UNIVERSITÀ
DEGLI STUDI
DI PADOVA

Sede amministrativa: Università degli studi di Padova

Dipartimento di Beni Culturali: archeologia, storia dell'arte, del cinema e della musica

SCUOLA DI DOTTORATO DI RICERCA IN: Studio e conservazione dei beni archeologici e architettonici
INDIRIZZO: Scienze e tecnologie per i beni archeologici e architettonici
CICLO XXV

STUDY OF THE PRODUCTION AND THE REGIONAL AND INTERREGIONAL RELATIONS BETWEEN THE PROTOHISTORY COMMUNITIES FROM THE NORTHERN ITALY, PARTICULARLY FOCUSING ON THE MIDDLE-EAST AREA, THROUGH THE ARCHAEOMETRICAL ANALISYS OF THEIR POTTERY

Direttore della Scuola : Ch.mo Prof. Giovanni Leonardi
Supervisore :Ch.mo Dott. Lara Maritan
Co-supervisore :Ch.mo Prof. Giovanni Leonardi

Dottorando : Marta Tenconi

CONTENTS

Abstract

Introduction

First chapter – Modern techniques of analysis applied to the study of ancient ceramics

1.1 Macroscopic analysis
1.2 Petrographic characterization through the optical polarizing microscope
1.3 Digital image analysis through scanning electron microscope
1.4 X-ray powder diffraction analysis (XRPD)
1.5 Chemical analysis trough X-ray fluorescence spectroscopy (XRF)
1.6 Statistical analysis
1.7 Electron probe microanalysis
1.8 High-resolution micro X-ray diffraction

Second chapter – Historical context of the protohistory of north-eastern Italy: a brief overview

Third chapter – The pottery assemblage from Castel de Pedena

3.1 Castel de Pedena, historical context
3.2 Macroscopic analysis
3.3 Petrographic fabric classification
3.4 Digital image analysis
3.5 Mineralogical composition
3.6 Chemical analysis and statistical treatment of the data
3.7 Geological setting and provenance considerations
3.8 Production technology
3.9 Discussion and conclusions
3.10 The pottery assemblage from Fondo Paviani
3.10.1 Historical context
3.10.2 Geological setting
3.10.3 Petrographic fabric classification
3.10.4 Mineralogical composition
3.10.5 Chemical analysis and statistical treatment of the data
3.10.6 Discussion and conclusions

Fourth chapter – Flared rim and flattened lip pottery

4.1 Historical context
4.2 Macroscopic analysis
4.3 Petrographic fabric classification
4.4 Digital image analysis
4.5 Mineralogical composition
4.6 Chemical analysis and statistical treatment of the data
4.7 Geological setting and provenance considerations
4.8 production technology
4.9 Discussion and conclusions

Fifth chapter – Postdepositional deterioration in buried ceramics

5.1 Secondary phosphates in ceramic fragments from Concordia Sagittaria
5.2 Secondary sulphates formed in potsherds coming from lagoon-like environments

Conclusion

References

ABSTRACT

In the archaeological record the ceramic remnants are among the strongest materials since their origin. The pottery study is therefore very important for archaeology for many different reasons. First of all the morphological features of the vase shapes, their decoration as well as the production technology are usually a peculiar element of the community that produced them. These elements make ceramic a craft-made expression and an artistic expression of a certain culture and the 'key fossil'. Pottery is also one of the most significant indicators to measure the technological development of a society in a particular period of time. Furthermore pottery gives relevant information about both the contacts and the social relations, which occurred between neighbouring and far away countries, and trades between different populations.

Through archaeological and archaeometric analysis of vase shards, this project aimed to highlight the contacts, the social relations and the trades occurred between the protohistorical populations from the north-east of Italy, particularly the Veneto region, and other populations settled in the Italian peninsula or up north the Alps. Secondly, the study was addressed to investigate the production technology adopted for manufacturing these artefacts and to characterize in detail the compositional variability of the pottery in terms of chemistry and petrography. Where possible, in addition to the archaeological finds, a series of clays and sands sampled from potential provenance sites were studied. The research were carried out through optical microscopy (petrographic microstructural and textural analysis) and image analysis on scanning electron microscopy (image and elemental maps), the mineral assemblages were gained by X-ray diffraction (XRD), geochemical analysis by X-ray fluorescence (XRF) and multivariate statistical analysis.

Three case studies were selected, each involving different regions and a wide chronological interval, in order to develop the research project:

a) The site of Castel de Pedena (Belluno, Italy), dated between the end of the Old Bronze age and the end of the Late Bronze age (XVIII-X Century b.C.). Particular interest was here addressed to some jars found in the site, typical of the Alpine Luco/Laugen-Meluno/Melaun culture. Although no ceramic trade could be identified for these vases with the regions where the Luco/Laugen culture was well attested -Italian South Tyrol and Trentino, Austrian East Tyrol, Liechtenstein and Swiss Grisons regions- a so high similarity in the shapes of vessels and in the production technology proves the existence of intensive contacts. Furthermore, the study of the pottery assemblage of Castel de Pedena allowed to delineate the evolution of the production technology from the Recent Bronze Age to the first Iron.

b) The flared rim and flattened lip ceramics (FRFL pottery), a peculiar type of vase that spread across the Friuli Venetia Giulia region (north-east of Italy), between the final Bronze Age and the beginning of the Iron Age, but found also in few sites of the neighboring Veneto region. The archaeometric analyses of FRFL pottery coming from three sites of Veneto (Concordia Sagittaria, Padova, Castion d'Erbè) revealed that they had high similarity in the preparation process since they were realised using similar recipes in

terms of abundance and type of temper. Inclusions were represented mostly by concretions of speleothems, a very peculiar type of rock. Moreover, comparison with the local Venetian products indicated that the FRFL pottery were compositionally distinct. On contrast they showed great similarity with FRFL shards coming from sites of the Friuli Venetia Giulia region. The presence of speleothems related this pottery to the Friuli Venetia Giulia, a karsic region with presence of more of seven-thousand caves, and it suggested that they were transported in Veneto for some specific product trade.
c) The site of Fondo Paviani (Verona, Italy), dated between the end of the Middle Bronze age and the beginning of the Late Bronze age (XIV-XII Century b.C.). During the Recent Bronze Age the common use of produce coarse pottery with macroscopically similar pastes spread in all the 'Palafitticolo Terramaricola' culture sites. Since in the coeval level of the site of Castel de Pedena specimens typical of the plain culture were found, some specimens from Fondo Paviani were selected with the intention to compare them with macroscopically similar shards from Castel de Pedena, dated at the same age. This third 'case study' concerned a small number of potsherds coming from the site of Fondo Paviani (Verona, Italy). It must be consider a preliminary study and not statistically representative of the real context of the site. For the same reason it was not possible to make any general correlation between the pottery productions of Fondo Paviani and Castel de Pedena.

ABSTRACT
I materiali fittili sono fra i prodotti più resistenti nel record archeologico a partire dalla loro invenzione nell'antico Neolitico. Per questo il loro studio è di grande importanza per l'archeologia sotto molteplici aspetti. In particolare le forme vascolari, le loro decorazioni e la tecnologia di produzione sono normalmente peculiari delle comunità che le hanno prodotte. Questi elementi fanno della ceramica espressione artigianale, e nelle fasi più recenti anche artistica, e tecnologica di una cultura, qualificando tale prodotto come 'fossile guida' d'eccellenza e come uno degli indicatori parziali più sensibili del livello di organizzazione del lavoro raggiunto da una data società in un determinato periodo. La ceramica inoltre fornisce importanti informazioni sui rapporti sia di integrazione sociale tra popolazioni confinanti o anche ad ampio raggio, sia indicando rapporti commerciali tra gruppi diversi.
Attraverso l'analisi archeologica e archeometrica di frammenti vascolari, col presente progetto si è cercato di fare luce principalmente sui rapporti di interazione sociale, di scambio o commerciali tra le popolazioni protostoriche dell'Italia settentrionale -con particolare riferimento alla zona veneta- e le popolazioni coeve della penisola e d'oltralpe. A tal fine si è ritenuta necessaria la distinzione tra manufatti realmente di importazione e manufatti che imitano modelli di provenienza alloctona, l'individuazione dei centri produttori di tali manufatti, l'identificazione delle vie percorse dai traffici e la definizione delle relazioni tra le culture locali. Non si è voluto tralasciare inoltre la comprensione e la ricostruzione della tecnologia ceramica adottata, della tipologia dei materiali utilizzati e

del luogo di approvvigionamento delle materie prime. Dove possibile al lavoro sui materiali fittili è stata associata l'analisi di campioni di argille o sabbie provenienti da potenziali aree di approvvigionamento preceduta dallo studio dettagliato della geologia dell'area di interesse.

Analisi petrografiche e microstrutturali sono state condotte attraverso osservazione al microscopio ottico ed elettronico (analisi di immagine). Lo studio delle fasi mineralogiche presenti nei campioni ceramici è stato condotto attraverso analisi diffrattometrica dei raggi X su polveri mentre la composizione chimica è stata ottenuta per fluorescenza dei raggi X sui cui risultati sono state condotte analisi statistiche multivariate. In particolare sono stati presi in considerazione tre casi studio:

a) Il sito d'altura di Castel de Pedena (Belluno), datato tra il tardo Bronzo antico e il tardo Bronzo finale/prima età del Ferro. Durante gli scavi sono stati raccolti numerosi reperti ceramici vascolari alcuni dei quali riconducibili alla cultura alpine Luco/Laugen-Meluno/Melaun. Sebbene non sia stata riscontrata nessuna testimonianza di rapporti commerciali riguardanti questa tipologia vascolare con le aree pertinenti -il Trentino, l'Alto-Adige, il Tirolo Orientale e la Bassa Engadina- la forte somiglianza tra i reperti rinvenuti presso sito e il cosiddetto boccale tipo Luco sembrerebbe provare intensi contatti tra le due culture.

Infine, lo studio dell'intero repertorio ceramico proveniente da Castel de Pedena ha permesso di ricostruire l'evoluzione della tecnologia di produzione della ceramica dall'età del Bronzo Recente fino alla prima età del Ferro.

b) La ceramica a orlo svasato superiormente appiattito (qui chiamata FRFL pottery) si diffusa nel Friuli Venezia Giulia (Italia nord-orientale) tra la fine dell'età del Bronzo Finale e la prima età del Ferro. Questa tipologia vascolare trova però confronti anche in reperti provenienti da alcuni abitati coevi di area veneta.

Le analisi archeometriche di alcuni reperti di vasi provenienti dai siti veneti di Padova, Concordia Sagittaria e Castion d'Erbé hanno rivelato che gli impasti dei campioni sono simili tra loro sia per l'abbondanza di inclusi sia nella peculiare scelta della tipologia litica adottata: sono stati fatti utilizzando frammenti di concrezioni di grotta (speleotemi). Inoltri il confronto con frammenti di vasi di tipologie tipiche venete, e quindi di probabile origine locale, ha dimostrato che questi vasi sono composizionalmente distinti mentre hanno grande somiglianza con ceramiche 'FRFL' di provenienza friulana e giuliana. La presenza di speleo temi le mette in relazione con la regione della Venezia Giulia, un'area carsica dove si conoscono oltre settemila grotte. Sembrerebbe quindi che fossero state trasportate in Veneto, probabilmente per scopi legati al commercio di qualche prodotto specifico.

c) I reperti provenienti dal sito arginato di Fondo Paviani (Legnago, Verona), datato tra la fine dell'età del Bronzo Medio e l'inizio del Bronzo finale (XIV-XII secolo a.C.). Il sito arginato di Fondo Paviani (Verona) si data tra la fine dell'età del Bronz Medio e l'inizio del Bronzo Finale. Durante l'età del Bronzo Recente è stato osservata nell'area ascrivibile alla cultura 'Palafitticolo Terramaricola' l'abitudine comune di produrre ceramica vascolare

grezza caratterizzata da impasti macroscopicamente simili. Materiali simili, ascrivibili all'età del Bronzo recente, sono stati trovati anche presso l'abitato di Castel de Pedena. Questo ha indotto a studiare un piccolo numero di questi reperti provenienti da Fondo Paviani con l'intenzione di confrontarli con i coevi materiali di Castel de Pedena. Dato l'esiguo numero di campioni, questo ultimo caso studio è da considerarsi uno lavoro preliminare i cui risultati non sono statisticamente rappresentativi del contesto reale del sito. Per lo stesso motivo non è stato possibile trovare alcuna correlazione coi reperti di Castel de Pedena, e con la tecnologia di produzione adottata in antichità presso il sito.

INTRODUCTION

The term *ceramic* derives from Greek *keramos* – *keramikós*, whose translation is "made of clay hardened by heat". Indeed, traditional ceramics are formed by clays, usually with varying amount of impurities or additives. When mixed with water they can be shaped in various forms, then after being dried and fired become a harder and a permanent object. In that way traditional ceramics were the first synthetic materials produced by humans. From an archaeometrical viewpoint, pottery can be considered like an artificial rock that can be compared to artificial metamorphism at high temperature and low pressure. From this process arises a transformation with a solid-state recrystallization of mineral phases originally . The result is a product formed by holes (pores), a matrix (former clay minerals), coarser minerals and rock fragments (non-plastic inclusions) either natural or purposely added (Maggetti 1991).forming in clay phases.

The production of every pot is the result of a series of decisions of potters, as the selection and preparation of the raw materials, the forming method, the decoration and firing technique. Potters affected the final material with choices and actions that express their cultural environment, as well as their own feelings.

The main aim of archaeological pottery studies is primary the reconstruction of its production, distribution and use, and in a secondary stage, through its interpretation, a better understanding of the related society. One of the best ways to do this is to reconstruct the production process, described as a *chaine operatoire* by Leroi Gourhan (1964, 1965), looking at each step in the operational sequence and questioning the choice of the particular techniques and tools used. With regards to this, any ceramic shard is of great importance because it brings a wide range of information about its history (Sillar, Tite 2000).

This project deals with the study of pottery coming from protohistorical sites of the north-east of Italy. The main aims were to answer important questions about short and long-lasting contacts and trades between people and cultures through the archaeometrical analysis of ancient pottery. Secondly, the study is addressed to investigate the production technology adopted for manufacturing these artefacts.

The term *archaeometry* implies the practice of scientific methods to the study of works of art covering the application of the physical and biological sciences to archaeology and history of art. Moreover, the archaeometry is deeply connected with the archaeological theory and the historical context of the studied artefacts. Therefore, this research was carried out in collaboration with scientists involved into more archaeological projects of the same protohistoric contexts and materials coming from there. In that way, it represents a part of a multidisciplinary work, realised thanks to the collaboration of a large team composed by researchers with scientists and archaeological expertises.

In order to gain these aims, two cases were developed. Based on a multidisciplinary approach, the first study involves the pottery collection coming from the site of Castel de Pedena (Belluno, Italy). Particular interest in this case was addressed to some jars found in the site, typical of the Alpine Luco/Laugen-Meluno/Melaun culture. The other example concerns a pottery type highly present in the Friuli Venetia Giulia region and in few sites of the neighbouring Veneto region. In both these examples, the research aimed to provide evidence about possible trades or relationships between cultures and people and to define the production technological level used by ancient potters.

The first chapter summarizes the analytical methods used for this work, their underlying principles and some consideration in applying these to the archaeological pottery study.

The second part introduces the protohistory of the north-east of Italy. It summarizes the main events from the Early Bronze Age up to the first Iron Age, the life-time of the sites considered in this research. The main aim was to illustrate the complexity and vitality, as well as the historical context of the studied sites.

Chapter three treats the study of the pottery collection from Castel de Pedena. A first part is about its historical context. It is followed by the analytical results: the vase shards characterisation, the description of the clayey pastes and the distinction of main different *fabrics*, the bulk chemistry analysis and the mineral assemblages existing in the potsherds. Then the results interpretation –namely the distinction between local products and allochthonous artefacts and the reconstruction of the production technology- is presented.

A further paragraph about the analysis of potsherds coming from the coeval site of Fondo Paviani (Verona, Italy) is finally introduced. This concerns only a small number of samples, therefore it must be consider a preliminary study preceding a larger-scale project.

Chapter four deals with the so-called flared rim and flattened lip pottery. Though it was highly present in the Friuli Venetia Giulia region during the late Final Bronze Age and early Iron Age, a few specimens were discovered also in several early Iron Age sites of the neighbouring Veneto region. The first part of the chapter is about the historical context of these sites, followed by the analytical results and their interpretation. The main aims were the distinction between local products and allochthonous artefacts and the reconstruction of possible trades, secondly their production technology. Here the same topics-sequence adopted for chapter three was here followed.

Finally, there is a last part concerning the alteration of pristine mineral phases and the formation of post-depositional secondary phases -phosphates and sulphates- in pottery coming from the sites of Concordia Sagittaria, Aquileia and Terzo Ramo del Timavo. A combined microchemical, microstructural and diffractometric approach was used to comprehend and describe them more completely.

First chapter

MODERN TECHNIQUES OF ANALYSIS APPLIED TO THE STUDY OF ANCIENT CERAMICS

Under an archaeometrical point of view, pottery can be considered as artificial rocks that have undergone metamorphism at high temperature and low pressure with a solid-state re-crystallization of minerals (Maggetti 1991, Veniale 1990). The resulted product is formed by voids (pores), a matrix (composed by very fine grained crystals and an amorphous phase formed during firing), coarser minerals and rock fragments (non plastic inclusions) either natural or purposely added. With regards to this, any ceramic shard is of great importance because it brings a wide range of information about his history and can be analyzed with the same technical methods used in geosciences to study soils, rocks and minerals.

The main aims of materials studies in archaeology are primary the reconstruction of the production, their distribution and use and in a secondary stage, through their interpretation, a better understanding of the related society. In this study, to avoid any prejudice, the analyses were first performed without considering the archaeological information a priori (pottery typology, chronology and provenance context).

In particular, this chapter summarizes the methods used for this work, their underlying principles and some consideration in applying them to archaeological pottery.

1.1 Macroscopic analysis

In the preliminary stage of investigation all the pottery samples selected for the analyses were subjected to a hand-examination following the methodology illustrated by P. Stienstra (1986) with Maritan's modifications (Maritan 2002, Whitbread 1995). The observations were conducted on the fresh cross sections resulted by the sampling of materials made with a diamond saw, leaving in this way an even surface.

The description, made with the help of a hand lens, considers the main pottery features: matrix and inclusions. Being the term matrix applied to the finest grained material not visible at the unaided eye, it was limited to the colour determination measured following the Munsell colour system, with the Munsell Soil Color Chart (2000). Some samples show differentiations along the internal or external surfaces or a dark "core", the so-called sandwich structure.

Non-plastic inclusions were reported considering the total concentration (expressed as abundant, common, rare), the maximum and average grain sizes, the estimation of the

roundness (rounded, sub-rounded, angular) by the comparison with a visual estimation chart (figure 1.1). Their characterization was deduced in a second moment by optical microscopy (Maritan 2002, Stienstra 1986).

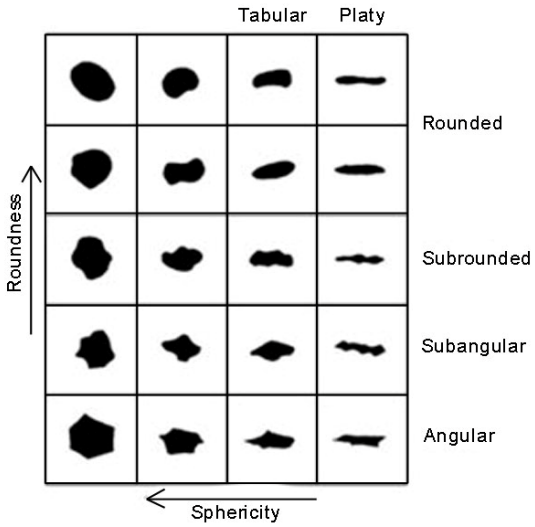

Figure 1.1. Shape of inclusions. After Hodgson 1974.

1.2 Petrographic characterization through the optical polarizing microscope

Optical microscopy was carried out on whole fragments with the aim to characterize their fabric and possibly their distinction in different groups. In fact thin-sections observation can give important information about the provenance and the production technology adopted: clay selection and processing choice, preparation technique and firing process (Reedy 1994, Reedy 2008, Riederer 2004).

Standard petrographic thin sections (30 μm thick) were prepared at the Geoscience Department, University of Padova. They were cut with a diamond saw perpendicularly to the base and rim of the vase (vertical section), as it is considered more useful for provenance and technological studies (Whitbread 1996, Woods 1982). The so cut slides were vacuum impregnated with epoxy to stabilize the sample enough for the following polishing process. At this point they were attached to a glass slide, grinded and polished with diamond abrasive powders until the achievement of a 30 μm thickness. They were then analyzed under polarizing light microscope following a modification of the thin section description protocol illustrated by Whitbread (1989, 1995).

Whitbread description methodology was developed by the soil micromorphology and sedimentary petrology systems. Their peculiarity, that makes them particularly useful in the ceramic description, is the adoption of a purely descriptive vocabulary that produces objective results, separating the interpretation from the observation (Freestone 1995, Josephs 2005, Whitbread 1995). The method considers the main characteristic features of a ceramic (groundmass or matrix, non plastic inclusions, voids/porosity) according to the following scheme:

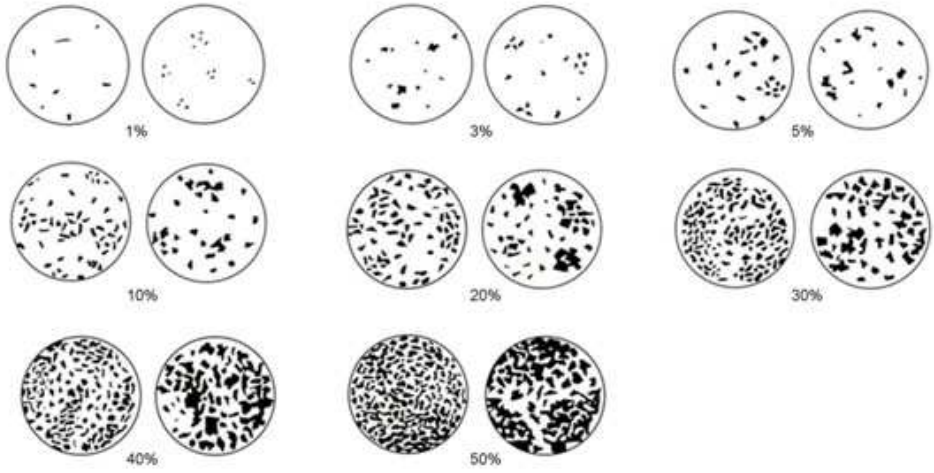

Figure 1.2. Comparative chart for the estimation of the percentage are of the non-plastic inclusions and voids. After Müller 1964 .

Matrix:

The matrix, composed by the clay minerals and occasionally by a glassy part, is the finest constituent of a ceramic (less than 10 μm) (Whitbread 1995). It is not easily solvable at the optical microscope and its description includes: the *homogeneity*, whether there are variations within or between the fabrics like in textural features, distribution of inclusions, type of voids, colour differentiations between core and margin. The *optical state*, the presence or absence of interference colours in the micromass under cross polars with indication of its intensity or variations. The *birefringent fabric* (*b-fabric*), the special disposition and nature of optically active zones in the ceramic. It can be described as crystallitic: small birefringent crystals other than clay mineral domains; speckled: random birefringent zones of a few microns in size; striated: elongate birefringent streaks; strial: preferred orientation of large (several mm/cm) birefringent streaks. The *orientation*, description whether the clay minerals, the elongate minerals and the elongate pores have specific orientation, for instance with respect to the vessel wall.

Voids:

Voids are the empty spaces present in the ceramic materials. Their study can provide important information about pottery productions. The voids description includes: the *concentration*, the total area percentage of the voids, measured by comparison with published estimation charts (figure 1.2). The *shape* described as planar voids: linear in thin section but planar in three dimensions; channels: linear in thin section but cylindrical in three dimensions; vughs: relatively large, irregular voids; vesicles: regular in shapes with smooth surfaces (figure 1.3). The size, the modal diameter of the biggest pore.

Inclusions:

The inclusions, or non-plastic inclusions, represent all the materials that compose a ceramic easily distinguishable at the optical microscope (grains sizes bigger than 10 μm). The term “inclusions” is here used, as suggested by Whitbread (1995), to describe generically discrete particles within the fabric regardless of their supposed origins. While the term “temper” will be employed referred to materials that, for some stated reason, are

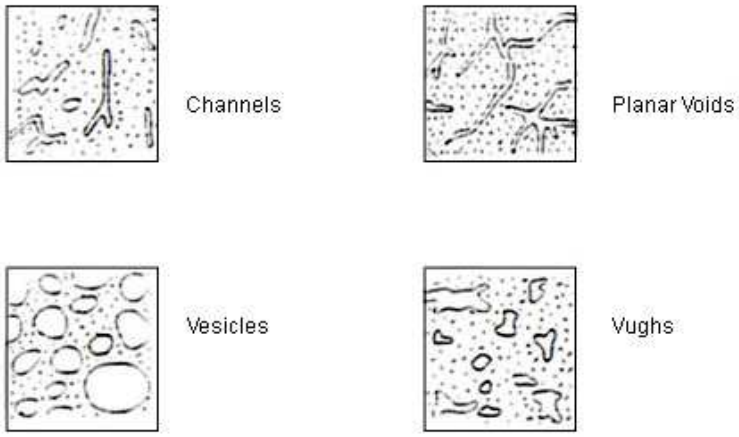

Figure 1.3. Shapes of voids. After Kemp 1985.

believed to be added by the potter (Rice 1987, Whitbread 1995). In this research their description includes: the *abundance*, their concentration expressed in percentage, measured by comparison with estimation charts (figure 1.2; table 1.1); the *size,* the modal grain-size, grain-size range and indication of the presence of a unimodal, a bimodal or a polymodal and a seriate size distributions; the *shape*: the roundness deduced from comparative charts (figure 1.1); the *composition*, the identification of the mineral phases and lithics with indication of the relative abundance in respect of all the other. If the fabric has more than one mode or a seriate grain-size distribution, the coarser (c) and finer (f) fractions were distinguished and the c:f ratio - the relative proportion of the coarser (c) and finer (f) fraction of the inclusions- was indicated. In this case they were described separately.

Predominant:	>70	%
Dominant:	50-70	%
Frequent:	30-50	%
Common:	15-30	%
Few:	5-15	%
Very few:	2-5	%
Rare:	0,5-2	%
Very rare:	< 0,5	%

Table 1.1. Semi-quantitative frequency for inclusions.

1.3 Digital image analysis through scanning electron microscope

The SEM observations were conducted particularly for characterizing pottery pastes through features quantification (the area percentage of matrix, voids and inclusions, average size and grain-size distribution, length of axes, degree of roundness) by image analysis. It was also performed for investigating secondary phosphates due to post-depositional precipitation, and the microstructure of speleothems fragments observed through the optical microscope in some of the studied pottery (Freestone, Middleton 1987, Reedy 2006, Reedy 2008, Tite, Freestone et al. 1982, Tite, Maniatis 1975). The analysis was carried out at the Department of Geosciences (University of Padova). Samples were prepared as polished thin sections, coated with a thin layer of the conductive material carbon. Both back-scattered electrons images and chemical maps were acquired.

Back-scattered electrons images (SEM-BSE)

SEM-BSE images were acquired with a SEM CamScan MX 2500 microscope, coupled with an energy dispersive spectrometer, equipped with a LaB_6 cathode, working in high vacuum mode (HV). The analytical parameters (working distance, spot size, luminosity, contrast,…) used during the acquisitions were changed time by time considering the distinctive features of each sample. A SEM-BSE image is a grey scale image where the discrimination of phases is based on the mean atomic number (Z), commonly associated to the grey hues: a "brighter" BSE intensity is correlated with greater average Z, and "darker" areas with lower average Z.

Chemical maps

For chemical semi-quantitative analysis an EDAX Genesis energy-dispersive X-ray spectrometer was used with accelerating voltage of 25 KeV. X-ray maps of nine chemical elements (Al, Ca, Fe, K, Mg, Na, O, Si, Ti), corresponding to the same number of separated TIFF files, were detected. Only for the phosphates investigation also P and Mn were added. An element map is a 2-dimensional image showing the spatial distribution of the single elements in a sample. In order to obtain a good accuracy and quality 512x400 pixels maps with a 12 hours mapping time were acquired.

Digital image analysis (DIA)

Petrographic thin-section analysis is an important tool for materials characterization and for studying deterioration and treatment effects on stone, cementitious materials, and ceramics. Combining thin-section examination with computer programs that analyze digital images is a standard procedure in geology. These programs allow rapid measurement and quantification of thin-section parameters as area percentage, length, width, distance between features, roundness, size distribution and clustering of features. DIA was traditionally gained by visual estimation, a method relatively fast but with low accuracy and reproducibility, or by point counting, a methodology that has higher accuracy but that is time consuming (Matthew, Woods et al. 1991, Middleton, Freestone et al. 1985, Reedy 2006, Reedy 2008, Stoltman 1989). Here, computerized analysis of digital images (DIA) was performed representing a considerable saving in time and increasing the precision and reproducibility of the work.

Both, back-scattered electrons micrographs (SEM-BSE) and elemental chemical X-ray maps were studied by DIA. A selection of samples characteristic of the fabrics groups identified by optical microscopy and of the different features of interest was chosen. For each sample nearly ten BSE images were acquired to guarantee statistical validity and to cover the whole section. Chemical mapping was performed only on a representative area of the sample, since the acquisition of several maps in different areas of each samples would had been very time consuming and expensive.

For DIA a modification of the protocol suggested by Gregorio Dal Sasso (2011) was adopted. Initially the images were "manipulated", when required, in order to emphasize particular features. For this aim the graphical software package ImageJ was used: each image was converted into 8-bit grey-scale, the brightness and contrast were enhanced and the noises were reduced and smoothed with the median filter. The files were saved as TIFF type (Tagged Image File Format), an uncompressed file format that prevent the loss of image quality.

For BSE images, the components (matrix, inclusions and voids) were differentiated, or segmented, considering the diverse grey tones[1]. Each pixel corresponds to a specific grey dye that strictly depends on Z and that is supposed to differ for the different pottery features (voids, matrix, inclusions = different mineral phases or lithics) and to be peculiar within the same ones. In this way it might be possible to classify the ceramic textural features on the bases of their different grey hues.

The preliminary selection of fabric groups defined by the previous optical microscope observation was the starting point. Than the classification, its evaluation and the extraction of the desired information were carried out through an *unsupervised classification mode*, using the MultiSpec (version 3.3) software. The grey tones were assigned to a set of classes, covering all the range of grey values of the image (from black to white). Different mineral phases or textural features may not correspond to a single class, but could be described by more classes. Therefore, each textural feature and, when possible, also mineral phase assigned by the operator, group successive classes. This methodology assigns all the pixels with the same grey hue or the most similar one to a same set. The aims is to find groups that are exhaustive, separable and of informational value.

After the first analyses it became evident that, due to the particular complexity of the ceramic constituents, for SEM-BSE images it was not possible to separate all the different kind of inclusions. So, for maintained high accuracy, only the distinction between matrix, voids and inclusions (in general) was considered.

With the purpose of obtaining a higher precision, it was observed that it is useful to adjust the parameters of the clustering in order to achieve a number of clusters higher than the number of the effective features present in the thin section. This number was decided time by time considering each sample situation. In this way it was less probable to wrongly cluster together different pottery features with similar Z, as some inclusions and the matrix. The different components, so split in several groups, were re-collected together in a second moment. The Gaussian Maximum Likelihood classification algorithms (Quadratic Likelihood) and ECHO (Extraction and Classification of Homogeneous Objects) were used. These algorithms are both maximum likelihood classifiers that segment the scene into spectrally homogeneous objects (Landgrebe 1997).

[1] Image segmentation is one of the most studied methods of grouping pixels in computer vision. It tries to find partitions of the image pixels into sets corresponding to coherent image properties such as brightness, color and texture (Malik, Belongie et al. 2001).

The results are displayed in a cluster classification image where each class is represented by a specific colour.

An element map is a 2-dimensional image showing the spatial distribution of the single elements in a sample. Chemical maps, as obtained by the SEM, were treated whit the MultiSpec software, in order to describe the different type of inclusions in terms of size, grain-size distribution and shape, and to quantify the m:i:v (matix:inclusions:voids). When working with X-ray elemental maps, all kind of inclusions were separately investigated. The multispectral image files were overlaid and linked together as one that contains all the channels (the single chemical maps). This allows to control the type of multispectral display (one, two or three channels at the same time) and to select which channels to display. The result was a series of thematic maps where each chemical element (for a maximum of three at the same time) was represented in false colour and the overlay of them was representative of the different mineralogical phases. As for the BSE-SEM images, then these components were investigated and quantified.

Finally the quantitative parameters of the binary segmented images were treated with the ImageJ software. For the images of inclusions these parameters were analyzed: the *area* occupied by each particle; the *Feret's diameter (Feret)*: the maximum size of the inclusion; and shape descriptors: the *aspect ratio (AR)* of the particle's fitted ellipse: it describes the elongation of particles (AR = Maximum axis/minimum axis) and the *roundness*: the inverse of the aspect ratio. Also a summary of the results was displayed in a table with indication of the particle count, the total particle area, the average particle size, the area fraction in percentage and the mean of all parameters listed above. For the images representing the voids distribution, only the summary table was displayed because of the complexity of their shapes; while the matrix area was calculated by subtraction of area fraction of inclusions and voids.

These results were statistically treated with the software packages Excel 2007 and STATGRAPHIC Centurion in order to analyze the grain-size distribution of the inclusions present in the thin sections, shapes and proportion of inclusions in order to highlight different assemblages and production recipes.

According with Whitbread (1995), the boundary between the inclusions and the matrix components of the ceramic body was set at 10 μm. For this reason particles with lower Feret values were not considered in the particles analysis. At first the m:i:v (matrix:inclusions:voids) ratio was estimated through the area fraction occupied by each of them and displayed in a 100% stacked bar chart. Then for each sample the Feret values were displayed in histograms overlaid by the probability distribution functions that fit better in order to show the particle-size distribution and whether one or more modes exist. Since the finest fraction of the inclusions is extremely greater in the particles number respect the coarser inclusions, they appeared predominant also when they were insignificant considering the total area fraction occupied. For this reason often it was difficult to see any real presence of one or more modes. Therefore the inclusions were divided on the basis of the different size distributions referred to the Wentworth grain-

size chart. The total area fraction occupied by each grain size classes were graphically represented in a 100% stacked bar chart. In doing this the Feret values were considered in order to be able to compare the information about the coarser inclusions with the optical microscope observations. Since for SEM-BSE the inclusions were analyzed all together without discriminating the different types, this result must be considered with great caution because they gather different type of litho-types that usually have different aspects (shape, angularity, size, ...).

1.4 X-ray powder diffraction analysis (XRPD)

X-ray powder diffraction (XRPD) analysis is a technique that allows the determination of the mineral phases on bulk of a ceramic by their crystalline structure. Through the measure of the diffraction effects intensities, it can provide also semi-quantitative information about the minerals phases present in amount more than 5%.

Before performing the analysis, the external surface of each shard was cleaned from possible alteration with a micro-drill. Then nearly 0,3 g of each sample was grounded in fine powder (less than 10 μm) with an agate mortar and, in some cases, with an industrial McCrone micronising mill.

XRPD analyses were carried out at the Geoscience Department, Univeristy of Padova, with a Philips X-Pert PRO diffractometer. The instrument is a PW3710 parafocusing geometry Bragg-Brentano diffractometer equipped with a copper anode, sample spinner, a goniometer PW3050/60 (Theta/Theta) with minimum step size 2Theta: 0,001, and a RTMS detector (X'Celerator). The analyses were conducted in the range 3–80° 2Theta using a step interval of 0.017° 2theta, with a counting time of 100 s. The phase identification and semi-quantitative analysis were performed using the software package X'Pert HighScore Plus (3.0 version) with whom the integral profile width and shape of multiple peaks were closely examined. The phase's identification was gained by the comparison with the reference pattern databases PDF2 (ICDD), Panalytical-ICSD and COD (Crystallography Open Database. It contains inorganic crystal structure data and includes structures from the American Mineralogist database) in order to find similar features. The semi-quantitative data were calculated through the estimation of the accepted phases' mass fraction with the RIR (Reference Intensity Ratio) values (Chung 1974).

The mineral assemblages identified in the potsherds yield information about production technology, particularly about the raw material originally used (the nature of the initial clay or the presence of different clays at the same time), the firing temperatures reached and post depositional mineralogical changes, data difficult to recognize with other techniques (Maggetti 1991, 5-7, Veniale 1990, 19-28).

The maximum firing temperatures can be obtained comparing the XRPD's results with tables of the stability of minerals (figure 1.4) at different temperatures in the reducing and oxidizing atmospheres, available in literature (Maggetti 1982, Maggetti 1991, Maritan 2002, 122-139, Maritan 2004).

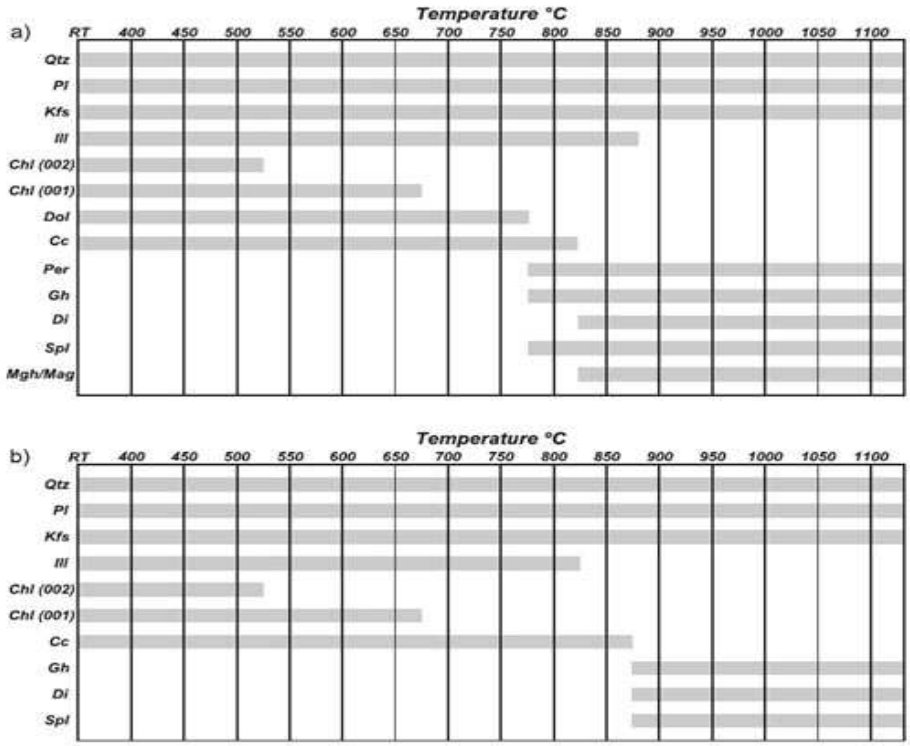

Figure 1.4. Mineralogical changes during firing of clays under oxidizing (a) and non-oxidising (b) conditions. Qtz: quartz; Pl: plagioclase; Kfs: K-feldspar; Ill: illite; Chl: chlorite; Dol: dolomite; Cc: calcite; Per: periclase; Gh: gehlenite; Di: diopside; Spl: spinel; Mgh/Mag: maghemite/magnetite. After Maritan 2004.

1.5 Chemical analysis trough X-ray fluorescence spectroscopy (XRF)

The bulk chemistry of the samples was determined by X-ray fluorescence spectroscopy at the Department of Geoscience, University of Padova.

The external surface of each shard was cleaned from possible alteration with a micro-drill and then ground in powder in an agate mortar. A known amount of the samples' powders (nearly 1,5 g) was heated in a furnace at 860°C for about 20 minutes and then at 980°C for about 2 hours for the determination of loss on ignition (L.O.I.). The L.O.I. can be affected by the volatile elements present: hydrogen, oxygen and carbon. These are not determined by XRF and are related to the organic matter and the water of primary phases or anions, such as CO_3, originally present. Samples for XRF analysis were then prepared as glass beads mixing 0,65 g of the calcined powder and the flux di-lithium tetraborate $Li_2B_4O_7$ with a dilution ratio of 1:10 and melted using a fluxer Claisse Fluxy (that operates at a temperature of about 1150°C). The samples analysis was carried out on a WDS sequential Philips PW2400 spectrometer, operating under vacuum conditions and equipped with a 3kW Rh tube, five analyzing crystals (LiF220, LiF200, Ge, PE, TlAP), two detectors (flow counter and scintillator), three collimators (150 µm, 300 µm and 700 µm) and four filters (Al 200 µm, Brass 100 µm, Pb 1000 µm and Brass 300 µm). The quantitative analyses were performed using the software package SuperQ; the concentration of the major and minor elements is expressed in wt% of their oxides (SiO_2, TiO_2, Al_2O_3, Fe_2O_3, MnO, MgO, CaO, Na_2O, K_2O, P_2O_5), and for trace elements the concentration is expressed in ppm (Sc, V,

Cr, Co, Ni, Cu, Zn, Ga, Rb, Sr, Y, Zr, Nb, Ba, La, Ce, Nd, Pb, Th, and U). Instrumental precision (defined by several measurements performed on the same sample) is within 0,6% relative for major and minor elements, and within 3% relative for trace elements. The XRF accuracy was checked by reference standards (Govindaraju 1994) and was within 0,5 wt% for Si, lower than 3% for other major and minor elements, and lower than 5% for trace elements. The lowest detection limits of XRF were within 0,02 wt% for Al_2O_3, MgO and Na_2O, within 0,4 wt% for SiO_2, within 0,005 wt% for TiO_2, Fe_2O_3, MnO, CaO, K_2O and P_2O_5 and within a range between 3 and 10 ppm for trace elements. The calibration curves were calculated using 60 reference standards (Govindaraju 1994).

Fe measured with XRF is expressed as Fe_2O_3. The FeO (Fe^{2+}) content was determined by the modified Pratt's method (Pratt 1894): about 0,5 g of powdered sample was dissolved in 15 ml of a solution of sulphuric acid (H_2SO_4), hydrofluoric acid (HF) and deionised water in a 1:1:1 ratio and heated at 180° for 8 minutes. The dissolved sample obtained was mixed with a solution of 300 ml of deionised water, 5,0 ml of H_2SO_4 and 0,6 g of boric acid (H_3BO_3), and titrated with potassium permanganate ($KMnO_4$ N/10). The concentration of FeO was calculated by:

$$\% \text{ FeO} = (\text{ml } KMnO_4 \text{ N/10} * 0{,}007185 * 100) / (\text{sample weight}).$$

The Fe_2O_3 concentration was calculated by the difference from total iron oxide (Fe_2O_{3tot}) determined by XRF and FeO content determined by titration as follow:

$$Fe_2O_3 = Fe_2O_{3tot} - (FeO * 1{,}111)$$

where 1.111 is the ratio between the percentage contents of Fe in FeO and Fe_2O_3, respectively.

1.6 Statistical analysis

Chemical data were statistically treated using descriptive and multivariate approaches to form clusters of similar materials and to determine paste compositional reference units (PCRU). PCRU can be useful in discriminating local production from the allochthonous ones, or different workshops. This is based on the *provenance postulate* that holds that the variations in chemical composition between different natural sources exceed the differences observed within a given source (Buxeda, Cau et al. 1996, Rice 1987, Weigand, Harbottle et al. 1977).

However, with coarse-paste pottery it is important to make great attention in using statistic techniques for separating reference groups. Therefore, it is always advisable to compare chemical and mineral-based analytical methods (Rice 1987). Besides, when the temper is added there is a *dilution problem* causing the decrease of the original concentrations of the elements (Buxeda 1999, Kilikoglou, Maniatis et al. 1988).

The work was carried on a n x p data matrix with (number of cases) $n > p$ (number of variables describing the geochemical composition of a sample). Twenty-nine variables corresponding to the following chemical elements (SiO_2, TiO_2, Al_2O_3, Fe_2O_3, MnO, MgO, CaO, Na_2O, K_2O, P_2O_5, V, Cr, Co, Ni, Cu, Zn, Ga, Rb, Sr, Y, Zr, Nb, Ba, La, Ce, Nd, Pb, Th, and U) were considered for the statistical treatment. The analyses were performed using the

programs packages of STATGRAPHIC Centurion XVI, Minitab 14.13 and Microsoft Excel 2007.

The preliminary chemical analyses were based on a descriptive approach on one variable procedures and on the graphical summary in order to investigate the general trend and the distribution type. The *median*, the *arithmetic mean*, the *variance*, the *standard deviation*, the *coefficient of variation* (a measure of relative variability that expresses the standard deviation of the data as a percentage of the mean), the *first* and *third quartiles* were calculated in order to describe the central values of the data distributions and the level of concentration or dispersion around these central values (Sheldon 2003). The normal probability plot was performed through the ECDF (Empirical Cumulative Distribution Function) *Anderson-Darling test* to examine whether or not the observations follow a normal distribution.

Also graphical displays were created including the *box-plot* with indication of the outliers, the *histogram* with fitted probability density function and the *density trace*.

In order to distinguish paste compositional reference units (PCRUs) and outliers, compositional data analyses, particularly multivariate statistical representation, were fulfilled. In that way simultaneous observations of all the statistical variables were presented. This was possible because the data were transformed so that lower-dimensional representations could be used (Baxter 1999, Bishop, Neff 1989, Rice 1987).

As the chemical results were at different scales (major elements were expressed in percentage while trace elements in parts per million (ppm)), a standardization or transformation process of the data was required. So all the data were transformed to base 10 logarithms, a procedure that requires all values $x_{ij}>0$ and produce a nearly equal weighting though, not exact equality (Baxter 2001, Baxter, Freestone 2006, Buxeda, Kilikoglou et al. 2001, Day, Kiriatzi 1999). The so transformed data were used to perform unsupervised learning techniques of cluster analysis and principal component analysis (PCA) (Baxter 2006).

Initially the analyses were performed on the total data set excluding the P_2O_5 because of the high concentrations observed in the studied pottery, interpreted as a contamination effect (Freestone, Middleton et al. 1994, Freestone 2001, Lemoine, Picon 1982, Maritan, Mazzoli 2004, Picon 1985). Then they were repeated excluding those samples that appeared to be outliers through the box-plot display and through the cluster analysis (Baxter 2006).

The cluster analysis is based on the definition of a measure of dissimilarity between pair of cases and on the choice of an algorithm for grouping them hierarchically on the basis of a dissimilarity coefficient. The *Euclidean distance* and the *Squared Euclidean distance,* as measure of dissimilarity, and different hierarchical agglomerative algorithms were here adopted (Papageorgiou, Baxter 2001, 688, Baxter 2001, 688, Baxter 2006). Results are usually displayed in a dendrogram. The interpretation of results and the choice of the (dis-)similarity level with the consequent division in clusters are subjective choices of the operator.

The PCA aims to take the original *p* variables and to convert in new *p* variables: the principal components. They are linear combinations of the transformed originals, where the first few components are often good approximation of the higher *p*-dimensional space and are sufficient to describe most of the variability. This happens when the variables are highly correlated (Baxter 2001, Baxter 2006). It is commonly accepted that the first components, whose proportion of variances' sum (cumulative proportion of *eigenvalues*) reaches the 70% of the total, can be considered a good approximation of the original multidimensional space. However, also lower values can provide useful interpretable plots and the first three principal components were here used. The results gained are graphically displayed in a dot-plot based on scores of the first three components, with the loading plot superimposed, that indicates the location of each variable (chemical element) in the space.

Both cluster and PCA analyses aim to identify the structure of the data-set and the presence of initially unknown distinct subsets as well as to identify outliers and to show how they relate to other cases in the sample.

1.7 Electron probe microanalysis (EMPA)

EMPA analysis was carried out to define the composition of two different type of phosphates. They were recognised by optical and electronic microscopy and formed some aggregates in one sample (sample 31290).

The EMPA technique was performed at the IGG-CNR of Padova. The sample was prepared as a polished thin section coated with a thin layer of conducting material (carbon). Quantitative analyses of major and minor elements (Na, Mg, Al, Si, P, K, Ca, Mn, Fe) were carried on through a CAMECA SX50 equipped with four wavelength-dispersive spectrometers (WDS), the TAP, PET and LIF analyzing crystals, SE, BSE and XR detectors and an energy-dispersive spectrometers (EDS). The following standards were adopted: synthetic oxides of MgO, Al_2O_3, Fe_2O_3 for Mg, Al and Fe, $MnTiO_3$ for Mn and Ti, apatite for P and Ca, plagioclase (amelia) for Na, wollastonite for Si and orthoclase for K. The analyses were carried out at a current of 20 kV and at 5 nA with acquisition time of 10 s for peaks and 5 s for backgrounds. Only for K an acquisition time of 7 s for peak and 3 s for background were adopted. The concentrations of the major and minor elements were detected with a precision respectively within 2% and 4-5%. This technique can detect only elements present in amount more than 300 ppm (0,03).

1.8 High-resolution micro X-ray diffraction

To further integrate the mineralogy of phosphate aggregates found in the sample 31290, profile high-resolution micro-X-ray diffraction was performed on the two aggregates. Since the sample was mounted on a thin-section, it had a glass carrier that contributes to the background intensity. For reducing as much as possible the noise caused by the background, the carrier was reduced by polishing from 1200 μm to 780 μm thickness.

Measurements were performed at the third-generation synchrotron radiation source BESSY II of the Helmholtz Centre Berlin for Materials and Energy. The beamline was constructed and installed by ACCEL instruments GmbH as a second branch (40 mrad off-centre) of the 7 T wavelength-shifter, utilizing the optical hutch of the BAMline (Gorner, Hentschel et al. 2001, Paris, Li et al. 2007). The accessible energy range s 1.9–30 keV, provided by a fixed exit double crystal monochromator with three sets of crystals (Si 111, Si 311 and Ge 111). The energy resolution can vary between $\Delta E/E = 10^{-4}$ (Si 311) and $\Delta E/E = 10^{-2}$ (Si/W multilayer on Si 311). Several flexible optical schemes make it a multi-purpose beamline for applications in X-ray scattering and X-ray spectroscopy (Erko, Schäfers et al. 2004, Paris, Li et al. 2007).

The micro-XRPD experiments were carried out in transmission geometry. Both point (spot size: 30 µm) and line scans (1 mm, line brought 30 µm) were performed. The focusing system of the beam line provided a beam diameter of 10 µm at a photon flux of 1 x 10^{-9} s^{-1} at a ring current of 200 mA. The experiments were carried on with a wavelength of 1.0657 Å using a double-crystal monochromator [Si(111)]. The diffracted intensities were collected 200 mm behind the sample position with a two-dimensional MarMosaic CCD X-ray detector with 3072 x 3072 pixels (Schlegel, Mueller et al. 2011).

The obtained scattering images were processed and converted into diagrams of scattered intensities versus scattering vector q ($q = 4\pi/\lambda \sin\theta$) employing an algorithm from the FIT2D software. For the graphical representations, q-values were transformed to the diffraction angle 2θ (Cu) to provide a direct comparison to results obtained by XRD with Cu radiation. Copper anodes are one of the most commonly used X-ray tube materials for laboratory XRD studies (Schlegel, Mueller et al. 2011).

Second chapter

HISTORICAL CONTEXT OF THE PROTOHISTORY OF NORTH-EASTERN ITALY: A BRIEF OVERVIEW

This work concerns the study of sites settled during a period of 2000 years of protohistory, between the Early Bronze Age (EB) and the first Iron Age (FI) in the modern regions of Veneto and Friuli Venetia Giulia (north east of Italy). Though the area is not wide, it is characterized by very different landscapes: the Po river flows between Garda Lake on the west and the coast on the east, with the Alps to the north, and the peculiar karstic landscape on the north-eastern region.
During this period a series of significant and crucial historical changes took place. At the beginning there was the presence of an open landscape with few human boundaries and small farming and pastoral family groups, proceeding towards an ownership of land system characteristic of "quasi-political" tribal systems. All these institutions showed a varied and complex structure, based on networks, and were societies where the expression of status and power was of extreme importance. However, this complex process was not uniform in its manifestations across all the north-east of Italy as a result of the variety of its landscapes which affected it (Balista, Leonardi 2003). The chronology of the Bronze Age is well assured thanks to the good knowledge about the settlements, metalwork, pottery production and radiocarbon dates (Bietti Sestieri 1996, De Marinis 1999, Peroni 2004).

The protohistorical sequence:

Early Bronze Age (2300-1700 B.C.)

During the Early Bronze Age (EB) in the north of Italy it is possible to recognize only one archaeological *facies*, the Polada culture. The main indicators of the Polada culture are the pottery type (mostly ovoid cups and bowls) and the unique settlements. Only in the eastern Friuli Venetia Giulia region the Polada vessels were rare, while there were other different typologies that seem to be related with the coeval western Pannonia plain cultures of Wieselburg-Gáta and Litzenkeramik (Bellintani 1987, Peroni 2004, Rapi 2002).
The biggest peculiarity of this period was the occupation practice: coastal sites characterized by pile-dwelling and by bank drainage structures settled in the wetlands constituted by the many lakes and peat bogs that formed in the moraine amphitheatres during the late glacial time (Balista, Leonardi 1998, De Marinis 1999, De Marinis 2000). A

great number of pile-dwellings are known. Some of the better preserved are Lavagnone, Lucone and Polada on the Garda lake, Arquà Petrarca in the Euganean hills and Fiavé and Ledro in the Trentino region, and there are many other examples in all the northern Italy, up to the Piedmont region (De Marinis 2000, Peroni 2004). Only in some rare cases different occupational choices were preferred, like in mountain sites. Moreover, there began to appear some minor sites, which played a strategic role, being located in naturally defended positions (Leonardi 2010).

During the EB another substantial transformation took place in the way how people obtained their sustenance. The food procurement of hunter-gatherers was still consistent but domesticated animals and plants acquired greater importance. The use of the plough is also significant of an even more sophisticate and intense agricultural practice (De Marinis 2000, Peroni 1971).

People of the Polada culture reached great technological knowledge in all the different fields. Very good timber working skills are documented by the complexity of the dwelling structures. As a result of the damp environment, wooden tools were found along with lithic, bone or horn objects. Although the presence of metallurgy in northern Italy is indicated by the large number of metalwork hoards and votive deposits stone was still the preferred material for the production of artefacts. Pottery was the earliest handcraft technology with coarse paste hand-made vessels: ovoid drinking pots and bowls, amphorae, bi-conical or truncated conical vases, ovoid pots and pans were the most frequent, often with *elbow* handles and plastic decorations (De Marinis 2000, Peroni 1971).

Most materials are likely to come from local sources but there was also a wide use of raw materials coming from specific places, such as the grey flint from the Lessini mountain, the obsidian from the Eolie islands and the Baltic amber. This testifies the intense exchanges and transmission of objects, people and ideas (Bietti Sestieri 1996, Peroni 1971).

Middle Bronze Age (1700-1350 B.C.)

In the Middle Bronze Age (MB) the archaeological situation changed and the "Palafitticolo Terramaricola" culture spread. There were still evidences of pile-dwelling settlements in the western Lombardy, Veneto, Trentino and South Tyrol regions, but in Emilia Romagna, part of the southern Lombardy and lower Venetian plain there also appeared some peculiar settlements called terramare, mostly along the main rivers Mincio, Adige and Tartaro (Bernabò Brea, Cardarelli 1997). The terramare were mainly quadrangular settlements surrounded by a ditch and an earthen rampart with defensive function. The water of a nearby river or natural canal were re-routed into the moat, redistributing the water resources as it was attested at Santa Rosa di Poviglio and Redù. Excavations documented that the ditch and earthwork were sometimes absent in the ancient phases of the villages but they always appeared at a certain point (Bernabò Brea, Cremaschi 1997, Cardarelli 2009).

The karstic region of Friuli Venetia Giulia, around Trieste and Gorizia, in Istria and in the northern part of the Dalmatia region (an important area of passage that links the northern Italy with the south-east of the continental Europe) is characterized by the Castellieri culture. The area was identified by peculiar fortified boroughs usually settled in strategic positions on hills or mountains, defended by one or more concentric walls (AA VV. 1984, 75-80, Bietti Sestieri 1996, Peroni 2004).

The MB was generally characterized by the reorganization of the settlements system, as demonstrated by the practice of woodland clearance that typically preceded occupations. The majority of the ancient pile-dwelling sites were abandoned and new ones appeared. Mountain sites in positions strategic for the control of the Alps passages were occupied, always with wide views on the landscape and naturally defended (Leonardi 2010). Parts of the landscape were bound to the field system that was selected through specific choices and addresses toward hill landscapes (De Marinis 1997, Balista, Leonardi 2003). The territory became domesticated: subsistence activities went mostly from domestic food resources, with cereals and legumes (as the principal plant food) and sheep, cattle and pig (as the mainstay of meat production). Wild resources were also present but rare.

The MB society was organized into medium tribal units involved in the farming (animals and cereals) and characterized by an ownership of land system, with socio-economical differentiations and technological specialization of people (Peroni 2004).

Craftwork was also of great importance: a large number of bronze objects including ornaments, sickles, razors, axes, daggers and swords, were easily found in all the sites. Although metal tools usually appeared in domestic contexts, only in a few sites there was evidence of metalwork, such as in the pile-dwelling area (in particular in Peschiera). Metal hoards and votive deposits were still present but characterized by broken objects. Wooden artefacts were popular, while bone or horn objects became less frequent and were used only for luxury objects. Lithic tools were rare too. Pottery was still the most important indicator of the different cultures: in the pile-dwelling area vessels were similar to the Polada types -where ovoid drinking pots, cups and bowls, bi-conical vases and big ovoid jars were frequent- showing certain continuity. In the Terramare area carinated cups, bi-conical vases, ollas, big jars were very common and their main peculiarity was the style of handles: raised and cylindrical handles and cattle horns-shaped handles (Cardarelli 2009, 487). In the Castellieri sites the ceramic was a hand-made production that differed from the near one of the Po river plain except for some few elements like a grooving decorations on the bottom of the pots. The main shapes were globular and truncated conical bowls, globular cups, ovoid jars and situla-shaped vessels (Bietti Sestieri 1996, 208).

Recent Bronze Age (1350-1200 B.C.)

The Recent Bronze Age (RB) in north-east Italy was a period of cultural continuity from the MB, where the same cultural and geographical differentiations were recognizable: the "Palafitticolo-Terramaricola" culture and the Castellieri region.
Archaeological indicators of the MB were metalwork and pottery that during the RB gradually changed and differentiated from the previous ones. The beginning of the RB was a lively period where the craftwork acquired great specialization with the introduction of innovative technologies and the production of standardized objects together with luxury goods. The craftwork was no longer domestic: metalwork was of great importance and this was fully testified by the remnants found in domestic contexts, metalwork hoards and weapons votive deposits found in the rivers that were visible as part of a water-associated cult that became increasingly important during the RB. Lithic tools were rare (Marzatico 2000).
Short and long distance exchanges are testified by exotic ceramic as sub-Apennine vessels (Bianchin Citton 1989, Damiani 1997, Pacciarelli 1997) and Aegean pottery imported from Greece and from the southern Italy as well as produced locally (Bettelli, Vagnetti 1997, Cupitò, Leonardi c.s., Jones, Vagnetti et al. 2002). Contacts were proved also by the so-called *metallurgical koiné* that affected all the Europe and the common funerary practice of cremation burials arose in all the north-east of Italy (Carancini, Peroni 1997).
In contrast with the first phase of the RB -characterized by great innovation and wealth, during which villages became large- toward the end of the period there was a strong demographic reduction and a consequent general trend of abandoning most of the sites. This process highlighted the presence of a significant organization of the territory and a political stable tribal organization lead by the military power in the first RB (Cardarelli 1997, Cupitò, Leonardi 2005) and, by contrary, of an unstable situation that brought to the system collapse in the second half of RB, at the transition between the RB and Final Bronze Age (FB) (Bernabò Brea, Cardarelli et al. 1997, Cardarelli 2009). Only the north-eastern Castellieri culture did not seem to be affected by this crisis.

Final Bronze Age (1200-1000 B.C.)

During the Final Bronze Age (FB) Italy (both the peninsula and the islands) was characterized by the Proto-Villanovan culture. The Proto-Villanovan was a homogeneous culture characterized by the same pottery style—with similar decorations and shapes, same metalwork and same funerary practice of cremation. This shows a general change towards a new life style including settlement strategy, production technology, economy of sustenance and of food procurement (Bagolan, Leonardi 2000, Leonardi 1979, Harari, Pearce 2000). However, the FB was still a lively period for craftwork with increasing technological specializations. Pottery was a hand-made production whose main characteristics were bi-conical vessels (mostly crematory urns) and carinated or ovoid pots -commonly decorated with geometric patterns and occasionally with bird elements- with grooves and incisions, made by impressing a cord on the clay surface or with combed

decoration (a special form of incision with a multiple-pronged tool) (Bietti Sestieri 1996, Peroni 2004).

The metalwork, that during the previous period saw a homogeneous phase called *metallurgic koiné,* was then characterized by regional differentiations (Pellegrini 1989). The habit of laying metalwork, both broken or not, in hoards was still widely practiced. Bone and horn continued to be used exclusively for luxury objects, together with ivory -occurring here for the first time- and glass beads. The use of such sophisticated goods implied specialist productions and workshops concentrated in few centres. Frattesina (Rovigo) was one of the most important, showing evidence of metalwork, glass processing, bone and horn manufacturing. Ivory, ostrich eggs and amber were also found and they are indicators of far away contacts. Other important production centres in the Veneto region were Fondo Paviani, Montagnana and Mariconda.

The funerary practice was the cremation burial where people were apparently grouped following their social rules, rather than on parental connections, with high differentiation in grave goods (AA VV. 2010).

The Proto-Villanovan culture did not arrive to the border upland regions of north-eastern Italy. Rather, it was the Luco/Laugen–Meluno/Melaun culture that spread in the Italian South Tyrol and Trentino, Austrian East Tyrol, Liechtenstein and Swiss Grisons (Lanzinger, Marzatico et al. 2000, Leonardi 2010, Metzer, Gleirscher 1992). Its main archaeological indicators were a coarse tempered rostrate globular cup and a double-conic or truncated conic jar with a spout and bands of decorations made by parallel oblique incisions, an effect that simulated a cord impressed on the clay. Metalwork was similar to the products of the coeval Proto-Villanovan culture. (Maggetti, Marro et al. 1979, Marzatico 2000, Metzer, Gleirscher 1992, Perini 1976).

In the Friuli Venetia Giulia region the S. Canziano and Leme culture blossomed. Although the pottery and metalwork productions were highly similar to the Proto Villanovan ones, it differed in the mortuary practice, as here they practised the burial of individuals together (Peroni 2004).

First Iron Age (1000-500 A.D.)

After the FB -when in the entire Italian peninsula the Proto-Villanovan with its secondary regional differentiations developed- with the first Iron Age (FI), these regionalisms evolved into independent archaeological cultures:

1. In the Veneto and eastern Lombardy spread the so-called “cultura Veneta” (Venetian culture) (Capuis 1993).
2. In the central-eastern Emilia and in the Romagna regions, around the centres of Bologna and Verrucchio, spread the Villanovan culture (Capuis 1993).
3. In the central alpine regions spread the second phase of the Luco/Laugen-Meluno/Melaun culture and the Bludenz culture (Metzer, Gleirscher 1992, Lanzinger, Marzatico et al. 2000).

4. The uplands of Friuli Venetia Giulia were a strategic place of passage for linking the northern Italy with the south-eastern continental Europe. Here a complex and fragmented archaeological reality arose, characterized by the multiple influences from several contacts with the neighbouring cultures (AA. VV. 1996).

In Veneto, after a first moment of continuity of occupation of the FB sites, a settlement system crises lead to a new territory organization. The sites that survived from the earlier period became of secondary importance while a few new ones were founded, bigger, with greater authority and considered proto-urban. Este, settled on the river Adige, and Padova, settled on the Brenta and closed to the Bacchiglione river, were the most important of them (Capuis 1993, Capuis 1999).

In the southern region, the Villanovan-Bolognese culture widely differed from the earlier period. Almost all the ancient sites were abandoned for long time, followed by the sudden appearance of new proto-urban ones, the most important of which were Verrucchio and Bologna (Capuis 1993).

Whereas the Valli Grandi Veronesi, the area of the lower Venetian plain (north-eastern Italy), was completely abandoned and a new territory organization appeared in the north east of the Veneto region. In fact new settlements, which would later achieve great importance during the Iron Age, were founded: Castion d'Erbé, Castellazzo della Garolda and Gazzo on the rivers system of Mincio, Tartaro and Tione; and the settlement of Montebelluna, Mel, Oderzo, Concordia Sagittaria and San Zeno, linked to the Brenta, Piave and Livenza-Tagliamento river systems.

The Friuli Venetia Giulia region showed influences on the neighbouring italic traditions (Este and the southern and central Italy societies) but also influences of the trans-alpine hallstattian and of south-eastern European populations (AA. VV. 1996).

Despite such a varied situation, the existence of models shared by all these different realities and mutual influences, as demonstrated by the metalwork, was evident. The Bolognese-Villanovan style, the so-called Certosa pins, and the situla production were well known and adopted in all the north-eastern Italy. Also pottery manufacturing had some common elements: combed decoration, particular to the Bolognese-Villanovan culture, and the red and black horizontal bands decoration, typical of Este, could be found almost everywhere. A great technological innovation was represented by the introduction of the wheel-forming technique, indicating the emergence of highly specialist potters aiming towards an increasing standardization of products (Peroni 2004).

The mortuary practice was still commonly represented by cremation burials with the use of double-conic or situla shaped urns.

Even from this short introduction, it becomes evident the vitality of the north-eastern Italian protohistory: a period characterized by social relations and tight networking, attesting to long-lasting contacts and trades between cultures and people. This research project developed from this complicate but doubtless exiting contest, tries to investigate and answer a variety of anthropological questions regarding technological skills and

social organization of production and distribution, trade routes and exchange patterns, as well as cultural contacts, exchange relationships, and cultural changes over time.

Third chapter

THE POTTERY ASSEMBLAGE FROM CASTEL DE PEDENA

3.1 Castel de Pedena, historical context

Castel de Pedena (S. Gregorio nelle Alpi, Belluno, Italy) was a fortified mountain village dated between the Early Bronze Age and the beginning of the Iron Age. This is the only site known in the Belluno area with a so longue life-time, though it is unlikely that it had been continuous. It was settled in the Venetian Prealps at 680 m above the sea level, in a strategic position important for the control of the Alps passage toward the Trentino and the South Tyrol. Moreover, it was placed on the confluence of the Cordevole stream and the Piave river, with a wide view on the valley (the Vallone Bellunese) and naturally defended (Leonardi 2010, Leonardi 2012). Many ceramic remnants, together with fewer metal objects, were found during the archaeological excavations, directed by Prof. G. Leonardi (University of Padova), allowing to date precisely the site thanks to the good knowledge of the protohistorical settlements, metalwork and pottery production in the north of Italy.

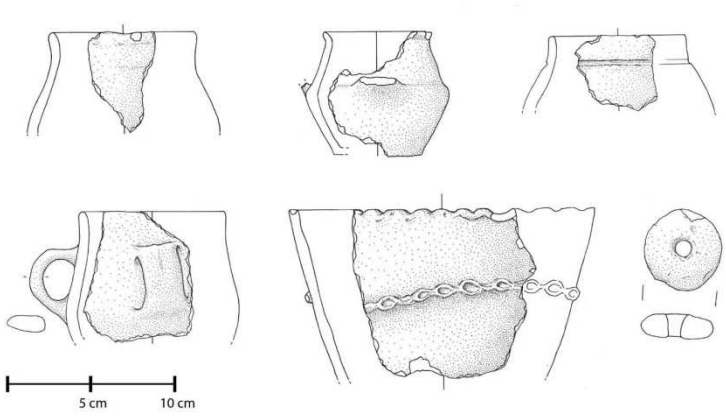

Figure 3. 1. Vessels shapes typical of the Polada culture (Early Bronze Age). After Dalla Longa 2012.

The found of pottery peculiar of the Polada culture (figure 3.1) allowed to date the more ancient phase of the site at the Early Bronze Age (2300-1700 b.C.). It consisted of coarse paste hand-made vessels: ovoid or bi-conical drinking pots and bowls, in few cases with *elbow* handle or plastic decorations, that find comparisons with vases coming from the more

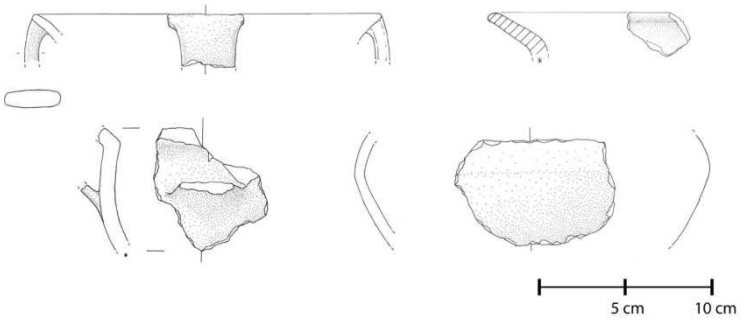

Figure 3. 2. Vessel shapes typical of the eastern Wiselburg-Gàta culture. After Dalla Longa 2012.

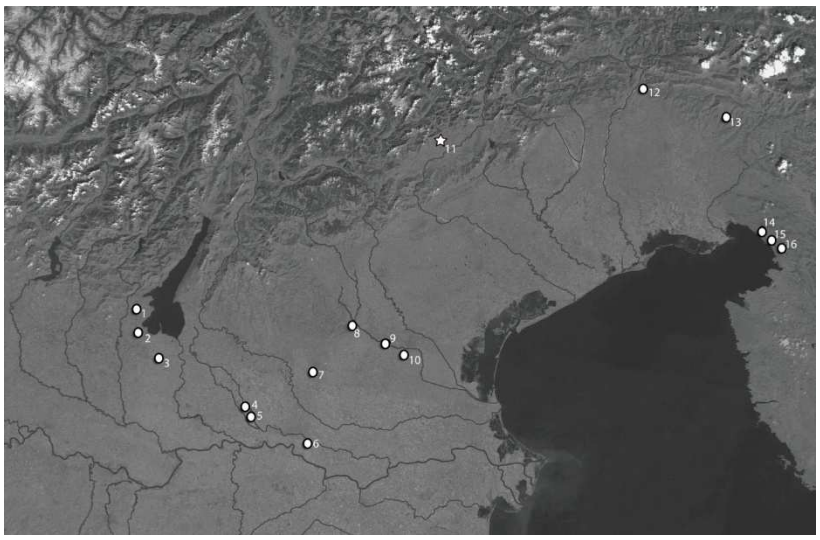

Figure 3. 3. Distribution of Wieselburg-Gàta ceramic in Italian settlements. Nr. 11: Castel de Pedena (BL). After Leonardi 2012.

important lake-dwelling sites of the northern Italian plain (Lavagnone (BS), Ledro (TN), Bande di Cavriana (MN)) (Dalla Longa 2012).

More surprising was the discover of vessel shapes typical of the eastern Wiselburg-Gàta culture (figure 3.2), that spread during the late Early Bronze age in the eastern Austria, in the south-western Slovacchia and western Hungary (Neugerbauer 1994). Wieselburg-Gàta pottery types are also known in the coeval sites of the Friuli Venetia Giulia region and of the eastern Venetian plain, in the Adriatic area, where the pile dwelling of Canàr (S.Pietro Polesine, Rovigo) is the main example (figure 3.3). Castel de Pedena can be considered out of this region, being the northern site and the only one in the Alpine area with pottery with elements peculiar of the Danubian and Carpatian regions (Bellintani 1987, Bellintani 1998, Leonardi 2012). These are good quality bi-conical amphoras with a truncated conical neck, one or two inflection points on the wall and elbow handles, with black burnished surfaces. Being these "exotic" vases usually amphoras, it seems likely that they were used for some specific products circulation, therefore, they should be imported objects (Dalla Longa 2012, Leonardi 2012). The occupation of the site during the late Middle Bronze Age-Recent Bronze Age was testified by the presence of typical cups, bowls, bi-conical ollas and one specimens of a raised handle. At RB were assigned some big bowls, one with the grooved rim and one with a raised cylindrical handle (figure 3.4).

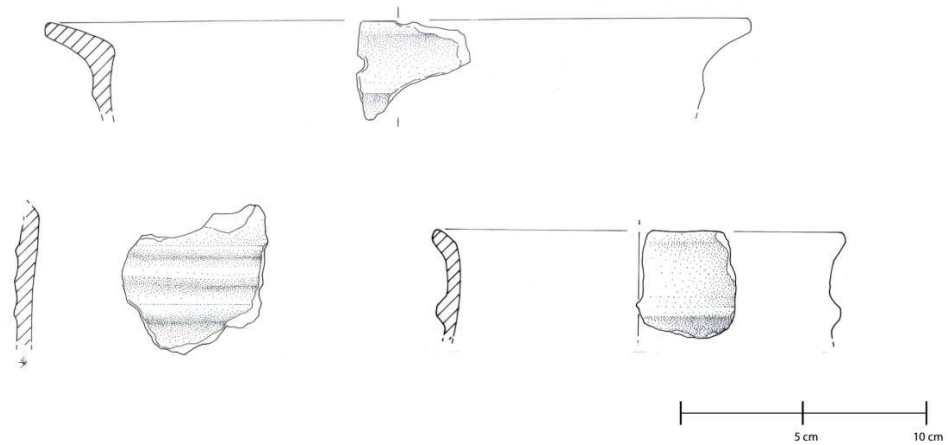

Figure 3. 4. Vassel shapes typical of the Recent Bronze Age. Modified from Donadel 2012.

These vessels found well comparison with the coeval pottery of the Padan plain, especially coming from the sites of Custoza, Fabrica dei Soci, Fondo Paviani and Mariconda di Melara (Dalla Longa 2012).

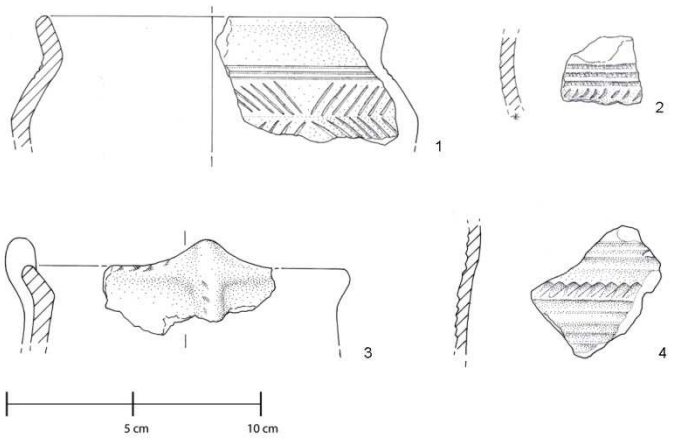

Figure 3. 6. Vessels shapes of Luco A type (3-4) and Luco B (1-2). Modified from Donadel 2012.

During the Final Bronze Age this situation changed and the pottery assemblage from Castel de Pedena seems to be related with the Luco/Laugen–Meluno/Melaun culture that spread in the Italian South Tyrol and Trentino, the Austrian East Tyrol, in Liechtenstein and the Swiss Grisons (Leonardi 2010, Lanzinger, Marzatico et al. 2000, Metzer, Gleirscher 1992). Potsherds were found that are related to the peculiar Luco ceramic, both "Luco A" and "Luco B" (figure 3.5): coarse tempered rostrate globular cups and double-conic or truncated conic jars with a spout and decorated with bands made of parallel oblique incisions, effect that simulates a cord impressed on the clay (Lanzinger, Marzatico et al. 2000, Perini 1976). They find good similarity with specimens coming from Appiano/Eppan S. Paul, Groa di Sopramonte, Montesei di Serso, Seeberg/Lago Nero and Monte Ozol all attributed to Luco A, and from Montesei di Serso related at Luco B (Donadel 2012). There were also present some other more common vessel types that find good comparison in the Alpine sites (figure 3.6) (Donadel 2012). The nearly totally absence of vase type peculiar of the Veneto region and the high concentration of pots typical of the Alpine regions may induce to consider Castel de Pedena linked to the Luco/Laugen–Meluno/Melaun culture, and not just a neighbouring

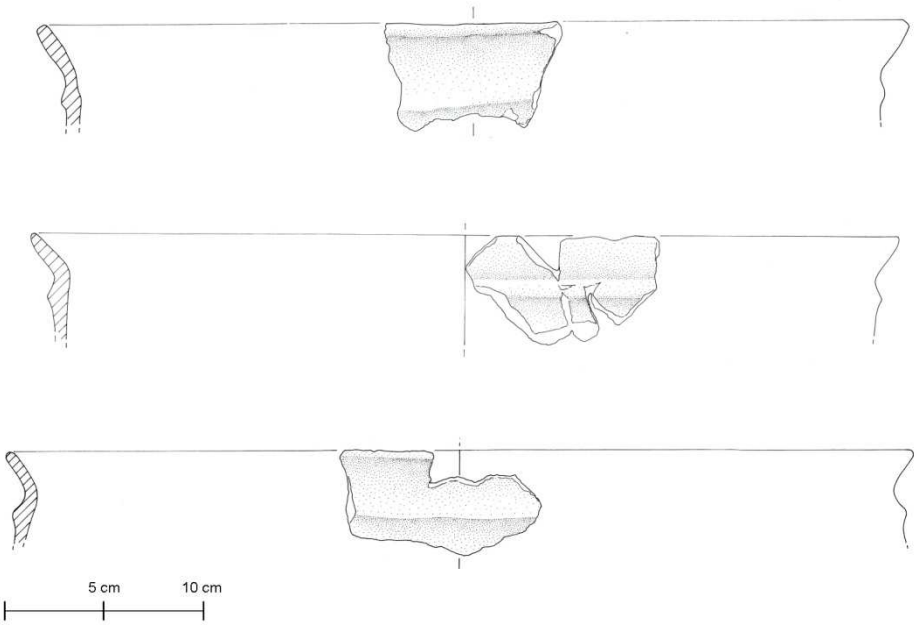

Figure 3. 5. Fragments of recurved rim jars (first Iron Age). After Donadel 2012.

site. In that way it should be the more eastern Luco/Laugen–Meluno/Melaun site known (Donadel 2012, Leonardi 2012).
This is a very short summary, though, enough to see the importance of this site and to comprehend the interest that it generates in archaeologists and scientists for its possible leading role, suggested by the strategic position, and for the several external contacts testified by the presence among the pottery assemblage of exotic types (Wieselburg-Gàta and Luco/Laugen–Meluno/Melaun). These vessels could had been manufactured locally (produced by locals, thanks to the circulation of different ceramic models) or even imported from the major regions pertaining to these cultures (due to the people circulation). In any way, they attest long-lasting contacts and trades among cultures and people.

3.2 Selection of samples and macroscopic description

Initially the potshards from the excavation campaigns held in 2006-2008 at the site of Castel de Pedena were considered. It is only afterwards that these potshards were integrated with other few significant samples from the next field campaigns. The Department of Cultural Heritage at the University of Padova is currently managing the dig at the site and the whole pottery collection is stored in the university deposits.
Because of the enormous number of potshards and the highly fragmented condition of them, only those samples representing a range of areas of the vessels (rim, appendages like supports, handles, spouts,..) and that provide additional information useful in the archaeological interpretation (type, decorative style, shape classes, chronological and regional variations, ...) were considered, from a total of four-hundred fragments.
All these fragments were analyzed with a hand lens with regard to the main features of a pottery: matrix and inclusions. This was carried out with the aim to firstly distinguish the different fabrics in the site and subsequently to select a set of samples for further archaeometrical analysis which were as representative as possible of the variation in the entire collection. In order to avoid bias, this first categorization was conducted without considering any archaeological information and only further all the data were joined together.
In this way five paste types were initially distinguished considering attributes like constituents, hardness and texture (figure 3.7):

- Paste A: hard ceramics with few pores, characterized by coarse inclusions that can even reach pebbles sizes, low in quantity (3-5%), with a polymodal grain-size distribution. Usually these potsherds have light colour, mostly with beige, reddish or brown hues, sometimes they present the typical sandwich structure, but there are also few examples with dark grey pastes. These represent 29% of the samples.
- Paste B: hard compact ceramics with few small inclusions (1-2%), usually with sub-millimetric sizes and angular or sub-angular shapes. They are generally of light colours, mostly light grey and reddish often with a grey internal core. These shards are 4-7 mm thick. They represent the 22% of the samples.

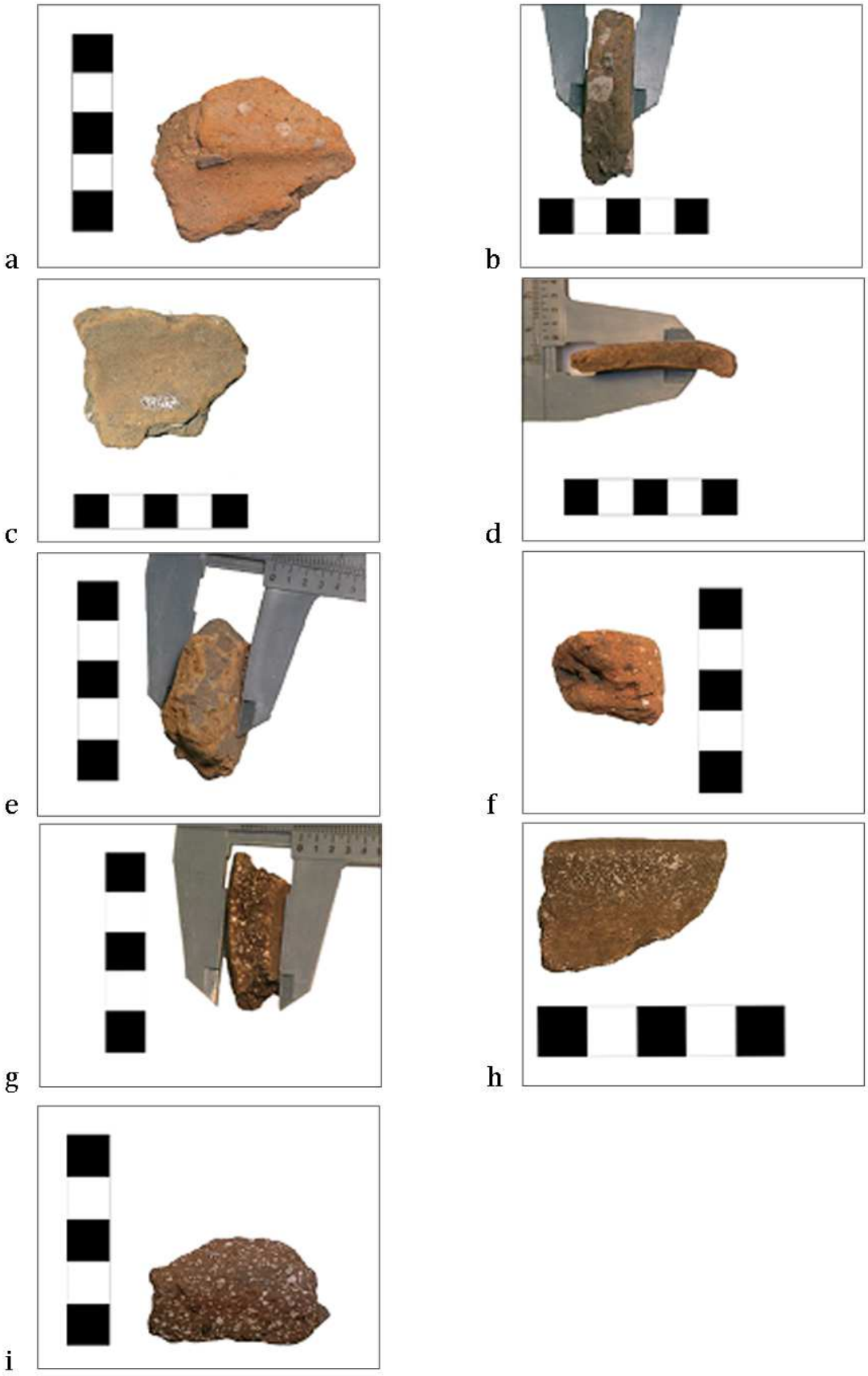

Figure 3. 7. Paste typologies identified by hand examination. a-b) Paste A; c-d) Paste B; e-f) Paste C; g-h) Paste D; i) paste E.

Samples	Form	Chronology
M001	Jar (Wieselburg-Gàta)	EB
M002	Cup with recurved rim	MB-RB
M003	Bowl/jar with flattened lip	MB-RB
M004	Carinated wall	RB
M005	Truncated conic bowl with incised rim	RB1
M006	Jar	BR2 ?
M007	Bowl with wide carved surface	FB1
M008	Jar with flattened lip	FB1
M009	Jar with recurved rim	FB1
M012	cup (Luco A?) with flattened lip	FB
M013	Jar with recurved rim	FB-IX/VIII sec.
M014	Jar with recurved rim	BZ F
M015	Cup (Luco B)	FB
M016	Carinated cup with symmetric helicoidal decoration	FB
M017	Jar with slightly recurved rim and plastic additions on the surface	IX sec.
M018	Jar with recurved rim and plastic additions on the surface	IX sec.
M019	Jar with recurved rim and plastic additions on the surface	IX sec.
M020	Jar with slightly recurved rim and plastic additions on the surface	IX sec.
M021	Jar with flattened lip	RB-FB
M022	Jar with plastic additions on the surface	RB1
M023	Indeterminate, surface with plastic addition on the surface	RB1
M024	Jar with flattened lip	RB-FB
M025	Jar with flattened rim	RB-FB
M026	Jar with flattened rim	RB-FB
M027	Indeterminate, surface with plastic addition on the surface	RB1
M028	Jar with flattened lip	RB-FB
M029	Jar with plastic additions on the surface	RB1
M030	Indeterminate, base	-
M031	Cup (Luco B)	FB
M032	Indeterminate, rim	RB1 ?
M033	Cup (Luco)	FB
M034	Truncated conic bowl	RB1
M035	Jar with recurved rim	FB-IX/VIII sec.
M036	Jar with recurved rim	FB-IX/VIII sec.
M037	Jar with recurved rim	FB-IX/VIII sec.
M038	Carinated pot	RB1
M039	Indeterminate, lip thickened to exterior	RB1
M040	Jar with recurved rim	FB-IX/VIII sec.
M041	Jar with recurved rim	FB-IX/VIII sec.
M042	Jar with recurved rim	FB-IX/VIII sec.
M043	Jar with recurved rim	FB-IX/VIII sec.
M044	Indeterminate, surface with plastic addition on the surface	RB1
M045	Indeterminate, surface with plastic addition on the surface	RB1
M046	Cup (Luco)	FB
M051	Bowl with recurved rim	RB1
M056	Indeterminate, base	-
M068	Jar with recurved rim	FB-IX/VIII sec.
M069	Jar with recurved rim and plastic additions on the surface	IX sec.
M071	Jar with recurved rim and plastic additions on the surface	FB-IX/VIII sec.
M075	Jar with shirt flattened lip, thickened to exterior	RB2
M079	Indeterminate	FB ?
M080	Indeterminate, base	FB-IX/VIII sec.
M081	Double-conic bowl	FB-IX/VIII sec.
M083	Indeterminate, base	-
M086	Indeterminate, base	-
M088	Indeterminate, base	-
M090	Carenated pot	FB
M092	Indeterminate, surface with plastic addition under the inflection point	IX sec.
M094	Indeterminate, surface with plastic addition	IX sec.
M097	Jar with recurved rim	FB
M098	Double-conic jar ?	FB
M101	Cup	IX sec.
M102	Indeterminate, surface with plastic addition	IX sec.
M103	Indeterminate, base	-

Table 3. 1. Details of the shards from Castel de Pedena analyzed in this study.

- Paste C: soft ceramics characterized by an apparently very light weight. The shards have a rounded shape and very light colours with reddish and orange hues, sometimes they have the peculiar sandwich structure. Inclusions are rare and very small with sub-millimetric sizes, however sometimes they can also reach 3 mm. These represent the 3% of the samples.
- Paste D: ceramics apparently characterized by a high number of voids. Inclusions are common (5-15% of the surface) and have average sizes of 1 mm. They are often on the brown or grey tones. They represent the 12% of the samples.
- Paste E: ceramics characterized by a high number of voids. Inclusions are abundant (> 15% of the surface) and measure on average 1 mm. Generally the potshards are 7-10 mm thick. They represent the 34% of the samples.

A bunch of specimens characteristic of these ceramic pastes was chosen for the archaeometric study (table 3.1). Moreover, some vessels found in the sites had an "exotic" fabric, with respect to the typical pottery assemblage of Castel de Pedena and they were archeologically attribute to the Wieselburg Gata and Luco/Laugen-Meluno/Melaun ceramics. As one of the main focus of this work was to investigate the production technology of the pottery assemblage from Castel de Pedena and their provenance, also these "exotic" potshards were analysed. All the selected samples (Table 3.1) had undergone a very detailed hand-examination to the unaided eye, following the methodology illustrated by P. Stienstra (1986) (see chapter 1.1). The pastes were described using the non-plastic inclusions (concentration, shape and size which were evaluated through comparison with visual estimation charts) and the matrix, and the results are reported in table 3.2.

The analysis of the chromatic variations evaluated by comparison with the Munsell's Soil Colour Charts (Munsell 2000) distinguished different situations (figure 3.8). The majority

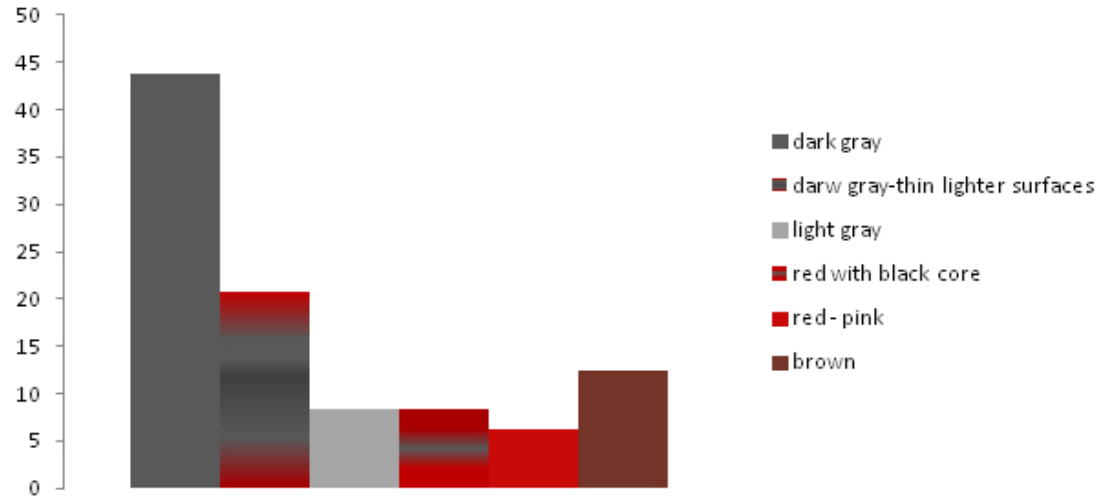

Figure 3. 8. Colour of the pastes of the studied potshards.

of the samples have an homogeneous grey or very dark grey body, sometimes with a lighter (pink or red) and an extremely thin external layer, probably too thin to be considered as a sandwich structure. Only few of them have homogeneous light bodies, grey and brown or reddish coloured, while only four samples present a sandwich structure (a dark "core" with lighter reddish surfaces) or colour differentiations along the external, usually reddish, and the internal, grey-dark grey, surfaces.

Samples	Paste typology	Thickness	External layers/sourfaces: colours		Matrix: colours		Inclusions				
			Colour	Munsell	Colour	Munsell	Amount	Sizes		Shapes	
								d_{max}	d_{media}	A	SA	R
M01	B	7	E: very dark gray I: dark reddish gray	E: 5YR 3/1 I: 5YR 4/2	black	5YR 2.5/1	rare	<<1	<<1			
M02	B	5	E: dark grayish brown I: brown	E: 10YR 4/2 I: 7.5YR 5/4	very dark gray	10YR 3/1	rare	3	<1		*	
M03	B	10	E: pale brown I: dark gray	E: 10YR 6/3 I: 10YR 4/1	gray	10YR 5/1	rare	4	<1			*
M04	A	11	E: light brownish gray - brown I: grayish brown	E: 10YR 6/2 - 10YR 5/3 I: 10YR 5/2	brown	10YR 5/3	rare	8	<1		*	*
M05	A	9	E: dark gray I: brown	E: 7.5YR 4/1 I: 7.5YR 5/3	dark gray	10YR 4/1	rare	4	<1		*	*
M06	E	7	E: yellowish red I: yellowish red – brown	E: 5YR 5/6 I: 5YR 5/6 – 7.5YR 4/2	light brown	7.5YR 6/4	abundant	2	1		*	
M07	E	8	E: very dark grayish brown – I: dark grayish brown	E: 10YR 3/2 - 10YR 4/2 I: 10YR 4/2	very dark gray	10YR 3/1	abundant	2	1			*
M08	E	7	E: dark gray I: grayish brown	E: 10YR 4/1 I: 10YR 5/2	dark gray	10YR 4/1	common	2	1			*
M09	E	8	E: pale brown I: brown – dark brown	E: 10YR 6/3 I: 10YR 5/3 - 10YR 4/1	Brown	10YR 5/3	abundant	1	<1		*	*
M12	D	8	E: brown I: brown	E: 7.5YR 5/4 I: 7.5YR 5/4	brown - very dark gray	7.5YR 5/4 - 7.5YR	common	2	<1			*
M13	E	9	E: brown I: brown	E: 7.5YR 5/2 I: 7.5YR 5/2	dark gray	10YR 4/1	abundant	5				*
M14	D	7	E: brown I: brown	E: 10YR 5/2 I: 10YR 5/2	dark gray	10YR 4/1	abundant	<1	<1			*
M15	B	6	E: brown – dark gray I: brown – dark gray	E: 7.5YR 5/4 - 7.5YR I: 7.5YR 5/4 - 7.5YR 4/1	dark gray	10YR 4/1	rare	<1	<1			*
M16	D	6	E: brown I: dark brown	E: 7.5YR 4/3 I: 10YR 4/1	dark gray	10YR 4/1	abundant	6	<1			*
M17	E	8	E: red I: light yellowish brown	E: 2.5YR 5/6 I: 10YR 6/4	dark grayish brown	10YR 4/2	common	2	1			*

Table 3. 2. Macroscopic description of the analyzed samples with indication of the paste typology described in chapter 3.2, thickness of the potsherds, colour determined using the Munsell colour charts, relative abundance of the inclusions, maximum and average dimensions and shape (A: angular, SA: subangular, R: rounded).

Samples	Paste typology	Thicknes	External layers/sourfaces: colours		Matrix: colours		Inclusions					
			Colour	Munsell	Colour	Munsell	Amount	Sizes	Shapes			
								Æmax	Æmedia	A	SA	R
M19	D	8	E: brown I: brown	E: 7.5YR 5/3 I: 7.5YR 5/2	dark grayish brown	10YR 4/2	abundant	1	1		*	*
M18	E	7	E: yellowish red I: yellowish red	E: 5YR 5/6 I: 5YR 5/6	dark grayish brown	10YR 4/2	rare	1,5	1		*	
M20	E	7	E: reddish brown I: reddish brown	E: 5YR 5/4 I: 5YR 4/3	dark gray	7.5YR 4/1	abundant	2	2		*	
M22	A	10	E: reddish yellow I: brown	E: 7.5YR 6/6 I: 7.5YR 5/4	dark gray	10YR 4/1	rare	6	<1		*	
M23	A	13	E: brown I: brown	E: 7.5YR 5/4 I: 7.5YR 5/2	dark gray	10YR 4/1	common	8	<1		*	*
M27	A	8	E: dark gray I: dark gray - brown	E: 7.5YR 4/1 I: 7.5YR 4/1 - 7.5YR 4/2	dark gray	7.5YR 4/1	rare	6	<1		*	*
M20	E	7	E: reddish brown I: reddish brown	E: 5YR 5/4 I: 5YR 4/3	dark gray	7.5YR 4/1	abundant	2	2		*	
M22	A	10	E: reddish yellow I: brown	E: 7.5YR 6/6 I: 7.5YR 5/4	dark gray	10YR 4/1	rare	6	<1		*	
M23	A	13	E: brown I: brown	E: 7.5YR 5/4 I: 7.5YR 5/2	dark gray	10YR 4/1	common	8	<1		*	*
M27	A	8	E: dark gray I: dark gray - brown	E: 7.5YR 4/1 I: 7.5YR 4/1 - 7.5YR 4/2	dark gray	7.5YR 4/1	rare	6	<1		*	*
M29	A	12	E: reddish yellow I: dark gray	E: 5YR 6/6 I: 10YR 4/1	dark gray	10YR 4/1	rare	5	<1		*	
M30	B	6	E: brown I: light brown	E: 7.5YR 5/4 I: 7.5YR 6/4	dark gray	7.5YR 4/1	rare	<1	<1			
M32	B	8	A: brown B: brown	A: 7.5YR 5/4 B: 7.5YR 5/4	very dark gray	7.5YR 3/1	Rare	5	1		*	
M34	B	9	E: light yellowish brown I: dark grayish brown	E: 10YR 6/4 I: 10YR 4/2	dark gray	10YR 4/1	rare	2	<1		*	
M38	B	7	E: reddish yellow I: reddish yellow	E: 7.5YR 6/6 I: 7.5YR 7/6	reddish yellow	7.5YR 6/6	rare	4	<1			*

Table 3. 2. Macroscopic description of the analyzed samples.

Samples	Paste typology	Thicknes	External layers/sourfaces: colours		Matrix: colours		Inclusions					
			Colour	Munsell	Colour	Munsell	Amount	Sizes	Shapes			
								Æmax	Æmedia	A	SA	R
M39	A	12	E: dark grayish brown I: dark grayish brown	E: 10YR 4/2 I: 10YR 4/2	dark grayish brown	10YR 4/2	rare	4	<1		*	
M44	A	10	E: strong brown I: dark brown	E: 7.5YR 5/6 I: 10YR 4/1	dark gray	10YR 4/1	rare	3	<1		*	
M45	A	10	E: brown I: brown	E: 7.5YR 5/4 I: 7.5YR 5/4	dark gray	7.5YR 4/1	rare	4	<1		*	
M51	C	10	E: reddish yellow I: reddish yellow	A: 5YR 6/8 B: 5YR 6/6	yellowish red - gray	5YR 5/8 – 2.5Y 5/1	common	4	<1		*	
M56	C	9	E: reddish yellow	E: 5YR 6/8	reddish yellow – yellowish red	5YR 6/8 - 5YR 5/8	rare	3	<1		*	*
M68	B	9	E: light brown I: dark gray	E: 7.5YR 6/4 I: 10YR 4/1	dark grayish brown	10YR 4/2	rare	2	1,5			*
M69	E	8	E: light brown I: light brown	E: 7.5YR 6/4 I: 7.5YR 6/4	brown	10YR 5/3	rare	2	1,5			*
M71	D	7	E: reddish yellow I: yellowish red	E: 5YR 6/6 I: 5YR 5/6	dark grayish brown	10YR 4/2	rare	3	<1			*
M75	D	9	E: light yellowish brown I: grayish brown	E: 10YR 6/4 I: 10YR 5/2	grayish brown	10YR 5/2	abundant	2	<1			*
M79	D	5	E: gray I: gray	E: 2.5y 5/1 I: 2.5y 5/1	gray	2.5y 5/1	common	1	<1		*	*
M80	D	7	E: brown I: very dark gray	E: 7.5YR 5/3 I: 7.5YR 3/1	very dark gray	7.5YR 3/1	abundant	2,5	<1			*
M81	D	7	E: light brown I: dark gray	E: 7.5YR 6/3 I: 10YR 4/1	dark gray	10YR 4/1	common	<1	<1			*
M83	E	13	E: brown I: brown	E: 7.5YR 5/4 I: 7.5YR 5/4	gray	7.5YR 5/1	abundant	5	<1			*
M86	E	8	E: dark gray I: light brown – dark reddish	E: GLEY1 4/N I: 7.5YR 6/4 – 2.5YR 4/1	dark gray	GLEY1 4/N	common	1			*	
M88	E	7	E: dark reddish gray I: dark reddish gray	E: 2.5Y 4/1 I: 2.5Y 4/1	dark gray	2.5Y 4/1	common	2				*
M90	E	8	E: reddish yellow I: reddish yellow	E: 7.5YR 6/6 I: 7.5YR 6/6	brown	10YR 5/3	abundant	1	1		*	

Table 3. 2. Macroscopic description of the analyzed samples.

Samples	Paste typology	Thicknes	External layers/sourfaces: colours		Matrix: colours		Inclusions					
			Colour	Munsell	Colour	Munsell	Amount	Sizes	Shapes			
								Æmax	Æmedia	A	SA	R
M92	E	7	E: reddish yellow I: reddish yellow	E: 5YR 6/6 I: 5YR 4/3	dark grayish brown	10YR 4/2	abundant	2	1,5			*
M94	E	8	E: yellowish red – brown I: brown	E: 5YR 5/6 – 10YR 5/3 I: 7.5YR 5/3	dark gray	7.5YR 4/1	common	2,5	1			*
M97	E	5	E: brown I: brown	E: 10YR 5/3 I: 10YR 5/3	grayish brown	10YR 5/2	rare	<1	<1			*
M98	E	7	E: brown I: brown	E: 7.5YR 5/4 I: 7.5YR 5/4	dark gray	10YR 4/1	abundant	3	<1			*
M101	E	7	E: brown I: reddish brown	E: 7.5YR 5/3 I: 2.5YR 4/4	grayish brown	10YR 5/2	rare	2	1,5			*
M102	E	6	E: brown I: very dark gray	E: 7.5YR 5/3 I: 7.5YR 3/1	dark gray	7.5YR 4/1	rare	2	1,5			*
M103	E	9	E: yellowish red I: reddish yellow	E: 5YR 5/6 I: 7.5YR 6/6	reddish yellow - gray	7.5YR 6/6 - 7.5YR	abundant	3	1,5		*	

Table 3. 2. Macroscopic description of the analyzed samples.

3.3 Petrographic fabric classification

The ceramic shards (sixty-four samples) were analyzed under polarizing light microscope following the description protocol illustrated in chapter 2.2, based on Whitbread terminology and descriptive procedure (1989, 1995)

The petrographic examination of the potsherds revealed a high variability due to the different mineralogical and petrographic types of inclusions, and due to the variety of fabrics. Nine petrographic groups were identified according to similarities and variation in voids, micromass and the nature, shape and arrangement of non-plastic inclusions, then further differentiated also according to their size into coarse inclusions (c) and fine inclusions (f) respectively (ref. *c:f ratio* chapter 1.2), (table 3.3, figures 3.9-3.10):

Fabric F1: carbonate inclusions rich potsherds with a bimodal grain-size distribution

The first fabric (nineteen samples) is characterized by a homogeneous active micromass with a birefringent fabric of spackeld type. Inclusions are generally abundant (on average 20%) with moderately sorted bimodal grain-size distributions (c:f ratio between 60:40 and 90:10) where the coarser fraction varies considerably in size, measuring 4,4 mm on average but reaching up to 9,0 mm. The coarser fraction is mainly composed by calcite and dolomite crystals and equant sub-rounded carbonatic fragments that are represented with a great variability of types (dolomite, carbonate mudstone, sparry calcite, ooid limestone, bioclast limestone with coral fragments and pelagic foraminifera bearing mudstone). This variability is due to the Mesozoic-Cenozoic carbonate sequences typical of this area of the Dolomite mountains with its moraine deposits. There are subordinate polycrystalline quartz, cherts and quartz crystals. The finer fraction is generally represented by a fine sand, which is composed of crystals of quartz and muscovite. Inclusions can reach large dimensions (maximum sizes of 9 mm, on average 1,8 mm). Voids occupy on average 10% of the area and consist mainly of vughs.

Fabric F2: carbonate inclusions rich potsherds with a seriate grain-size distribution

The fabric F2 (fifteen samples) is characterized by a homogeneous active micromass with a birefringent fabric of spackeld type. Inclusions are abundant (on average 25%) with a seriate grain-size distribution, in which the coarser fraction is mostly represented by sub-angular carbonatic inclusions (mainly carbonate mudstone and sparry calcite) generally smaller than the ones of the group F1 (average dimension of the coarse fraction: 1,5 mm). The finer fraction is mainly represented by quartz crystals and carbonate mudstone fragments.

Fabric F3: carbonate inclusions rich potsherds associated with metamorphic rocks fragments

This group (nine samples) is characterized by a moderately sorted bimodal grain-size distribution. It distinguishes from the other two subgroups because of a high percentage of metamorphic rocks fragments (polycrystalline quartz, gneiss, mica schists, graphite shists) that can represent up to the 50% of all the non-plastic inclusions and also because of the occasional presence of groundmass of volcanic intermediate or acid igneous rocks. Carbonate inclusions are abundant. The ground mass is inactive or slightly active.

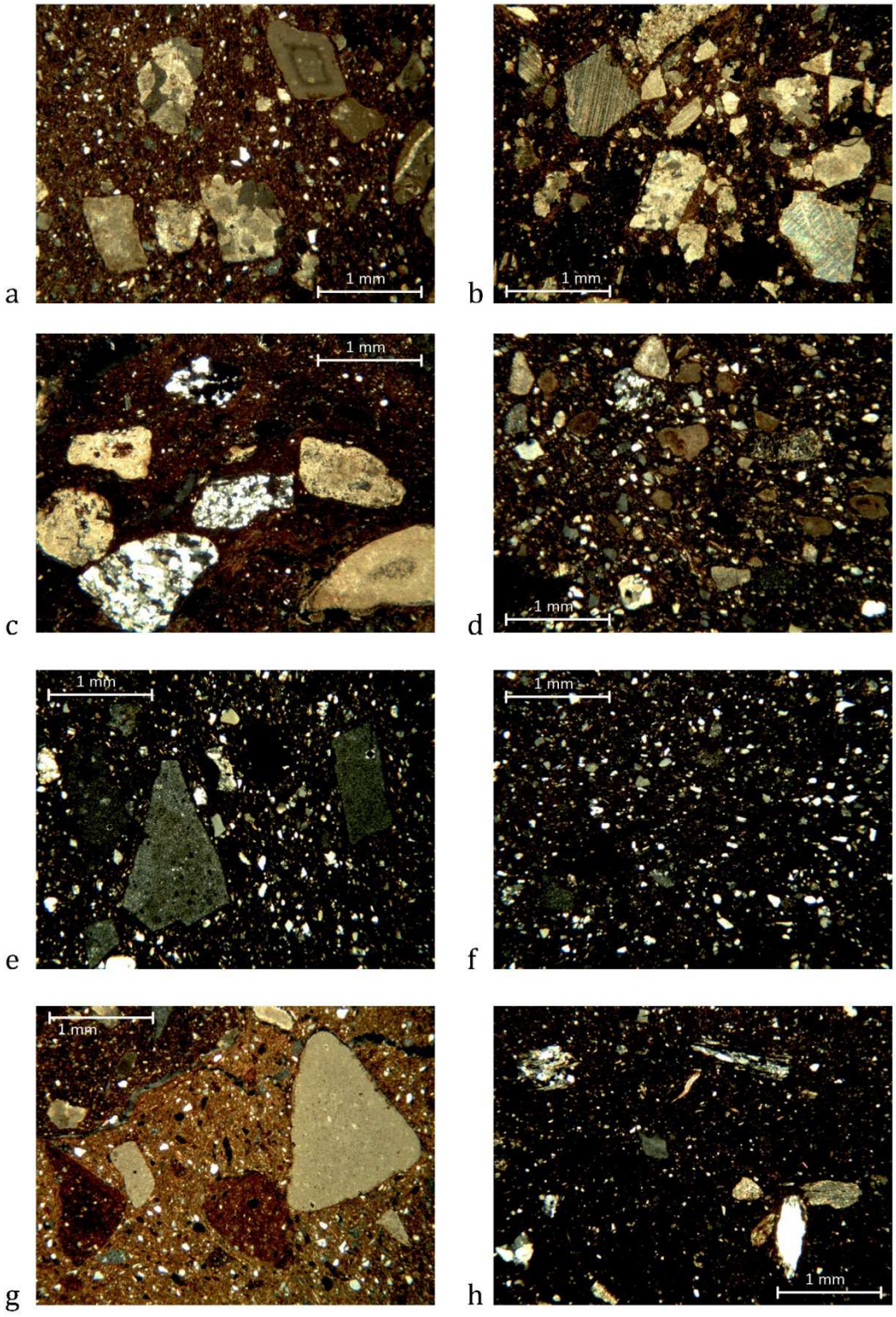

Figure 3. 9. Thin section photomicrographs of selected ceramics analysed in this study belonging to fabrics 1-8. a) Fabric F1: carbonate rich potshards, b) Fabric F2: carbonate rich potshards with a seriate grain-size distribution, c) Fabric F3: carbonate rich potshards associated with metamorphic rocks fragments, d) Fabric F4: quartz and carbonate sand rich potshards, e) Fabric F5: chert and quartz rich potshards, f) Fabric F6: quartz sand rich potshards, g) Fabric F7: grog and carbonatic inclusions rich potshard, h) Fabric F8: metamorphic rocks rich potshard. The images were all taken in crossed polars

Fabric F4: quartz and carbonate sand rich potsherds

This is a small group (two samples) characterized by a quartz and carbonate sand, with a moderately sorted bimodal grain-size distribution. The finer fraction equates with a high percentage (nearly 40-50%) of all the inclusions and has generally bigger grain sizes (maximum and average dimension: 0,4 mm and 0,2 mm) than in the other fabrics.

Fabric F5: big angular chert fragments rich potsherds associated with carbonate mudstone

The fabric F5 (twelve samples) is a homogeneous group, characterized by an optically active (birefringent fabric of spackeld type) and weakly-oriented groundmass and different amounts of pores (from 5 to 15%), mainly vughs, planar voids and channels. There are abundant inclusions (20-30%) with a good bimodal grain-size distribution (c:f ratio from 30:70 to 50:50). The coarser fraction is mainly represented by big, angular fragments of chert (coarse sand-pebbles range sizes), while quartz crystals are the main components of the finer fraction (fine silt-medium sand range sizes). Sometimes it is also possible to see a smaller quantity (always less than the 5% of all the inclusions) of metamorphic rock fragments (polycrystalline quartz, mica shist, graphite shist), carbonate mudstone, groundmass of intermediate volcanic igneous rocks and highly weathered intermediate plutonic rocks. plutonic and volcanic.

Fabric F6: quartz sand rich potsherds

This is a small group (four samples) with abundant inclusions (nearly 30%), characterized by a quartz sand, where the rock fragments are nearly absent. They are mostly rounded and sub-rounded quartz crystals with rare chert and polycrystalline quartz fragments. Inclusions have a unimodal grain-size distribution (average dimension: 0,45 mm). Only the sample M033 has a bimodal grain-size distribution, where the coarser fraction (10% of total inclusions) is represented by large grog fragments. The groundmass is generally active or slightly active with a birefringent fabric of spackeld type.

Fabric F7: grog rich potsherd

This unique sample is formed by a weakly active groundmass with a birefringent fabric of spackeld type. It is characterized by low porosity (7%), mostly represented by vughs and planar voids. The inclusions, 25% of the total area, have a seriate grain-size distribution and the majority of them are represented by large fragments of grog, associated to few carbonate mudstone.

Fabric F8: metamorphic rocks (mica schist, graphite schist, polycrystalline quartz) rich potsherd

Fabric F8, composed by a lonely sample, is characterized by dominant metamorphic rock fragments, rare chert and carbonate mudstone. The inclusions, 25% of the area, have a well bimodal grain-size distribution. The groundmass is weakly active with a speackled birefringent fabric. It is characterized by a high porosity (10%) mostly represented by vughs and planar voids.

Fabric F9: volcanic igneous rocks rich potsherd

This potsherd presents an optically active birefringent fabric and a groundmass with a great number of pores (10%), especially channels. There are abundant rounded and sub-rounded inclusions showing a bimodal grain-size distribution where the coarser fraction is subordinate (c:f ratio of inclusions 40:60). They are mainly composed of groundmass of intermediate and acidic volcanic igneous rocks, associated with few carbonate mudstone fragments.

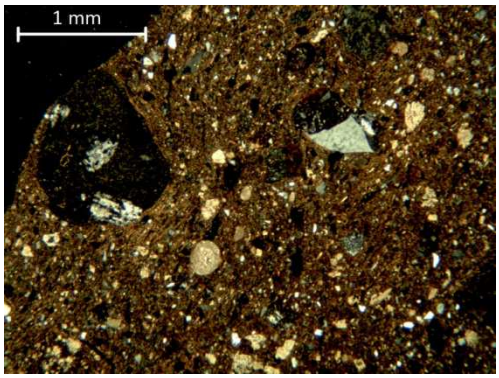

Figure 3.10. Thin section photomicrographs of sample M038 (Fabric F9): acid volcanic igneous rocks rich potshard. The image was taken in crossed polars

Table 3. 3. Minero-petrographic and micro-structural features of pottery samples analyzed under optical microscope. MATRIX: area fraction occupied by the matrix (A.%); homogeneity (Hom); optical state (Opt.Ac.) optical state; birefringent fabric (b-fab); orientation (Or). VOIDS: total area fraction occupied by the voids (A.%); maximum size (max.size); shape: channel (Ch), planar voids (Pb), vugh (Vu). INCLUSIONS: total area fraction occupied by the inclusions (A.%); orientation (Or); grain-size distribution of the inclusion: unimodal (u), bimodal (bi), seriate (S), kind of sorting of the inclusions: well sorted (ws), moderately sorted (ms),poorly sorted (ps), very poorly sorted (vps); distinct description of the course and fine fractions of the inclusions (where there are present more than one mode): relative abundance of the inclusions of the fine and coarse fractions (Rel.Ab.%); maximum size of the inclusions (max.size); average size of the inclusions (av.size); shapes: equant (eq), elongate (el), angular (A), sub-angular (SA), sub-rounded (SR), rounded (R). Composition of the mineral phases and lithics: qz: quartz crystals; Fsp: feldspars in general; KF: alkali feldspar; Pl: plagioclase; Cal-Dol: calcite and dolomite crystals, Amp: amphibole; Px: pyroxene; Ms: muscovite; Bt: biotite; Op: opaque minerals; Glt: glauconite; Grt: garnet; Qzt: polycrystalline quartz; Mcsc: mica schist; FllGr: Phyllite graphite; Vlc: volcanic rock; Plt: plutonic rock; acd: acidic rock; itmd: intermediate rock; Ch: chert; Dol: dolomite; CMt: carbonate mudstone; CSpr: sparrycalcite; OO-Pld: ooid limestone; Crl: bioclastic limestone with corals; Bio: bioclastic limestone; CP: clay pellets; Grog: grog; ARF; CalSc: secondary calcite. Abundance of mineral phases: 8: predominant (>70%); 7: dominant (50-70%); 6: frequent (30-50%); 5: common (15-30%); 4: few (5-15%); 3: very few: (2-5%); 2: rare (0,5-2%); 1: very rare (<0,5%).

Samples	MATRIX						VOIDS					INCLUSIONS:				INCLUSIONS-COARSE FRACTION								INCLUSIONS-FINE FRACTION						
	A. %	Hom.	Opt. Ac.	b-fab.	Or.	d-sp.	A. %	max. size	Shape			Or.	A. %	Dist.	kind of sor.	Rel. Ab. %	max. size	av. size	Shape					Rel. Ab. %	max. size	av. size	Shape			
								mm	Ch	Pb	Vu						mm	mm	eq/el	A	SA	SR	R		mm	mm	eq/el	SA	SR	R
FABRIC 1																														
M013	70	o	a	sp	i	cl-s	5	1,4x0,3			x	i	25	bi	ms	80	4,4	2	eq		x		x	20	0,3	0,1	eq	x	x	
M017	70	o	a	sp	o	cl-s	10	4,4x1,0			x	i	20	bi	ms	85	5,4	1,8	eq			x	x	15	0,3	0,14	eq	x	x	
M018	60	e	a	sp	o↓	cl-d	15	1,5x0,6		x	x	i	25	Bi	ms	70	5,6	2,2	eq-el		x		x	30	0,4	0,12		x	x	
M020	70	o	a	sp	o↓	cl-s	10	4x1,6		x	x	wo	20	Bi	ms	85	3,4	2	eq-el		x	x	x	15	0,2	0,06	eq-el	x	x	
M028	77	o	↓a	sp	i	cl-d	8	1,7x1	xx		x	i	15	Bi	ms	90	2,2	1	eq			x	x	10	0,4	0,14	eq	x	x	
M029	60	o	i	-	i	cl-s	10	4,3	x		x	wo	30	bi	ms	60	9	2,04	eq-el		x	x	x	40	0,4	0,14	eq	x	x	
M035	87	o	a	sp	o↓	cl-d	3	3,8	x		xx	o	10	bi	ms	70	3,6	1,8	eq			x	x	30	0,3	0,1	eq	x	x	
M037	-	o	a	sp	o↓	cl-s	-	-	-	-	-	wo	20	bi	ms	90	4	2	eq		x	x		10	0,3	0,2	eq	x	x	
M040	87	o	a	sp	o↓	cl-d	3	3,8x1	xx		xx	wo	10	bi	ms	60	4,2	1,4	eq		x	x		40	0,2	0,12	eq	x	x	
M068	60	o	a	sp	i	cl-s	10	3,1x1,2			x	o	30	Bi	ws	60	3,4	1,8	eq			x		40	0,4	0,08	eq-el	x	x	
M069	50	o	a	sp	o	cl-s	20	5,4x2,6		x	x	wo	30	Bi	ms	60	4,4	1,8	eq		x	x		40	0,32	0,1	eq-el	x	x	
M083	60	o	a	sp	o↓	cl	10	2,4x1,2		x	x	wo	30	Bi	ps	90	5,2	2	eq			x	x	10	0,4	0,1	eq	x	x	
M088	73	o	a	sp	o↓	cl-d	7	2,2x1,2		x	x	wo	20	bi	ms	65	4,6	2	eq			x	x	35	0,3	0,08	eq	x	x	
M094	70	o	↓a	sp	i	cl-d	5	4x0,6	x		x	wo	25	bi	ms	75	4,3	2,6	eq			x		25	0,3	0,06	eq	x	x	
M097	75	o	a	sp	i	cl-d	10	8x2,6			x	i	15	bi	ps	70	2,3	1,2	eq		x	x		30	0,2	0,04	eq	x	x	
M098	1.1	o	a	sp	o	cl-d	15	6,4x0,5	x			i	25	bi	vps	90	2,9	1,8	eq	x		x	x	10	0,24	0,08	eq	x	x	
M101	75	o	↓a b	sp	o	s-d	5	4x0,4	x			o	20	bi	ps	70	5	1,6	eq-el		x	x	x	30	0,5	0,1	eq	x	x	
M102	70	o	a	sp	i	s-d	10	3,6x1,3		x		i	20	bi	ms	80	4	2	eq		x	x		20	0,4	0,1	eq	x	x	
M103	65	o	a	sp	o↓	cl-s	15	9x3,0			x	wo	20	bi	ms	75	5,2	2	eq			x	x	25	0,2	0,04	eq	x	x	
FABRIC 2																														
M006	65	o	↓a	sp	o↓	cl-d	10	1,6x0,3	x		x	i	25	S	ps	70	3,2	1,2	eq-el		x	x		30	0,16	0,04	eq	x	x	
M012	60	o	a	sp	o	cl-s	10	3,8x0,2	x	x		i	30	S	ps	90	5	1,2	eq		x	x		10	0,4	0,06	eq	x	x	
M014	60	e	a	sp	o	cl-s	15	0,8x0,6	x		x	i	25	S	vps	70	2,2	1,2	eq-el		x			30	0,18	0,04	eq-el	x	x	
M025	72	o	a	sp	o	cl-s	8	6x2,0	xx		x	i	20	S	vps	70	5	1,2	eq		x	x	x	30	0,4	0,1	eq-el	x	x	
M026	75	o	i	-	o	cl-d	5	3x	xx			i	20	s	ps	90	3	1,8	eq		x	x		10	0,3	0,1	eq-el	x	x	
M036	-	o	i	-	o	cl-s	-	-	-	-	-	i	20	S	vps	70	4,4	1,4	eq	x	x	x		30	0,4	0,1	eq	x	x	
M041	85	o	a b.	sp	o_p.	cl-s	5	-	xx			i	10	S	p s	90	3,4	1,8	eq	x	x			10	0,2	0,1	eq	x	x	
M042	72	o	a	sp	o	cl-s	8	1,3x1,3	xx		x	i	20	S	vps	80	2	1,1	eq	x	x	x		20	0,3	0,1	eq	x	x	
M043	80	o	↓a	sp	i	cl-s	5	1x1,0	xx		x	i	15	S	ps	80	2,2	1,4	eq	x	x	x		20	0,3	0,08	eq	x	x	
M075	63	o	a	sp	o	cl-d	7	1,4x	x		x	i	30	S	vps	60	3,86	2	eq		x	x		40	0,16	0,1	eq	x	x	
M079	50	o	↓a	sp	o	cl-s	15	1,7x0,14	x			i	35	S	vps	75	2	2	eq		x	x	x	25	0,14	0,04	eq	x	x	
M080	55	o	a	sp	o↓	cl-s	15	1,8x0,8		x	x	i	30	S	vps	80	3,1	1	eq		x	x		20	0,16	0,04	eq	x	x	
M081	55	e?	↓a	sp	i	cl-s	15	3,1x0,8		x		i	30	S	vps	80	3,2	1,2	eq		x	x		20	0,16	0,04	eq	x	x	
M086	1.2	o	a	sp	o	cl-s	15	5,8x1,1	x			i	20	S	ps	90	3,84	2	eq			x	x	10	0,2	0,06	eq	x	x	
M092	1.2	e?	a↓	sp	o	cl-d	10	3,3x1,5		x	↓x	i	25	s	vps	80	3,6	1,5	eq	x	x	x		20	0,14	0,04	eq	x	x	

Table 3. 1. Minero-petrographic and micro-structural features of pottery samples analyzed under optical microscope.

samples	MATRIX						VOIDS					INCLUSIONS				INCLUSIONS-COARSE FRACTION								INCLUSIONS-FINE FRACTION						
	A. %	Hom.	Opt. Ac.	b-fab.	Or.	d-sp.	A. %	max. size	Shape			Or.	A. %	Dist.	kind of sor.	Rel. Ab. %	max. size	av. size	Shape					Rel. Ab. %	max. size	av. size	shape			
								mm	Ch	Pb	Vu						mm	mm	eq/el	A	SA	SR	R		mm	mm	eq/el	SA	SR	R
FABRIC 3																														
M007	45	o	i	-	i	cl-s	20	2x0,9	x		x	i	35	Bi	ms	95	6,4	1,6	eq			x	x	5	0,24	0,04	eq	x	x	
M008	47	o	i	-	o	cl-s	28	3,6x1,6		x	x	i	25	Bi	ms	95	3,7	1,6	eq			x	x	5	0,24	0,04	eq	x	x	
M009	52	e	a	sp	o	cl-d	23	2,9x0,8	x		x	i	25	Bi	ms	90	3	1,6	eq			x	x	10	0,16	0,04	eq	x	x	
M021	82	o	a↓	sp	o	cl-s	8	2,6x	xx		x	wo	10	Bi	ps	90	4	1,2	el-eq			x	x	10	0,1	0,08	eq	x	x	
M024	77	o	i	-	o	cl-s	8	2x1,0	xx		x	wo	15	Bi	ms	90	3,6	1,4	eq			x	xx	10	0,16	0,06	eq	x	x	
M031	80	o	a↓	sp	o	cl-d	5	2,2x0,4	x			i	15	Bi	ms	90	1,8	1	eq		x		xx	10	0,2	0,06	eq	x	x	
M046	65	o	a	sp	o	s-d	15	3,2x0,4	xx		x	i	20	Bi	ms	95	1,7	1,2	eq	x		x	xx	5	0,1	0,04	eq	x	x	
M071	1.4	e	↓a	sp	o	cl-d	10	3,2x0,9	x		x	wo	25	Bi	ps	70	6,7	1,8	eq	x		x	x	30	0,16	0,1	eq	x	x	
M090	65	o	a	sp	o	cl-d	10	3,4x1,4	x		x	i	25	Bi	ms	80	3	1,8	eq		x	x		20	0,2	0,06	eq	x	x	
FABRIC 4																														
M016	45	o	a↓	sp	o	cl-s	15	1,7x0,4	x			wo	40	Bi	ms	50	1,8	1,2	eq-el	x	x	x		50	0,4	0,2	eq	x	x	
M019	55	o	a	sp	o	cl-s	15	1,8x1,0		x	x	i	30	Bi	ms	60	3	1,4	eq		x	x	x	40	0,3	0,1	eq	x	x	
FABRIC 5																														
M003	60	o	a↓	sp	i	cl-s	5	1,1x0,9		x		wo	35	Bi	ws	30	4	1,8	eq-el	x	x			70	0,5	0,06	eq		x	x
M004	60	o	a↓	sp	i	s	5	3,3x1,4	x		x	i	35	Bi	ms	30	4,2	1,8	eq	x	x	x		70	0,3	0,08	eq		x	x
M005	55	o	i	-	o↓	s	15	2,3x1,0	x		x	i	30	Bi	ms	60	3	1,4	eq	x	x			40	0,46	0,14	eq		x	x
M022	70	o	a	sp	o	s-d	5	0,44x0,4		x	x	i	25	Bi	ms	60	6,2	2	eq	x	x	x		40	0,5	0,1	eq		x	x
M023	55	o	i	-	o↓↓	s-d	15	4x1,7		x	x	i	30	Bi	ms	30	5,6	2	eq	x	x	x		70	0,4	0,1	eq		x	x
M027	60	o	a	sp	o↓	s	15	8,6x0,6		x		wo	25	Bi	ms	60	6	1,6	eq	x	x	x		40	0,3	0,14	eq		x	x
M032	60	o	a	sp	o↓↓	cl-s	5	2,5x			x	i	35	Bi	ms	25	7,64	2	eq	x	x	x		75	0,36	0,18	eq		x	x
M034	73	o	a	sp	o↓	s	7	1,6x			x	i	20	Bi	ms	50	2	1,6	eq	x	x	x		50	0,34	0,1	eq		x	x
M039	55	o	a	sp	o↓	s	20	7x2,0	x		x	i	25	Bi	ms	50	3,2	1,4	eq	x	x	x		50	0,2	0,1	eq		x	x
M044	70	o	a b	sp	o	s	10	2x0,4	x	x		i	20	Bi	ps	40	4	1	eq	x	x	x		60	0,5	0,16	eq		x	x
M045	70	o	a	sp	o↓↓	s	5	4x1,9		x	x	i	25	Bi	ws	40	4,6	1,8	eq	x	x			60	0,3	0,14	eq		x	x
M051	70	e	a↓	sp	o	s-d	10	4,7x	x		x	wo	20	Bi	ps	50	6	1,6	eq-el	x	x			50	0,4	0,14	eq		x	x
FABRIC 6																														
M001	50	e?	i	-	i	cl-s	15	2,9x1,6	x	x	x	i	35	u	ws	-	3,4	0,26	eq			x	x	-	-	-	-	-	-	-
M002	60	o?	a↓ b	sp	o	cl-s	5	1,9x1,1	x		x	i	35	u	ws	-	1,7	0,3	eq			x	x	-	-	-	-	-	-	-
M030	65	?	a	sp	o↓↓	cl-s	5	3,14x	x	x		i	30	u	ps	-	6,98	0,16	eq	x				-	-	-	-	-	-	-
M033	84	o	a	sp	i	cl-s	1	0,36x			x	i	15	Bi	ms	10	3,8	1,1	eq	x	x	x		90	0,8	0,2	eq		x	x
FABRIC 7																														
M056	68	o	a↓	sp	i	s-d	7	2,4x1,3		x	x	i	25	S	ws	60	5	3	eq	x	x	x	x	40	0,34	0,14	eq		x	x
FABRIC 8																														
M015	65	o	a↓	sp	o	s-d	10	2,4x1,0		x	x	o	25	Bi	ms	50	2,6	1,74	eq		x	x	x	50	0,4	0,1	eq		x	x
FABRIC 9																														
M038	70	e	a	sp	o↓↓	s-d	10	5x1,4	x			i	20	Bi	ms	40	4,8	1,6	eq		x	x	x	60	0,3	0,14	eq		x	x

Table 3. 2. Minero-petrographic and micro-structural features of pottery samples analyzed under optical microscope.

COARSE FRACTION																											
samples	CRYSTALS									METAMORPHIC R.			IGNEOUS R.				SEDIMENTARY R.								TEXTURES		
	Qz	Fsp	KF	Pl	Cal-Dol	Px	Bt	Op	Glt	Qzt	Mcsc	FllGr	vlc		plt		Ch	Arn	Dol	CMt	CSpr	OO-Pld	Crl	Bio	CP	Grog	ARF
													acd	int	acd	int											
FABRIC 1																											
M013	3												2				6		6	6	2	5			1	1?	
M017																	4		6	6	2				3		1
M018										4		3					4		5	6	4	4					
M020																	1?		6	7	3		2		1		1
M028		2			3					4							4		5	6	3	1					
M029	3									3		3					2		6	6	2				1?		
M035	2									4							5		6	6							
M037					3					5							5		6								
M040	4	3	*		3			3		5		4					5		6	6							
M068										1							1			8							
M069																	5		6	6		5			3		1
M083	1																5		6	6		5		1			1?
M088																	4		5	4	7		1		?		
M094			1														4			7	4						
M097										5							4			7	5		4		1		
M098										2							4		5	7	5						?
M101										5							4		5	5	6				1		1
M102				2									3				5		6	6					2		
M103										3							3		6	6	1	6			2		2
FABRIC 2																											
M006										1										6	7		1				
M012																	4		6	6	5	4			2	2	
M014																					6		6		3		
M025	2	2															2	3	4	7	6				2		
M026	2				3															4	7		1		2?		
M036					3														6		7		5				
M041					3														6								
M042					3																7		4?				
M043					3														6								
M075	1				3														6		6						
M079												1	2				5		1	7	1	5					
M080					3														3		7		4				
M081																			4	4	8		5				
M086																	4		6	6	4	4	2			2	
M092					3															4	6		3		5		

Table 3. 3. Minero-petrographic and micro-structural features of pottery samples analyzed under optical microscope.

COARSE FRACTION																											
Sample	CRYSTALS									METAMORPHIC R.			IGNEOUS R.				SEDIMENTARY R.								TEXTURES		
	Qz	Fsp	KF	Pl	Cal-Dol	Px	Bt	Op	Glt	Qzt	Mcsc	FllGr	Vlc		plt		Ch	Arn	Dol	CMt	CSpr	OO-Pld	Crl	Bio	CP	Grog	ARF
													Acd	int	Acd	int											
FABRIC 3																											
M007	3									6	2	2	1				4			7	2				3		
M008	2							2		5	2	4		4			3		2	7					3		1
M009	2			2						6	3	4	2				3			6	3				2		
M021			1							4	2	5	1				4		5	5	1						
M024	2									5	4	4	4		1				5	5	2						
M031	2					2				5		5				1	5			7	2						
M046	4									4		4	3				6			6	2				4		
M071										6		4					3			7	5	1					
M090	2				2			3		4	3	4					3			7	6		3				2
FABRIC 4																											
M016	2							2	2	5		1					4		3	7	2				2		
M019	2									5	1	4					4			5	6		5				
FABRIC 5																											
M003										5							8			2					2		
M004								2	2	5		4	1?				8			4					3		
M005	2																8								4		
M022	2		2						1	4	5	2	2				7		2	3					2		
M023						1						3					8			4					2		1
M027										3		2					8										
M032	2							2		6	?	2					7			3							1
M034	1																8										
M039																	8			2					2		
M044	1								1	3							8								2		
M045	2									3		2				4	8										
M051	2									2							8			2							
FABRIC 6																											
M001	4		1	1	1	1	1	1	2	2			1?				1			1				1			
M002	7	x	3	3			1	4	1	4							5			2							
M030	7			3				4	1	3	1						5								4	4	
M033	1									2							3									7	
FABRIC 7																											
M056																	4			6	2	2				6	
FABRIC 8																											
M015	2									6		6					4			2					2		
FABRIC 9																											
M038	3		2						2	2		2	6				5			6					3	3	

Table 3. 4. Minero-petrographic and micro-structural features of pottery samples analyzed under optical microscope.

FINE FRACTION																												
Sample	CRYSTALS													METAMORPHIC R.			IGNEOUS R.		SEDIMENTARY R.							TEXTURES			
	Qz	Fsp	KF	Pl	Cal-Dol	Amp	Px	Ms	Bt	Op	Glt	Tur	Grt	Qzt	Mcsc	FllGr	vlc	plt	Ch	Dol	CMt	CSpr	OO-Pld	Crl	Bio	CP	Grog	ARF	CalSc
																	acd	itmd											
FABRIC 1																													
M013	7	2	x	x				4	1	1	1								6	4	3								
M017	7	2	x	x		1?		4	1	1	3	1	1	3					5		3								
M018	7				1			2		3	4	1	1	4		2			3		4								1
M020	7				1			1				1	1								3								
M028	7				4					2									3		1								
M029	7		1	1				2		2	4			3					3		3								
M035	7	x						2		2	3			3					5										
M037	8	?	1		3			3		3									2										
M040	7	3		1	2	1		5	1	3				1					4										
M068	7		1					4	1	2	2			3					3										
M069	7	?				1		4	1	3	3	1	1						5										2
M083	7			1	1			2	1	2	2			3					4		2								
M088	7					1		2	1	2	3		1																1
M094	7		1	1		1		4		2	1	1		1					6										
M097	7							4	1	2	2			3					4		3								
M098	6						1	2		2									2		6	4							
M101	8			2	2			2		2	2								4		3								
M102	7			2		2		4	2	2	2		1	3					4		2								
M103	7				1	1		4	1	2	2	1	1						5										
FABRIC 2																													
M006	6				1			2		2	2	1							5		6								
M012	6		3					2		2	3								4		6								
M014	4				?			4		2												6							
M025	4	2			6																7								
M026	5	2		1	2		1	3		3									3		7								
M036	1				7			1																					
M041	8				5			2		2																			
M042	1				7			1														6							
M043	1				8			3		2																			
M075	6			1	3?			2	1	2		1	1	2					3			6							
M079	6							3		2				1		1			4		6								
M080	6				2?			1	1	2		1										7							
M081	5				6?			2											1		7	5							
M086	1				1			1											1	3	3	2	2	1	1		1		
M092	6				6	1		3		2				1					1			5							

Table 3. 5. Minero-petrographic and micro-structural features of pottery samples analyzed under optical microscope.

FINE FRACTION																												
sample	CRYSTALS													METAMORPHIC R.			IGNEOUS R.		SEDIMENTARY R.							TEXTURES			
	Qz	Fsp	KF	Pl	Cal-Dol	Amp	Px	Ms	Bt	Op	Glt	Tur	Grt	Qzt	Mcsc	FllGr	vlc	plt	Ch	Dol	CMt	CSpr	OO-Pld	Crl	Bio	CP	Grog	ARF	CalSc
																	acd	itmd											
FABRIC 3																													
M007	6		2			?		2		2				4	3	2			4		4								
M008	6		4					2		2				5	4	2	4		4		4								
M009	7	2	2			?	1	2		2		1		4	4		2		4		5								2
M021	8	2			1			5	1	3									2										
M024	8	2		1				5	1	3									3										
M031	8		1		1					1									1										
M046	7							4			2								4		6								
M071	6		1	1				2		2	2			4							6								
M090	6							3	1	3				4		2			4		6								
FABRIC 4																													
M016	7	3	2	2		1	1	3	2	2	4	1	1	4		2			4		4								
M019	7			2	4			3	2	3	4	1	1	5	1	1			5										
FABRIC 5																													
M003	7			2		2		3	1	2		1	1	4	2				4										?
M004	7		3	3		2		3	1	4	3	1		5	4				4		2								
M005	7		3	3		2		2	1	2	1	1	1	4					5										1
M022	7		3	3			2	2	1	3	2	1		4					6										
M023	7		3	3			2	3		2	2			5		2			6										
M027	7		3	3				2	1	2			1	4		2			6										
M032	7		2	2				2		2	2		1	4		2			5										?
M034	7		3	2				4		2	2	1	1	2					6							1		1	
M039	6							4	1	2				3					6										1
M044	7		3			2		2	1	2			1	4					5										
M045	7		2	2			1	2	1	2	1	1	1	4					4										
M051	6						1	3	1	2	1	1		6					6										1
FABRIC 6																													
M001	-	-	-	-	-	-	-	-	-	-	-	-	-	-	-	-	-	-	-	-	-	-	-	-	-	-	-	-	-
M002	-	-	-	-	-	-	-	-	-	-	-	-	-	-	-	-	-	-	-	-	-	-	-	-	-	-	-	-	-
M030	-	-	-	-	-	-	-	-	-	-	-	-	-	-	-	-	-	-	-	-	-	-	-	-	-	-	-	-	-
M033	7	5	**				3	2			1			3					4										
FABRIC 7																													
M056	6	2	2					2	1	2		1		2					6										
FABRIC 8																													
M015	8							3	1	2		1		4					4										2
FABRIC 9																													
M038	6		3	3			3	2	1	2	2			4					4		5								?

Table 3. 6. Minero-petrographic and micro-structural features of pottery samples analyzed under optical microscope.

3.4 Digital image analysis (DIA)

Digital image analysis (DIA) is a tool recently developed on archaeological ceramic useful in the study of ceramic pastes and production technology. It gives information, particularly on the quantity, grain-size distribution and shape of inclusions, as well as on the ratio between matrix, inclusions and pores. Here, it was performed on a selection of samples characteristic of the different fabrics groups identified by the optical microscopy.
For this purpose SEM-BSE images were acquired for eight samples (M003, M012, M015, M018, M045, M051, M056, M102). For each sample approximately ten SEM-BSE images were taken, in order to obtain a good representation of each thin section. Before performing the DIA, it was necessary to process all of them as described in chapter 1.6. The files so elaborated were then segmented and the information about the pottery features were extracted (figures 3.11-18). In the samples with closed-spaced inclusions, those fragments very closed one to the other or in contact, were considered by the software like one single grain. In these cases the grains that merged together were separated manually. A further problem occurred with sample M056 (fabric F7), rich in grog fragments. Since the temper and the matrix were of similar composition it was not always possible to discriminate automatically the grog. In this case grog was detected and isolated from the surrounding matrix thanks to the shrink rim and was selected manually (figure 3.17).

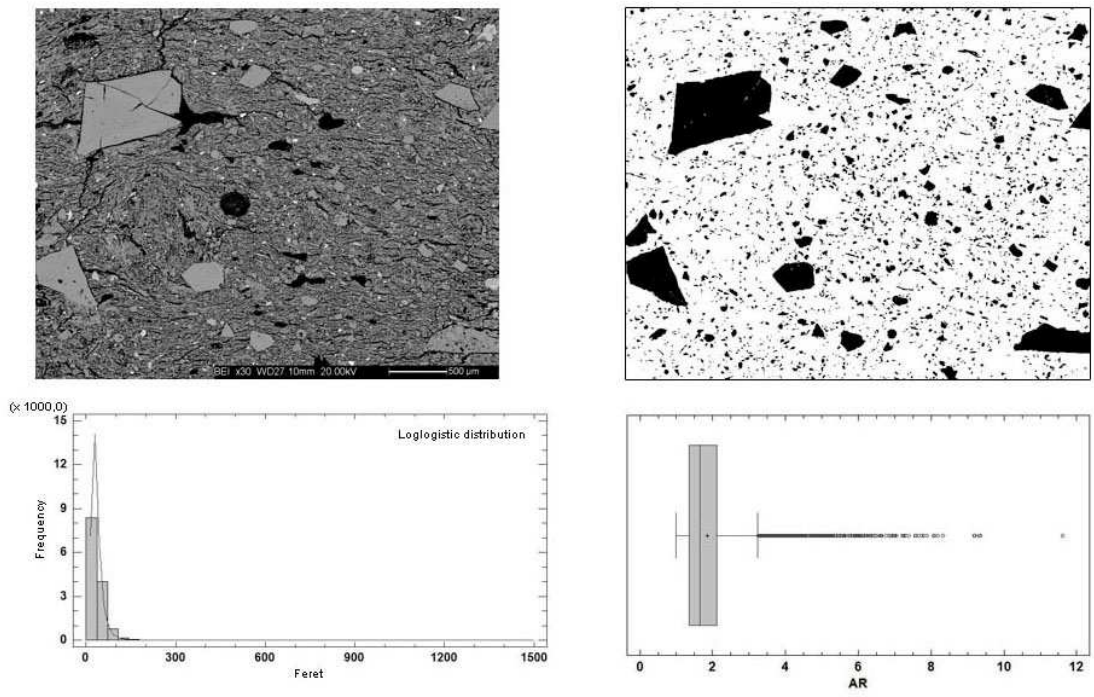

Figure 3.11. a) SEM-BSE image of the sample M003 (fabric F5); b) segmented image of the inclusions present; c) frequency distribution diagram of the whole inclusions; d) AR values of the inclusions.

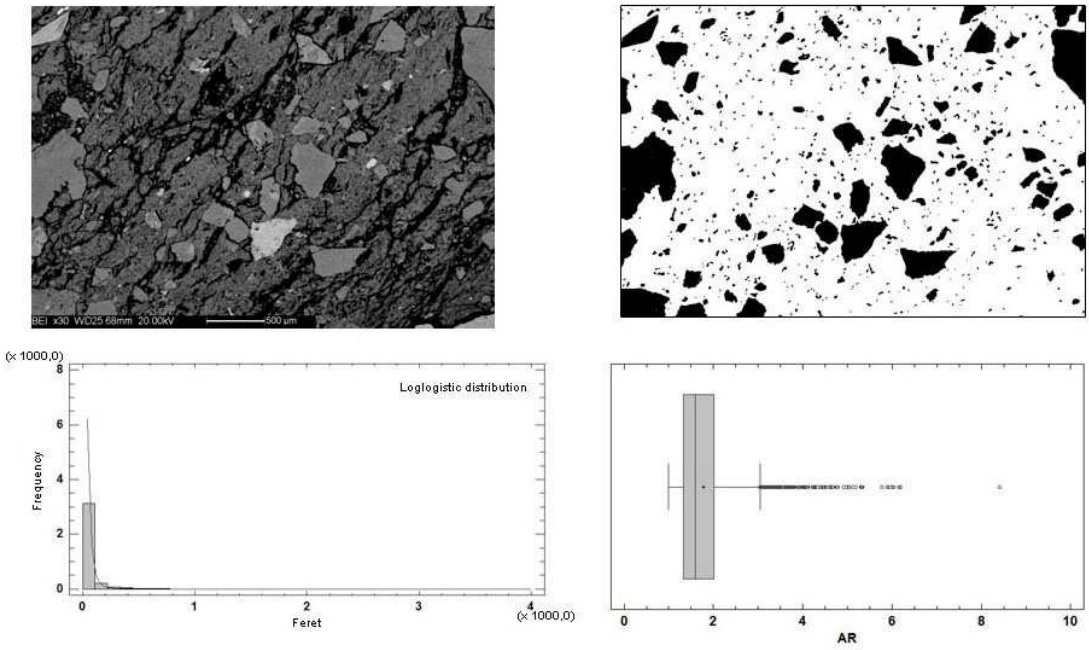

Figure 3.12. a) SEM-BSE image of the sample M012 (fabric F2); b) segmented image of the inclusions present; c) frequency distribution diagram of the whole inclusions; d) AR values of the inclusions.

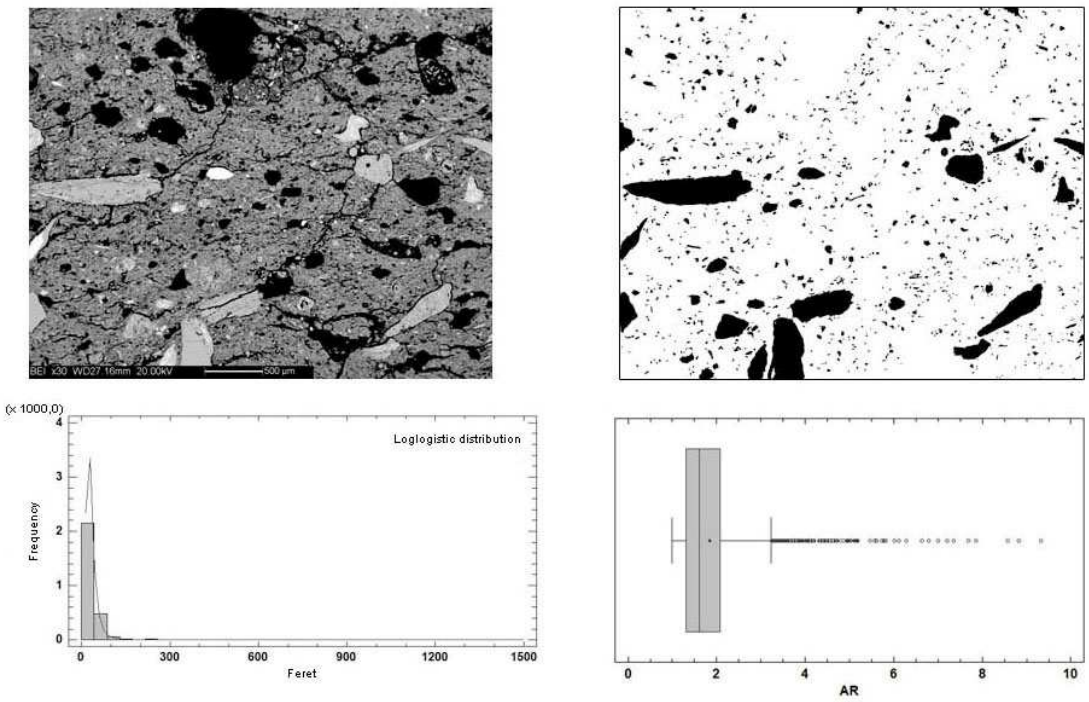

Figure 3.13. a) SEM-BSE image of the sample M015 (fabric F8); b) segmented image of the inclusions present; c) frequency distribution diagram of the whole inclusions; d) AR values of the inclusions.

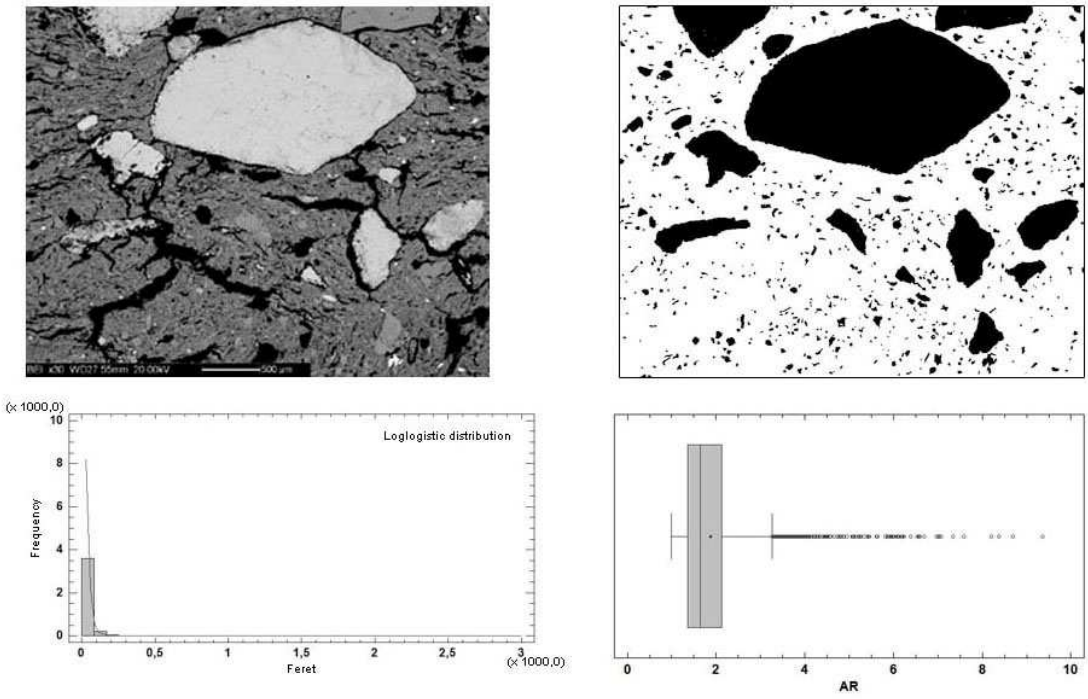

Figure 3.14. a) SEM-BSE image of the sample M018 (fabric F1); b) segmented image of the inclusions present; c) frequency distribution diagram of the whole inclusions; d) AR values of the inclusions.

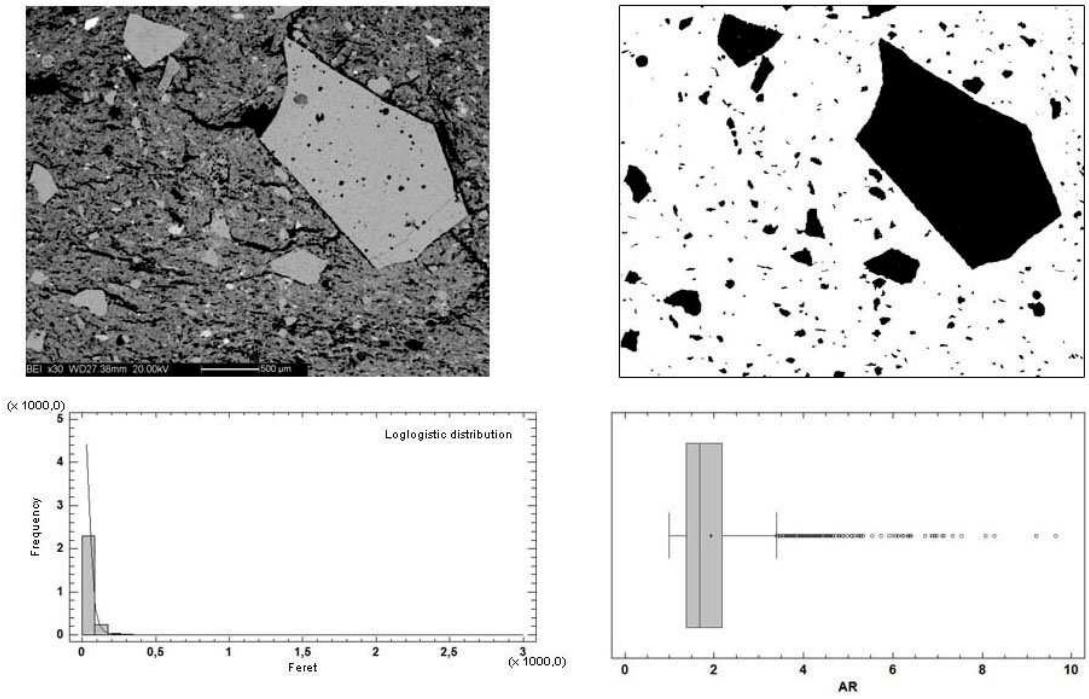

Figure 3.15. a) SEM-BSE image of the sample M045 (fabric F5); b) segmented image of the inclusions present; c) frequency distribution diagram of the whole inclusions; d) AR values of the inclusions.

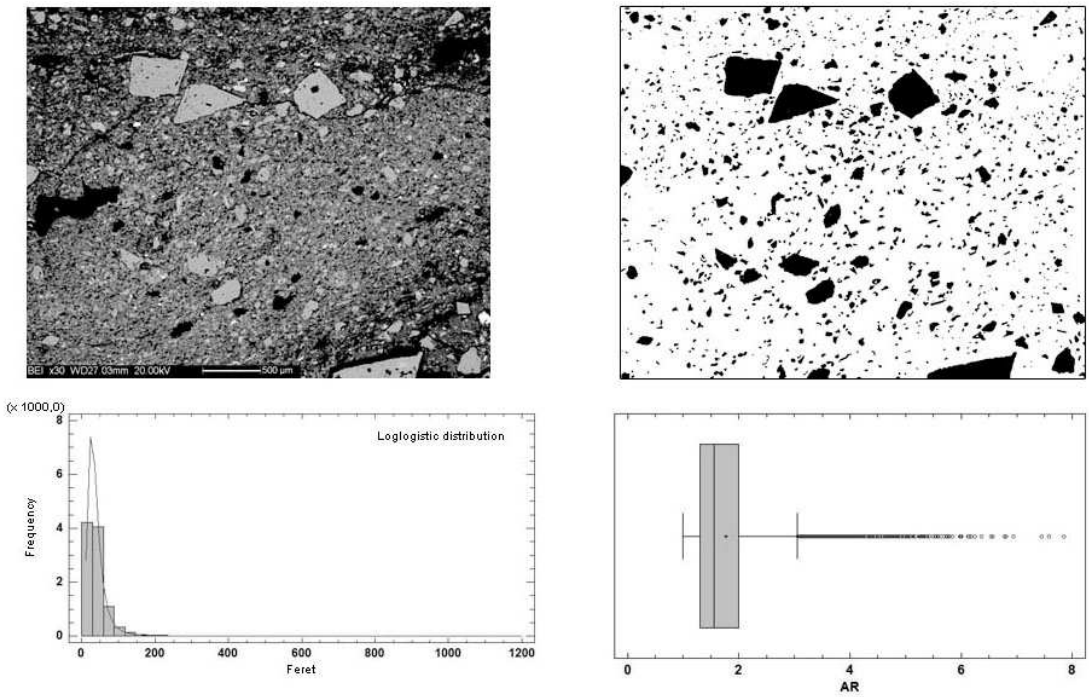

Figure 3.16. a) SEM-BSE image of the sample M051 (fabric F5); b) segmented image of the inclusions present; c) frequency distribution diagram of the whole inclusions; d) AR values of the inclusions.

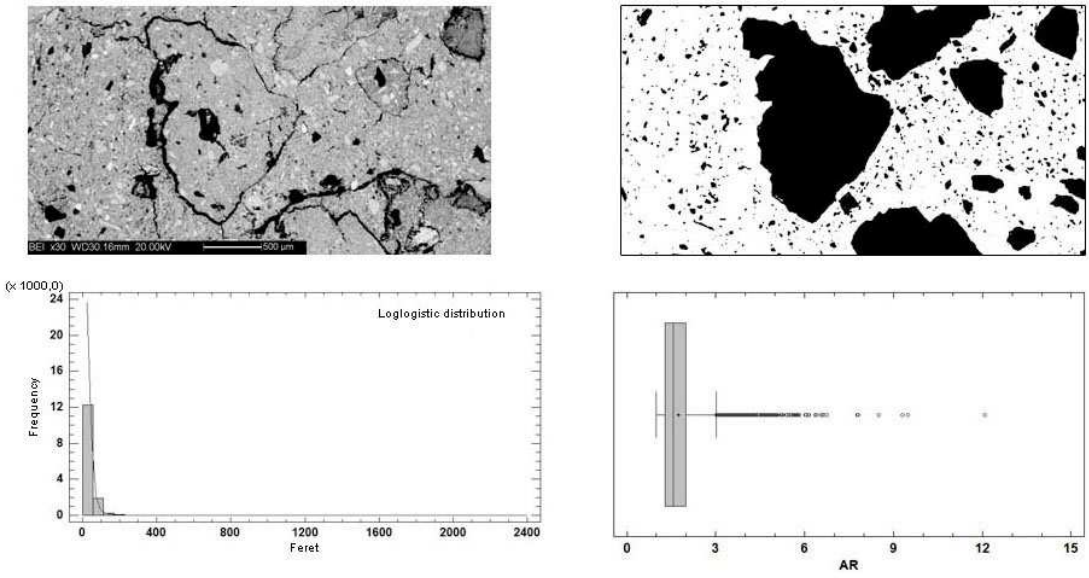

Figure 3.17. a) SEM-BSE image of the sample M056 (fabric F7); b) segmented image of the inclusions present; c) frequency distribution diagram of the whole inclusions; d) AR values of the inclusions.

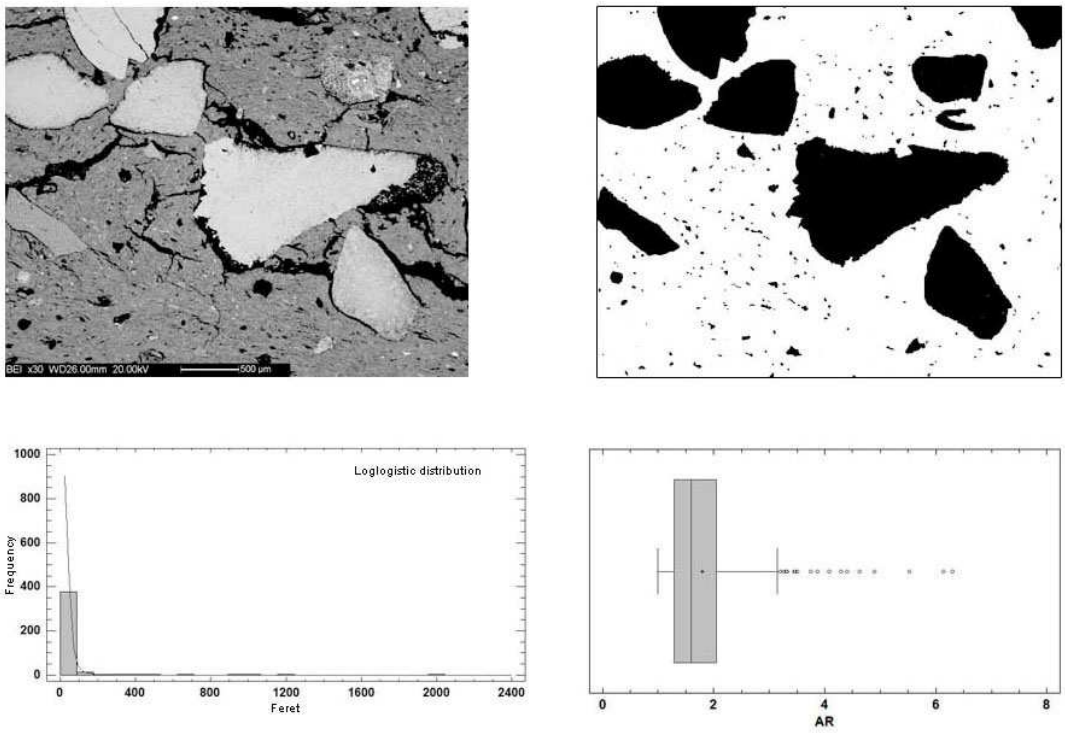

Figure 3.18. a) SEM-BSE image of the sample M102 (fabric F1); b) segmented image of the inclusions present; c) frequency distribution diagram of the whole inclusions; d) AR values of the inclusions.

Chemical maps were acquired for those samples (M001, M009, M016, M086, M101) whose components (inclusions and matrix) showed comparable average atomic numbers. That caused high similarity of grey tones and it was not possible any distinction between them (figures 3.19-3.26).

At this point, particle analysis was performed on the segmented images gained by SEM-BSE pictures and by chemical maps. For each one the *area fraction,* the maximum size of the inclusions *(Feret)* and the *aspect ratio (AR)* were statistically treated.

One of the main goals of DIA was to differentiate the pottery components (single type of inclusions, matrix and voids) and to analyze them separately. After the first analyses it was evident that, due to the particular complexity of the ceramic constituents, it was not possible to separate all the different kind of inclusions from the SEM-BSE images. Therefore only the distinction between matrix, voids and inclusions in general was considered for them.

For each sample, the analysis of the Feret results of the inclusions data-set were illustrated through histograms overlaid by the probability distribution functions (figures 3.11-3.26). As the finer inclusions were extremely greater in terms of number of particles than the coarser ones, they appeared predominant also when the total occupied area was insignificant. This type of representation made very difficult to define whether the grain-sizes distribution of the fragments in the thin section had one or more modes. For this reason they were divided on the basis of the different size distribution referred to the

Wentworth grain-size chart and the total area fractions occupied by each grain-size classes were calculated. According with Whitbread (1995) only the fragments greater than 10 μm were considered as inclusions.

Box-plots of the Aspect Ratio (AR) values were displayed in order to give the average lengthening of the fragments for each sample (figure 3.11.d-3.18.d). Inclusions were analyzed all together without discriminating the different types. This result must be considered with great caution because the AR is referred to diverse rocks and minerals that can have different aspects (angularity, elongation, size). Moreover, finer inclusions were extremely greater in the number of particles than the coarser ones. They were mostly represented by small sub-angular equant quartz crystals. This aspect deeply affects the results displayed in the box-plots where the median and the first-third quartiles range had low values of AR, indicating a high sphericity, always together with great numbers of outliers.

A different situation was for the chemical map images where it was possible to examine the different inclusions types. Sample M001 (fabric F6) was characterized by abundant quartz (mostly chert fragments and subordinate quartz crystals) representing 10% of the total area of the thin section (figure 3.19). The other inclusions (alkali-feldspar, plagioclase, calcite and Fe and Ti oxides) were always present in amounts less than 1%. Considering the grain-size distribution of quartz appeared continuous. Calcite and other minerals had a less well delineated situation with some sporadic presences in the coarser fraction.

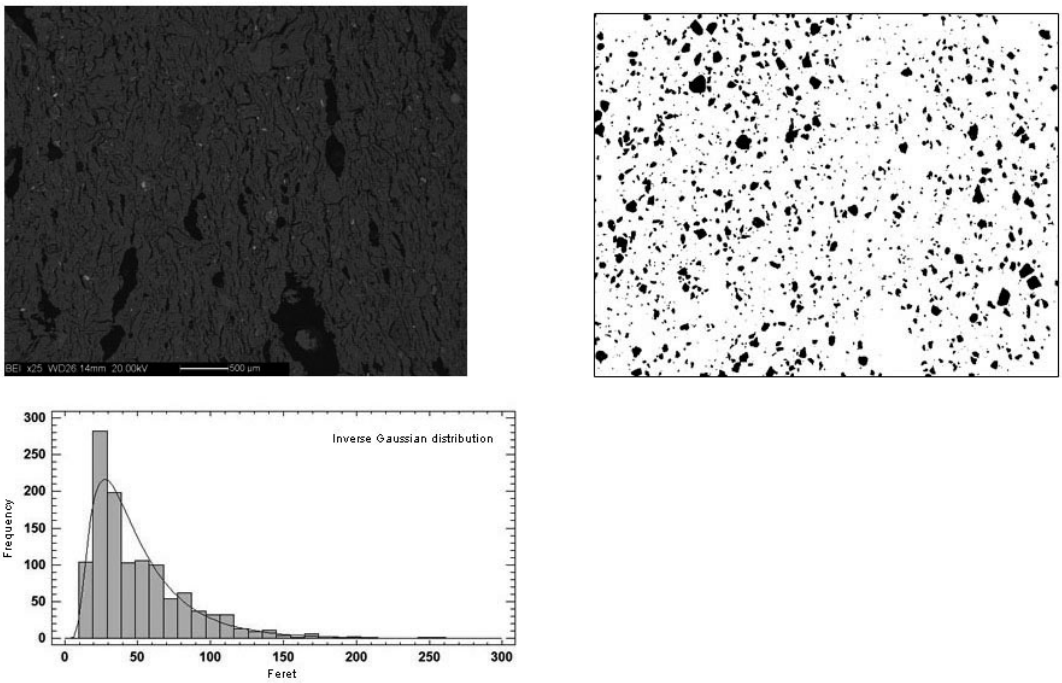

Figure 3.19. a) SEM-BSE image of the sample M001 (fabric F6), image of the area acquired by elemental chemical map; b) segmented image of the quartz inclusions present; c) frequency distribution diagram of the quartz inclusions.

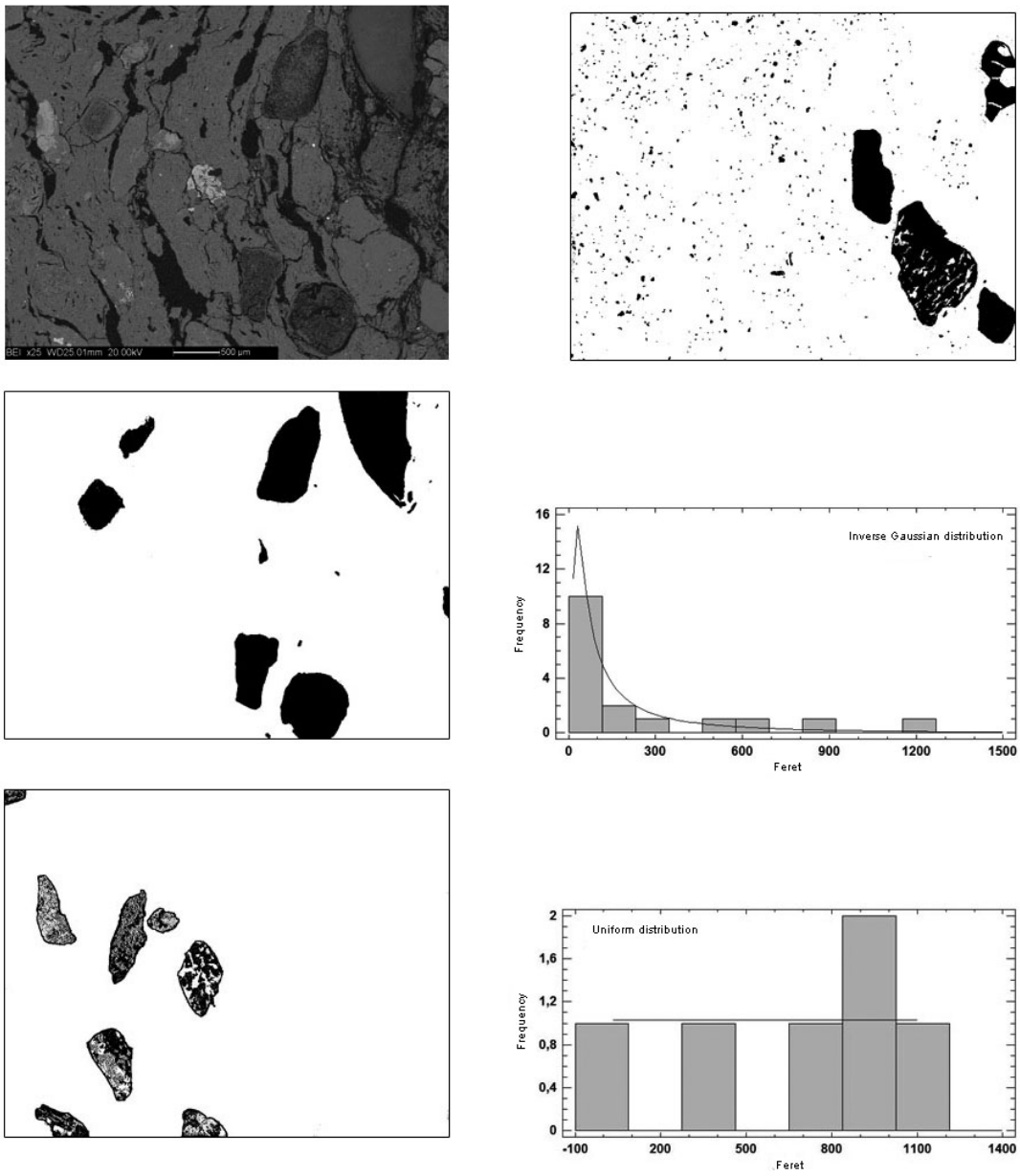

Figure 3.20. a) SEM-BSE image of the sample M009 (fabric F3), image of the area acquired by elemental chemical map; b) segmented images of the quartz inclusions present; c) segmented images of the carbonate (calcite) inclusions present; d) frequency distribution diagram of the calcite inclusions; e) segmented images of the metamorphic rocks present; f) frequency distribution diagram of the metamorphic rocks.

Sample M009 (fabric F3) was characterized by a great amount of carbonate inclusions (6%), metamorphic rock fragments (6%) and quartz (8%), mostly present in the finer fraction (figure 3.20). The other crystals (alkali-feldspar, plagioclase, and Fe and Ti oxides) were always present in amounts less than 1%. Quartz had a continuous grain-size distribution with the larger number of grains falling in finer fraction range and rare isolated cases in the coarser grain-size fraction. Calcite was represented by more modes while the metamorphic rocks fragments had a uniform distribution with one peak in the range 800-1100 μm.

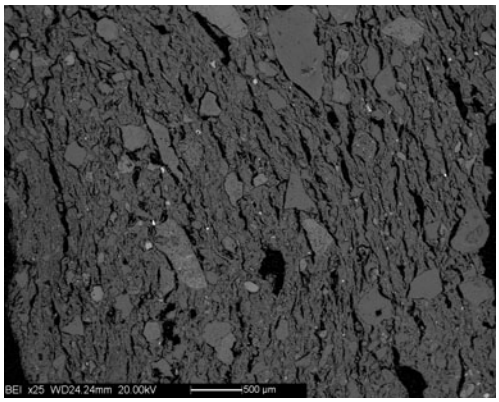

Figure 3.21. SEM-BSE image of the sample M016, image of the area acquired by elemental chemical map.

Sample M016 (fabric F4), was characterized by abundant inclusions with a bimodal grain-size distribution (c:f ratio 50:50), mainly represented by quartz (10% of the total area fraction), dolomite (4%) and calcite (2%) (figure 3.21-3.22). The other minerals (alkali-feldspar, plagioclase, and Fe and Ti oxides) were always present in amounts less than 1%. Quartz showed a continuous grain-size distribution with the largest number of grains falling in the range between 30 and 80 µm. Dolomite presented two populations: one continuous distribution among small grain-sizes and a second distribution represented by few bigger

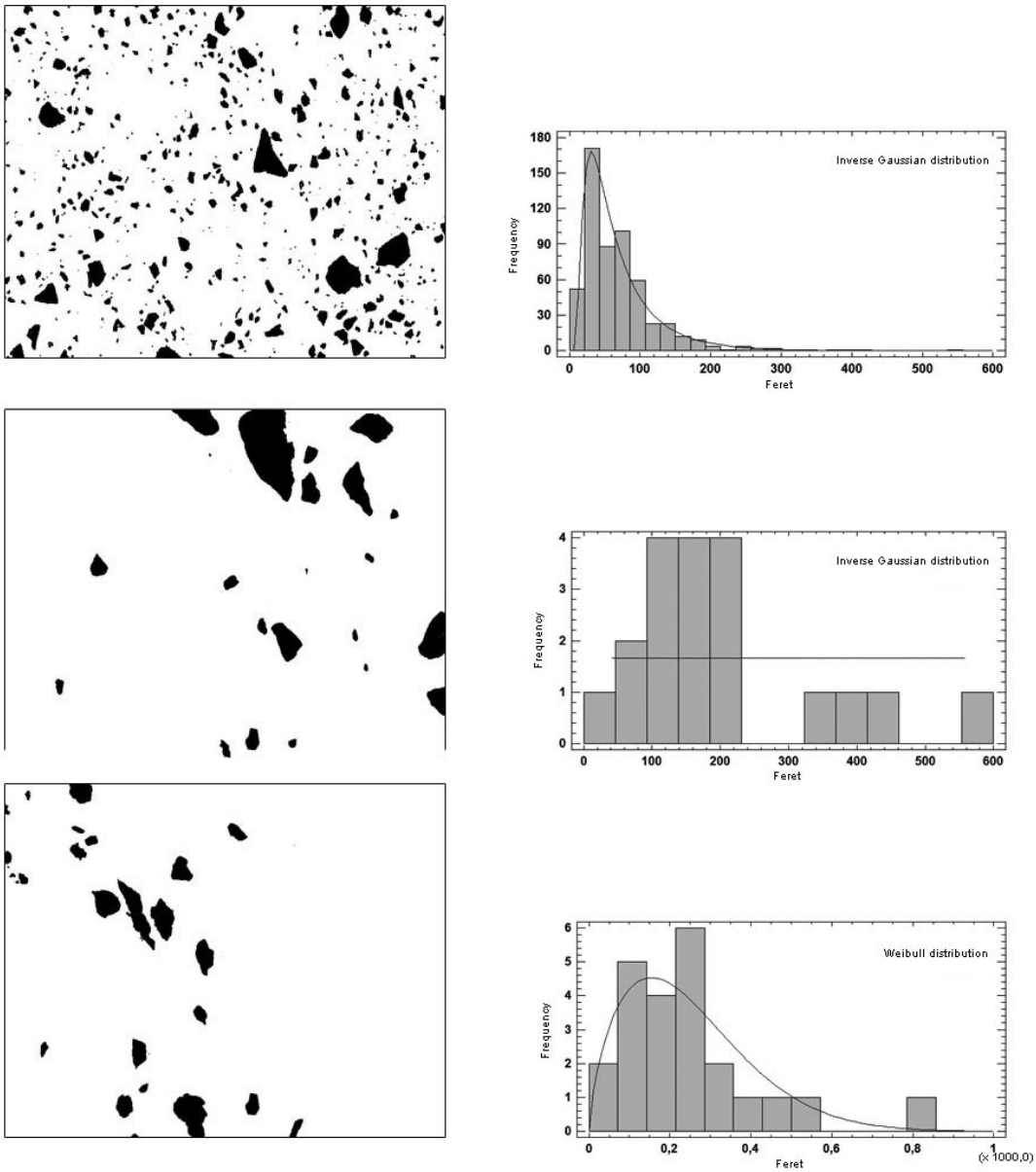

Figure 3.22. Segmented images of the inclusions present in sample M016 with the corresponding frequency distribution diagrams: a) quartz inclusions; b) calcite inclusions; c) dolomite inclusions.

grains. Calcite is represented by more and uniform modes both in the finer and in the coarser fractions.

Sample M086 (fabric F2), was characterized by abundant inclusions of dolomite (12% of the total area fraction), calcite (10%) and subordinate quartz (1%) (figures 3.23-3.24). All the other inclusions (alkali-feldspar, and Fe oxides) were present in amounts less than 0,3%. Quartz presented a continuous grain-size distribution with most of the grains falling in the range between 10 and 100 μm, and just few with coarser size. Calcite was represented by a polymodal distribution, while dolomite present a uniform grain-size distribution, mostly in the coarser grain-size classes. This happened probably because the two carbonate phases are both present mostly with few coarse grains.

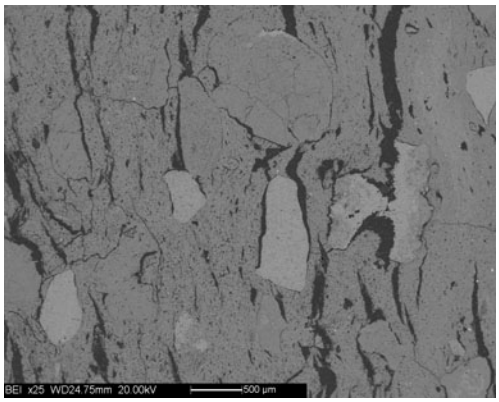

Figure 3.23. SEM-BSE image of the sample M086, image of the area acquired by elemental chemical map.

Sample M101 (fabric F1) was characterized by abundant carbonate inclusions (figures 3.25-3.26). It had a coarser fraction mostly constituted by dolomite (6% of the total thin sections area) and calcite (2,3%), while quartz (6%) was the main component of the finer fraction. All the other inclusions (alkali-feldspar, and Fe and Ti oxides) were present in amounts less than 1%. Similarly to sample M009, M016 and M086, where it was the main

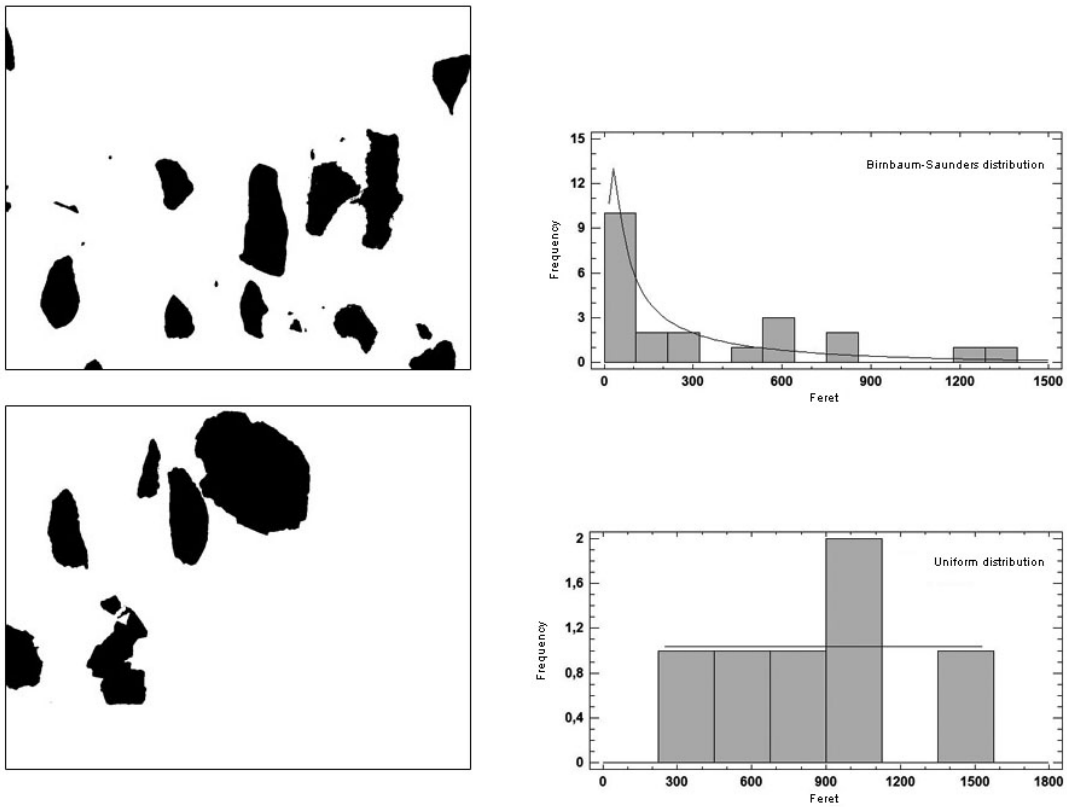

Figure 3.24. Segmented images of the inclusions present in sample M086 with the corresponding frequency distribution diagrams: a) calcite inclusions; b) dolomite inclusions

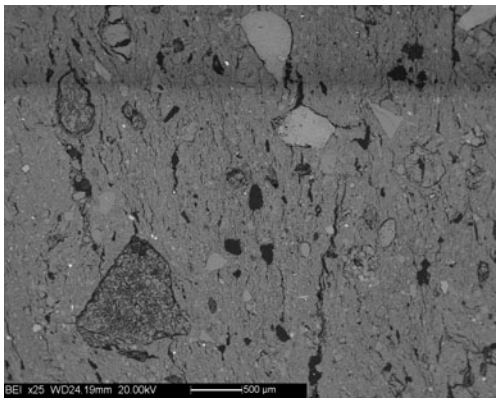

Figure 3.25. SEM-BSE image of the sample M101, image of the area acquired by elemental chemical map.

constituent of the finer fraction, quartz occurred with a continuous grain-size distribution with most of the grains falling in the range between 10 and 100 µm, and only few in the coarser fractions. Calcite and dolomite were characterized by a polymodal grain-size distribution, with higher frequency in the coarser fraction range classes.

Then, the m:v:i (matrix:voids:inclusions) ratio typical of each petrographic fabric group was estimated through the average area fraction

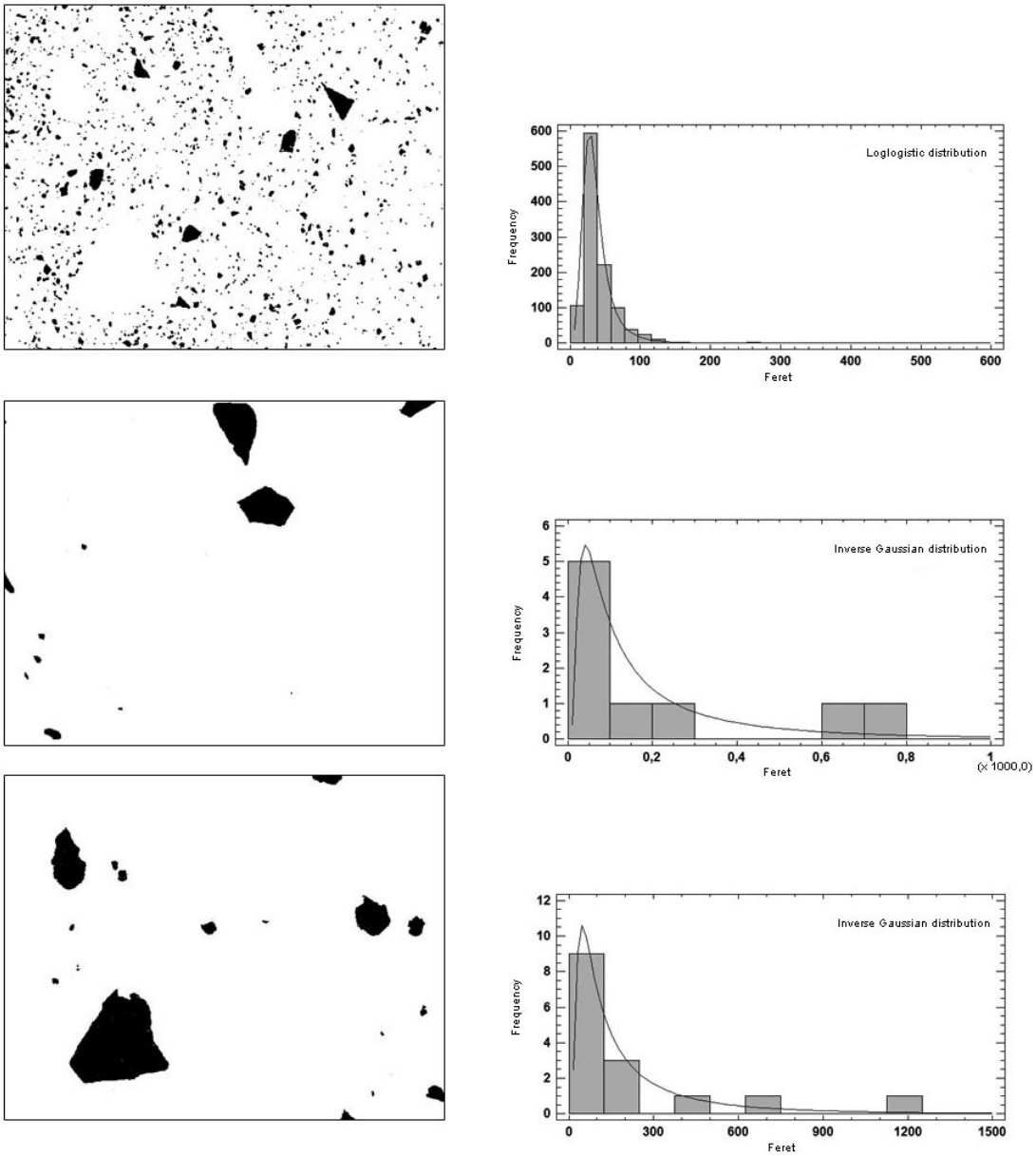

Figure 3. 26. Segmented images of the inclusions present in sample M101 with the corresponding frequency distribution diagrams: a) quartz inclusions; b) calcite inclusions; c) dolomite inclusions.

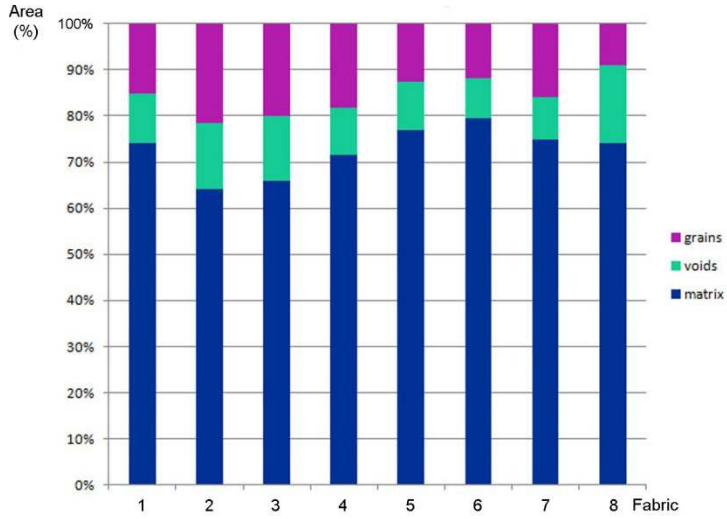

Figure 3. 27. Typical area fraction of each fabric group occupied by the inclusions, voids and matrix.

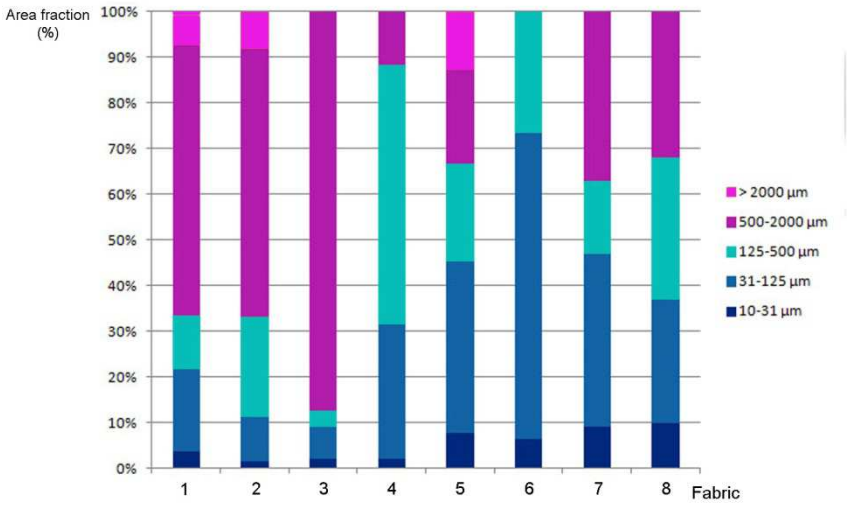

Figure 3. 28. Area fraction of each grain-size class of the inclusions typical for each fabric group.

occupied by the matrix, voids and all the inclusions, respectively, and displayed in a 100% stacked bar chart (figure 3.27).

A similar representation of the different size-distribution referred to the Wentworth grain-size scale and the total area fractions occupied by each grain-size class were adopted also for underling the characteristics of each fabric group (figure 3.28). Where more than one sample for fabric was available, their average data were adopted. It was observed that clustering together two by two the Wentworth grain-size classes makes the results more clear and still well comparable with the fabric description.

Comparing the results obtained from DIA with those gained by microscopy observations (table 3.3, reassumed above), it appeared that there was a good correspondence. Only the m:v:i ratio gained by visual estimation charts sometimes was slightly overestimated.

3.5 Mineralogical composition

The mineralogical association of the samples was identified by X-ray powder diffraction (XRPD) analysis. This technique is particularly useful to get information about the raw material originally used (in particular the nature of the base-clay and of any possible added temper), the mineral phases formed during the firing (e.g. hematite, gehlenite, diopside, spinel, cristobalite, mullite, cordierite, wollastonite, anorthite) and the presence of secondary phases formed after burial for post-depositional processes, all information difficult to be recognized with any other method. (Maggetti 1982, Maggetti 1991, Rice 1987, Veniale 1990).

The high mineralogical and petrographic variability noticed through the thin sections observation was also confirmed by the XRPD data: observing the presence or absence and the relative abundance of some specific mineral phases, it was possible to distinguish different mineral assemblages (table 3.4; table 3.5; figure 3.29):

The first group ($A1_{xrd}$) is characterized by abundant quartz and calcite and scarce illite and feldspars (both plagioclases and alkali-feldspars, like microcline). Traces of dolomite and anatase can also be occasionally present. In some samples ($A3_{xrd}$) traces of smectites and chlorite, or of hematite ($A2_{xrd}$) also occur. In two specimens the peaks of zeolite were also observed. In these potsherds this mineral is a secondary phase formed for the re-crystallization of the glassy phase after the clay minerals break-down (Buxeda, Mommsen et al. 2002, Schwedt, Mommsen et al. 2006). All the samples of this first group belong to the petrographic fabrics F1, F2, F3, F4.

Samples	XRD groups	Qz	Pl	Kfs	Kfs	Cal	Dol	Ilt	Sme	Chl	Spl	Zeo	Px	Hem	Amp	Ant
			Ab	Mc	An/Sd											
M006, M016, M029, M068, M079, M081, M090, M094, M102	A1 xrd	****	*/**	*		**/***	-/*	*				-/*?				-/*
M014, M020, M036, M043, M092	A2 xrd	****	*	*		****	*	*						*		
M019, M037, M041, M042, M080, M088, M097	A3 xrd	***/****	*	*		***/****	*/**	*/**	-/*	-/*		-/*?				
M012, M017, M025, M035, M040, M069, M075, M083, M086, M103	B1 xrd	****	*/**	*	-/*	**/***	**/***	*/**				-/*?				
M013, M018, M028, M098, M101	B2 xrd	****	*	*		**	**/***	*/**	*			-/*?				-/*
M007, M008, M009, M021, M071	C xrd	****	*/**	*		*/**	-/**	*/**			*		-/*			
M001, M002, M003, M004, M005, M023, M027, M030, M032, M034	D1 xrd	****	*/**	*/**		-/*		*/**							-/*	
M026, M051, M056	D2 xrd	****	*	*		*	-/*	*	-/*					*		
M022, M039, M044, M045	D3 xrd	****	*	*/**		-/*		**	-/*	-/*					-/*	
M038	E xrd	****	**		***	*		**					*	*		

Table 3. 4. Mineralogical associations in the studied pottery. Qz: quartz; Pl: plagioclase (albite like); KF: alkali feldspar (microcline like); Cal: calcite; Dol: dolomite; Ilt: illite; Sme: smectites; Chl: chlorite; Spl: spinel; Zeo: zeolite; Px: pyroxene; Hem: hematite; Amp: amphibole; Gp: gypsum; Pyr: pyrite; Ant: Ti oxide atanasio.

samples	Fabric	XRD groups	Qz	Pl	Kfs	Kfs	Cal	Dol	Ilt	Sme	Chl	Spl	Zeo	Px	Gh	Hem	Gp	Amp	pyr	Ant
				Ab	Mc	Ano/Snd												Tr		
M013	F1	$B2_{xrd}$	****	*	**		**	**	*	*										
M017	F1	$B1_{xrd}$	****	**	*		**	**	*											
M018	F1	$B2_{xrd}$	****	*	*		**	**	*	*										
M020	F1	$A2_{xrd}$	****	*	*		****	*	*							*				
M028	F1	$B2_{xrd}$	****	*	*		**	***	**	*										
M029	F1	$A1_{xrd}$	****	*	*		***	*	*											
M035	F1	$B1_{xrd}$	****	*	*		**	**	*											
M037	F1	$A3_{xrd}$	****	*	*		***	*	**	*										
M040	F1	$B1_{xrd}$	****	**	*		**	**	*											
M068	F1	$A1_{xrd}$	****	**	*		**		*				*							
M069	F1	$B1_{xrd}$	****	*	*		*	**	**											
M083	F1	$B1_{xrd}$	****	*	*		***	***	**											
M088	F1	$A3_{xrd}$	****	*	*		***	**	**	*										
M094	F1	$A1_{xrd}$	****	*	**		**		*											
M097	F1	$A3_{xrd}$	****	**	*		***	*	*	*										
M098	F1	$B2_{xrd}$	****		*		**	**	**	*										*
M101	F1	$B2_{xrd}$	****	*	*		*	**	*	*										
M102	F1	$A1_{xrd}$	****	*	*		**	*	**											
M103	F1	$B1_{xrd}$	****	*	*		**	**	**											
M006	F2	$A1_{xrd}$	****	*	*		***	*	*											
M012	F2	$B1_{xrd}$	****	*	*		**	***	*											
M014	F2	$A2_{xrd}$	***		*		****	*	*	*						*				
M025	F2	$B1_{xrd}$	***	**	SAN	**	***	***	**											
M026	F2	$D2_{xrd}$	****	*	*		*	*	**	*						*				
M036	F2	$A2_{xrd}$	***	*	*		****	**	**	*						*				
M041	F2	$A3_{xrd}$	***	*	*		****	***	*	*										
M042	F2	$A3_{xrd}$	***	*	*		****	**	**	*										
M043	F2	$A2_{xrd}$	***	*	*		***	**	**	*						*				
M075	F2	$B1_{xrd}$	****	*	*		**	***	*											
M079	F2	$A1_{xrd}$	****	*	*		***		*											
M080	F2	$A3_{xrd}$	***	*	*		****	**	**	*										
M081	F2	$A1_{xrd}$	****	*	*		***	*	**				*							
M086	F2	$B1_{xrd}$	****	*	**		**	**	**											
M092	F2	$A2_{xrd}$	****	*	**		***	*	*							*				
M007	F3	C_{xrd}	****	**	*		**		*			*								
M008	F3	C_{xrd}	****	*	*		**		**			*		*						
M009	F3	C_{xrd}	****	*	*		*		*			*								
M021	F3	C_{xrd}	****	*	*		*	**	**			*								
M071	F3	C_{xrd}	****	**	**		**		*			*								
M090	F3	$A1_{xrd}$	****	**	*		***		*											*
M016	F4	$A1_{xrd}$	****	**	*		**		*											
M019	F4	$A3_{xrd}$	****	*	*		***		*	*										
M003	F5	$D1_{xrd}$	****	*	*				*											
M004	F5	$D1_{xrd}$	****	**	**		*		*											
M005	F5	$D1_{xrd}$	****	*	*				*											
M022	F5	$D3_{xrd}$	****	*	**				**		*							*		
M023	F5	$D1_{xrd}$	****	**	**				*											
M027	F5	$D1_{xrd}$	****	*	*				*											
M032	F5	$D1_{xrd}$	****	*	**				*									*		
M039	F5	$D3_{xrd}$	****	**	*		*		**		*									
M044	F5	$D3_{xrd}$	****	*	*		*		**	*										
M045	F5	$D3_{xrd}$	****	*	**				*		*									
M051	F5	$D2_{xrd}$	****	*	*		*		*							*				
M001	F6	$D1_{xrd}$	****	**	*				**											
M002	F6	$D1_{xrd}$	****	*	*		*		*											
M030	F6	$D1_{xrd}$	****	**	*				**											
M034	F6	$D1_{xrd}$	****	*	*		* ?		*											
M056	F7	$D2_{xrd}$	****	*	*		*		*	*						*				
M038	F9	E_{xrd}	****	**	SAN	***	*		**					*		*				

Table 3. 5. XRPD results. Samples are here ordered following the petrofabric classification. For the minerals abbreviations see table 3.4.

The second group (B_{xrd}) is similar to the first one, but it is characterised by higher dolomite content and by the absence of chlorite, hematite and zeolite. In five specimens ($B2_{xrd}$) there are also visible traces of smectites and in another one (M025) of alkali-feldspar (like sanidine). Alkali-feldspars like sanidine are generally absent in all the other studied pottery from Castel de Pedena. All the samples of this group belong to the petrographic fabrics F1-F2.

The third group (C_{xrd}) is composed by only five samples all belonging to the petro-fabric F3. They are characterized by dominant quartz and subordinate feldspars (plagioclases and alkali-feldspars), calcite and illite. Dolomite can be present in small amounts and also in sample M08 where is visible rare pyroxene and trace of spinel, a mineral that generally forms in the ceramics as a secondary phase at temperature higher than 950° (Maggetti 1982, Veniale 1990).

The fourth assemblage (D_{xrd}) is characterized by seventeen sample with predominant quartz and subordinate feldspars (both plagioclases and alkali-feldspar like microcline) and illite. Occasionally traces of calcite and amphibole can be present. Few samples ($D2_{xrd}$, $D3_{xrd}$) bear also clay minerals like smectites and chlorite, while three of them also contain hematite ($D2_{xrd}$). All the samples belong to the fabrics F5, F6 and F7, while only one sample (M026) belongs to the fabric F2, this being justified by the rare calcite and dolomite among its minerals.

The last group only consists of sample M038. It is characterized by abundant quartz and alkali-feldspar like sanidine or anorthoclase. Plagioclase and illite are few and there are traces of pyroxene, hematite and calcite. The presence of alkali-feldpas like sanidine and anorthoclase, and of pyroxene is well explained by the abundant igneous rock fragments among its inclusions (ref. chapter 3.3).

Since any special treatments of the powders (e.g. ethylene glycol-solvation) was performed to distinguish the mineral species within the smectite group, here I refer to smectites in general (Bradley 1945, Moore, Reynolds Jr. 1997).

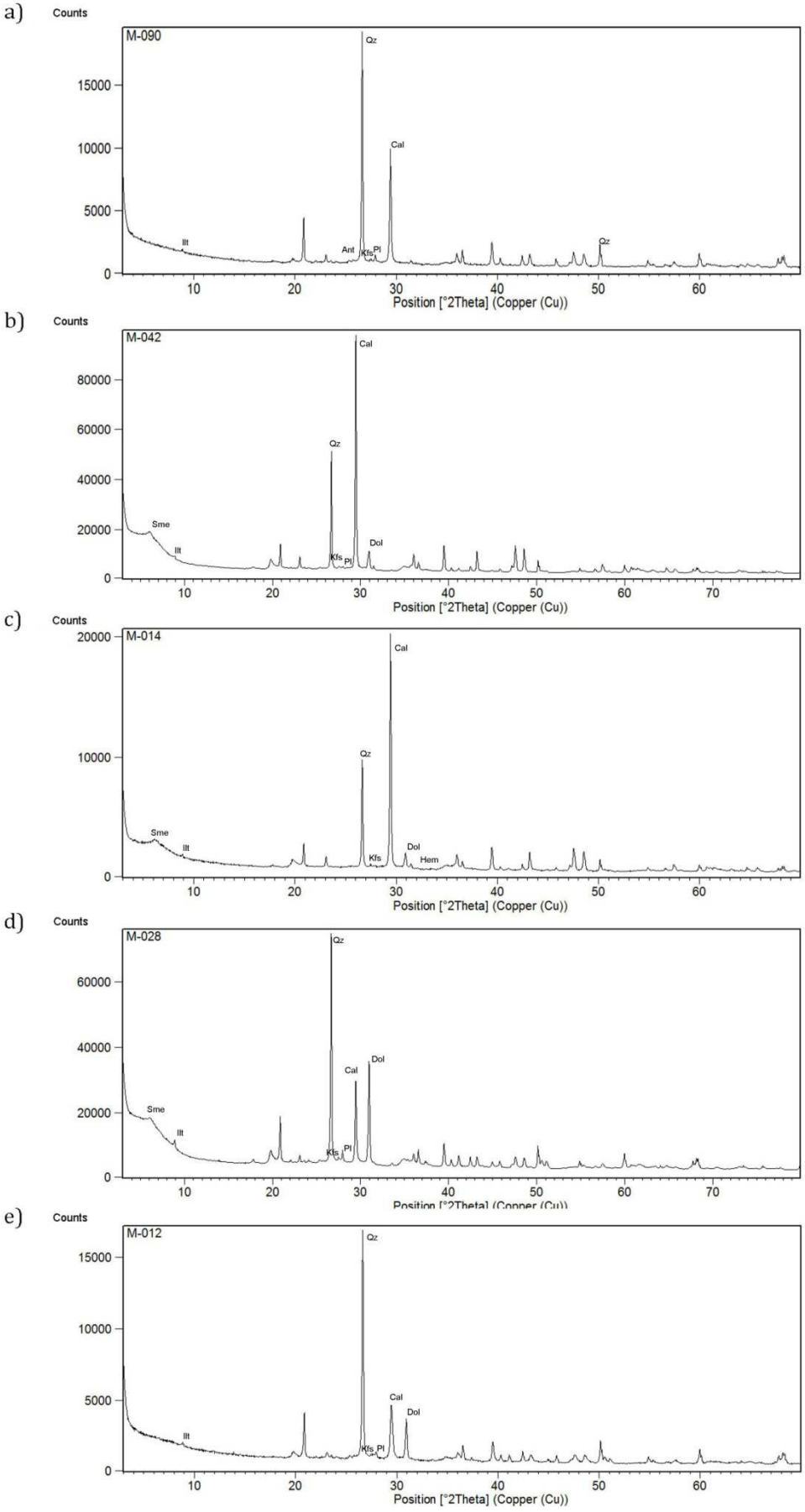

Figure 3. 29.1. Examples of diffractograms representative of the different XRPD groups: a) group $A1_{xrd}$, sample M090: b) group $A3_{xrd,}$ sample M042; c) group $A2_{xrd}$, sample M014; d) group $B2_{xrd}$, sample M028; e) group $B1_{xrd}$, sample M012.

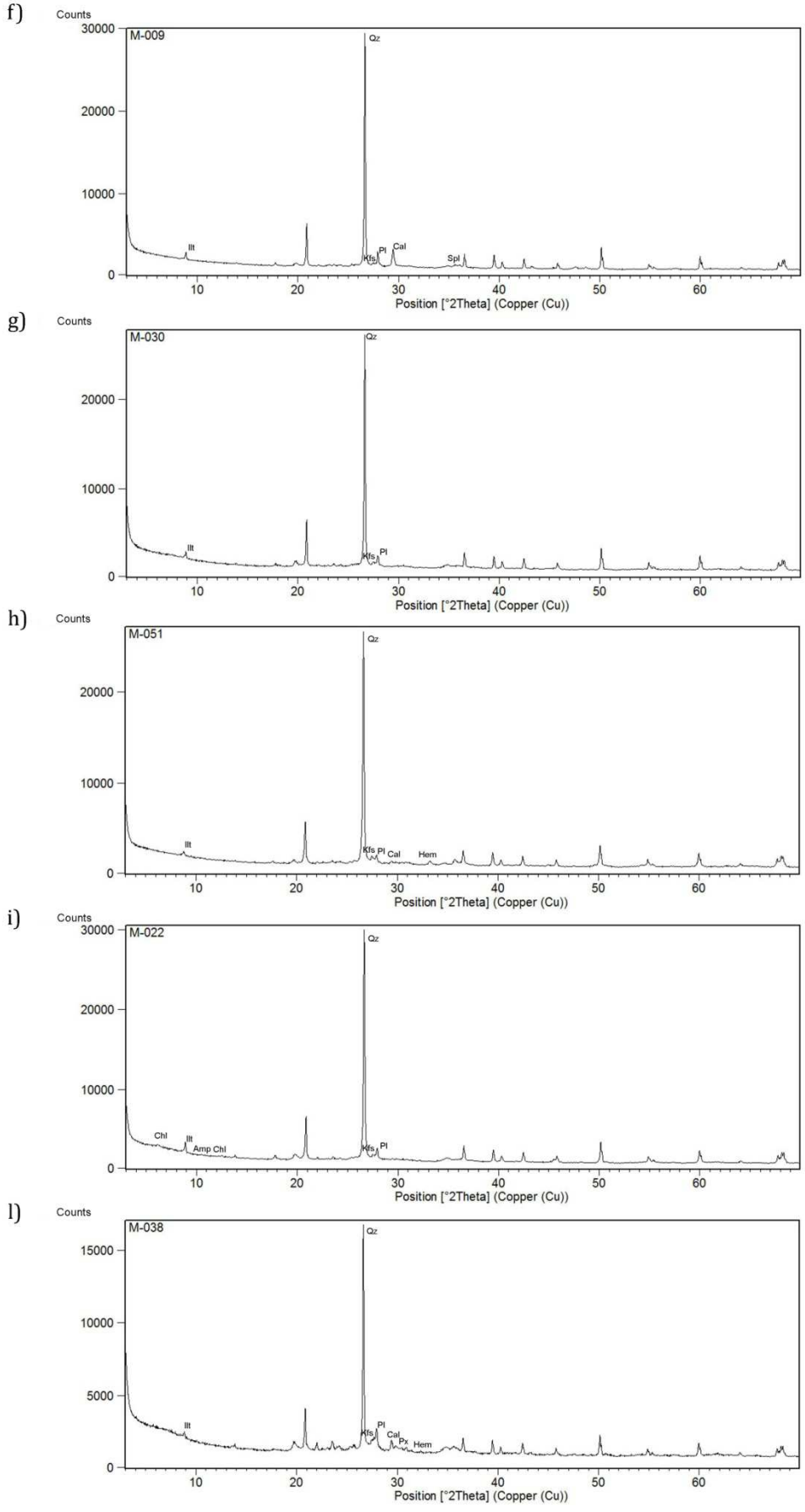

Figure 3.29.2. Examples of diffractograms representative of the different XRPD groups: f) group C_{xrd}, sample M009: g) group $D1_{xrd,}$ sample M030; h) group $D2_{xrd}$, sample M051; i) group $D3_{xrd}$, sample M022; l) group E_{xrd}, sample M038.

3.6 Chemical and statistical analysis

The bulk chemistry of fifty-three samples was determined by X-ray fluorescence spectroscopy at the Department of Geoscienze, University of Padova. For each sample the quantitative analyses were performed calculating the concentration of the major and minor elements, expressed in wt% of their oxides (SiO_2, TiO_2, Al_2O_3, Fe_2O_3, MnO, MgO, CaO, Na_2O, K_2O, P_2O_5), and of trace elements, expressed in ppm (Sc, V, Cr, Co, Ni, Cu, Zn, Ga, Rb, Sr, Y, Zr, Nb, Ba, La, Ce, Nd, Pb, Th, and U). Chemical data were statistically treated using descriptive and multivariate approaches in order to form clusters of similar materials and to determine compositional reference groups. The work was carried on on a *n* x *p* data matrix with (n= number of cases) *53 > 30* (p= number of variables describing the geochemical composition of the artefacts) (table 3.7).

The preliminary chemical analyses were based on a descriptive approach on one variable procedures and the graphical summary in order to investigate the general trend and the distribution type. The *median*, the *mean*, the *variance*, the *standard deviation*, the *coefficient of variation*, the *first* and *third quartiles* were calculated. The normal probability plot was performed through the *Anderson-Darling test*. Also graphical displays were created including the *histogram* with fitted probability density function and the *box-plot* with indication of the outliers (figures 3.30-31).

Variable	A	SD	V	CV	MIN	IQ	MED	IIIQ	MAX	p-value
SiO2	58,02	8,49	72,13	14,64	38,74	51,17	59,14	65,71	70,88	**0,14**
TiO2	0,85	0,09	0,01	10,38	0,59	0,79	0,85	0,91	1,07	**0,86**
Al2O3	16,76	1,82	3,33	10,88	13,30	15,59	16,52	18,01	21,65	**0,06**
Fe2O3	7,52	0,99	0,98	13,13	5,50	6,91	7,29	8,26	10,03	**0,12**
MnO	0,18	0,05	0,00	29,29	0,07	0,14	0,18	0,22	0,29	**0,19**
MgO	2,40	1,34	1,80	55,96	0,64	1,37	2,03	3,21	7,12	<0,005
CaO	10,85	8,17	66,69	75,30	1,45	2,11	9,50	17,54	28,73	<0,005
Na2O	0,52	0,25	0,06	48,32	0,09	0,37	0,53	0,62	1,41	0,03
K2O	1,59	0,37	0,14	23,46	1,02	1,34	1,60	1,83	2,97	**0,14**
P2O5	0,64	0,36	0,13	56,56	0,10	0,35	0,62	0,87	1,68	**0,16**
V	123,83	18,20	331,30	14,70	69,00	113,00	124,00	135,50	177,00	**0,52**
Cr	160,92	37,40	1398,84	23,24	52,00	142,00	159,00	174,00	274,00	<0,005
Co	22,66	7,03	49,46	31,04	11,00	17,00	21,00	28,00	38,00	**0,12**
Ni	121,06	39,00	1521,21	32,22	29,00	97,50	112,00	146,00	212,00	0,01
Cu	98,30	30,33	919,91	30,85	37,00	79,00	91,00	114,50	216,00	0,05
Zn	199,72	51,09	2610,51	25,58	111,00	161,00	186,00	233,00	344,00	<0,005
Ga	17,28	4,31	18,55	24,92	7,00	14,50	18,00	20,00	27,00	**0,51**
Rb	93,45	20,60	424,41	22,04	49,00	83,00	93,00	109,00	142,00	**0,66**
Sr	86,49	34,82	1212,45	40,26	49,00	70,00	78,00	89,50	268,00	<0,005
Y	57,96	19,33	373,65	33,35	28,00	43,00	56,00	68,00	109,00	**0,10**
Zr	207,74	33,58	1127,85	16,17	133,00	187,50	209,00	230,00	276,00	**0,69**
Nb	14,59	1,47	2,17	10,10	12,00	14,00	14,00	15,00	19,00	<0,005
Ba	514,50	102,70	10542,80	19,96	259,00	425,00	504,00	588,50	729,00	**0,36**
La	50,00	13,75	189,08	27,50	24,00	38,00	47,00	59,50	86,00	0,04
Ce	77,91	13,66	186,63	17,54	43,00	70,50	79,00	87,00	117,00	**0,63**
Nd	32,13	11,98	143,62	37,30	12,00	23,00	31,00	36,00	64,00	0,04
Pb	34,75	40,04	1603,03	115,20	18,00	25,50	29,00	32,00	318,00	<0,005
Th	8,55	3,46	11,98	40,50	1,00	6,50	8,00	10,00	19,00	<0,005
U	3,15	1,98	3,90	62,67	1,00	1,00	3,00	5,00	7,00	<0,005

Table 3. 6. Average (A), standard deviation (SD), variance (V), coefficient of variation (CV), minimum (MIN), first quartile (IQ), median (MED), third quartile (IIIQ) and maximum (MAX) values and the p-value of the Anderson–Darling normality test for the studied potsherds

samples	SiO_2	TiO_2	Al_2O_3	Fe_2O_3	MnO	MgO	CaO	Na_2O	K_2O	P_2O_5	V	Cr	Co	Ni	Cu	Zn	Ga	Rb	Sr	Y	Zr	Nb	Ba	La	Ce	Nd	Pb	Th	U		L.O.I.	FeO
M001	67,78	0,79	15,59	7,83	0,15	0,82	1,92	0,49	1,45	1,4	120	157	14	93	82	219	17	87	67	68	209	14	493	59	82	44	35	4	3		17,98	1,50
M002	68,87	0,72	15,47	6,94	0,12	1,4	1,81	0,54	1,62	0,7	110	190	17	98	105	269	19	103	64	64	203	13	575	48	58	34	30	6	5		13,53	1,24
M003	69,41	0,91	15,67	7,31	0,22	1,03	1,54	0,67	1,74	0,62	120	154	21	97	87	258	10	86	69	59	246	15	453	37	87	34	29	8	5		12,64	1,46
M004	66,44	0,96	17,2	7,94	0,23	1,07	2,17	0,72	1,91	0,96	125	164	21	101	143	237	20	93	77	64	267	16	494	66	98	36	32	7	6		14,22	1,17
M005	57,74	0,83	17,18	7,1	0,12	3,6	7,85	1,41	2,97	0,18	125	193	20	129	69	111	23	142	268	31	158	14	425	38	78	26	27	8	4		14,96	1,69
M006	57,61	0,94	18,32	7,89	0,23	1,5	11,23	0,43	1,42	0,47	141	191	24	142	100	160	21	60	76	72	206	15	373	51	77	49	29	7	1		24,35	0,72
M007	53,69	0,88	19,49	9,04	0,19	3,15	9,71	0,53	1,83	0,71	143	172	25	176	114	232	18	93	74	51	196	14	505	52	80	32	27	6	1		19,52	1,40
M008	54,21	0,84	18,59	8,65	0,22	3,9	10,22	0,52	2,22	0,71	132	149	28	134	99	166	16	114	86	48	180	16	652	41	85	16	34	7	5		17,69	0,94
M009	60,56	0,83	18,49	8,56	0,14	1,49	6,45	0,58	1,44	0,62	134	160	28	129	115	211	20	71	65	45	188	15	380	54	81	35	41	5	4		17,55	1,04
M012	53,16	0,77	15,98	7,01	0,17	3,67	16,06	0,35	1,62	0,86	126	159	19	146	109	194	15	89	73	65	166	14	503	44	72	35	30	6	1		22,77	0,76
M013	60,11	0,76	13,76	5,73	0,13	3,72	12,61	0,54	1,39	0,15	109	138	17	81	90	157	18	96	80	30	205	12	462	38	79	16	24	9	3		17,60	0,84
M014	44,59	0,79	16,65	6,91	0,14	2,51	26,48	0,2	1,02	0,18	129	112	29	117	81	160	24	117	113	43	151	13	604	38	80	12	30	11	4		25,35	0,78
M016	59,74	0,83	15,88	8,78	0,09	1,92	9,33	0,76	1,46	0,93	113	158	15	75	67	159	11	75	86	42	263	14	381	52	79	35	23	8	5		18,12	1,70
M017	61,28	0,86	14,97	6,23	0,08	3,57	9,5	0,8	1,88	0,34	101	127	12	64	46	151	14	115	90	36	231	14	502	34	71	18	24	13	1		15,27	0,97
M018	60,91	0,93	18,04	8,45	0,22	1,84	7,04	0,53	1,63	0,3	139	174	21	116	123	184	21	87	70	59	233	14	504	54	76	31	29	9	4		17,44	1,21
M019	53,95	0,85	15,58	7,2	0,16	0,82	19,16	0,44	1,25	0,2	117	161	15	93	82	134	12	69	76	37	230	14	364	35	71	22	25	10	5		22,87	1,14
M020	48,52	0,94	16,79	8,09	0,24	1,87	20,8	0,32	1,07	0,76	120	274	32	212	105	194	12	64	96	83	210	16	402	62	95	52	24	11	5		25,23	0,99
M022	68,6	0,81	15,75	7,14	0,2	1,59	1,9	0,61	1,94	0,7	116	142	22	105	82	265	10	109	74	62	222	16	612	56	81	29	28	8	1		11,43	1,11
M023	68,97	0,83	16,92	7,86	0,19	0,93	1,84	0,51	1,57	0,6	128	163	24	103	102	169	14	82	62	78	221	14	402	61	86	43	30	5	3		15,60	1,60
M025	38,74	0,59	19,97	5,5	0,09	6,55	24,62	0,23	1,02	1,68	69	52	12	29	59	162	12	49	95	51	231	15	425	40	117	51	51	19	3			
M026	58,26	0,86	17,98	8,21	0,22	3,37	7,45	0,56	1,6	0,71	150	160	29	173	73	218	21	103	76	56	194	14	635	47	73	31	32	13	7			
M027	66,62	0,77	17,05	8,98	0,29	1,03	1,86	0,39	1,42	0,99	137	150	17	111	109	247	21	85	54	95	190	14	547	86	82	46	31	5	4		17,34	1,46
M029	56,95	0,77	13,3	6,56	0,15	1,06	17,23	0,74	1,66	0,91	97	136	15	81	86	149	15	84	211	63	230	13	498	59	70	35	27	8	4		18,98	1,35
M030	63,39	1,02	20	8,93	0,26	1,12	1,45	0,56	1,86	0,36	155	197	28	130	143	186	19	90	53	63	257	17	518	58	92	36	33	8	5		17,02	1,55
M032	66,9	0,93	16,16	8,69	0,17	0,92	1,7	0,82	1,55	1,4	115	150	15	87	102	234	16	75	70	97	276	17	365	84	87	64	32	7	4		13,45	1,29
M034	70,88	0,9	15,27	6,29	0,25	0,64	1,5	0,42	1,34	0,71	118	161	20	102	216	223	7	80	49	47	216	15	406	47	81	34	33	6	5		14,32	1,07
M035	60,66	0,89	16,14	6,91	0,13	2,86	8,71	0,58	1,82	0,57	124	194	24	153	65	192	16	110	70	41	217	14	562	31	58	30	29	17	1			
M036	43,14	0,71	15,37	6,52	0,14	3,22	28,73	0,22	1,13	0,1	135	114	34	109	79	220	17	111	105	33	133	14	514	32	59	25	28	13	1			
M037	59,14	0,76	13,96	6,17	0,07	2,16	13,61	0,67	1,56	0,16	103	120	12	72	37	210	17	128	83	28	186	14	496	39	56	24	20	14	1			
M038	56,95	1,07	20,6	10,03	0,19	2,08	3,76	1,22	2,52	1,12	143	118	20	74	105	250	15	115	120	52	257	15	729	45	101	27	38	4	6		15,04	0,82
M039	70,43	0,81	14,89	6,6	0,18	1,93	1,79	0,58	2	0,52	118	123	23	101	97	215	21	98	76	58	203	13	581	42	82	17	22	9	3		10,04	1,32
M040	59,19	0,84	14,26	6,26	0,14	2,84	12,33	0,54	1,49	0,44	107	160	19	101	62	180	13	88	81	32	222	13	503	24	67	21	30	13	1			
M041	42,84	0,75	16,8	7,29	0,13	3,19	26,9	0,17	1,02	0,19	132	123	34	134	78	320	20	109	104	45	142	12	635	37	70	22	34	13	1			
M043	47,61	0,77	16,52	7,36	0,18	3,73	21,28	0,28	1,24	0,16	133	151	34	166	79	344	19	121	89	39	151	14	596	38	55	24	30	14	1			
M044	68,81	0,8	16,14	7,18	0,17	1,97	2,05	0,54	1,75	0,2	124	142	24	112	104	263	20	125	70	52	201	13	571	46	77	27	27	8	7		10,76	0,92
M045	68,63	0,84	16	7,33	0,2	1,74	1,58	0,63	1,96	0,63	115	145	17	110	116	281	18	109	69	62	224	13	609	60	72	24	30	6	5		11,25	1,00
M051	64,97	0,87	17,35	8,2	0,2	1,62	2,05	0,39	1,75	0,87	92	149	28	112	145	191	19	66	67	81	223	15	396	79	87	48	36	1	1		10,20	1,10

Table 3.7. Geochemical composition of samples obtained by XRF. The FeO values ware obtained by titration.

samples	SiO_2	TiO_2	Al_2O_3	Fe_2O_3	MnO	MgO	CaO	Na_2O	K_2O	P_2O_5	V	Cr	Co	Ni	Cu	Zn	Ga	Rb	Sr	Y	Zr	Nb	Ba	La	Ce	Nd	Pb	Th	U		L.O.I.	FeO
M056	69,61	0,9	15,24	6,72	0,16	1,81	2,4	0,67	1,85	0,29	96	157	17	103	85	179	22	105	62	43	232	14	491	39	87	29	29	7	5		9,32	0,83
M068	62,87	0,96	16,86	7,3	0,1	1,08	7,74	0,92	1,85	0,6	112	176	13	177	76	164	15	91	80	44	254	17	503	39	84	26	22	12	5		16,63	1,61
M069	64,14	0,93	16,69	7	0,09	2,41	5,95	0,89	1,8	0,46	116	151	11	79	75	160	16	95	82	48	263	17	499	38	89	28	24	10	1		15,76	1,56
M071	60,27	0,98	18,68	8,54	0,22	2,03	6,49	0,4	1,34	0,31	136	259	33	181	124	172	20	51	69	97	228	18	259	70	95	62	37	6	1		18,43	1,73
M075	49,15	0,85	14,74	6,95	0,23	7,12	18,02	0,38	1,38	0,74	128	194	25	146	130	235	16	84	75	72	197	15	565	61	65	44	24	10	1		24,53	0,98
M079	47,61	0,78	15,8	7,08	0,12	2,88	23,01	0,16	1,2	1,16	111	174	20	105	89	134	8	63	104	35	187	14	406	36	54	19	18	8	6		25,68	1,18
M080	42,55	0,79	16,77	7,19	0,22	2,57	27,07	0,2	1,22	0,46	128	123	32	118	90	165	18	117	106	68	162	14	716	55	76	16	24	7	1		26,66	0,81
M083	50,14	0,69	14,58	6,36	0,26	3,93	20,14	0,34	1,43	0,95	109	169	19	162	127	154	14	89	119	59	167	13	564	47	43	31	24	8	1		22,74	0,71
M086	47,64	0,84	20	8,92	0,2	4,38	14,77	0,09	1,97	1,18	160	171	32	186	118	184	25	119	98	88	165	14	622	65	68	41	32	9	1		23,46	1,18
M088	52,91	0,87	16,01	7,21	0,18	1,96	18,09	0,53	1,25	0,46	115	129	22	94	73	139	19	100	89	55	195	15	608	66	76	22	27	8	3		22,27	0,86
M090	51,88	0,93	17,42	8,22	0,21	1,34	17,09	0,44	1,2	0,37	136	271	31	194	91	170	20	55	86	109	215	19	349	71	90	57	318	1	1		23,59	0,83
M092	49,35	0,91	19	8,3	0,2	1,32	17,84	0,33	1,1	0,84	143	181	35	162	113	172	16	88	84	75	194	15	662	60	73	31	31	9	1		25,38	1,23
M098	50,45	0,89	21,65	9,33	0,21	3,45	10,38	0,1	1,62	1,06	177	192	38	212	167	330	27	109	78	89	179	15	692	57	97	36	32	7	3		21,77	0,91
M101	61,53	0,85	16,08	6,69	0,13	3,03	8,33	0,57	1,68	0,38	125	173	21	98	89	157	20	103	74	42	224	15	532	49	73	20	26	9	1		16,77	0,64
M102	57,2	1	18,8	7,93	0,22	2,06	9,94	0,5	1,63	0,65	143	172	25	119	117	190	25	100	86	65	219	17	564	46	95	34	34	8	6		20,09	
M103	57,46	0,86	15,96	7,28	0,2	3,15	11,36	0,58	1,67	0,69	113	154	18	112	90	165	14	86	84	51	191	13	565	37	62	22	26	8	4		18,70	1,54

Table 3.7. Geochemical composition of samples obtained by XRF. The FeO values ware obtained by titration.

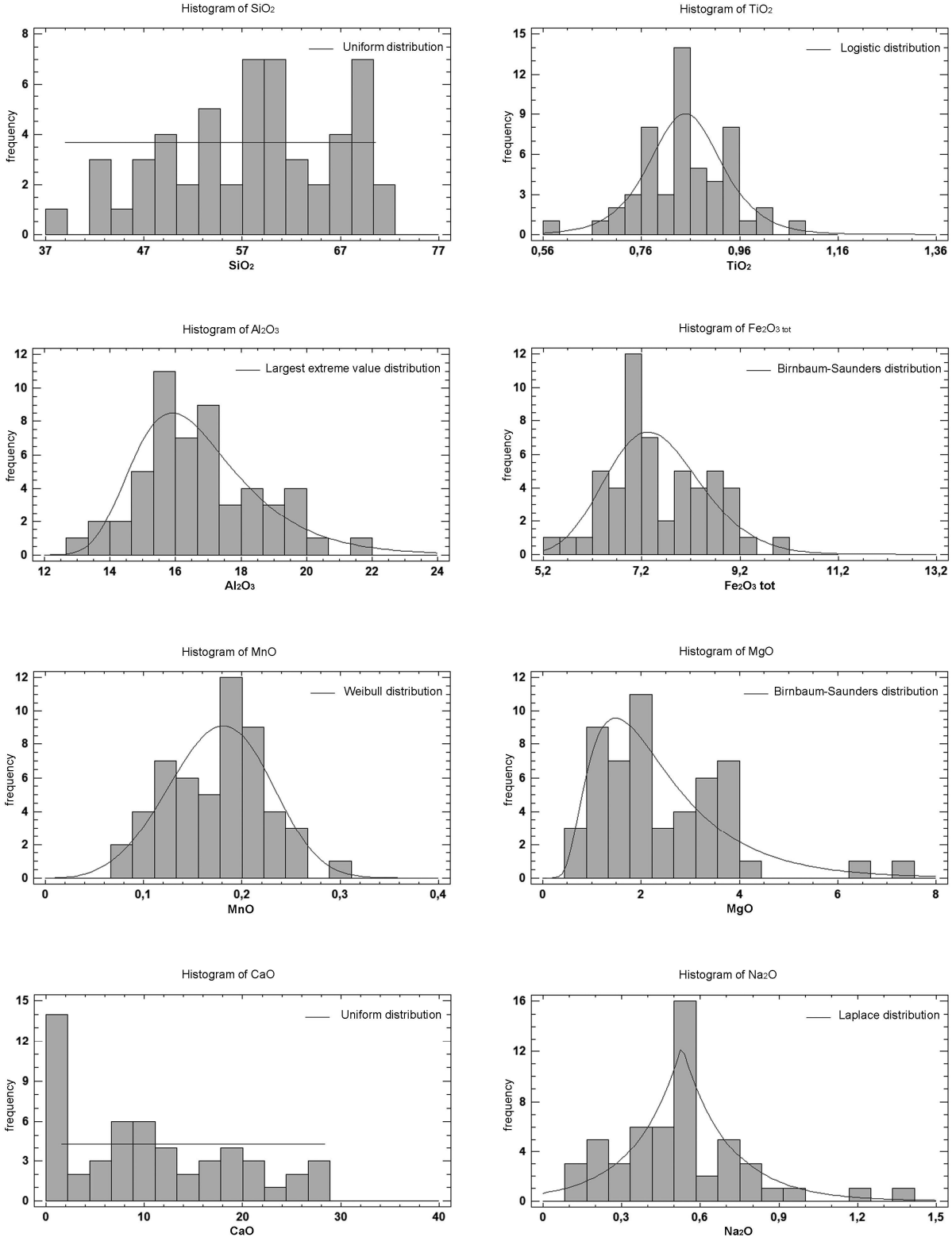

Figure 3.30 a. Histogram with fitted probability density function of the chemical data.

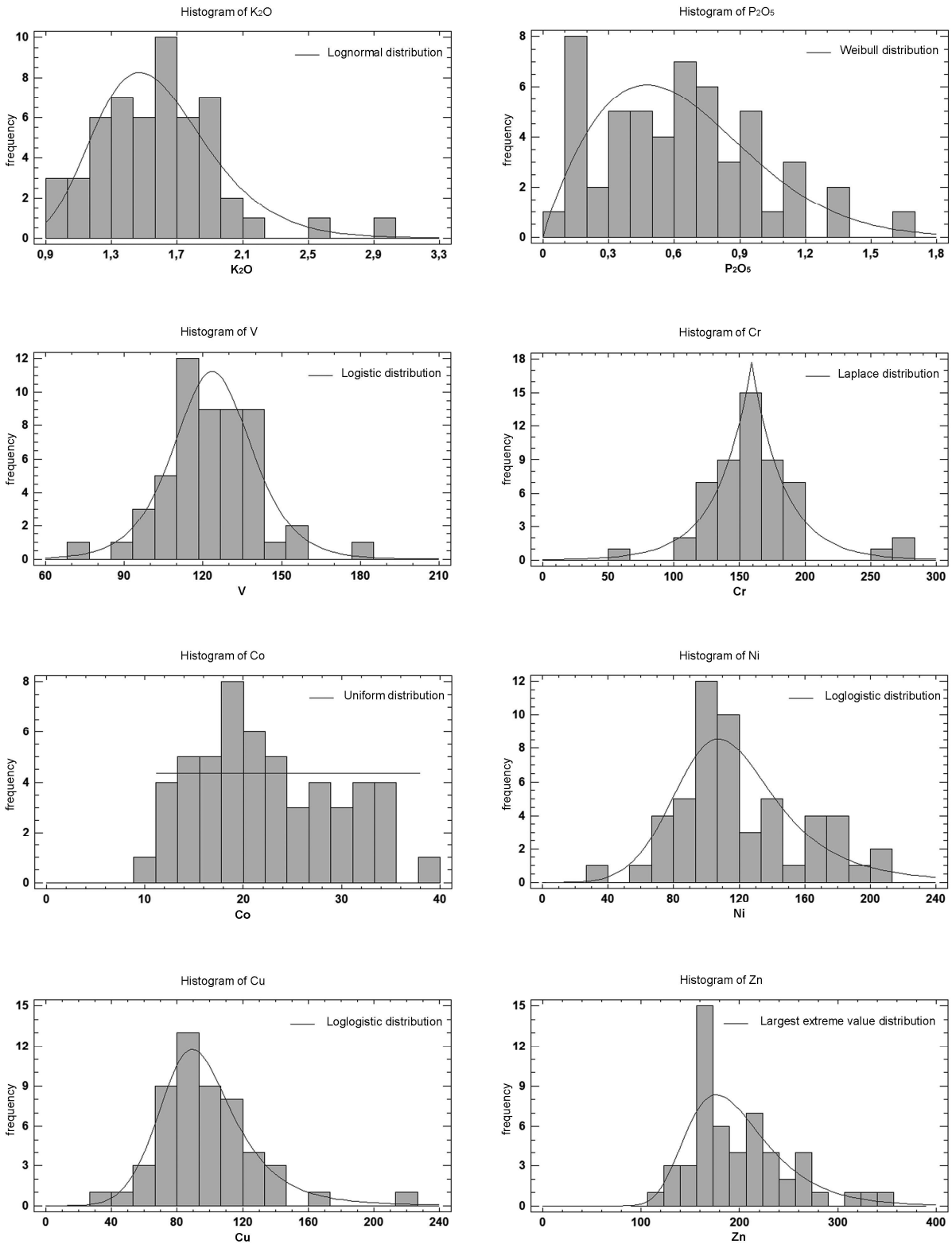

Figure 3.30.b. Histogram with fitted probability density function of the chemical data.

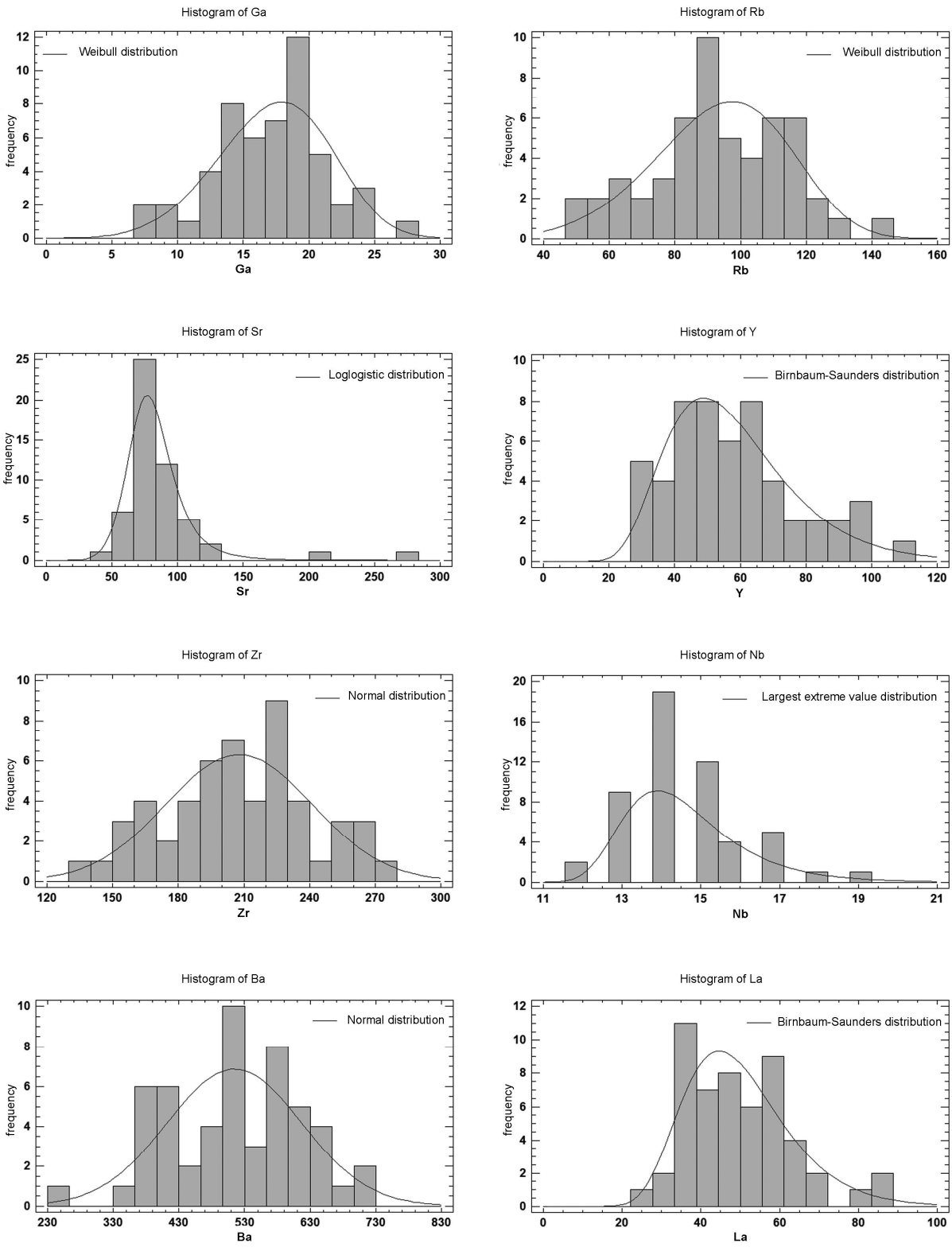

Figure 3.30.c. Histogram with fitted probability density function of the chemical data.

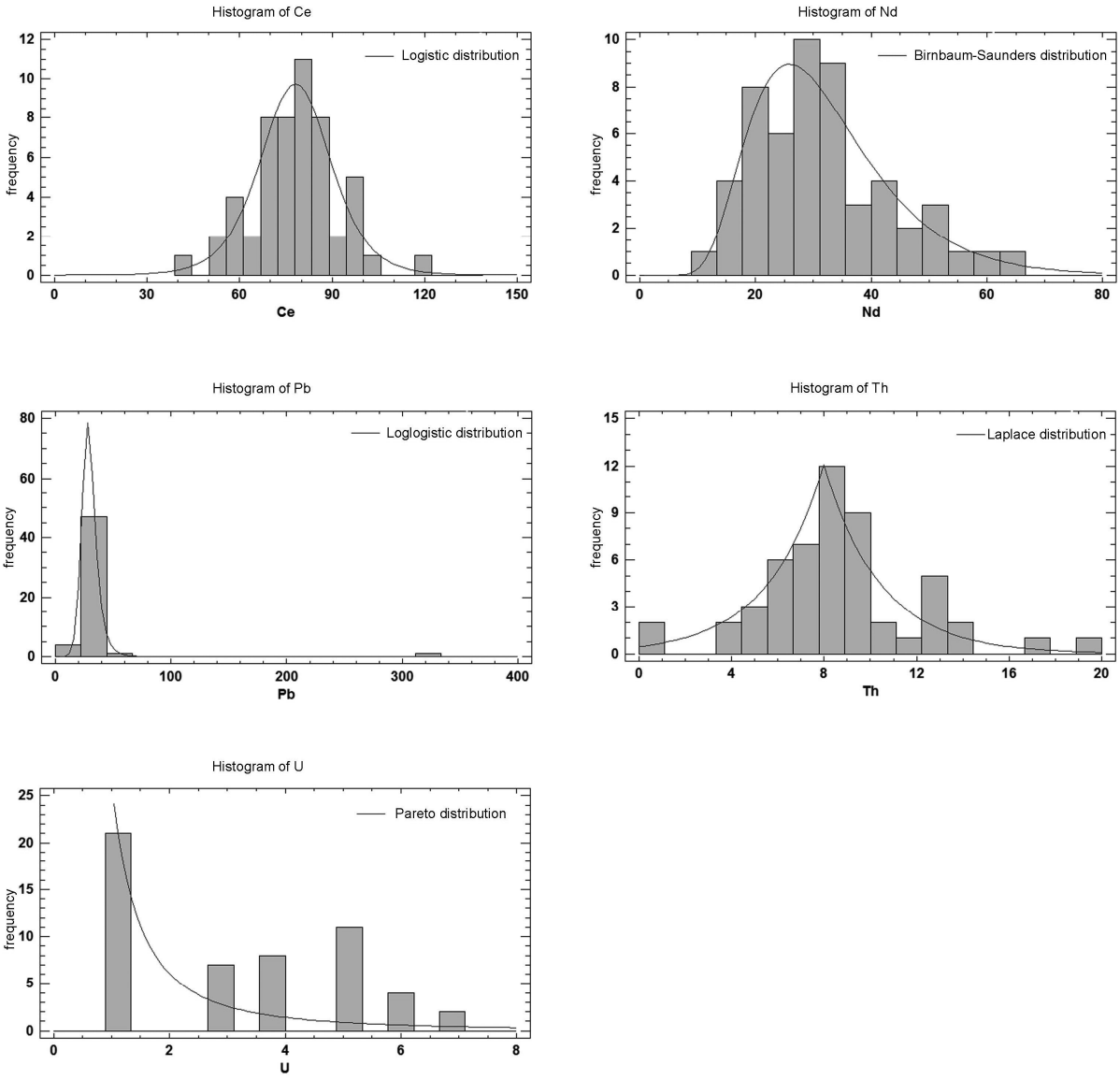

Figure 3.30.d. Histogram with fitted probability density function of the chemical data.

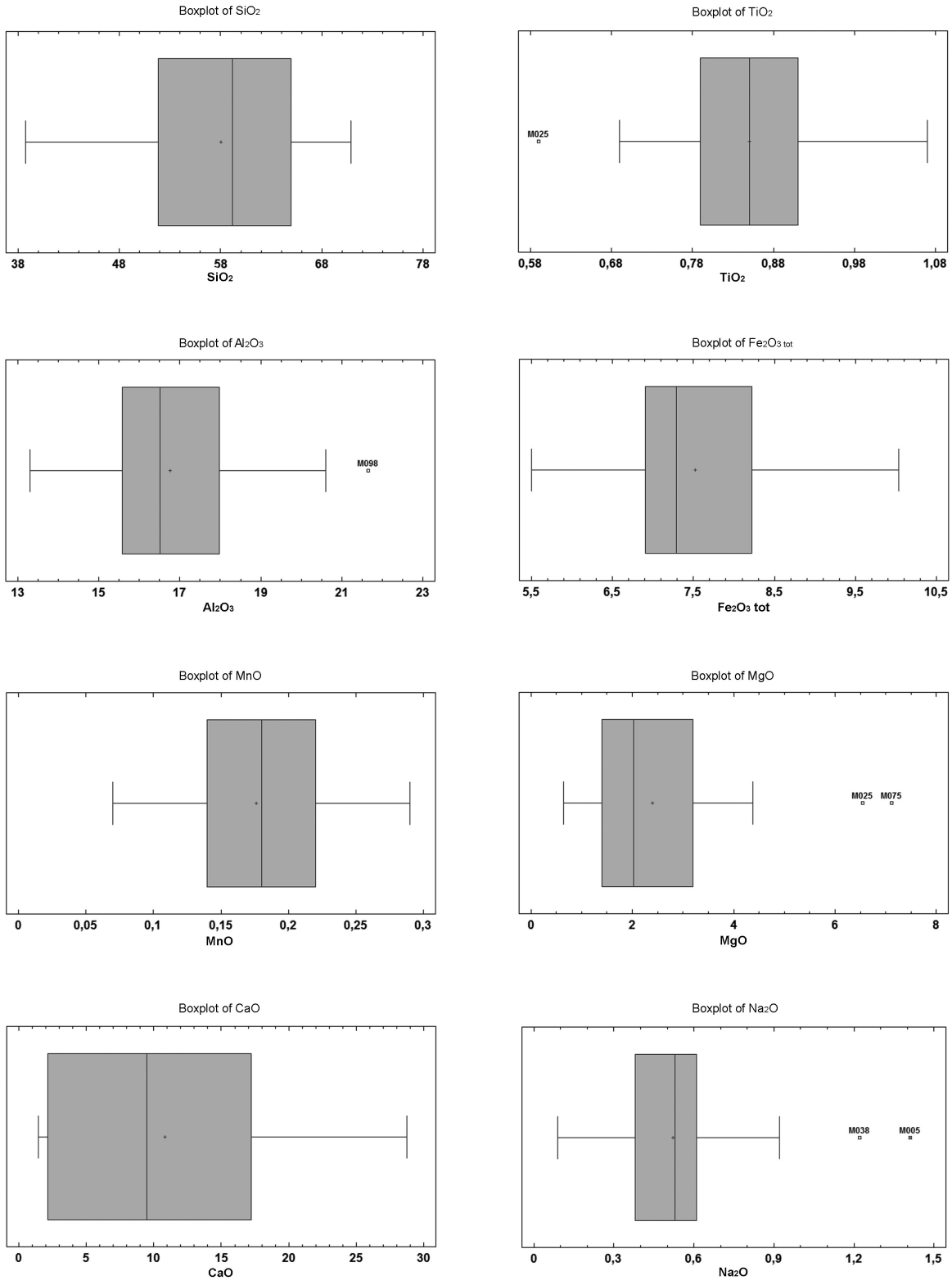

Figure 3.31.a. Box-plot representing the chemical data with indication of the outliers.

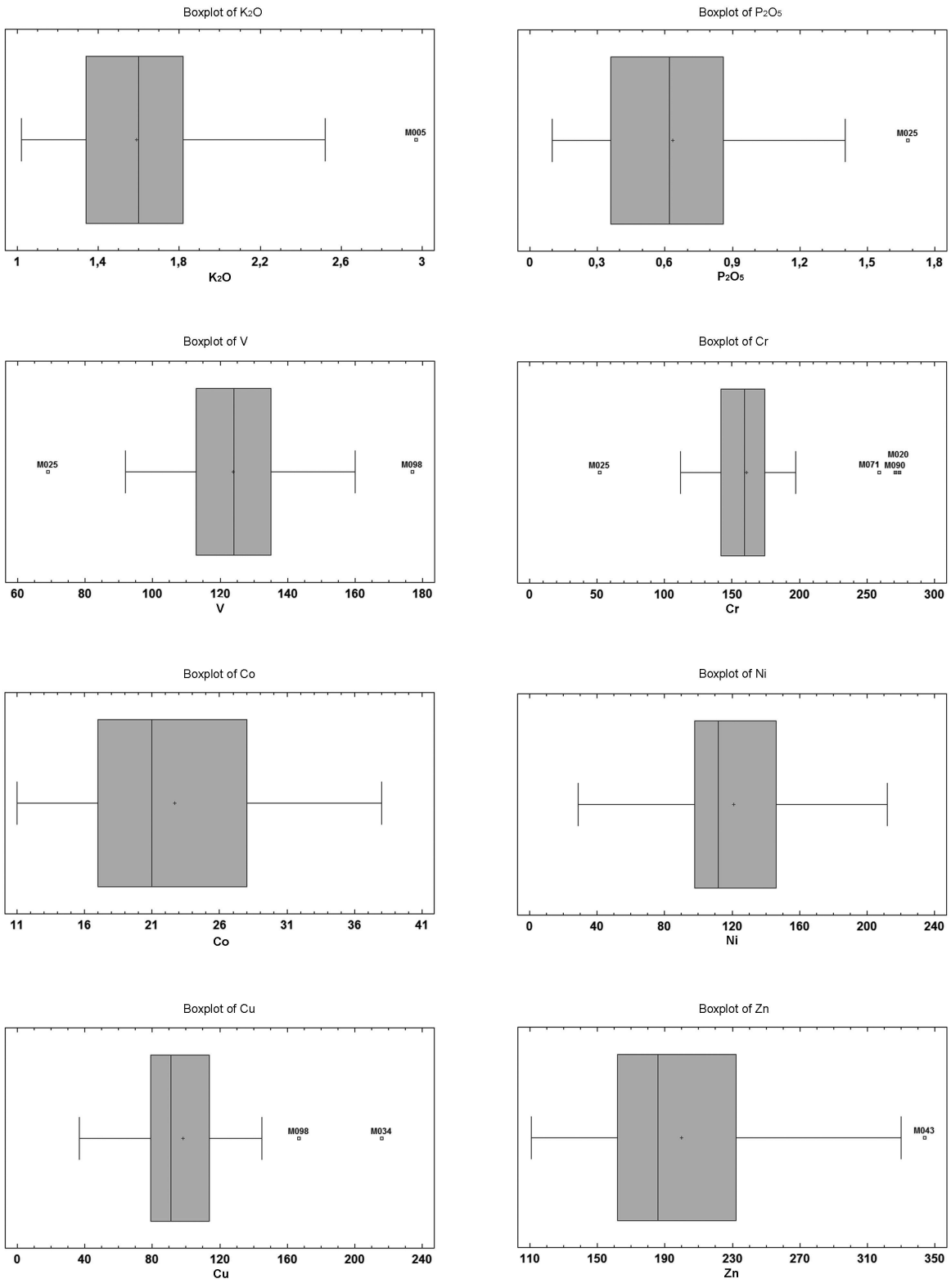

Figure 3.31.b. Box-plot representing the chemical data with indication of the outliers.

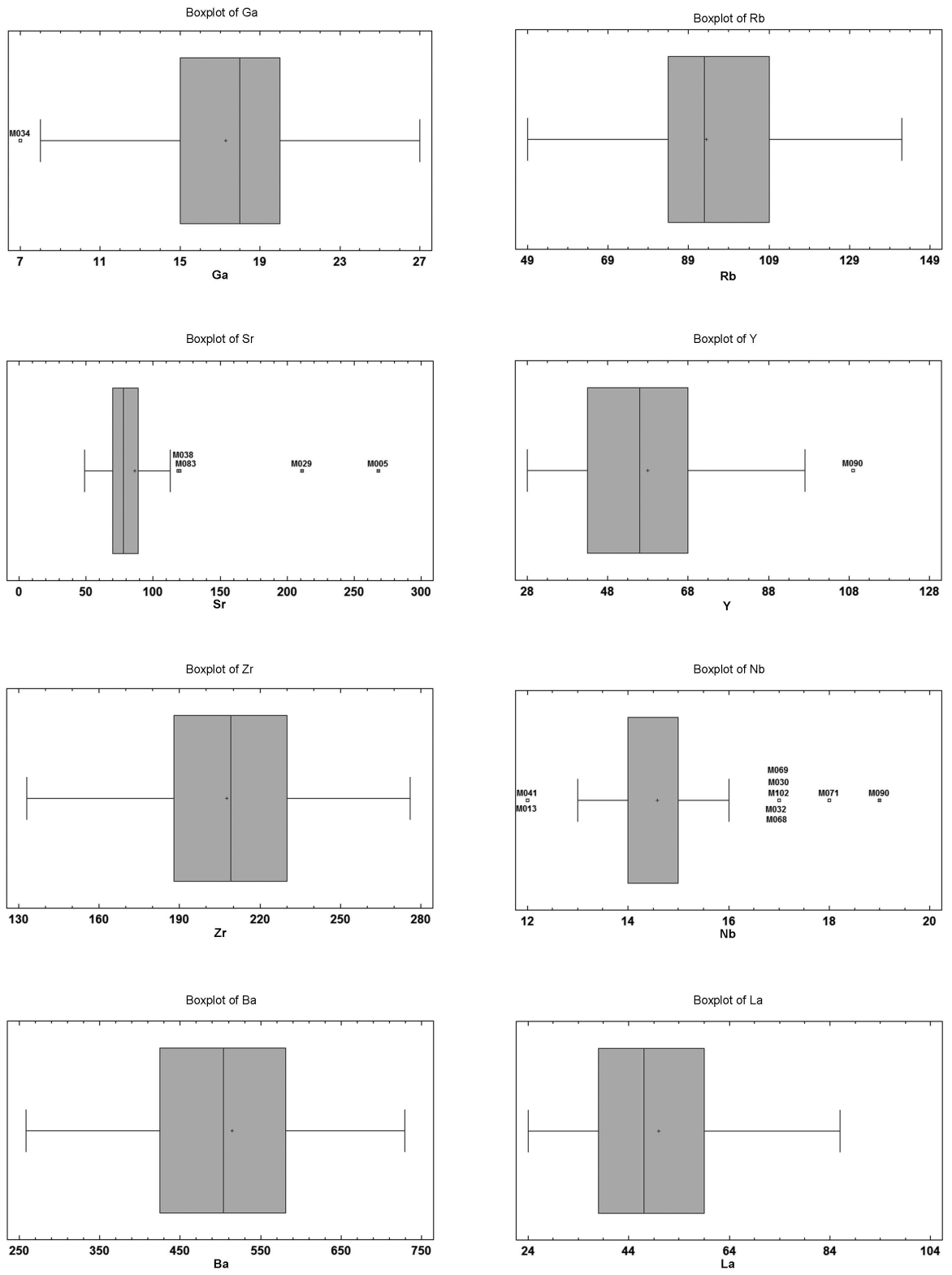

Figure 3.31c. Box-plot representing the chemical data with indication of the outliers.

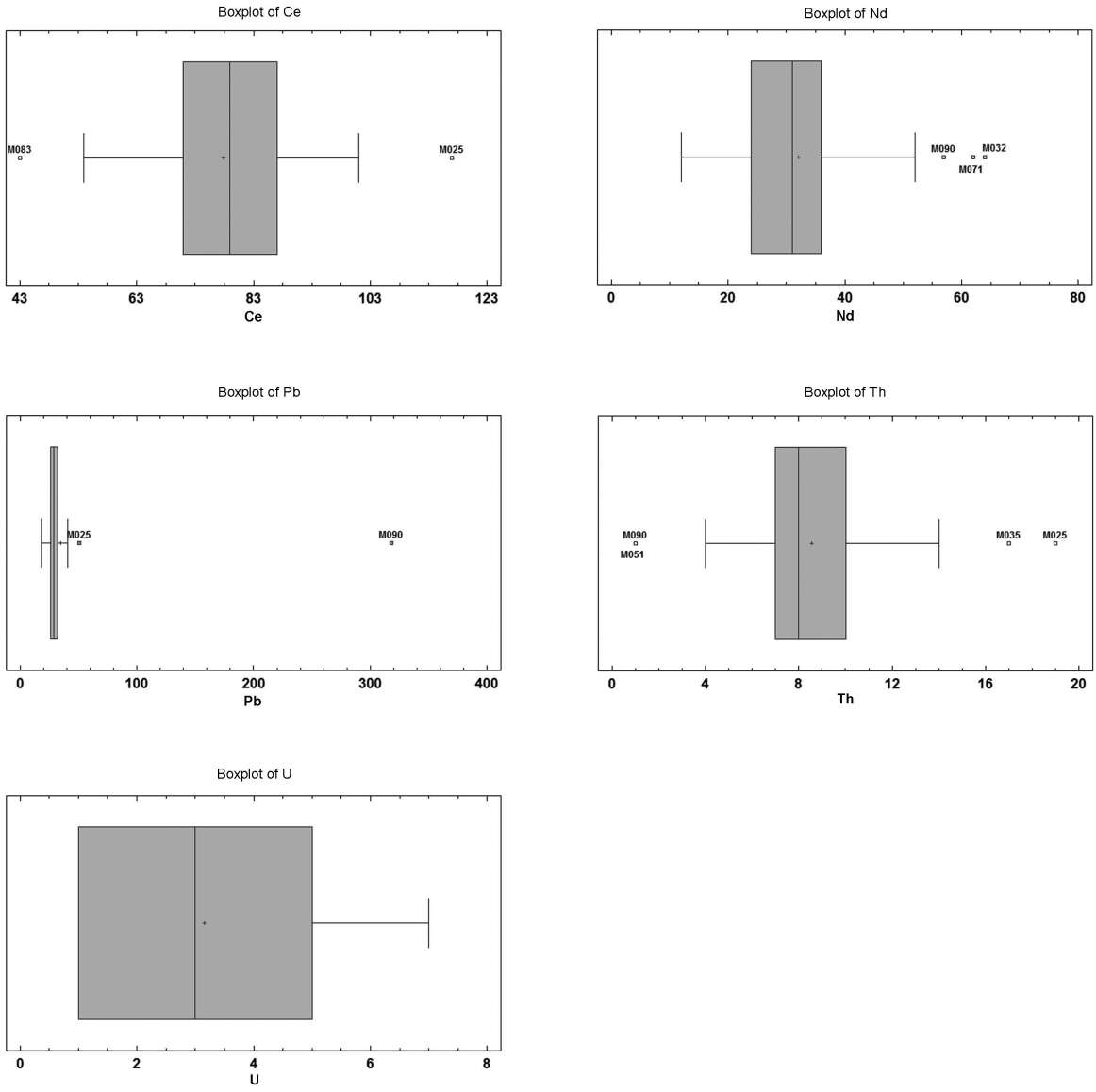

Figure 3.31.d. Box-plot representing the chemical data with indication of the outliers.

The samples analyzed showed compositional heterogeneity, expressed by the standard deviations and the wide distribution intervals. Furthermore, the coefficient of variations for several elements was greater than 50% and for the Pb reaches the 115% and the Anderson Darling normality test indicated that only the 52% of the variables follow a normal distribution (p-value > 0,05) (table 3.6). Examining the *box-plot*, it appeared that only seventeen variables had at least one sample that could be considered an outlier. The samples with anomalous values for the higher number of chemical elements are the M025 and M090 (figure 3.32). These situations is due to the coarse-paste pottery, to the different mineralogical and petrographic inclusions types and to the several fabrics recognized. In order to distinguish paste compositional reference units (PCRUs) and outliers, multivariate statistical representation (cluster analysis and principal component analysis) were fulfilled. The analyses were performed on the standardized values of the elements transformed to base 10 logarithms (table 3.8).

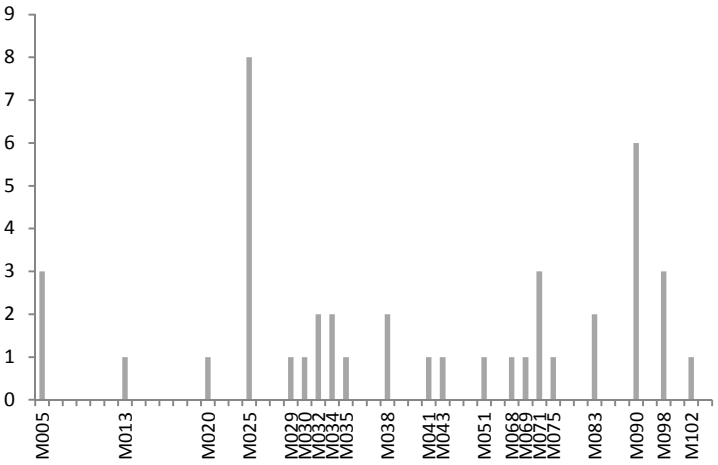

Figure 3.32. Frequency of the outliers observed respect of all the variables (chemical elements) analyzed.

Buried pottery may undergo post-depositional alterations. Temperature cycles, freezing, load pressure, groundwater composition, acidity, saturation and redox conditions are the main environmental parameters controlling burial alteration processes. Of these, groundwater is the main weathering agent determining chemical and mineralogical transformations of pottery by dissolution, alteration and/or precipitation of secondary mineral phases on the surface or, through open pores, inside the potsherds (Freestone 2001, Maritan, Mazzoli 2004, Schwedt, Mommsen et al. 2006). Variations in the pristine chemical composition of the pottery represent good evidence of chemico-physical alterations of archaeological finds during burial. This suggests caution when interpreting archaeometrical data in provenance studies and when estimating firing conditions (Secco, Maritan et al. 2011). Phosphate oxide is commonly considered a good indicator of the alteration processes that can take place during burial (Lemoine, Meille et al. 1981, Lemoine, Picon 1982, Freestone 2001). In this work the multivariate analyses were carried out excluding the concentration of P_2O_5, since here it varied over an interval (0,10-1.68 wt%) much wider than that observed in the clayey materials sampled closed to the site (0,08-0,20 wt%) with the most of the samples that exceeded this value. This so high concentration observed was interpreted as a contamination effect (Freestone, Middleton et al. 1994, Freestone 2001, Lemoine, Picon 1982, Maritan, Mazzoli 2004, Picon 1985).

The cluster analysis was performed using the squared Euclidean distance and the average algorithm. The dendrogram indicates that samples tend to group into three main clusters (figure 3.33) that only partially match with the petro-fabrics observed at microscope: cluster 1 (CL1) is formed by all the samples belonging to fabrics F5, F6 and F9 (except sample M005), rich in chert fragments, crystals of quartz and volcanic rocks, respectively. These potsherds have abundance of SiO_2 as it was well conformed also by the XRD analysis. The cluster 2 (CL2) is composed by twenty-one samples mostly related to the fabrics F1, F4 and F3, all rich in carbonatic inclusions associated to polycrystalline quartz, chert fragments and -fabric F3- also to mica shist and graphite shist. There are also few samples of fabrics F2, rich in carbonatic inclusions but differentiated in the shapes, arrangements and c:f ratio of non plastic inclusions, and sample M005 (fabric F5) rich in chert fragments.

	SiO_2	TiO_2	Al_2O_3	Fe_2O_3	MnO	MgO	CaO	Na_2O	K_2O	V	Cr	Co	Ni	Cu	Zn	Ga	Rb	Sr	Y	Zr	Nb	Ba	La	Ce	Nd	Pb	Th	U
M001	1,83	-0,10	1,19	0,89	-0,82	-0,09	0,28	-0,31	0,16	2,08	2,20	1,15	1,97	1,91	2,34	1,23	1,94	1,83	1,83	2,32	1,15	2,69	1,77	1,91	1,64	1,54	0,60	0,48
M002	1,84	-0,14	1,19	0,84	-0,92	0,15	0,26	-0,27	0,21	2,04	2,28	1,23	1,99	2,02	2,43	1,28	2,01	1,81	1,81	2,31	1,11	2,76	1,68	1,76	1,53	1,48	0,78	0,70
M003	1,84	-0,04	1,20	0,86	-0,66	0,01	0,19	-0,17	0,24	2,08	2,19	1,32	1,99	1,94	2,41	1,00	1,93	1,84	1,77	2,39	1,18	2,66	1,57	1,94	1,53	1,46	0,90	0,70
M004	1,82	-0,02	1,24	0,90	-0,64	0,03	0,34	-0,14	0,28	2,10	2,21	1,32	2,00	2,16	2,37	1,30	1,97	1,89	1,81	2,43	1,20	2,69	1,82	1,99	1,56	1,51	0,85	0,78
M005	1,76	-0,08	1,24	0,85	-0,92	0,56	0,89	0,15	0,47	2,10	2,29	1,30	2,11	1,84	2,05	1,36	2,15	2,43	1,49	2,20	1,15	2,63	1,58	1,89	1,41	1,43	0,90	0,60
M006	1,76	-0,03	1,26	0,90	-0,64	0,18	1,05	-0,37	0,15	2,15	2,28	1,38	2,15	2,00	2,20	1,32	1,78	1,88	1,86	2,31	1,18	2,57	1,71	1,89	1,69	1,46	0,85	0,00
M007	1,73	-0,06	1,29	0,96	-0,72	0,50	0,99	-0,28	0,26	2,16	2,24	1,40	2,25	2,06	2,37	1,26	1,97	1,87	1,71	2,29	1,15	2,70	1,72	1,90	1,51	1,43	0,78	0,00
M008	1,73	-0,08	1,27	0,94	-0,66	0,59	1,01	-0,28	0,35	2,12	2,17	1,45	2,13	2,00	2,22	1,20	2,06	1,93	1,68	2,26	1,20	2,81	1,61	1,93	1,20	1,53	0,85	0,70
M009	1,78	-0,08	1,27	0,93	-0,85	0,17	0,81	-0,24	0,16	2,13	2,20	1,45	2,11	2,06	2,32	1,30	1,85	1,81	1,65	2,27	1,18	2,58	1,73	1,91	1,54	1,61	0,70	0,60
M012	1,73	-0,11	1,20	0,85	-0,77	0,56	1,21	-0,46	0,21	2,10	2,20	1,28	2,16	2,04	2,29	1,18	1,95	1,86	1,81	2,22	1,15	2,70	1,64	1,86	1,54	1,48	0,78	0,00
M013	1,78	-0,12	1,14	0,76	-0,89	0,57	1,10	-0,27	0,14	2,04	2,14	1,23	1,91	1,95	2,20	1,26	1,98	1,90	1,48	2,31	1,08	2,66	1,58	1,90	1,20	1,38	0,95	0,48
M014	1,65	-0,10	1,22	0,84	-0,85	0,40	1,42	-0,70	0,01	2,11	2,05	1,46	2,07	1,91	2,20	1,38	2,07	2,05	1,63	2,18	1,11	2,78	1,58	1,90	1,08	1,48	1,04	0,60
M016	1,78	-0,08	1,20	0,94	-1,05	0,28	0,97	-0,12	0,16	2,05	2,20	1,18	1,88	1,83	2,20	1,04	1,88	1,93	1,62	2,42	1,15	2,58	1,72	1,90	1,54	1,36	0,90	0,70
M017	1,79	-0,07	1,18	0,79	-1,10	0,55	0,98	-0,10	0,27	2,00	2,10	1,08	1,81	1,66	2,18	1,15	2,06	1,95	1,56	2,36	1,15	2,70	1,53	1,85	1,26	1,38	1,11	0,00
M018	1,78	-0,03	1,26	0,93	-0,66	0,26	0,85	-0,28	0,21	2,14	2,24	1,32	2,06	2,09	2,26	1,32	1,94	1,85	1,77	2,37	1,15	2,70	1,73	1,88	1,49	1,46	0,95	0,60
M019	1,73	-0,07	1,19	0,86	-0,80	-0,09	1,28	-0,36	0,10	2,07	2,21	1,18	1,97	1,91	2,13	1,08	1,84	1,88	1,57	2,36	1,15	2,56	1,54	1,85	1,34	1,40	1,00	0,70
M020	1,69	-0,03	1,23	0,91	-0,62	0,27	1,32	-0,49	0,03	2,08	2,44	1,51	2,33	2,02	2,29	1,08	1,81	1,98	1,92	2,32	1,20	2,60	1,79	1,98	1,72	1,38	1,04	0,70
M022	1,84	-0,09	1,20	0,85	-0,70	0,20	0,28	-0,21	0,29	2,06	2,15	1,34	2,02	1,91	2,42	1,00	2,04	1,87	1,79	2,35	1,20	2,79	1,75	1,91	1,46	1,45	0,90	0,00
M023	1,84	-0,08	1,23	0,90	-0,72	-0,03	0,26	-0,29	0,20	2,11	2,21	1,38	2,01	2,01	2,23	1,15	1,91	1,79	1,89	2,34	1,15	2,60	1,79	1,93	1,63	1,48	0,70	0,48
M025	1,59	-0,23	1,30	0,74	-1,05	0,82	1,39	-0,64	0,01	1,84	1,72	1,08	1,46	1,77	2,21	1,08	1,69	1,98	1,71	2,36	1,18	2,63	1,60	2,07	1,71	1,71	1,28	0,48
M026	1,77	-0,07	1,25	0,91	-0,66	0,53	0,87	-0,25	0,20	2,18	2,20	1,46	2,24	1,86	2,34	1,32	2,01	1,88	1,75	2,29	1,15	2,80	1,67	1,86	1,49	1,51	1,11	0,85
M027	1,82	-0,11	1,23	0,95	-0,54	0,01	0,27	-0,41	0,15	2,14	2,18	1,23	2,05	2,04	2,39	1,32	1,93	1,73	1,98	2,28	1,15	2,74	1,93	1,91	1,66	1,49	0,70	0,60
M029	1,76	-0,11	1,12	0,82	-0,82	0,03	1,24	-0,13	0,22	1,99	2,13	1,18	1,91	1,93	2,17	1,18	1,92	2,32	1,80	2,36	1,11	2,70	1,77	1,85	1,54	1,43	0,90	0,60
M030	1,80	0,01	1,30	0,95	-0,59	0,05	0,16	-0,25	0,27	2,19	2,29	1,45	2,11	2,16	2,27	1,28	1,95	1,72	1,80	2,41	1,23	2,71	1,76	1,96	1,56	1,52	0,90	0,70
M032	1,83	-0,03	1,21	0,94	-0,77	-0,04	0,23	-0,09	0,19	2,06	2,18	1,18	1,94	2,01	2,37	1,20	1,88	1,85	1,99	2,44	1,23	2,56	1,92	1,94	1,81	1,51	0,85	0,60
M034	1,85	-0,05	1,18	0,80	-0,60	-0,19	0,18	-0,38	0,13	2,07	2,21	1,30	2,01	2,33	2,35	0,85	1,90	1,69	1,67	2,33	1,18	2,61	1,67	1,91	1,53	1,52	0,78	0,70
M035	1,78	-0,05	1,21	0,84	-0,89	0,46	0,94	-0,24	0,26	2,09	2,29	1,38	2,18	1,81	2,28	1,20	2,04	1,85	1,61	2,34	1,15	2,75	1,49	1,76	1,48	1,46	1,23	0,00
M036	1,63	-0,15	1,19	0,81	-0,85	0,51	1,46	-0,66	0,05	2,13	2,06	1,53	2,04	1,90	2,34	1,23	2,05	2,02	1,52	2,12	1,15	2,71	1,51	1,77	1,40	1,45	1,11	0,00
M037	1,77	-0,12	1,14	0,79	-1,15	0,33	1,13	-0,17	0,19	2,01	2,08	1,08	1,86	1,57	2,32	1,23	2,11	1,92	1,45	2,27	1,15	2,70	1,59	1,75	1,38	1,30	1,15	0,00
M038	1,76	0,03	1,31	1,00	-0,72	0,32	0,58	0,09	0,40	2,16	2,07	1,30	1,87	2,02	2,40	1,18	2,06	2,08	1,72	2,41	1,18	2,86	1,65	2,00	1,43	1,58	0,60	0,78
M039	1,85	-0,09	1,17	0,82	-0,74	0,29	0,25	-0,24	0,30	2,07	2,09	1,36	2,00	1,99	2,33	1,32	1,99	1,88	1,76	2,31	1,11	2,76	1,62	1,91	1,23	1,34	0,95	0,48
M040	1,77	-0,08	1,15	0,80	-0,85	0,45	1,09	-0,27	0,17	2,03	2,20	1,28	2,00	1,79	2,26	1,11	1,94	1,91	1,51	2,35	1,11	2,70	1,38	1,83	1,32	1,48	1,11	0,00
M041	1,63	-0,12	1,23	0,86	-0,89	0,50	1,43	-0,77	0,01	2,12	2,09	1,53	2,13	1,89	2,51	1,30	2,04	2,02	1,65	2,15	1,08	2,80	1,57	1,85	1,34	1,53	1,11	0,00
M043	1,68	-0,11	1,22	0,87	-0,74	0,57	1,33	-0,55	0,09	2,12	2,18	1,53	2,22	1,90	2,54	1,28	2,08	1,95	1,59	2,18	1,15	2,78	1,58	1,74	1,38	1,48	1,15	0,00
M044	1,84	-0,10	1,21	0,86	-0,77	0,29	0,31	-0,27	0,24	2,09	2,15	1,38	2,05	2,02	2,42	1,30	2,10	1,85	1,72	2,30	1,11	2,76	1,66	1,89	1,43	1,43	0,90	0,85
M045	1,84	-0,08	1,20	0,87	-0,70	0,24	0,20	-0,20	0,29	2,06	2,16	1,23	2,04	2,06	2,45	1,26	2,04	1,84	1,79	2,35	1,11	2,78	1,78	1,86	1,38	1,48	0,78	0,70
M051	1,81	-0,06	1,24	0,91	-0,70	0,21	0,31	-0,41	0,24	1,96	2,17	1,45	2,05	2,16	2,28	1,28	1,82	1,83	1,91	2,35	1,18	2,60	1,90	1,94	1,68	1,56	0,00	0,00

Table 3.8. Matrix used for multivariate statistical analysis: Log10 of the geochemical composition of samples obtained by XRF.

	SiO_2	TiO_2	Al_2O_3	Fe_2O_3	MnO	MgO	CaO	Na_2O	K_2O	V	Cr	Co	Ni	Cu	Zn	Ga	Rb	Sr	Y	Zr	Nb	Ba	La	Ce	Nd	Pb	Th	U
M056	1,84	-0,05	1,18	0,83	-0,80	0,26	0,38	-0,17	0,27	1,98	2,20	1,23	2,01	1,93	2,25	1,34	2,02	1,79	1,63	2,37	1,15	2,69	1,59	1,94	1,46	1,46	0,85	0,70
M068	1,80	-0,02	1,23	0,86	-1,00	0,03	0,89	-0,04	0,27	2,05	2,25	1,11	2,25	1,88	2,21	1,18	1,96	1,90	1,64	2,40	1,23	2,70	1,59	1,92	1,41	1,34	1,08	0,70
M069	1,81	-0,03	1,22	0,85	-1,05	0,38	0,77	-0,05	0,26	2,06	2,18	1,04	1,90	1,88	2,20	1,20	1,98	1,91	1,68	2,42	1,23	2,70	1,58	1,95	1,45	1,38	1,00	0,00
M071	1,78	-0,01	1,27	0,93	-0,66	0,31	0,81	-0,40	0,13	2,13	2,41	1,52	2,26	2,09	2,24	1,30	1,71	1,84	1,99	2,36	1,26	2,41	1,85	1,98	1,79	1,57	0,78	0,00
M075	1,69	-0,07	1,17	0,84	-0,64	0,85	1,26	-0,42	0,14	2,11	2,29	1,40	2,16	2,11	2,37	1,20	1,92	1,88	1,86	2,29	1,18	2,75	1,79	1,81	1,64	1,38	1,00	0,00
M079	1,68	-0,11	1,20	0,85	-0,92	0,46	1,36	-0,80	0,08	2,05	2,24	1,30	2,02	1,95	2,13	0,90	1,80	2,02	1,54	2,27	1,15	2,61	1,56	1,73	1,28	1,26	0,90	0,78
M080	1,63	-0,10	1,22	0,86	-0,66	0,41	1,43	-0,70	0,09	2,11	2,09	1,51	2,07	1,95	2,22	1,26	2,07	2,03	1,83	2,21	1,15	2,85	1,74	1,88	1,20	1,38	0,85	0,00
M083	1,70	-0,16	1,16	0,80	-0,59	0,59	1,30	-0,47	0,16	2,04	2,23	1,28	2,21	2,10	2,19	1,15	1,95	2,08	1,77	2,22	1,11	2,75	1,67	1,63	1,49	1,38	0,90	0,00
M086	1,68	-0,08	1,30	0,95	-0,70	0,64	1,17	-1,05	0,29	2,20	2,23	1,51	2,27	2,07	2,26	1,40	2,08	1,99	1,94	2,22	1,15	2,79	1,81	1,83	1,61	1,51	0,95	0,00
M088	1,72	-0,06	1,20	0,86	-0,74	0,29	1,26	-0,28	0,10	2,06	2,11	1,34	1,97	1,86	2,14	1,28	2,00	1,95	1,74	2,29	1,18	2,78	1,82	1,88	1,34	1,43	0,90	0,48
M090	1,71	-0,03	1,24	0,91	-0,68	0,13	1,23	-0,36	0,08	2,13	2,43	1,49	2,29	1,96	2,23	1,30	1,74	1,93	2,04	2,33	1,28	2,54	1,85	1,95	1,76	2,50	0,00	0,00
M092	1,69	-0,04	1,28	0,92	-0,70	0,12	1,25	-0,48	0,04	2,16	2,26	1,54	2,21	2,05	2,24	1,20	1,94	1,92	1,88	2,29	1,18	2,82	1,78	1,86	1,49	1,49	0,95	0,00
M098	1,70	-0,05	1,34	0,97	-0,68	0,54	1,02	-1,00	0,21	2,25	2,28	1,58	2,33	2,22	2,52	1,43	2,04	1,89	1,95	2,25	1,18	2,84	1,76	1,99	1,56	1,51	0,85	0,48
M101	1,79	-0,07	1,21	0,83	-0,89	0,48	0,92	-0,24	0,23	2,10	2,24	1,32	1,99	1,95	2,20	1,30	2,01	1,87	1,62	2,35	1,18	2,73	1,69	1,86	1,30	1,41	0,95	0,00
M102	1,76	0,00	1,27	0,90	-0,66	0,31	1,00	-0,30	0,21	2,16	2,24	1,40	2,08	2,07	2,28	1,40	2,00	1,93	1,81	2,34	1,23	2,75	1,66	1,98	1,53	1,53	0,90	0,78
M103	1,76	-0,07	1,20	0,86	-0,70	0,50	1,06	-0,24	0,22	2,05	2,19	1,26	2,05	1,95	2,22	1,15	1,93	1,92	1,71	2,28	1,11	2,75	1,57	1,79	1,34	1,41	0,90	0,60

Table 3.8. Matrix used for multivariate statistical analysis: Log10 of the geochemical composition of samples obtained by XRF.

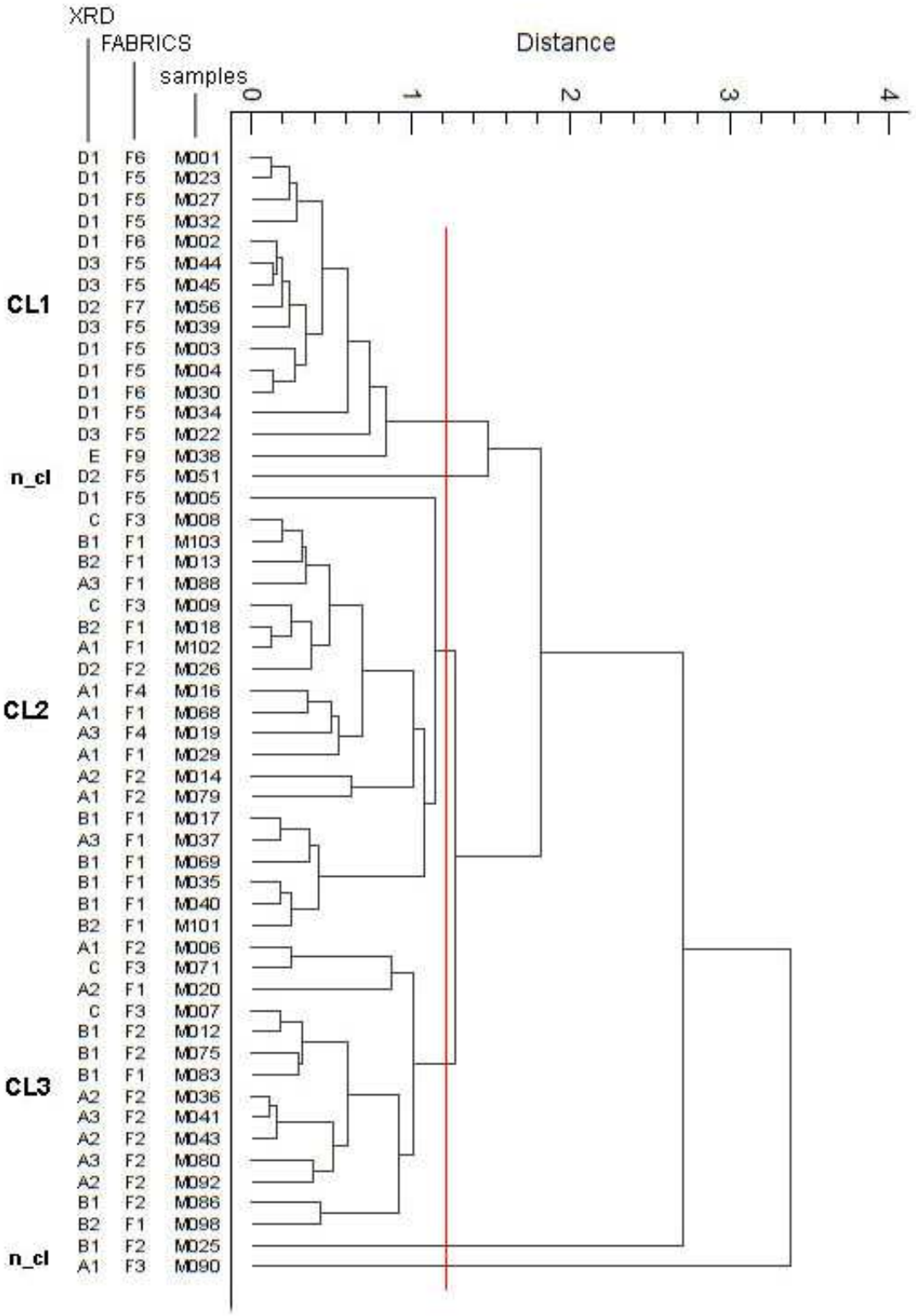

Figure 3. 33 Dendrogram obtained by cluster analysis (average linkage) of pottery from Castel de Pedena. Petrographic and XRD groups are also displaied.

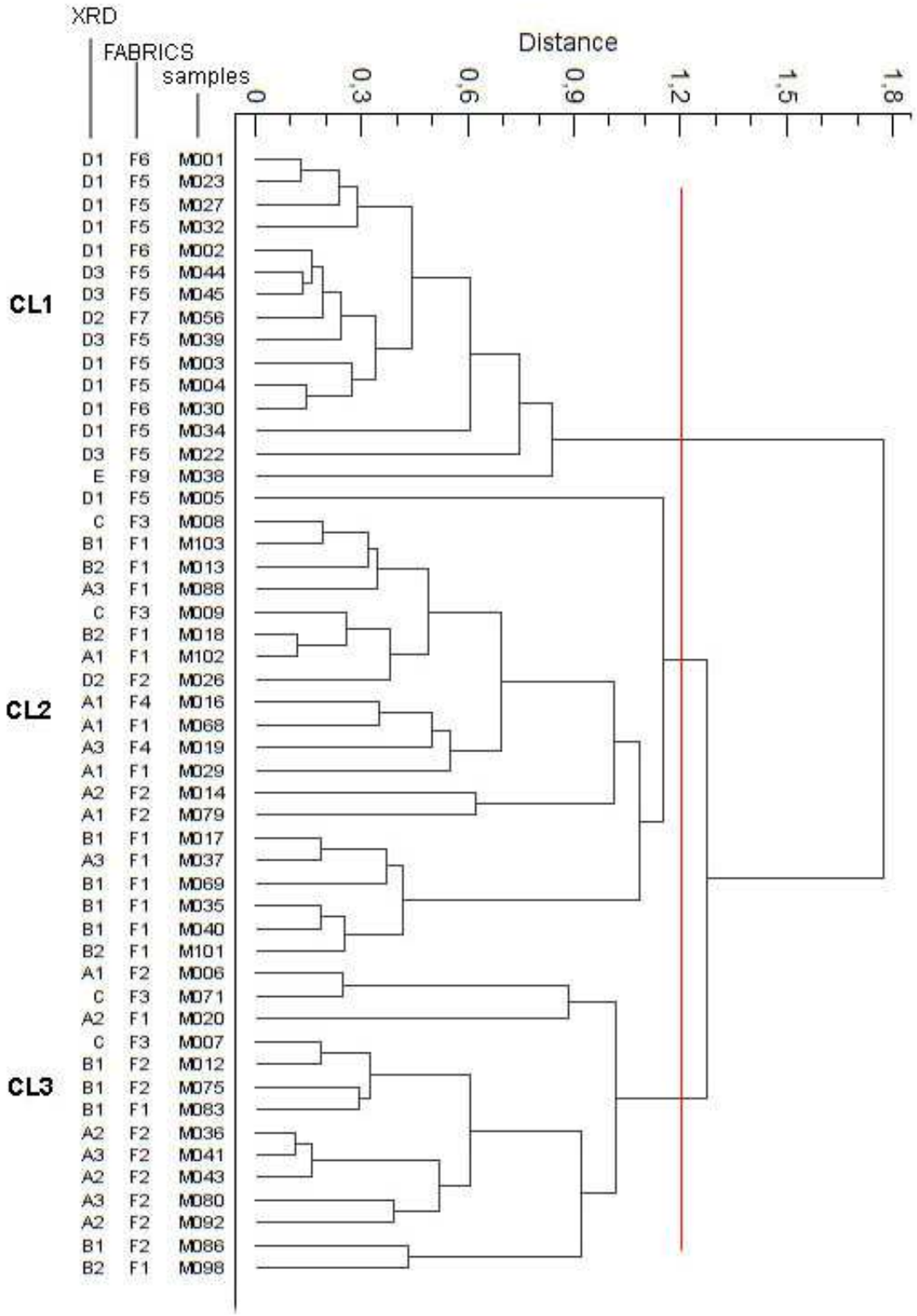

Figure 3. 34. Dendrogram obtained by cluster analysis (average linkage) excluding the outliers (M25, M51, M90) of pottery from Castel de Pedena. Petrographic and XRD groups are also displaied.

The claster 3 (CL3) is a smaller heterogeneous group. It is composed of fourteen samples mostly related to the fabric F2 with the exception of five samples belonging to the fabrics F1 and F3. Only three samples were considered outliers: M025, M051 and M090. Samples M025 and M090 resulted also outliers for more than six chemical elements, from the box-plot display. The analysis was performed again excluding the outliers. The new dendrogram was similar to the first one and the same clustering arised (figure 3.34). The score plot of principal component analysis (PCA) showed a less well defined situation (figures 3.35-38). Samples belonging to the fabrics F5, F6 and F7, rich in chert, quartz fragments and grog respectively, that were well grouped in the cluster analysis (CL1), are concentrated at low value of pc1, toward the direction of high content in SiO_2, Na_2O and K_2O. Samples of fabric F1 are well grouped toward high value of pc2 but they divided in two subgroups respect the pc3. Samples M017, M035, M037, M040, M069, M101 -that were also clustered together at smaller ultrametric distance in the cluster analysis- toward the direction of MgO and Na_2O and the other samples of fabric F1 toward the direction of U. Samples belonging to the fabric F2, mostly corresponding to cluster CL3, are generally grouped together for high value of pc1, toward the direction where the CaO

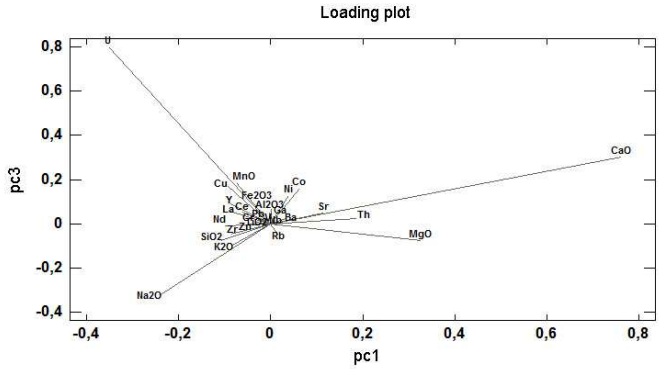

Figure 3. 35. Loading plot of the variables considered for the pca, respect pc1-pc3.

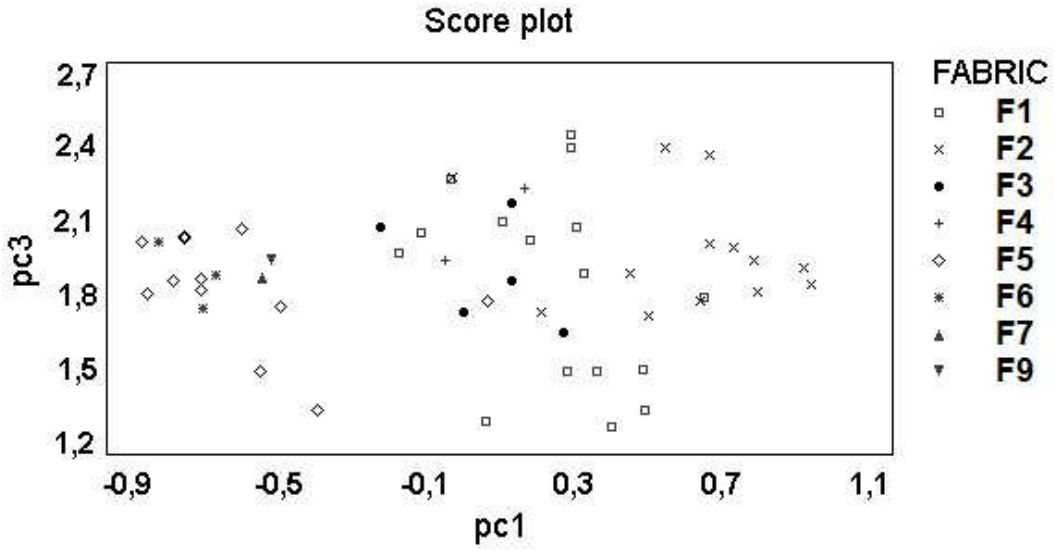

Figure 3.36. Principal component analysis of the chemical data with indication of the fabric groups. Plot of pc1 versus pc3, explaining 39% and 10,% of the total variance, respectively.

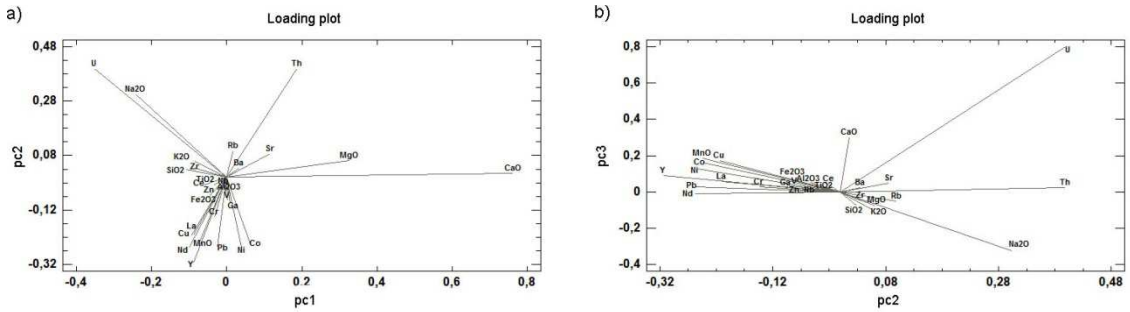

Figure 3. 37. Loading plot of the variables considered for the pca, respect pc1-pc2 (a) and pc2-pc3 (b).

content is more consistent. If we consider the dot plot originated by pc2 and pc3 we observed that all the samples form a large group, while those samples of fabric F1 that were separated also in the pc1-pc3 diagram, are still isolated (figure 3.38.b).

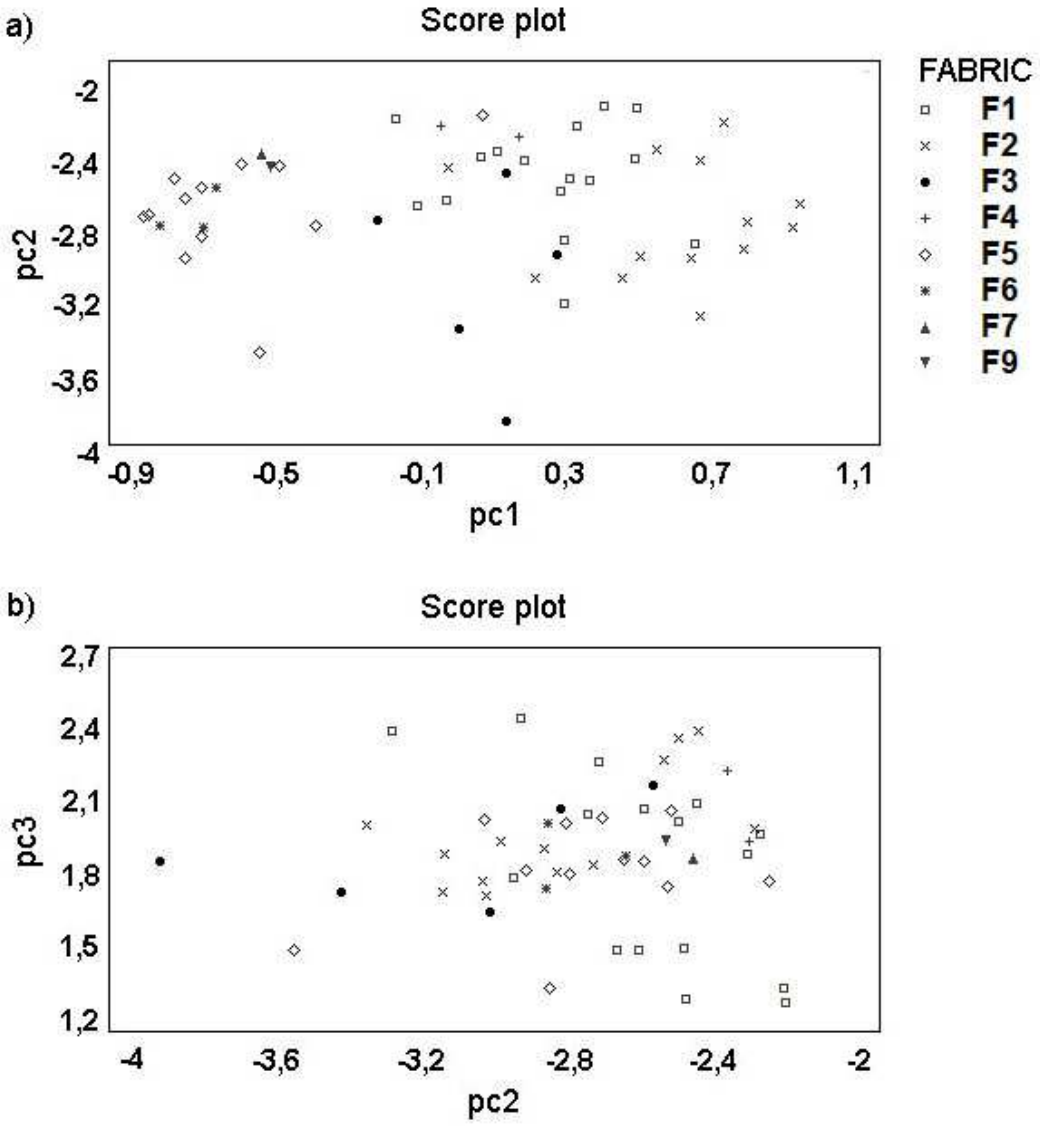

Figure 3. 38 Principal component analysis of the chemical data with indication of the fabric groups. a) Plot of pc1 versus pc2, explaining 39% and 17% of the total variance, respectively; b) plot of pc2 versus pc3, explaining 17% and 10% of the total variance, respectively.

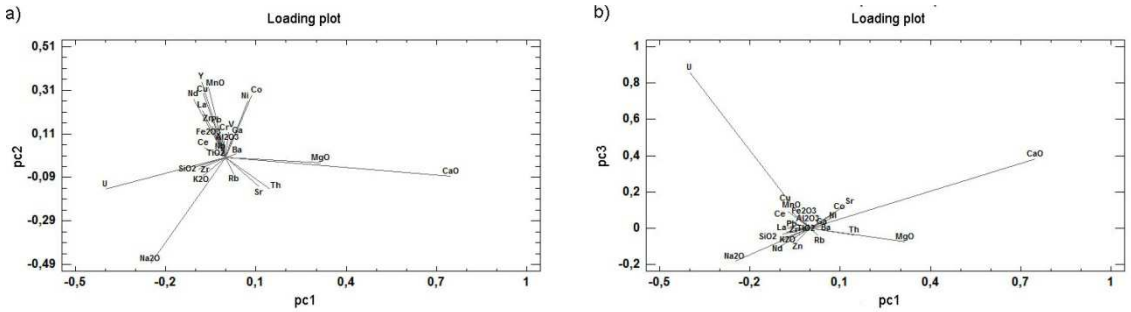

Figure 3. 39. Loading plot of the variables considered for the pca, respect pc1-pc2 (a) and pc1-pc3 (b). They were carried on excluding the outliers (M025, M051, M090).

As for the cluster, the analysis was repeated excluding the outliers (M025, M051, M090). The results so obtained are of great interest. The score plot shows a better defined situation (figures 3.3940). Considering the plot of the first and second components,

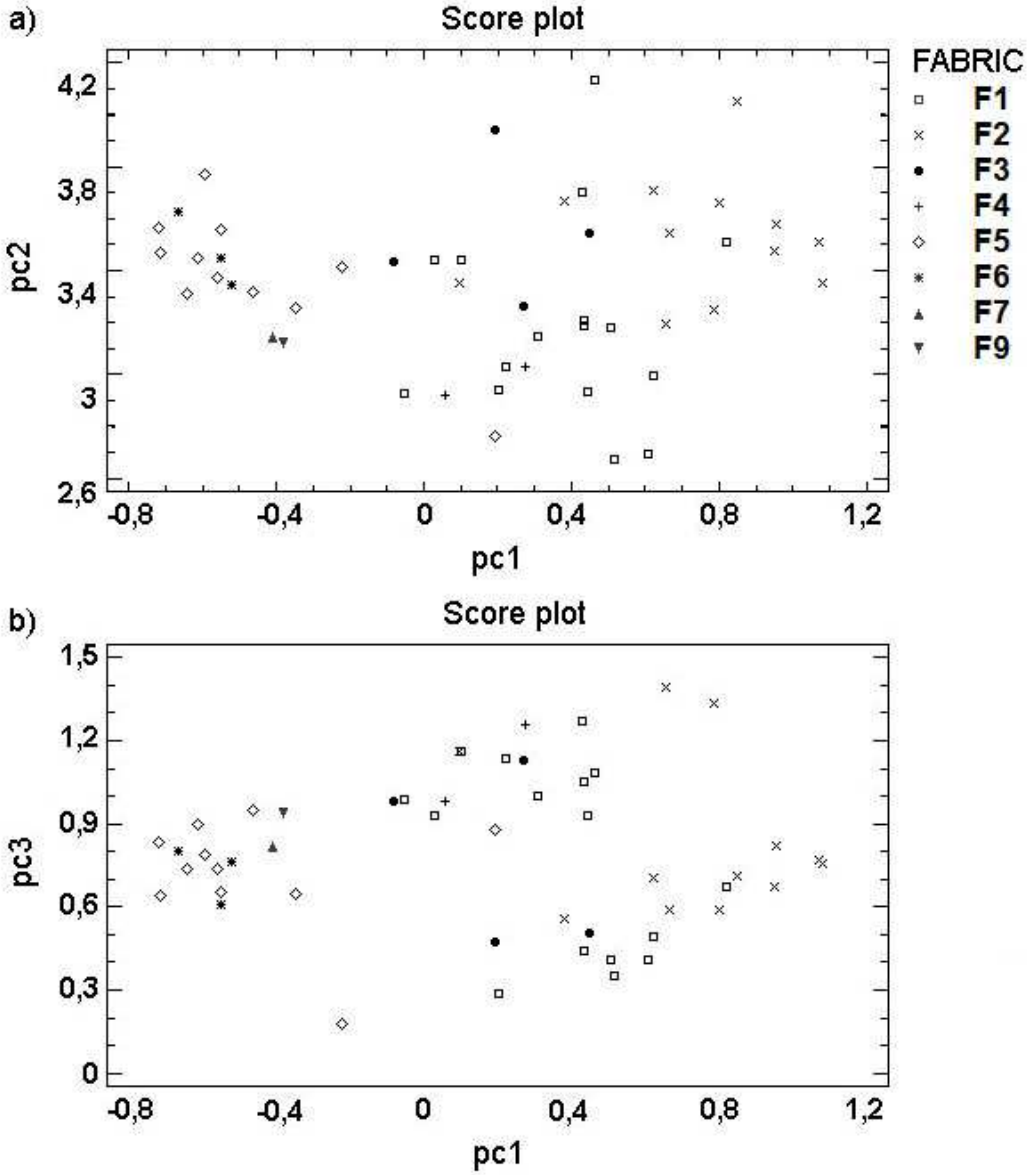

Figure 3. 40. Principal component analysis of the chemical data, excluding the outliers, with indication of the fabric groups. a) Plot of pc1 versus pc2, explaining 44% and 16% of the total variance, respectively; b) plot of pc1 versus pc3, explaining 44% and 12% of the total variance, respectively.

samples of fabric F1, F2, F3 and F4 are concentrated toward the direction of high content of CaO and MgO. Samples of fabric F5, F6 and F7 are concentrated toward the direction where the SiO_2 and Na_2O content is more consistent. In the dot-plot resulting from the first and third principal components samples of fabric F5, F6 and F7 are still concentrated toward the direction where the SiO_2 and U content is more consistent (low values of pc1). Samples of fabric F1, F2, F3 and F4 are laid along two imaginary regression lines comprising the fabrics F1,F4 and part of F2 (mostly representing the $A1_{xrd}$) the first and fabric F1 and part of F2 (mostly representing the $B1_{xrd}$) the second. They are divided respect the higher or lower amount of MgO (that means higher or lower amount of dolomite). Samples of fabric F3 are shared.

3.7 Geological setting and provenance considerations

Castel de Pedena (S. Gregorio nelle Alpi, Belluno, Italy) is a mountain village (*castelliere*) settled in the Venetian Prealps at 680 m above the sea level in the toe of the southern slope of the Pizzocco mountain. The site rises in the Vallone Bellunese, a valley crossed by the Piave river, on a ridge formed for erosion of the Pleistocene fluvial terraces for the action of the Brentaz (south/south-east) and the Rumarna (south-west) streams.

During the last glaciations the Piave basin, and so the Vallone Bellunese comprehending the Mis and Cordevole streams valleys, were completely covered by the same glacier. After its retreat, important morainic deposits remained, a long phase of stream aggradation of the valley bottom occurred and subsequently, during the Holocene, stream downcutting and formation of terraces took place. Today the site of Castel de Pedena is closed to the morainic deposit of Roncoi, and it is partially covered by fluvial deposits (gravels, sands and clays) cemented in conglomerates. Along the streams Brentaz and Rumarna the Miocene sandstones (mudstones and sandstones) bedrocks drop out (figure 3.41).

The geology northern of the site is characterized by important carbonate sequences: along the southern slope of the Pizzocco mountain there are bioclast carbonate grainstone, carbonate mudstone and clayey mudstone (marly limestones and clayey marls); chert-bearing limestone and foraminifera-bearing mudstone; ooid limestone, pelagic foraminifera carbonate mudstone and dolomite. Moving northern, along the main rivers and streams, the geological situation changes. Following the stream Mis up to the source, there are at first outcrops of the dolomite and then metamorphic rocks mainly constituted by quartz phyllites, occasional graphite phillytes, and subordinated carbon-rich phyllites and muscovite paragneiss. The Cordevole stream, a tributary that flows into the Piave river not far from Castel the Pedena, towards north crosses grainstones and chert nodules bearing carbonate mudstone, metamorphic rocks (quartz phyllites, graphite phillytes, carbon-rich phyllites and muscovite paragneiss), and, near Agordo, crosses the ooid carbonate mudstone and the dolomite outcrops. Some smaller streams (Tegnas, Liéra, ..), tributaries of the Cordevole, bring among its debris some volcanic igneous rocks gravels as monzonite, andesite, alkali basalt-andesite.

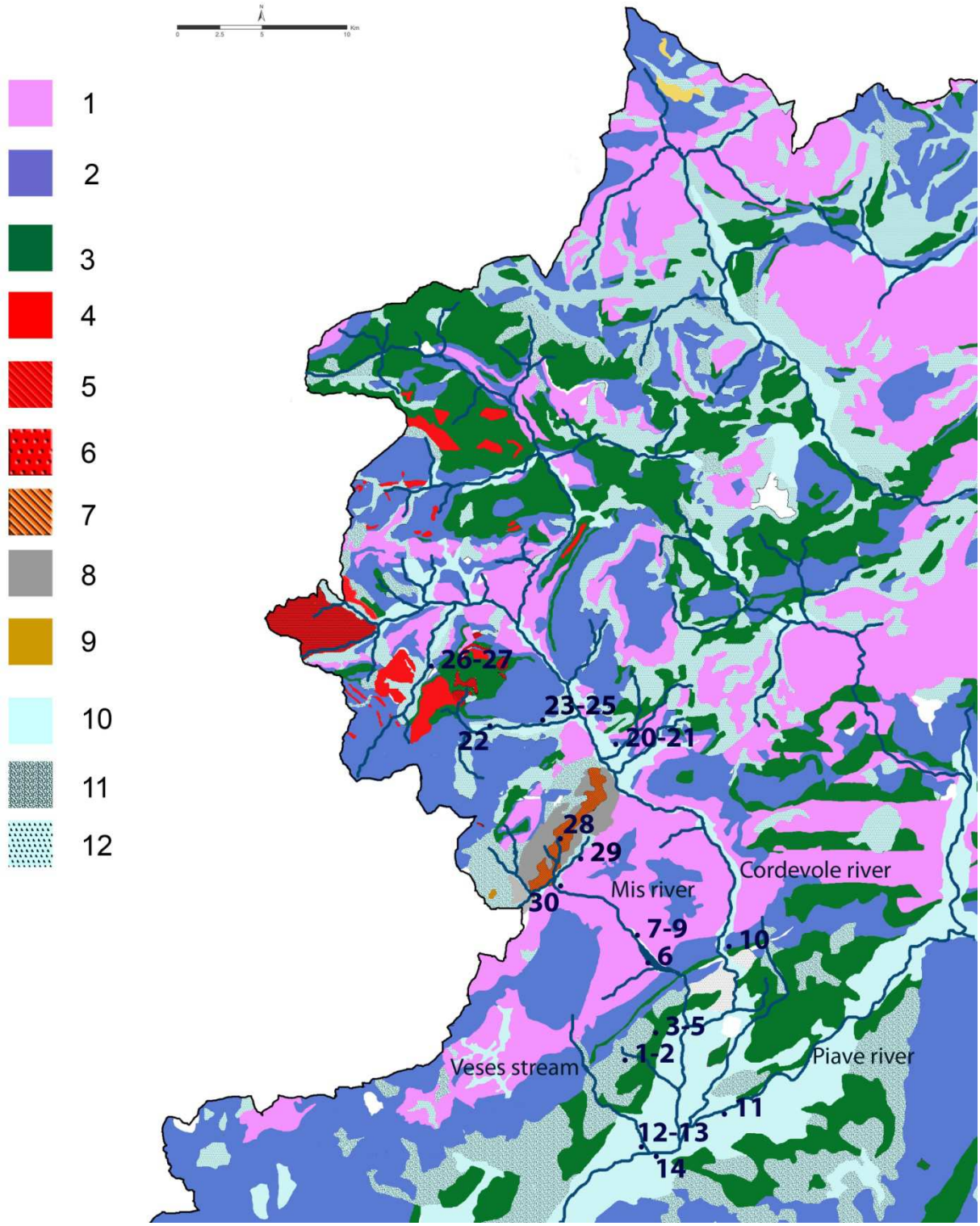

Figure 3. 41. Geology of the interested area with indication of the locations of the sediments sampling. Lithotypes: 1: dolomite; 2: carbonate mudstone; 3: detritic sedimentary rocks (sandstone); 4: volcanic igneous rocks (andesite); 5: volcanic igneous rock (monzonite); 6: volcanic igneous rocks (ignimbrite); 7: meta-rhyolite; 8: metamorphic rocks (phyllite); 9: detritic sedimentary rocks (conglomerates); 10: alluvial and fluvioglacial deposits; 11: morainic deposits; 12: detritic deposits. Location of the sediments sampling: 1, 2: Castel de Pedena; 3-5: Rumarna stream; 6-9: Mis lake; 10: Cordevole river; 11; 12-13: Veses stream; 14: Piave river; 20-21: Agordo; 22-25: Tegnas stream; 26-27: Gares lake; 28: Gosaldo; 29: stream repository of the Mis stream; 30: Mis stream.

sample	provenance	place	sample type	coordinate (DMS) N	coordinate (DMS) E
S1	Castel de Pedena	Loc_Roncoi	Silty clay	46°06.898'	12°01.913'
S2	Castel de Pedena	Loc_Roncoi	Silty clay	46°06.899'	12°01.915'
S3	Rumarna stream	Paderno	Clay	46°07.023'	12°03.142'
S4	Rumarna stream	Paderno	Clay	46°07.023'	12°03.142'
S5	Rumarna stream	Paderno	Clay	46°07.023'	12°03.142'
S6	Mis lake	Mis lake	Sand	46°09.880'	12°03.691'
S7	Mis lake	Mis lake, Soffia falls	Clay	46°11.135'	12°02.849'
S8	Mis lake	Mis lake, Soffia falls	Sand	46°11.135'	12°02.849'
S9	Mis lake	Mis lake, Soffia falls	Sand	46°11.135'	12°02.849'
S10	Cordevole river	Sedico, Peron	Sand	46°09.958'	12°07.168'
S11	Piave river, befor the Cordevole flows into	San Felice bridge	Sand	46°05.463'	12°07.428'
S12	Veses stream	S.Giustina, Brustolade	Sand	46°04.065'	12°03.133'
S13	Veses stream	S.Giustina, Brustolade	Sand	46°04.065'	12°03.133'
S14	Piave river, after the Cordevole flow into	S.Giustina, Brustolade	Sand	46°04.029'	12°03.202'
S20	Polane lake	Agordo, Polane clay quarry	Clay	46°16.399'	12°02.089'
S21	Polane lake	Agordo_cava_d'argilla_Loc_Polane	Clay	46°16.399'	12°02.089'
S22	Tegnàs stream	Valle_S.Lucano_frazione_col_di_Prà	Sand	46°17.763'	11°55.677'
S23	Tegnàs source	Valle_S.Lucano_tra_Loc_Mezzavalle_Loc_Peschiere	Sand	46°17.704'	11°57.816'
S24	Tegnàs stream	Valle_S.Lucano_Loc_Peschiere_chiesetta_S.Lucano	Sand	46°17.752'	11°58.170'
S25	Tegnàs stream	Valle_S.Lucano_Loc_Peschiere_chiesetta_S.Lucano	Sand	46°17.752'	11°58.170'
S26	Gares lake	Canale_Agordo_Loc_Pian_de_Giare	Sand	46°18.561'	11°52.965'
S27	Gares lake	Canale_Agordo_Loc_Pian_de_Giare	Sand	46°18.561'	11°52.965'
S28	Gosaldo	Gosaldo_via_laveder	grapite phyllite	46°13.431'	11°59.290'
S29	stream repositary of the Mis	Gosaldo_via_Lambroi	Sand	46°13.177'	11°59.544'
S30	Mis stream	Gosaldo_Loc_Bitti	Sand	46°12.734'	11°59.253'

Table 3. 9. Detail of the locations of sediments sampling.

As it appears from this brief report, the area around Castel de Pedena is characterized by a wide variety of lithologies: sedimentary rocks both carbonatic and detritic, metamorphic rocks and igneous rocks. These complex situation is well represented in the non-plastic inclusions of the studied pottery. The petrographic examination of the potshards had revealed a high mineral-petrographic variability, due to the different type of inclusions that are all consistent with the lithotypes present in the area around the site. Most of the studied potsherds -in particular those of fabric F1, F2, F3 and F4 (carbonate inclusions-rich potsherds) and fabric F5 (chert-rich potshards)- contained inclusions referable to the geology of the area nearby the site. They were characterised by carbonate outcrops and chert-bearing carbonate mudstone. The presence of metamorphic rocks in some of the samples (fabrics F3, F8) is correlated with the geology of the area just northern the site, closed to the Mis stream source, at a maximum distance of about 20 km. The volcanic igneous rocks (fabric F9) are related with the igneous rocks outcrops in the northern regions, at a distance of nearly 45-50 km.

In order to define more in detail the possible provenance of the raw materials, a clay and sand sediments sampling was planned. The places for the sampling were set with the help of local informants and consulting soil and geological maps of the region. In that way twenty-five samples of clay and sand sediments were collected (table 3.9), closed to the site and along the main streams. We tried to cover all the interest geological outcrops present in the region. Major attention was given to collect samples of sands more than

clays because of the varied and peculiar situation of the pottery a-plastic inclusions noticed during the microscopy observation. Moreover, with coarse pottery it is easier to make comparison with the inclusions than with the groundmass finer materials. The location of the sampling site was recorder using a GPS device. Chemical analyses were performed on the clayey sediments (samples S1, S2, S3, S4, S5, S7), while X-ray diffraction analysis and optical microscopy were conducted on the whole assemblage.

The sediments collected were dried in a oven at 50° for 24h, since at this temperature the minerals present in the pottery do not undergo irreversible transformations. Sand sediments were sieved for separating the size-fraction corresponding at that of the inclusions. To be sure to obtain subsamples as representative as possible, the method normally used in sedimentology was adopted: the powder or sediments were heaped up into a pile and quartered, then one quarter was selected and this procedure was repeated on the cut down material until it was reduced to the amount needed. Then a part of each sample was grounded in fine powder, while the other part was used for the thin sections preparation.

Through X-ray fluorescence spectroscopy the bulk chemistry of the clayey samples was determined (table 3.10). Clays S20 and S21 were not treated by XRF because the results of XRD analysis demonstrated the presence of gypsum and ettringite, mineral phases typical of the cements probably due to debris present in the soil. The main purpose was to investigate potential similarities between the sampled clays and the ceramic pastes. The concentration of the major elements expressed as percentage of their oxides (SiO_2, TiO_2, Al_2O_3, Fe_2O_3, MnO, MgO, CaO, Na_2O, K_2O, P_2O_5) were compared with those of the studied potsherds through descriptive statistics (mean, standard deviation, first quartile, median, third quartile) carried out selectively on the samples of the single fabric groups (table 3.10). In general, it was observed that there was not great similarities: samples of fabric F1, characterized by the high presence of carbonatic rocks among their inclusions seemed to be related more with the clays S5 and S2, since their percentage of TiO_2, Al_2O_3, Fe_2O_3, MgO, Na_2O well matched. The sediment S5 had also values of SiO_2, Mg, and CaO comprised between the samples' first and third quartiles.

Samples of the fabric F2, characterized by the high presence of carbonatic rocks among their inclusions, found low similarities with clays S1, S2, S3 and S5. In general the composition of these clays was comparable for the concentrations of SiO_2, TiO_2, MgO, K_2O, P_2O_5. The S2 had also corresponding concentrations of Al_2O_3, Fe_2O_3, MnO, but differed in the P_2O_5 and SiO_2, while S5 had higher concentration of K_2O, but CaO and Al_2O_3 were similar.

Samples of the fabric F3, characterized by the presence of both carbonate and metamorphic rocks inclusions, were slightly related to clays S2, S3 and S5. These latest had always lower values of Al_2O_3, Fe_2O_3, MnO and P_2O_5 and higher of Na_2O. Sediment S2 had TiO_2, MgO and K_2O values always comprised in the inter-quartile range, clay S3 matched for SiO_2, CaO and K_2O, while clay S5 had similar value for the SiO_2, MgO and CaO.

	samples	SiO_2	TiO_2	Al_2O_3	Fe_2O_3	MnO	MgO	CaO	Na_2O	K_2O	P_2O_5
Clays:	clay 1	40,61	0,43	6,90	3,07	0,12	4,47	40,60	0,44	1,27	0,11
	clay 2	72,89	0,90	14,24	6,37	0,12	1,54	0,95	0,83	1,95	0,08
	clay 3	58,29	0,80	10,11	4,23	0,06	5,16	17,07	1,20	1,96	0,20
	clay 4	46,45	0,54	7,33	3,84	0,05	7,77	30,30	0,72	1,52	0,19
	clay 5	59,93	0,78	15,53	5,31	0,05	3,27	10,17	0,87	2,77	0,16
	clay 7	39,81	0,66	13,26	4,26	0,10	13,66	24,05	0,73	2,84	0,15
Fabric F1:	Mean	57,72	0,86	16,12	7,09	0,16	2,56	12,11	0,57	1,59	0,56
	StDev	4,78	0,08	2,13	0,96	0,06	0,89	4,68	0,21	0,22	0,27
	Variance	22,84	0,01	4,54	0,92	0,00	0,80	21,88	0,04	0,05	0,07
	Minimum	48,52	0,69	13,30	5,73	0,07	1,06	5,95	0,10	1,07	0,15
	Q1	53,92	0,79	14,34	6,29	0,11	1,89	8,43	0,51	1,45	0,35
	Median	59,17	0,87	16,05	6,96	0,15	2,63	10,87	0,56	1,63	0,52
	Q3	61,19	0,93	16,84	7,77	0,22	3,38	16,33	0,72	1,77	0,74
	Maximum	64,14	1,00	21,65	9,33	0,26	3,93	20,80	0,92	1,88	1,06
Fabric F2:	Mean	48,75	0,81	17,33	7,41	0,18	3,43	19,28	0,29	1,31	0,65
	StDev	6,49	0,10	1,68	0,90	0,05	1,68	7,39	0,13	0,28	0,47
	Variance	42,14	0,01	2,81	0,80	0,00	2,81	54,54	0,02	0,08	0,22
	Minimum	38,74	0,59	14,74	5,50	0,09	1,32	6,49	0,09	1,02	0,10
	Q1	43,07	0,77	15,94	6,94	0,14	2,39	13,89	0,19	1,08	0,19
	Median	47,63	0,79	16,79	7,24	0,19	3,21	19,65	0,26	1,23	0,59
	Q3	54,27	0,87	18,76	8,23	0,22	3,89	26,59	0,39	1,47	0,94
	Maximum	60,27	0,98	20,00	8,92	0,23	7,12	28,73	0,56	1,97	1,68
Fabric F3	Mean	55,09	0,87	18,50	8,62	0,19	2,47	10,87	0,52	1,67	0,60
	StDev	3,78	0,05	0,85	0,34	0,04	1,26	4,47	0,06	0,45	0,16
	Variance	14,32	0,00	0,72	0,11	0,00	1,58	20,00	0,00	0,20	0,03
	Minimum	51,88	0,83	17,42	8,22	0,14	1,34	6,45	0,44	1,20	0,37
	Q1	52,33	0,83	17,69	8,31	0,15	1,38	7,27	0,46	1,26	0,43
	Median	53,95	0,86	18,54	8,61	0,20	2,32	9,97	0,53	1,64	0,67
	Q3	58,97	0,92	19,27	8,94	0,22	3,71	15,37	0,57	2,12	0,71
	Maximum	60,56	0,93	19,49	9,04	0,22	3,90	17,09	0,58	2,22	0,71
Fabric F4	Mean	56,85	0,84	15,73	7,99	0,13	1,37	14,25	0,60	1,36	0,57
	StDev	4,09	0,01	0,21	1,12	0,05	0,78	6,95	0,23	0,15	0,52
	Variance	16,76	0,00	0,05	1,25	0,00	0,61	48,31	0,05	0,02	0,27
	Minimum	53,95	0,83	15,58	7,20	0,09	0,82	9,33	0,44	1,25	0,20
	Q1	-	-	-	-	-	-	-	-	-	-
	Median	56,85	0,84	15,73	7,99	0,13	1,37	14,25	0,60	1,36	0,57
	Q3	-	-	-	-	-	-	-	-	-	-
	Maximum	59,74	0,85	15,88	8,78	0,16	1,92	19,16	0,76	1,46	0,93
Fabric F5	Mean	67,37	0,86	16,30	7,55	0,20	1,51	2,32	0,64	1,83	0,70
	StDev	3,49	0,06	0,83	0,80	0,04	0,79	1,76	0,28	0,42	0,34
	Variance	12,16	0,00	0,68	0,65	0,00	0,63	3,08	0,08	0,18	0,11
	Minimum	57,74	0,77	14,89	6,29	0,12	0,64	1,50	0,39	1,34	0,18
	Q1	66,49	0,81	15,69	7,11	0,17	0,96	1,61	0,44	1,56	0,54
	Median	68,62	0,84	16,15	7,32	0,20	1,33	1,85	0,60	1,75	0,67
	Q3	69,30	0,91	17,15	8,14	0,23	1,88	2,05	0,71	1,96	0,94
	Maximum	70,88	0,96	17,35	8,98	0,29	3,60	7,85	1,41	2,97	1,40
Fabric F6	Mean	66,68	0,84	17,02	7,90	0,18	1,11	1,73	0,53	1,64	0,82
	StDev	2,90	0,16	2,58	1,00	0,07	0,29	0,25	0,04	0,21	0,53
	Variance	8,42	0,02	6,66	0,99	0,01	0,08	0,06	0,00	0,04	0,28
	Minimum	63,39	0,72	15,47	6,94	0,12	0,82	1,45	0,49	1,45	0,36
	Q1	63,39	0,72	15,47	6,94	0,12	0,82	1,45	0,49	1,45	0,36
	Median	67,78	0,79	15,59	7,83	0,15	1,12	1,81	0,54	1,62	0,70
	Q3	68,87	1,02	20,00	8,93	0,26	1,40	1,92	0,56	1,86	1,40
	Maximum	68,87	1,02	20,00	8,93	0,26	1,40	1,92	0,56	1,86	1,40
Fabric F7	M056	69,61	0,90	15,24	6,72	0,16	1,81	2,40	0,67	1,85	0,29
Fabric F9	M038	56,95	1,07	20,60	10,03	0,19	2,08	3,76	1,22	2,52	1,12

Table 3. 10 Major element compositions of sediments materials. For comparison, statistical data for population of the fabrics observed are also reported: mean, standard deviation, variance, minimum, first quartile (Q1), median, third quartile (Q3), and maximum (MAX).

Fabric F4 was a very small fabric group composed by only two samples characterized by a quartz and carbonate sand. Chemical comparisons indicated that clays S3 and S5 were the more similar to fabric F4: the first had equal values of SiO_2, TiO_2, CaO and P_2O_5, while the second for SiO_2, TiO_2, Al_2O_3 and CaO. Lower analogies could be found with sediments S1 and S4. In general the clays had lower values of Al_2O_3, Fe_2O_3, MnO and MgO than the potsherds of this fabric.

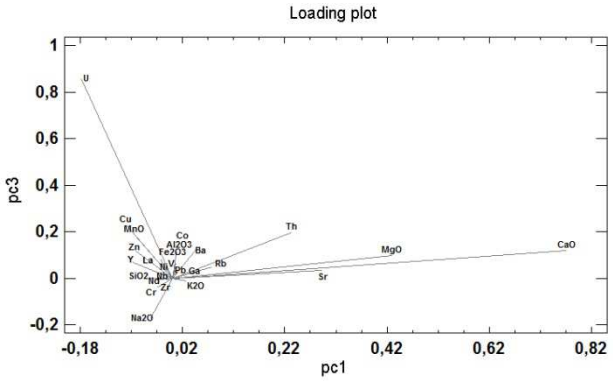

Figure 3. 42. Loading plot of the variables considered for the pca, respect pc1-pc3.

The fabric F5, rich in chert fragments and quartz crystals, had chemical similarity with clay S2, whose elements generally equaled those of pottery, and TiO_2, MgO and K_2O were comprised between the inter-quartile range. Only the clay concentrations of CaO and P_2O_5 were appreciably lower.

The fabric F6 presented greater analogies with S2 whose TiO_2, Al_2O_3, Fe_2O_3, MnO, MgO and CaO values were comparable , whereas Na_2O, K_2O clay elements were higher.

Sample M056, the only potsherd of fabric F7, was characterized by the abundant fragments of grog and fewer carbonate mudstone and chert inclusions. It found correspondence with the clay S2, since it had similar amount of SiO_2, TiO_2, Al_2O_3, Fe_2O_3, MgO and K_2O. But, the clay concentrations of MnO and CaO were lower and Na_2O was more abundant.

Sample M038, the only component of fabric F9, was characterized by volcanic intermediate and acidic rock fragments. It had not found good correspondence with any clay.

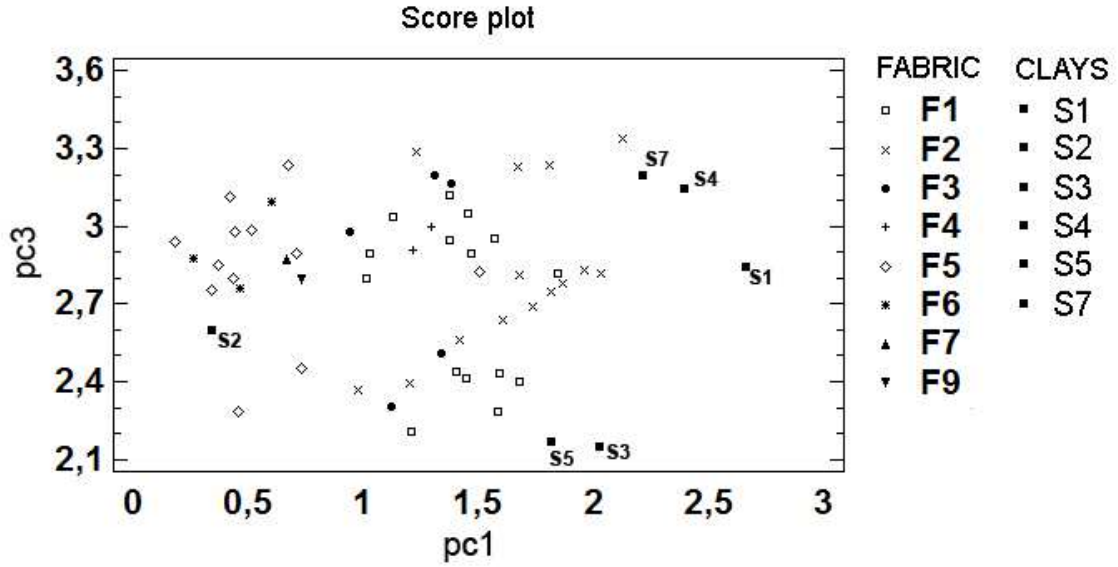

Figure 3. 43. Principal component analysis of the chemical data potsherds samples and sediments. Plot of PC1 versus PC3, explaining 39% and 10,% of the total variance, respectively.

samples	Qz	Pl	Kf	Kf	Cal	Dol	Ilt	Sme	Chl	Kln	Spl	Zeo	Px	Amp	Ant	Ett	Gp	Lz
		Ab	Mc	Snd														
S01	***	*			****	**	*		*									
S02	****	*	*				**		**									
S03	****	*	*		**	**	*		**					*				
S04	***	*			***	***	*		*					*				
S05	****	*	*		**	**	**		**			*		?				
S07	***	*	*		*	****	*		**	*				?	*?			
S09	*				*	****							*					
S10	***	**	**		**	***	**		*									
S11	***				***	***	*		*									
S13	****	**	**		**	***	*		*					*				
S14	***	**			**	****	*		*									
S20	**	*			****	***	**									**	**	*
S21	**	**			****	**	**									**	**	
S22	****	***		***	***	*	***	*	***	*		*	*					
S23	*				***	****	*	*	*									
S24	**	**		**	***	****				*	*		**					
S25	*	**			**	****	*	*	*	*			*					
S26		***	**			****	**	**				*	***					
S27	*	*	**		*	****	**	*				*	*					
S29	****	**		*			***		**				*					
S30	***	*			****	**	*	*										

Table 3. 11. Mineral assemblages of sediments gained by XRPD. Qz: quartz; Pl: plagioclase (albite like); KF: alkali feldspar both microcline like (Mc) and sanidine/anorthoclase like (Snd); Cal: calcite; Dol: dolomite; Ilt: illite; Sme: smectites; Chl: chlorite; Kln: kaolinite; Spl: spinel; Zeo: zeolite; Px: pyroxene; Amp: amphibole; Ant: atanasio; Ett: ettringite; Gp: gypsum; Lz: lizardite.

It was observed that clays concentrations of TiO_2, Al_2O_3, Fe_2O_3 and Mn were often lower than in the potshards. This may be related to clay minerals (kaolinite, chlorite, illite, smectites) concentrations higher in the pottery, than in the samples collected in the present research. On the contrary Na_2O and K_2O had often higher values in the clays than in the potshards, probably related to the dilution effect due to the coarse inclusions in the pottery.

The principal component analysis was performed on the based 10 logratio values of clay and potshards chemical elements confirming the results just discussed. The clay S2 was placed towards the direction of Na_2O, SiO_2 and U, and it well matched with samples of fabric F5. The other clay sediments were placed towards the direction of Na_2O, MgO, Sr, Th and CaO, closed to samples of fabric F1, F2, F3 and F4 but they did not cluster together (figures 3.42-43).

X-ray diffraction analysis was conducted on all the geological samples, both clays and sands (table 3.11). Clays S1 and S2, sampled closed to the site, were characterized by abundant calcite and quartz and subordinate illite and chlorite and abundant quartz, common illite and chlorite. Clays S3, S4, S5, coming from the Rumarna stream, and S7, sampled on the Mis lake bank, contain abundant quartz and dolomite (consistently with the geology of the area), subordinate calcite, plagioclase, alkali feldspar, illite and chlorite. Clays S20 and S21 presented among the other phases also gypsum and ettringite, minerals typical constituent of the cements. It seems reasonable that they had undergone alterations due by debris present in the soil. The sand (S9) coming from the confluence of the Mis stream into the homonymous lake was rich in dolomite. This is not surprising because the Mis stream cross an area characterized by dolomite outcrops. Some sand

samples collected along the Cordevole stream (S10), the Veses stream (S13), the Piave river (S13) and the Mis stream north of the lake Mis (S30 and S30m), presented similar minerals assemblages: they had great amount of quartz and dolomite and fewer calcite, traces of plagioclase and alkali-feldspar (of sanidine type) and abundant illite and chlorite. The remaining sediments were collected northern, along those streams that cross the metamorphic and volcanic outcrops. Sample S22 was characterized by a abundant clay minerals (illite, chlorite, smectites minerals, kaolinite), abundant quartz and common plagioclase, alkali-feldspar (like sanidine or anorthoclase), calcite, and traces of zeolite. Samples S24, S25, S26, S27 and S29 presented all the peaks typical of the pyroxene, had abundant dolomite, except sample S29, associated with different concentrations of quartz, plagioclases, alkali feldspars and clay minerals. Sample S23, coming from the same area, presented abundant calcite and dolomite and few quartz and clay minerals.

All these sediments were analyzed under polarizing light microscope, described following a simplification of the thin section description protocol illustrated by Whitbread (1989, 1995) and compared with the studied potshards (figure 3.44.a-b). Previously, it is important to specify that all the ceramics had a coarse paste and amount of inclusions higher than the clay samples. These evidences suggested that pottery was probably deliberately tempered. Once more, the results revealed high similarity between clay S2 and the samples of fabric F5, in accordance with the XRF analysis. This is rich in big angular and sub-angular chert fragments and subordinate carbonate mudstone and quartz crystals. The ceramics of this fabric generally showed higher amount of inclusions that may had been intentional added. Clay S2 appeared compatible also with samples of fabrics F1, F2, F3 and F6 because of the predominant presence of quartz and subordinate chert among the finer grain-size fraction. The absence of large chert fragments of great dimension in the pottery could be interpreted in terms of preparation of the clay, through levigation and decanting or sieving processes. The other clays and silt sediments coming from nearby the site (S1, S3, S4, S5, S7) were similar to the groundmass and fine fraction of samples of fabrics F1, F2, F3, f4, both in the type of inclusions and in the textural aspects (average dimensions, shapes, ..). Only sediments S3, S4 and S5 differed in the presence of biogenic limestone fragments (scaglia rossa) and microfossils in sediments. They were all collected along the Rumarna stream, one of the streams that brought to the erosion of the terrace where Castel de Pedena is settled.

The sand sediments represent the geological situation of the region and in general they had great similarity with the coarser fraction of the pottery inclusions. In particular samples of the first four fabrics (rich in carbonate rocks fragments) are similar to the sediments collected along the Mis stream (S6, S8, S9), the Cordevole stream (S10) and the Veses stream (S12, S13). According with the geology of the area , sediments coming from the Mis stream basin are rich in carbonate rocks (mostly dolomite, and less carbonate mudstone and oolitic limestone); sample S8 has also metamorphic rocks fragments.

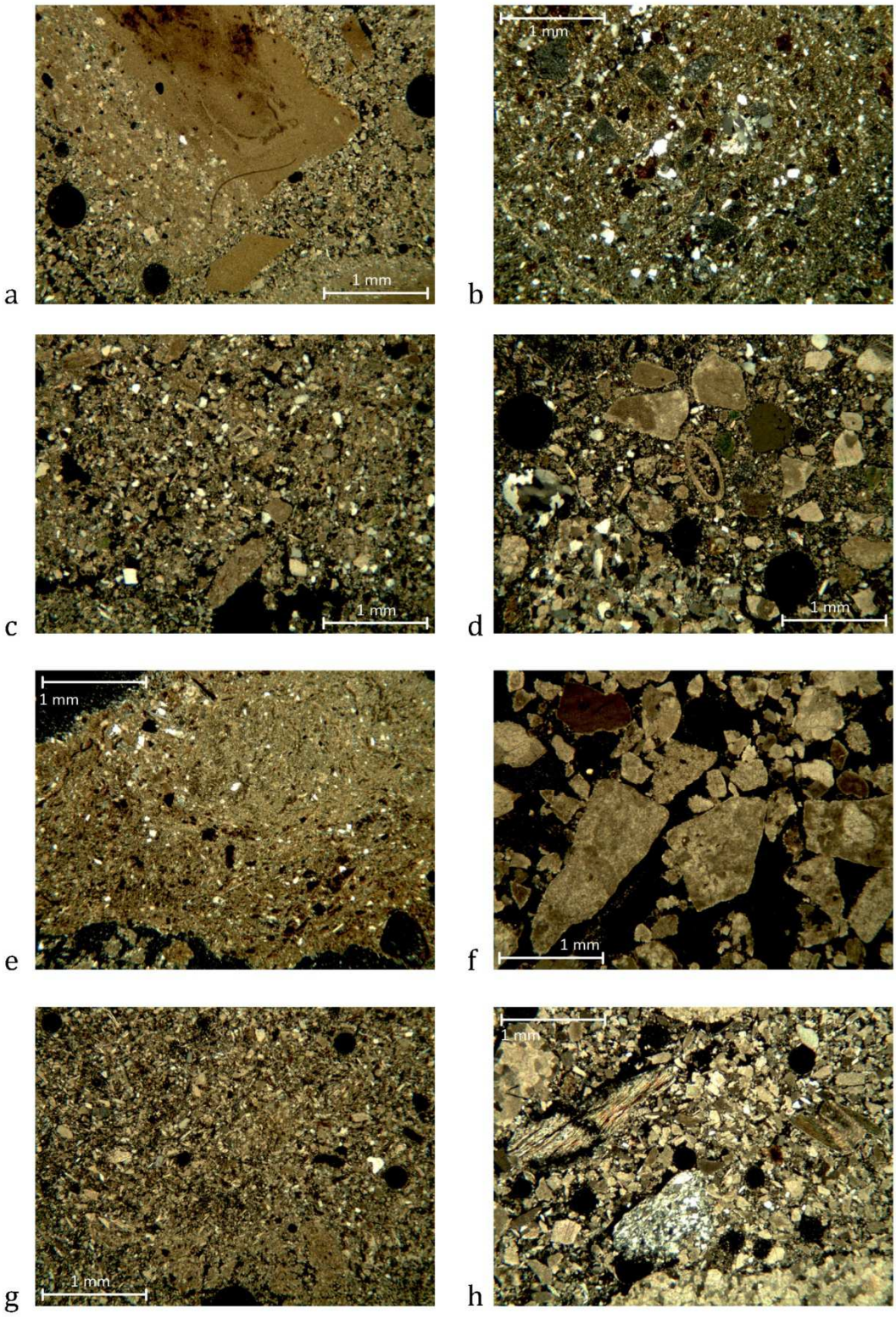

Figure 3. 44 a. Thin section photomicrographs of the sampled sediments. a) silty clay S1; b) Silty clay S2; c) caly S3; d) silty clay S4; e) clay S5; f) sand S6; g) clay S7; h) sand S8. The images were all taken in crossed polars.

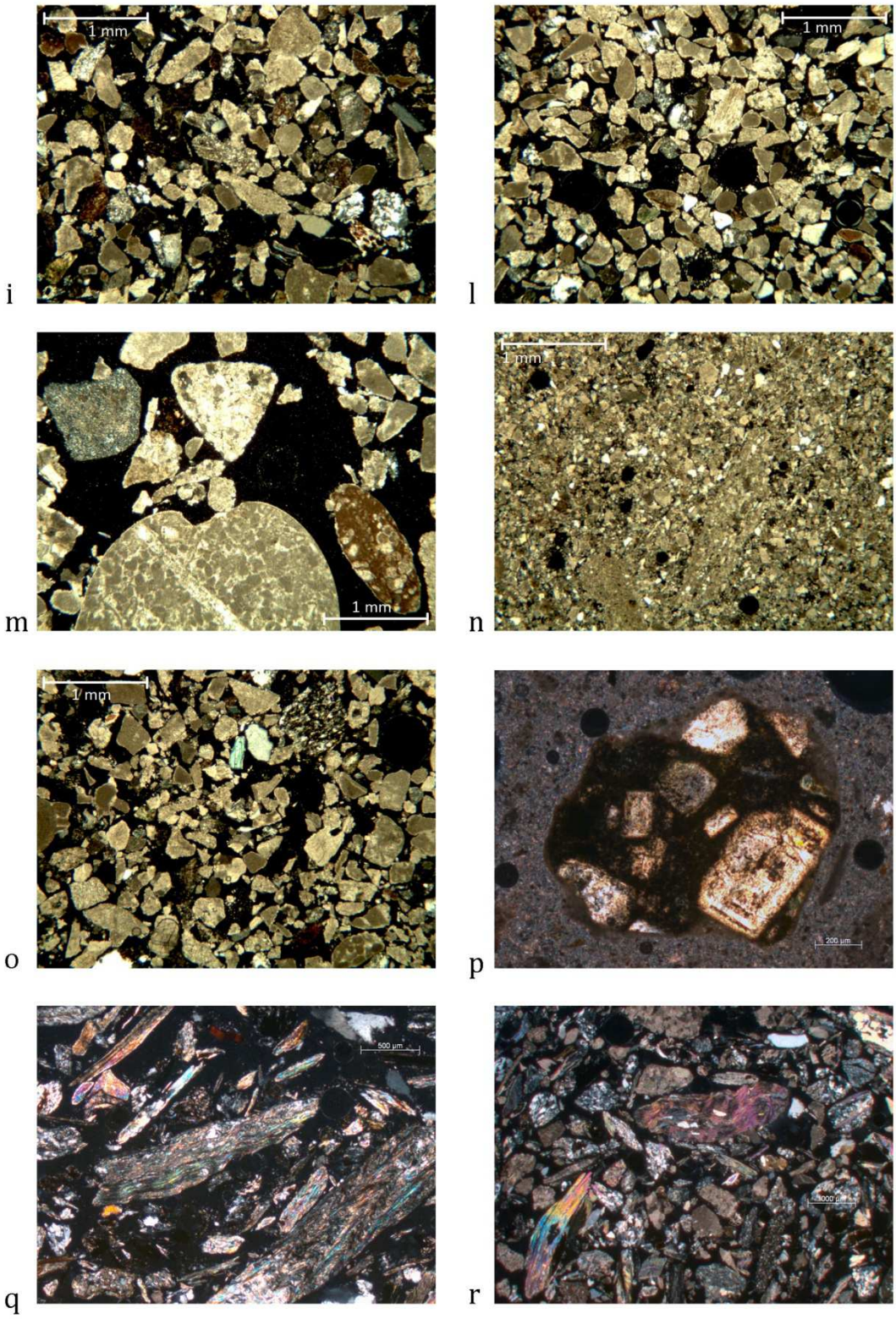

Figure 3.44. b. Thin section photomicrographs of the sampled sediments. i) sand S10; l) sand S11; m) sand S12; n) sand S13; o) sand S14; p) volcanic rock fragment in clay S20; q) sand S29; r) sand S30. The images were all taken in crossed polars.

Those sands collected northern along the Mis and closer to the metamorphic outcrops (S29, S30) are rich in polycrystalline quartz, mica-schist and graphite-phyllate. All these rock types are comparable with the a-plastic inclusions of sample M015 (fabric F8). Sands collected along the Cordevole stream have mostly carbonate mudstone, subordinate dolomite, and metamorphic polycrystalline quartz, phillyte, graphite-phyllite and few volcanic intermediate rocks. Samples of the Veses stream (S12, S13) are rich in carbonate mudstone and dolomite; sand S12 contains also few polycrystalline quartz and phyllite and rare intermediate volcanic rocks fragments.

Sediments coming from the volcanic area (S20-S27), rich in basalts, do not have any correspondence with the a-plastic inclusions of the studied potshards. Sample M038 itself, rich in intermediate volcanic inclusions, found major correspondence with the volcanic rocks observed in the other sediments (table 3.12) and with the few fragments observed in clay S21.

Several exotic pottery type were found during the excavations related to the Wieselburg-Gàta and to the Luco/Laugen–Meluno/Melaun cultures. These vessels could had been manufactured locally or even been imported from the major regions pertaining to these cultures. Specific provenance studies were carried out on these sherds. Only one sherd related to Wieselburg Gàta (late Early Bronze age) were studied under the petrographyc, mineralogical and chemical approach. The microscopic analysis indicated that this specimen (M001) was comparable with potsherds of fabric F6, characterized by predominant quartz sand inclusions, with a unimodal grain-size distribution. Unlikely it did not present among its a-plastic elements any rock type petrographically significant that could relate this fragment to any specific geographic area. Moreover, archeologically it is the only sample studied attributed at the Early Bronze Age and it belong to a very small group, so it was not possible to make any comparison with other coeval fragments and the few sample that may have petrographic similarity with it are much more recent. Moreover, this pottery type is not archaeometrically studied by other research groups, and there is not the possibility to make comparisons. In that way it is not possible to make any real consideration about its provenance.

The pottery assemblage coming from the Final Bronze Age phases seemed to be related to the Luco/Laugen–Meluno/Melaun culture. The Luco/Laugen-Meluno/Melaun ceramic style spread in the areas of the Italian South Tyrol and Trentino, the Austrian East Tyrol, the Swiss Grisons and the Swiss–Liechtensteinian–Austrian Alpine Rhine valley between the Final Bronze Age and the first Iron Age. This style was characterized by coarse tempered rostrate globular cups and double-conic or truncated conic jars with a spout (Leonardi 2010, Lanzinger, Marzatico et al. 2000, Metzer, Gleirscher 1992, Perini 1976).

Among the whole pottery assemblage studied, five specimens (M012, M015, M031, M033, M046) of Luco ceramic, of both Luco A (XI-Xcent. B.C.) and Luco B (X-IX cent. b.C.), were selected, especially to carry out provenance analyses. Unlikely the highly fragmented conditions and the small sizes of the potsherds did not allow to sample material enough to

samples	Av.size	Shapes					A%	CRYSTALS AND ROCKS																								
								Qz	Fsp	Snd	Pl	Cal-Dol	Px	Ms	Bt	Op	Glt	Chl	Grt	Qzt	Mcsc	FllGr	Vlc		Plt	Ch	Snd	Dol	CMt	CSpr	OO-Pld	Crl	Bio	ARF
	(mm)	eq/el	A	SA	SR	R																	acd	itmd	itmd								
S.1		eq			xx	x	C	3				2		1	1		2	1								2			8				1	1
S.2	0,8	eq		x	xx	x	A	6				1		2	1	2	2			4						6								4
S.3		eq			xx	xx	A	5				2		2	1	2	3	1	1	2						3		1	5				3	1
S.4	0,9	eq		x	xx	xx	A	3				2		1	1	1	2	1	1	1						4	2?	5	6		4	2	5	
S.5	0,06				xx	x	F	5				2		1			1	1		1												1	2	
S.6	1,6	eq-ql			xx	x		1															1i					8	3	2	3			4
S.7	0,04	eq			xx	x	A	3				2		1	1	1		1											6					
S.8	1,7	eq-el			xx	xx		3	1			2		1		1		1		5	4	3				3		8	4	5	3			
S.9	0,5	eq-el			xx	xx		1				1		1														5	7	5				
S.10	0,6	eq			xx	xx		2	2	1	2	1	1							4	4	4	4			4	1	4	7	5	2			
S.11	0,3	eq-el		x	xx	xx		2				1					1			3	2		3			4		3	7	2	1			2
S.12	1	eq			xx	xx		1				1			1		1			4	3		1			5	1	7	5		2		4	3
S.13	0,16	eq-el			xx	xx	A	5				1		1	1	2	1	1								2			6					
S.14	0,6	Eq			xx	xx		2	2		2	1	3		1	2	1	1		4	3	2	3		1	3		3	7		3		1	
S.20																																		
S.21																																		
S.22	0,6	eq-el	x	x	xx	xx					1	1	3			2	1	2			2	1	3			3	1		5	3	2			4
S.23	1	eq-el	x	xx	x	x						1				1											1	1	6	5	2			
S.24	0,7	eq-el	xx	xx	x	x		1				1	2			2	1	1					3		1	1		1	7	4				1
S.25																																		
S.26	1,5	eq	x	xx	xx	x						1	4			3	1	1					4	4				1	7	4				
S.27	0,6	eq	xx	xx	x	x		1				1	2			2							2					1	4	6				
S.29	1,2	eq	x	x	xx	xx		3			1				1	2		1		4		8												
S.30	1,4	eq-el	x	x	xx	x		1			1					1	1			2						3	1	2	5	4			5	1

Table 3.12. Brief description of the sampled sediments analyzed under optical microscope. Indication of the abundance of the inclusions (A.%) expressed like few (F), common (C) and abundant (A), it was indicated only for the clay sediments; average size of the inclusions (av.size); shapes: equant (eq), elongate (el), angular (A), sub-angular (SA), sub-rounded (SR), rounded (R). Composition of the mineral phases and lithics: qz: quartz crystals; Fsp: feldspars in general; KF: alkali feldspar; Pl: plagioclase; Cal-Dol: calcite and dolomite crystals, Amp: amphibole; Px: pyroxene; Ms: muscovite; Bt: biotite; Op: opaque minerals; Glt: glauconite; Grt: garnet; Qzt: polycrystalline quartz; Mcsc: mica schist; FllGr: Phyllite graphite; Vlc: volcanic rock; Plt: plutonic rock; acd: acidic rock; itmd: intermediate rock; Ch: chert; Snd: sandstone; Dol: dolomite; CMt: carbonate mudstone; CSpr: sparrycalcite; OO-Pld: ooid limestone; Crl: bioclastic limestone with corals; Bio: bioclastic limestone; CP: clay pellets; Grog: grog; ARF; CalSc: secondary calcite.

performXRPD and XRF analyses and multivariate statistical treatments except for sample M012. Optical microscopy thin-section observation was carried out on all the samples.
The petrographic classification of the Luco type potsherds show heterogeneous pastes belonging to different fabrics group (chapter 3.3): sample M012 fitted into the fabric F2, and it is characterized by abundant inclusions with a well sorted bimodal grain-size distribution. The coarser fraction, representing the 90% of the whole, is rich of carbonate inclusions (dolomite, carbonate mudstone, sparry calcite and oolitic limestone) and subordinate chert fragments. Sample M031 and M046 belongto fabric F3, and are characterized by well sorted bimodal grain-sized distribution of the inclusions where the c:f ratio is 90:10. The coarser fraction is mostly composed by carbonate mudstone associated to chert, polycrystalline quartz and graphite-phillyte fragments; samples M046 contains also few acidic volcanic rocks fragments, like rhyolite. Sample M015 is the lonely sample of fabric F8 whose peculiarity is the predominant quantity of metamorphic rocks (polycrystalline quartz and graphite-phyllite) associated to fewer chert fragments in the coarser fraction of the inclusions. Sample M033 belongs to fabric F6, characterized by a unimodal distribution of the inclusions mainly composed by a quartz sand. Though the pottery of Luco type differed one each other, they found petrographic correspondence with the supposed local potsherds, except sample M015, and fitted well with the fabrics described in chapter 3.3. Moreover their composition could be associated to the lithotypes present nearby the site and have good correlation with sand sediments collected along the streams near Castel de Pedena (S6, S9, S11, S12, S14). Although specimen M015 differed from the other shards, it could be related to the area just north the site, characterized by metamorphic outcrops, since its inclusions are similar to those of sand sediments S8, S10 and, just for the metamorphic inclusions, with S29, S30 (figure 3.41). Sample M033 did not present among its inclusions any rock type really petrographically significant that could allow to precisely relate the pot to any specific geographic area. Moreover it belongs to a small fabric class that groups sampled all attributed to different periods. Based on these considerations it was not possible to say if it is local or imported.
A study of a small assemblage of pottery coming from Castel de Pedena was carried out by Doct. Sara Levi few years ago and the results were presented at the conference “Il castelliere di Castel de Pedena. Un sito di frontiera del II e I millennio a.C.” in 2009. These shards include four samples of local type and two of Luco ceramic (sample named cdp2 of Luco A, and cdp6 of Luco B). For gentle concession of Doct. S. Levi it was possible to observe and compare the thin sections of these samples with those of the Luco pottery studied in this thesis. According with the results obtained by Levi, samples of Luco type A and B well matched with fabric F2 (sample cdp6) and F3 (sample cdp2), respectively. Sample cdp2 (Luco B) contains among its inclusions metamorphic and sedimentary carbonate rock fragments together with subordinate intermediate volcanic fragments, as observed also in sample M046. The other samples she studied, archaeologically classified

as local typology, are petrographically classifiable in fabric F1 (cdp5), fabric F2 (cdp3) and fabric F3 (cdp1, cdp4).

Provenance studies on Luco ceramic were carried out by Maggetti in the 70' with the intention to understand the trade routes and to distinguish between local productions and imported artifacts. This research involved all the geographical regions where the Luco culture spread: Italian South Tyrol and Trentino, the Austrian East Tyrol, the Swiss Grisons and the Swiss–Liechtensteinian–Austrian Alpine Rhine valley (figure 3.45). A total of four hundred and fifty-four samples from the three time horizons (Luco A, Luco B, Luco C) and thirty archaeological sites were analysed and published (Maggetti et al. 1979, 1982, 1983, Maggetti 2005, Marro *et al*. 1979, Stauffer *et all*. 1979).

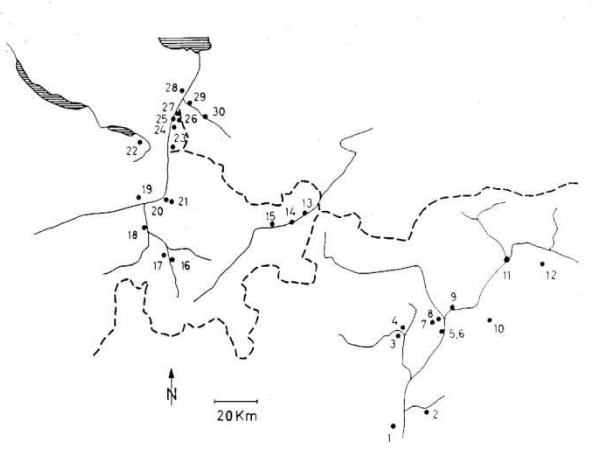

Figure 3. 45. Distribution of the site of Luco/Laugen-Meluno/Melaun culture studied by Maggetti. After Maggetti, Waeber et al. 1983. Italia settlements: 1-12; Swiss and Liechtenstein settlements: 13-15; the Rhine valley: 16-30

The Luco samples found at Castel de Pedena were compared with the pottery studied by Maggetti. At a previous stage of the analysis the published references and the geological map of the interested areas were considered. The areas investigated by Maggetti are all geologically distinct and differ from the Vallone Bellunese situation, so it seemed immediately that it was difficult to hypothesize a possible provenance from there:

The Italian settlements (Italian South Tyrol and Trentino).

Between Bozen and Trento, the area to the east and west of the Etsch River is marked by the presence of volcanic and/or carbonatic (dolomite) rocks. The volcanic elements form the so-called quartz–porphyric plateau, a mighty sequence of rhyolites and basalts. In addition to these components, the valley's unconsolidated sediments contain lithic fragments of gneiss, schist and granite. These occur north of the quartz–porphyric outcrops and were transported to the investigated area via glaciers and rivers (Maggetti 2005). Samples studied by Maggetti coming from the sites located at the centre of the volcanic complex resulted of local origin. In contrast to the central group, the peripheral sites (Brixen and St.Lorenzen-Sonnenburg) were partly of local origin and partly not manufactured on site. Instead, they were imported from the area of the central group (Maggetti 2005).

The Swiss and Liechtensteinian settlements. The Inn valley group

The area surrounding the Inn river is geologically characterized by gneiss, schist, amphibolite, serpentinite and dolomitic limestone. Only 57% of the analyzed pottery contains this types of rocks as non-plastic constituents. The remaining 43% contains a larger or smaller amount of volcanic rock fragments of the same petrographic composition found at the Italian sites. Therefore, the author concluded that the shards

from the Inn valley with volcanic rock temper were produced in the vicinity of the Italian central group and subsequently exported to the Inn Valley (Maggetti 2005).

The Rhine valley group

The temper of samples coming from the sites located in the Rhine Valley was characterized by either sedimentary or metamorphic constituents, that correspond to the respective geological–petrographic environment. The ceramic from the Flums-Gräpplang site revealed a rich schist temper, consistent with the Triassic 'Quartenschiefer' and Permian Verrucano schists occurring locally. Specimens from Altenstadt are rich in amphibolite rock fragments. This is compatible with the hinterland of the Ill River, that contains a lot of amphibolites (Maggetti 2005).

For gentle concession of Doct. Marino Maggetti, it was possible to observed the thin sections collection of pottery coming from the sites of the Luco culture. In that way we could make a direct comparison with the Luco type samples found at Castel de Pedena. According with the geological conditions of the interested areas, pottery from Castel de Pedena are different from those coming from the other sites where Luco pottery was found. Particularly they lacked in those lithotypes distinctive of the different geographical regions. Also a-plastic inclusions of sample M038, mainly composed of volcanic rocks fragments, are diverse rocks types than those peculiar of neighboring Bozen and Trento area. These results confirmed our assumption about a local origin of the Luco ceramic from Castel de Pedena.

3.8 Production technology

This archaeometrical study was conducted with the aim to define the production technology of pottery from Castel de Pedena (clay selection and processing choices, pottery forming methods, firing conditions...), to characterize in detail their compositional variability and to distinguish between local and imported artefacts. The combined petrographic and chemical analyses of the ceramic samples revealed compositionally diverse assemblages and recipes (corresponding to the different fabrics, chapter 3.3) related to different chronological phases of the site (figure 3.46).

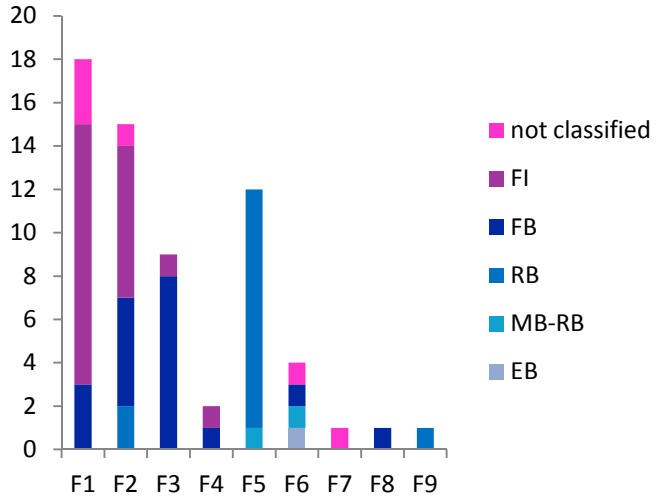

Figure 3. 46. Distribution of the studied potsherds related to the different chronological phases of the site.

According to the petro-fabric classification, different choices in the raw materials selection and use by potters resulted. Despite the heterogeneous situation in terms of inclusions composition, it was also possible to identify in the surrounding area of the site (or at small distances) potential sources for the raw materials geologically compatible. The sediments sampled allowed to make some more reflections.

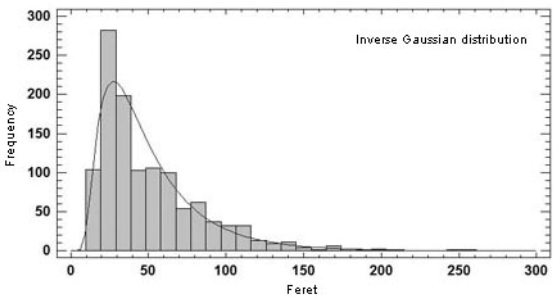

Figure 3. 47 Frequency distribution diagram typical of quartz inclusions in sample M001 (fabric 3).

In details, it arose that all the pots dated at the beginning of the Recent Bronze Age (BR1 for the Italian date) belong to fabric F5, except of sample M038, that is the only one pertinent to the fabric F9, and two samples attributed at the late Recent Bronze Age. These samples (fabric F5, chert and quartz rich potshards) were closely related both in its coarse and fine fraction to clay S.2, collected few hundred meters far from the site. Moreover, the DIA performed on the chemical map of potsherd M001 showed a continuous grain size distributions of quartz with the larger number of grains that fall in the finer fraction range (between 20-30 μm) and only rarely few peaks in the coarser fraction grain-size. This situation is typical of fragments naturally present in the clay (figure 3.47).

From the end of the Recent Bronze Age the situation was less well delineated. Samples attributed at the Final Bronze Age are well grouped in the fabric F3 and F2, only few of them are referred to the fabric F1. During the beginning of the Iron Age pastes of the first type (fabric F1) were preferred, but pastes of type 1.2 were still adopted.

Considering the raw material processing, if we assume the removal by the potters of the coarse particles through sieving and the further addition of temper materials, S.2 is also similar to potshards of fabrics F1,F3, F4 and F7. As well, their coarser inclusions found high petrographic correspondence with the sand sediments of some streams that flow near the site. The hypothesis of a artificial addition of a-plastic elements was supported also by the textural characteristics of the pastes. As observed through the microscopy analysis, and confirmed by the digital image analysis, inclusions are always present in high amount. In addition, pastes F1, F3, F5, F7, F8 and F9 present a well or moderately

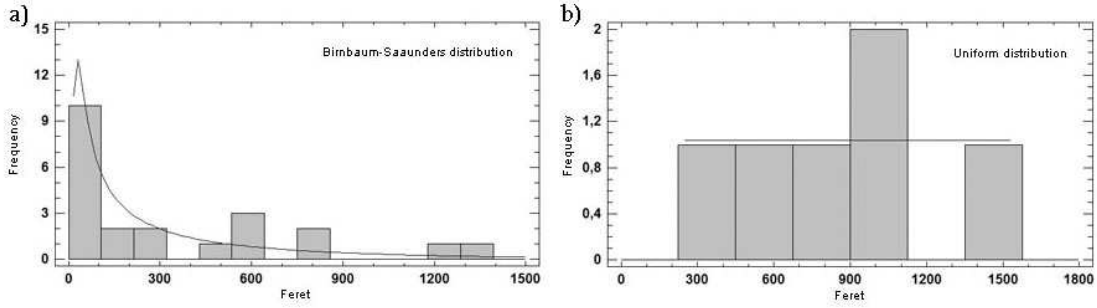

Figure 3. 48. Frequency distribution diagram typical of calcite (a) and dolomite inclusions in sample M086 (fabric F2).

sorted hiatal grain-size distribution. The DIA results obtained on the chemical maps images showed, in all the samples of fabrics F1, F2 and F3, a continuous grain-size distribution of quartz with the larger number of grains falling in the finer fraction range (usually between 20-40 μm). Calcite is usually represented by a continuous grain size distribution with the larger number of grains falling in the finer fraction range with some peaks in higher size ranges, significant of more than one modes (figure 3.48.a). While dolomite can have a grain-size distribution similar to that of calcite or, more often, a uniform grains size-distribution (figure 3.48.b). A similar situation is assumed by the metamorphic rock fragments in fabric F3. A distribution similar to that of calcite is usually related to its natural presence in the clay, in the fine fraction range size, and its addition, after sieving, for the coarse fraction range size. A distribution as that assumed by dolomite is usually related at the tempering of the clay.

As the temper grains are often rounded or at least have rounded edges, it can be concluded that potters mostly used natural sand as temper. Paste 1.2, the lonely with a seriate grain-size distribution, has carbonate elements angular in shape. This suggests the deliberately addition of the inclusions after being crushed. The addition of grog was extremely rare and always less than 10%, except for samples M056 and M030.

Few samples (Fabric F4) were characterized by a quartz and carbonate sand with a moderately sorted bimodal grain-size distribution. The DIA showed a continuous grain-size distribution of quartz (10%), two populations for dolomite: one continuous distribution among small grain sizes and a second distribution represented by few bigger grains. Calcite is represented by more uniform modes both in the finer fraction than in coarser one. In this situation it was not possible to say if samples were tempered or not.

Chronologically, these different pastes are related at the more recent occupational phases of the site. Therefore it can be inferred that the manufacturing techniques changed significantly throughout the centuries and was standardized during the different periods (figure 3.46).

Since fabrics F4, F6, F7, F8 and F9 are formed by few samples or lonely ones, they are statistically scarcely represented, and cannot be considered to draw a general trend in the pottery changes over time. Moreover, since there is not a representative assemblage of pottery coming from the earlier phases (Middle and Late Bronze Ages) of occupation of Castel de Pedena, it was not possible to make significant consideration about them.

An important aspect concerning the production technology is the firing process (redox condition and maximum temperature reached).

As the colour of the ceramic paste is strictly related to the redox conditions of firing (oxidising or reducing), chromatic variations of pottery were initially evaluated (see chapter 3.2) and different situations were described. The majority of the samples have homogeneous grey or very dark grey body, sometimes with a lighter (pink or red) extremely thin external layer. Usually, this is indicative of cooling in reducing atmosphere, independently of the organic matter content, or with a fast exposure to oxidising atmosphere. Only few of potsherds have homogeneous light bodies, grey and brown or

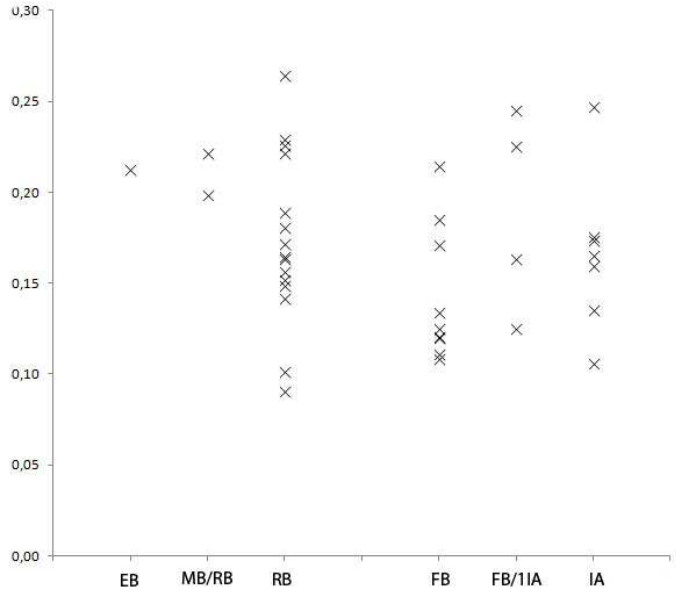

Figure 3. 49. Reduction Index estimated for the potsherds grouped respect their chronological phases.

reddish coloured, probably due to cooling in scarce oxidising atmosphere (grey and brown colours) and oxidising atmosphere, without or with scarce organic matter. Only four samples present a sandwich structure (a dark "core" with lighter reddish surfaces) or colour differentiations along the external, usually reddish, and the internal, grey-dark grey, surfaces. This is usually related to a reducing atmosphere during firing and oxidising cooling, or oxidising firing and cooling atmospheres in presence of organic matters.

The redox conditions of firing were deduced also from the reduction index (RI). The RI is defined as the ratio of the iron (FeO (Fe^{2+})) content determined by the modified Pratt's method (Pratt, 1894) as described in chapter 2.4 and the FeO_{tot}. The FeO_{tot} was calculated as (Fe_2O_{3tot}/1,111), where the total iron oxide (Fe_2O_{3tot}) is the iron content estimated through XRF analysis. Conventionally RI values higher than 0,20 are related to a reducing firing atmosphere. The RI calculated for the analyzed samples highly varies and range between 0,09 and 0,26. The 73% of the samples have value related to a oxidising firing atmosphere, and the other 27% are related to slightly reducing oxidising atmospheres. Since pottery has mostly grey or dark grey pastes, we could expect especially reducing atmosphere; this result can be explain with the lighter external layers, on brown tones often present, indicative of oxidizing cooling. In the samples with black cores and red margins (sandwich structure), the RI values vary over a wide variable firing conditions. These variations were related to the evolution in production technology, according to archaeological evidence (figure 3.49). The wider intervals of pottery dated at the Recent Bronze Age and the slighter differences of ceramics during the first Iron Age may indicate the passage from less standardized production towards better technological skills.

The firing temperatures were deduced from the stability range of selected critical minerals phases, defined by X-ray powder diffraction. Based on the results of XRPD analysis, the samples were clustered in groups and sub-groups considering the main

minerals present (table 3.4) and a temperature interval was suggested for each of them. Samples of group A_{XRD} and B_{XRD} are characterized by an illitic calcareous clay. For pottery fired in oxidizing condition, the presence of calcite and illite , and dolomite in group B_{xrd}, and the absence of chlorite indicate firing temperature between 650-850°C ($A1_{XRD}$) and between 650-750°C ($B1_{XRD}$), respectively. The nucleation of hematite in presence of carbonates (calcite and dolomite) indicates a temperature interval of 750-850°C (group $A2_{xrd}$). Since it was not possible to distinguish between smectites minerals of primary or secondary post-depositional formation, for groups $A3_{xrd}$ and $B2_{xrd}$ was suggested temperature lower than 650°C. Though higher temperatures between 650-800 ° C could occur.

Samples of groups C_{xrd}, D_{xrd} and E_{xrd} are characterized by a non calcareous illitic clay. The crystallization of spinel (maghemite and magnetite like) and the contemporary presence of illite (group C_{xrd}) indicate a temperature interval between 800-950°C. In samples of group $D1_{xrd}$ the absence of chlorite and the presence of illite suggest temperature between 650-950°C, while the nucleation of hematite in group E_{xrd} and $D2_{xrd}$ rises the temperature interval at 750-950 °C and the chlorite detected in group $D3_{xrd}$ lowers it at less than 650°C.

Therefore, very different firing temperatures were noticed, indicative of different techniques. It is likely that samples of groups D_{xrd}, dated at the Late Bronze Age and Recent Bronze Age, were fired using pit firing method as they present a wide temperature interval with temperatures ranging from less than 650°C and only in few cases restricted between 800-950 °C. Samples of groups A_{xrd}, B_{xrd} and C_{xrd}, dated between the Final Bronze Age and the first Iron Age, were probably fired using kiln firing conditions. Several samples present high temperature mineral phases: nucleation of hematite and spinels. Spinel is present only in few samples, attributed at moment of passage between the Bronze Age and the beginning of Final Bronze Age, all belonging at the fabric F3, that confirms a different production technology (different recipe for the paste and different fire technique).

3.9 Discussion and conclusions

The study of the pottery assemblage from Castel de Pedena provided important results under an archeological viewpoint: it was possible to delineate the evolution of the production technology from the Recent Bronze Age to the first Iron Age. Particularly, the combined petrographic and chemical analyses of the ceramic samples revealed compositionally diverse assemblages, related to the different chronological phases of the site. This high correlation suggests that the groups identified can be considered real "paste compositional reference units" (PCRUs), archaeologically meaningful. Moreover, this is significant of changes over time in the potters technological habits: variations in the geological source selection for supplying a-plastics (temper) and clays, in the clay processing choice and in the production technology.

During the Recent Bronze Age, it is likely that the raw material was selected in the surroundings of the site. The comparison between the raw clay materials and shards shows great similarity both in the clay and in the natural presence of angular chert fragments. However the inclusions are in great amount and have splintery, angular outlines. Therefore, it is not possible to say if potters used the raw material without processing it or if they added chert, rocks that were naturally present and available in the same clay outcrops. This type of pottery was formed by the coiling technique. It is likely that these samples were fired using pit firing as they present a wide temperature interval (low of 650-900°C).

During the Final Bronze Age, it seems that potters were used to select a non calcareous illitic clay at which added artificially non-plastic elements. Inclusions, mostly carbonatic rocks and metamorphic components sometimes associated with volcanic fragments, were collected in the nearby, probably along the Mis or Veses streams. They have a hiatal texture and are rounded or sub-rounded in shape. It can therefore be concluded that potters added natural sand. Ceramic were fired at temperature of 800-900°C in reducing atmosphere.

In few samples illitic non calcareous clays were tempered with crushed rocks, that are present with a seriate grain-size distribution (paste 1.2). The a-plastics inclusions are mainly carbonate, probably collected in the nearby. Ceramic were probably fired in kiln firing conditions at temperature between 650 and 850°C.

At the beginning of the Iron Age, it seems that potters were still using the same technique consisting in adding crushed carbonate mudstone at illitic non calcareous clays, but they associated also a new recipe. They started to select non calcareous illitic clays at which artificially added non-plastic elements. Inclusions, mostly carbonatic rocks, were collected in the nearby, probably along the streams that flow closed to Castel de Pedena. It can therefore be concluded that potters added natural sand. Ceramic were fired at temperature of 650-800°C, probably in fired in kiln firing conditions.

Other pastes and recipes must be considered as outliers since only few samples or lonely one belong to them. Therefore it is not possible to make any consideration about them. In addition, they are related to different chronological periods. Only one sample, a carinated vase, could be related to ceramic trade or contacts as it has among its inclusions, fragments of volcanic rocks peculiar of other area; geologically consistent with the Vallone Bellunese effusive rocks, that were also found in the sediments of the Cordevole basin.

The Luco/Laugen-Meluno/Melaun ceramic was produced locally using several recipes: addition of carbonate and metamorphic rocks collected along the streams; addition of crushed carbonate fragments; tempered with metamorphic rock fragments or with a fine quartz sand. No ceramic trade could be identified for these vases with the regions where the Luco/Laugen culture was well attested, especially with the closer Trentino and Suouth Tyrol.

Only one sample was probably made close to the sources of the Mis stream, at a distance of nearly 30-35 km. Therefore these data prove the existence of intensive contacts with the neighboring regions. This type of ceramic may had been manufactured by local people who adopted a new style or potters, who had migrated, may had continued to use their traditional methods.

3.10 FONDO PAVIANI

The occupation of the site of Castel de Pedena during the beginning of the Recent Bronze Age is testified by the presence of pottery that found well comparison with the coeval ceramic of the Po plain. In particular, big bowls, two of which with a grooved rim and a raised cylindrical handle, found good similarity with pots coming from the sites of Custoza, Fabrica dei Soci, Fondo Paviani and Mariconda di Melara (Dalla Longa 2012, Donadel 2012). The retrieval in the site of specimens typical of the "Palafitticolo Terramaricola" culture induced to analyze also a small assemblage coming from the site of Fondo Paviani dated at the middle of the Recent Bronze Age (Figure 3.50). A total of ten samples coming from Fondo Paviani were analyzed (table 3.13). This is a very small number and it is not statistically representative of the pottery assemblage coming from the site, therefore, these results presented here must be considered preliminary and a large-scale study needs to be carried out to better understand the relationship between these sites.

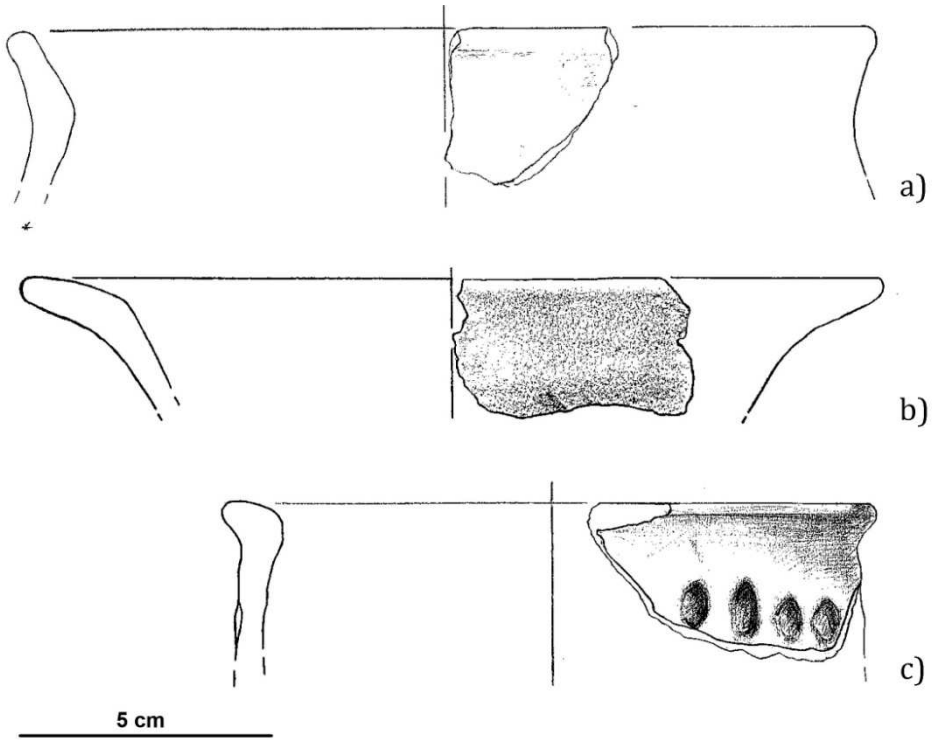

Figure 3. 50. Pottery types from Fondo Paviani corresponding to samples FP06 (a), FP09 (b), FP01 (c).

Samples	Form	Chronology
FP01	Ovoid jar with flattened lip	mature RB
FP02	Jar with flattened lip	mature RB
FP03	Jar with flattened lip	mature RB
FP04	Truncated conic bowl with flattened lip	mature RB
FP05	Ovoid jar with flattened lip	mature RB
FP06	Jar with flattened lip	mature RB
FP07	Jar with flattened lip	mature RB
FP08	Ovoid Jar with flattened lip, thickened to exterior	mature RB
FP09	Truncated conic bowl with flattened lip	mature RB
FP10	Indeterminate, wall with plastic additions (ribbon like) on the surface	mature RB

Table 3. 13. Details of the studied potsherds.

3.10.1 Historical context

Fondo Paviani (Legnago, Verona, north-eastern Italy) is a Bronze Age terramara located north of the Po River in the Valli Grandi Veronesi area settled at the transition between the middle Bronze Age and the late Bronze Age. Near the end of the late Bronze Age the site reached its maximum size of nearly 20 ha and was surrounded by a moat and fortified by a quadrangular earthen rampart. In this period the site assumed great vitality and a linking role connecting the Po plain, the continental Europe, the peninsular Italy, the Aegean and the eastern Mediterranean. This vivacity is testified by the high specialized craftworks with the introduction of innovative technologies and by short and long distance exchanges (Balista, De Guio 1997, Cupitò, Leonardi c.s., Fasani, Salzani 1975, Leonardi, Cupitò 2008). Exotic and luxury artefacts are bronze objects, Baltic amber ornaments, glass beads, sub-Apennine vessels and Aegean pottery imported from Greece and southern Italy as well as produced locally (Bettelli, Vagnetti 1997, Cupitò, Leonardi c.s., Jones, Vagnetti et al. 2002). Between the end of the Recent Bronze and the beginning of the Late Bronze Age, it seems to be one of the few terramare sites not affected by the general settlement system collapse and is well insert in the new system of the Po plain until the end of the Final Bronze Age (Bernabò Brea, Cardarelli et al. 1997, Cardarelli 2009, Leonardi, Cupitò 2008).

3.10.2. Geomorphological setting

The Valli Grandi Veronesi area corresponds to a wide subsiding alluvial basin between the major rivers Adige and Po in the southern Venetian plain (Mozzi 2005, Nicosia, Balista et al. 2010). The area is located at the margins of the so-called ancient Adige alluvial fan ("Conoide Antico dell'Adige"), a late-Pleistocene fluvioglacial fan deriving from the outwash of the Garda glacier (Sorbini, Accorsi et al. 1984). The Adige river appears to had downcut its course since the early Holocene, leaving a series of relict terraced strips on the surface of the ancient Adige fan. Since then, these exposed surfaces were subject to weathering (ARPAV 2005, Costantini 1992).

A series of small, incised valleys, formed during the Late-Glacial Age, were re-occupied by spring-fed rivers (Tartaro, Tregnone, Menago) that originate at the passage between the

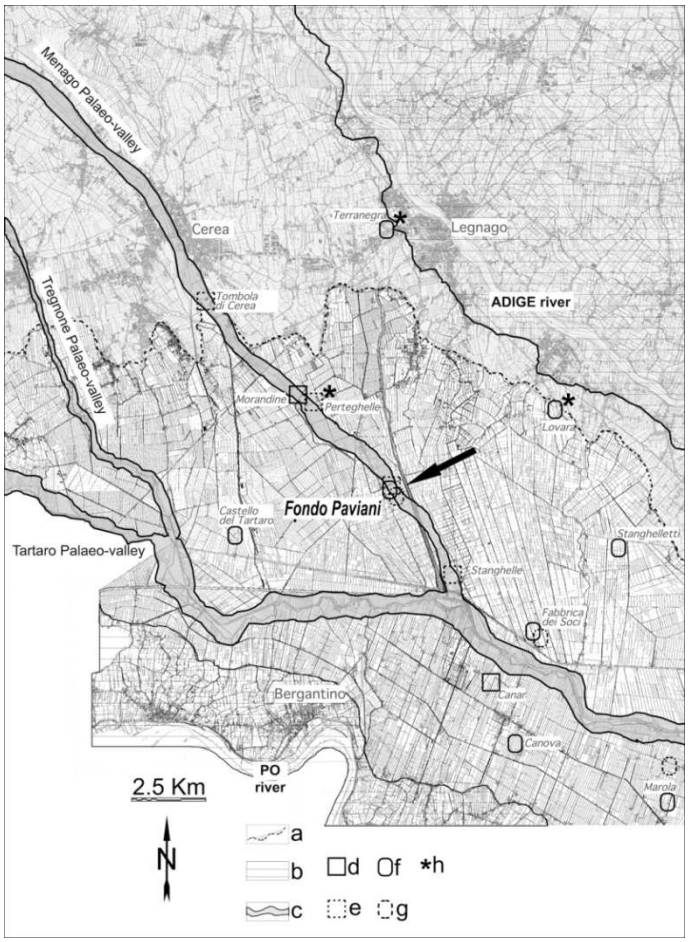

Figure 3. 51. Central part of the Valli Grandi Veronesi area, with indicated the position of Fondo Paviani (arrow). Symbol legend: (a) Terrains higher than 14m a.s.l., at the margins of the lowermost central part of the Valli Grandi Veronesi basin. (b) Po and Adige river courses of historical era. (c) Palaeo-river valleys incised in the late-Pleistocene ancient Adige alluvial fan. (d) Ancient Bronze Age pile-dwelling sites. (e) Middle Bronze Age sites on reclaimed terrains. (f) Recent Bronze Age sites with moat and rampart. (g) Sites still inhabited in the final Bronze Age. (h) Sites re-occupied during the early Iron Age. After Nicosia 2011.

high and medium portions of the plain (Sorbini, Accorsi et al. 1984). The site of Fondo Paviani is located within the Menago palaeo-river valley (figure 3.51). The Holocene infilling of these valleys consists of alluvial and peat deposits, controlled by climatic fluctuations since the Late-Atlantic/Sub-Boreal periods; the activity of spring-fed streams inside the valleys led to the formation of sandy alluvial ridges within palustrine successions (Balista, De Guio 1997, Nicosia, Balista et al. 2010).

3.10.3. Petrographic fabric classification

The ceramic shards (ten samples) were analyzed under polarizing light microscope following a modification of the thin section description protocol illustrated by Whitbread (1989, 1995). The petrographic examination of the thin sections revealed a high compositional variability, due to the different mineralogical and petrographic types of inclusions and to the diverse fabrics present (table 3.14).

Fabric 1: sand (quartz, polycrystalline quartz, volcanic acidic rocks -rhyolite- and carbonate mudstone) rich potsherds (three samples)

This fabric is a small group characterized by abundant inclusions (nearly 30%) with a good bimodal grain-size distribution (figure 3.52. a-b). The c:f ratio is 80:20 (maximum sizes 4,0 mm, average sizes 0,8 mm). The coarser fraction is composed by sand made of rounded crystals of quartz, polycrystalline quartz, volcanic acidic rocks (rhyolite), carbonate mudstone, and subordinated feldspars (both alkali feldspar and plagioclase). Voids are mainly channels and vughs (nearly 5%).

samples	MATRIX					VOIDS					INCLUSIONS:				INCLUSIONS-COARSE FRACTION								INCLUSIONS-FINE FRACTION							
	A %	Hom.	Opt. Ac.	b-fab.	Or.	A %	max. size	Shape			Or.	A %	Dist.	kind of sor.	Rel. Ab. %	max. size	av. size	Shape					Rel. Ab.	max. size	av. size	Shape			
							mm	Ch	Pb	Vu						mm	mm	eq/el	A	SA	SR	R	%	mm	mm	eq/el	SA	SR	R
FABRIC 1																													
FP-01	65	e?	i		i	5	1,6	x		x	i	30	bi	Ms	80	1,6	0,8	eq		x	xx	xx	20		5	eq	x	x	x
FP-03	62	e?	↑a	sp	o	8	2,3	xx	xx	x	i	30	bi	Ms	80	4	1	eq			x	x	10	0,3	10	eq		x	
FP-09	72	e?	↓a	sp	↓o	8	10	x		x	i	20	bi	Ms	80	2,6	0,8	eq		x	xx	xx	30	0,2	4	eq	x	x	
FABRIC 2																													
FP-06	82	e?	a	sp	i	8	2,2	x		xx	i	10	u	Ms		0,42	0,2	eq	x	x	x								
FP-08	87	o	a	sp	i	3	2	x		xx	i	10	u	Ms		1	0,3			x	x	x							
FP-07	85	o	a	sp	i	5	1,6	x		xx	i	10	u	Ps		1,5	0,3	el/eq		xx	xx	x							
FABRIC 3																													
FP-02	75	e?	a	sp	↓o	5	2	x		xx	i	20	Bi	Ms	90	2,5	1,2	eq	x	x	x		10	0,3	5	eq	x	x	
FP-04	75	e?	a	sp	↓o	5	1,5	x		xx	i	20	Bi	Ms	80	1,4	0,8	eq		x	xx	xx	20	0,2	4	eq	x	x	
FABRIC 4																													
FP-05	80	o	↓a	Sp	i	5	5	x		xx	i	15	S	vps	20	4	1,7	eq			x	x	80	0,5	5	eq		x	x
FABRIC 5																													
FP-10	70	o	i		i	5	2,6			x	i	25	S	Ps	50	5,2	1,4	el/eq		x	x	x	50	0,3	5	eq		x	x

COARSE FRACTION DESCRIPTION																								FINE FRACTION DESCRIPTION													
samples	CRYSTALS												M. R.	I. R.			SED. R.						OTHER FEATURES				CRYSTALS										M.R	I R	S. R.	
	Qz	Fsp	KF	Pl	Mcl	Amp	Px	Ms	Bt	Op	Glt	Grt	Qzt	vlc		plt	Ch	CMt	CSpr	OO	Crl	Bio	CP	Gg	ARF	CalSc	Qz	Fsp	KF	Pl	Cal-Dol	Amp	Ms	Bt	Op	Grt	Qzt	vlc	Ch	CMt	Ox
FABRIC 1														int	ac	ac																							
FP-01	4	4	*	*						3			5		5	3	4	5					2			2	7	4					2	1	3					
FP-03	5	4	*	*			1		2			1	4	3	5		3	5		4		2	2				5	6?	**	**		2	4		4	1	3	2	2		3
FP-09	5	5	*	*	*	1		1	1	1			5		5	5	3	5	3	1			1				7	5	**			2	3		4		1	3	3		3
FABRIC 2																																							
FP-06	7	6				3		2	2				3		2	1	3	1	1				1	3															
FP-08	7	5	*	*		1	1	2	1	2	1				4								3																
FP-07	5	5	*	*		2		2	2	3		1	5		4			1	1				4	2																
FABRIC 3																																							
FP-02	4	4	*	*		2						2	5		6		3	2							2		6	6		**	2	2	5	1	1	1				
FP-04	5	5	*	*	*								6	1	6		3	3	2				5				6	6	**		1	2	4	1	3	1				2
FABRIC 4																																							
FP-05	4	4	?	1									2	2	3			7				4		5			6	6	**	**		2	3	1	2		2	2	2	3	?
FABRIC 5																																							
FP-10	2	3												1		1		6			2	6				4	6	5			6		2		1		1		2		?

Table 3.14. Minero-petrographic and micro-structural features of pottery samples analyzed under optical microscope.

Table 3.14. (page 105) Minero-petrographic and micro-structural features of pottery samples analyzed under optical microscope. MATRIX: area fraction (A.%); homogeneity (Hom); optical state (Opt.Ac.); birefringent fabric (b-fab); orientation (Or). VOIDS: tarea fraction (A.%); maximum size (max.size); shape: channel (Ch), planar voids (Pb), vugh (Vu). INCLUSIONS: orientation (Or); total area fraction occupied by the inclusions (A.%); grain-size distribution of the inclusion: unimodal (u), bimodal (bi), seriate (S), kind of sorting of the inclusions: moderately sorted (ms), poorly sorted (ps), very poorly sorted (vps); distinct description of the course and fine fractions of the inclusions (where there are present more than one mode): relative abundances (Rel.Ab.%); maximum and average sizes (max.size; av.size); shapes: equant (eq), elongate (el), angular (A), sub-angular (SA), sub-rounded (SR), rounded (R). Composition of the mineral phases and lithics: qz: quartz crystals; Fsp: feldspars; KF: alkali feldspar; Pl: plagioclase; Mcl: microcline; Cal-Dol: calcite-dolomite crystals; Amp: amphibole; Px: pyroxene; Ms: muscovite; Bt: biotite; Op: opaque minerals; Glt: glauconite; Grt: garnet; Qzt: polycrystalline quartz; Vlc: volcanic rock; Plt: plutonic rock; ac: acidic rock; int: intermediate rock; Ch: chert; Dol: dolomite; CMt: carbonate mudstone; CSpr: sparry calcite; OO: ooid limestone; Crl: bioclastic limestone with corals; Bio: bioclastic limestone; CP: clay pellets; Gg: grog; ARF; CalSc: secondary calcite. Abundance of mineral phases: 8: predominant (>70%); 7: dominant (50-70%); 6: frequent (30-50%); 5: common (15-30%); 4: few (5-15%); 3: very few: (2-5%); 2: rare (0,5-2%); 1: very rare (<0,5%)

Fabric 2: quartz sand and grog rich potsherds (three samples)

This group has few inclusions (nearly 10% of the total thin section are), characterized by a unimodal grain-size distribution (figure 3.52. c-d). A-plastic elements are composed by grog and less large rock fragments (maximum dimension 1,50 mm) together with a quartz sand. There are also subordinate sub-rounded and sub-angular crystals of feldspar (both alkali feldspare and plagioclase), polycrystalline quartz, volcanic acidic rocks (rhyolite) and rare chert. Voids are rare (5%) mainly represented by vughs and channels.

Fabric 3: Rhyolite and polycrystalline quartz rich potsherds (two samples)

It is a small group, characterized by an optically active heterogeneous groundmass and small amount of pores (5%), mainly vughs and less channels (figure 3.52. e-f). Inclusions have a moderately sorted bimodal grain-size distribution with a c:f of 80:20. They are mainly represented by volcanic acidic rocks (rhyolite) and polycrystalline quartz. Crystals of quartz, feldspar, chert, carbonate mudstone and grog fragments are also present. They are associated to abundant clay pellets.

Fabric 4: carbonate mudstone rich potsherd (one sample)

This sample is characterized by few inclusions (on average 15%) showing a seriate grain-size distribution (c:f ratio of 80:20) where the coarser fraction can reach 4 mm in size and has average size of 1,7 mm (figure 3.52. g). It is composed of dominant carbonate mudstone, bioclastic limestone and grog. The finer fraction is a sand with abundant quartz crystals and subordinate feldspar crystals and few volcanic igneous rocks (rhyolite and trachyte). The fine fraction has a composition similar to the fabrics 1-3's samples.

Fabric 5: carbonate inclusions rich potsherd (one sample)

This sample is characterized by abundant inclusions (25%) showing a seriate grain-size distribution whit a c:f ratio of 50:50 (figure 3.52. h). The coarser fraction is represented by big sub-rounded and sub-angular carbonate mudstone and bioclastic limestone fragments (maximum dimension 5 mm). There are also rare volcanic acidic rocks, quartz and feldspar crystals (< 15%). Voids are few (on average 5%), mainly vughs.

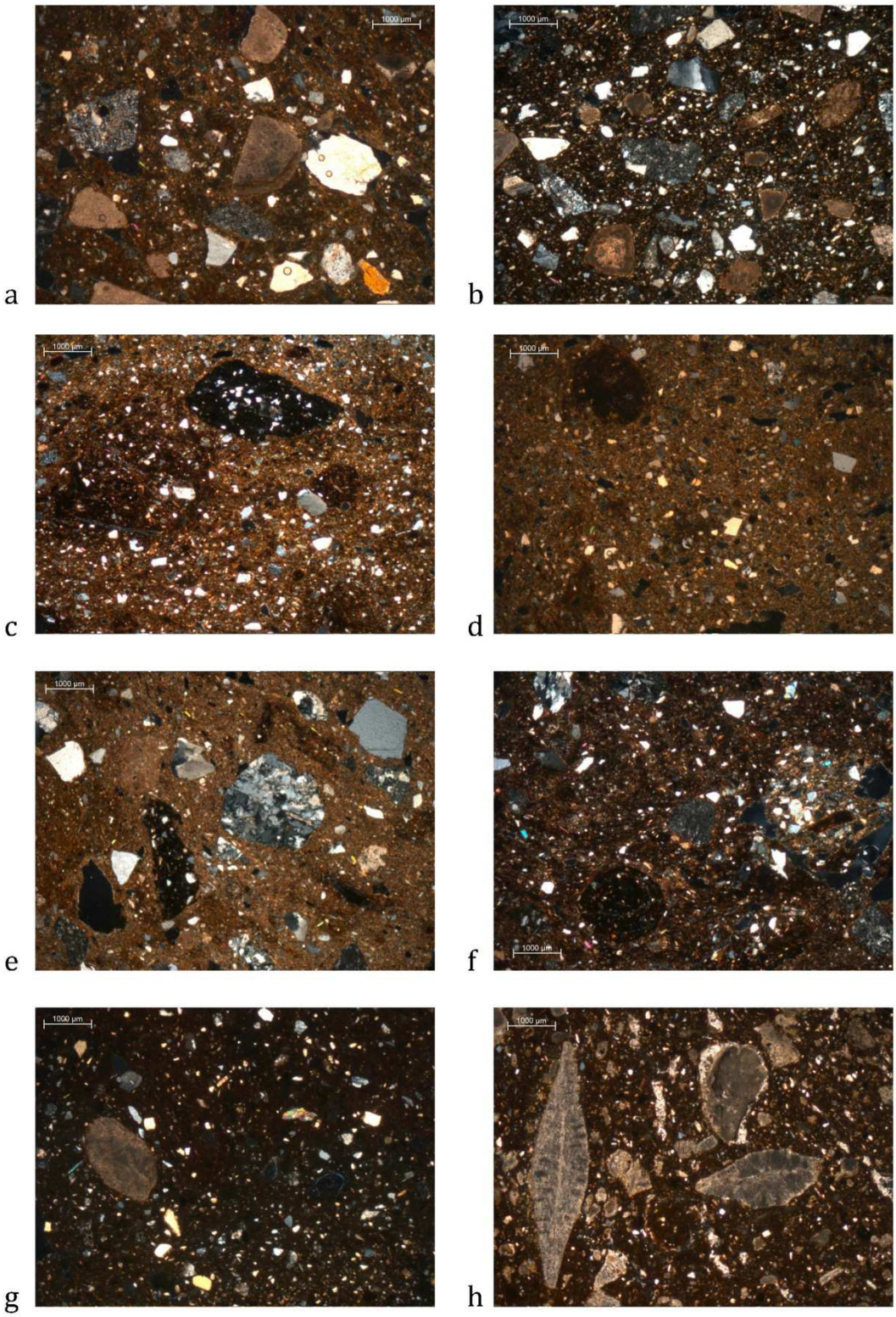

Figure 3. 52. Thin section photomicrographs of selected ceramics analysed in this study belonging to fabrics 1-5. a-b) Fabric 1: sand (quartz, polycrystalline quartz, volcanic acidic rocks -rhyolite- and carbonate mudstone) rich potsherds (samples FP03 (a), FP09 (b); c-d) Fabric 2: quartz sand and grog rich potsherds (samples FP06 (c), FP08 (d); e-f) Fabric 3: Rhyolite and polycrystalline quartz rich potsherds (samples FP02 (e), FP04 (f); g) Fabric 4: carbonate mudstone rich potsherd (sample FP05); h) Fabric 5: carbonate inclusions rich potsherd (sample FP10). The images were all taken in crossed polars.

3.10.4. Mineralogical composition

The mineralogical association of the samples, detected by X-ray powder diffraction (XRPD) analysis, revealed the following situation (table 3.15): all the samples have abundant quartz and subordinate plagioclase, alkali feldspar (like microcline/orthoclase), calcite and amphibole, sometimes there are trace of smectite minerals or chlorite. Between these, samples FP01, FP10 and FP05 presented also few hematite and pyroxene the first tow and hematite the last one. The sample FP02 is the lonely with dolomite. Samples FP06 and FP08 do not contain calcite neither dolomite.

samples	Fabrics	Qz	Pl	Kfs	Cal	Dol	Ilt	Sme	Chl	Zeo	Px	Hem	Amp
FP01	1	****	***	*	*					*	**	*	
FP02	4	****	*	**	**	*	*		*				*
FP03	1	****	**	**	**		*	*					*
FP04	4	****	**	**	**		*		*	*			*
FP05	3	****	**	**	*		*	*?				*	*
FP06	2	****	**	**			*	*					*
FP07	2	****	**	**	*		**	*					*
FP08	2	****	**	**			**		*				*
FP09	1	****	*	**	*		*						*
FP10	5	****	*	**	**		*				*	*	

Table 3. 15. Mineralogical associations in the studied pottery. Qz: quartz; Pl: plagioclase (albite like); Kfs: alkali feldspar (microcline like); Cal: calcite; Dol: dolomite; Ilt: illite; Sme: smectites; Chl: chlorite; Zeo: zeolite; Px: pyroxene; Hem: hematite; Amp: amphibole.

3.10.5 Chemical analysis and statistical treatment of the data

The chemical composition of seven samples was determined by XRF. Their major elements (SiO_2, TiO_2, Al_2O_3, Fe_2O_3, MnO, MgO, CaO, Na_2O, K_2O, P_2O_5) whose concentrations are expressed in wt% of their oxides, and trace elements (S, Sc, V, Cr, Co, Ni, Cu, Zn, Ga, Rb, Sr, Y, Zr, Nb, Ba, La, Ce, Nd, Pb, Th, and U), expressed in ppm were calculated (table 3.16).

Despite the very small number of the inclusions, not sufficient to be considered statistically representative, the potsherds had undergone statistical analyses. Descriptive statistic analyses were performed on the variable concentrations calculated for the whole

Samples	SiO_2	TiO_2	Al_2O_3	Fe_2O_3	MnO	MgO	CaO	Na_2O	K_2O	P_2O_5	S	Sc	V	Cr	Co	Ni
FP.02	59,22	0,66	15,42	6,32	0,08	2,08	8,03	1,12	2,86	2,75	1075	3	96	77	18	115
FP.03	62,72	0,72	14,56	5,45	0,07	1,65	8,09	1,13	2,46	2,02	423	3	89	83	17	62
FP.04	62,51	0,88	17,05	5,77	0,08	1,55	3,97	1,14	3,03	2,68	434	13	117	107	23	120
FP.05	61,15	0,89	16,59	6,44	0,09	1,88	5,92	1,17	2,90	1,73	392	6	110	104	18	72
FP.07	64,36	0,84	16,01	6,23	0,07	2,00	3,35	1,26	2,86	1,78	333	19	111	108	27	114
FP.08	66,43	0,82	15,66	5,72	0,08	1,62	2,43	1,40	3,06	1,74	88	17	95	83	22	144
FP.09	64,80	0,72	15,13	5,32	0,09	2,00	6,19	1,33	2,63	1,00	274	3	97	94	17	78
Samples	Cu	Zn	Ga	Rb	Sr	Y	Zr	Nb	Ba	La	Ce	Nd	Pb	Th	U	L.O.I.
FP.02	61	130	18	139	311	37	178	12	1974	35	84	5	44	6	4	13,57
FP.03	47	117	17	130	264	33	174	12	1465	42	84	5	37	9	5	12,06
FP.04	80	145	19	150	261	37	210	14	1715	25	85	5	39	9	4	11,60
FP.05	52	155	20	136	282	43	291	17	1480	39	97	5	37	11	6	6,74
FP.07	67	184	17	147	233	40	252	14	1308	41	83	5	39	10	8	8,70
FP.08	76	154	18	145	221	36	275	13	1329	36	89	5	38	10	8	7,62
FP.09	48	160	17	126	185	41	213	12	912	57	80	12	39	12	5	6,79

Table 3. 16. Geochemical composition of samples obtained by XRF.

Sample	SiO_2	TiO_2	Al_2O_3	Fe_2O_3	MnO	MgO	CaO	Na_2O	K_2O	*S*	Sc	V	Cr	Co	Ni
FP.02	1,77	-0,18	1,19	0,80	-1,10	0,32	0,90	0,05	0,46	3,03	0,48	1,98	1,89	1,26	2,06
FP.03	1,80	-0,14	1,16	0,74	-1,15	0,22	0,91	0,05	0,39	2,63	0,48	1,95	1,92	1,23	1,79
FP.04	1,80	-0,06	1,23	0,76	-1,10	0,19	0,60	0,06	0,48	2,64	1,11	2,07	2,03	1,36	2,08
FP.05	1,79	-0,05	1,22	0,81	-1,05	0,27	0,77	0,07	0,46	2,59	0,78	2,04	2,02	1,26	1,86
FP.07	1,81	-0,08	1,20	0,79	-1,15	0,30	0,53	0,10	0,46	2,52	1,28	2,05	2,03	1,43	2,06
FP.08	1,82	-0,09	1,19	0,76	-1,10	0,21	0,39	0,15	0,49	1,94	1,23	1,98	1,92	1,34	2,16
FP.09	1,81	-0,14	1,18	0,73	-1,05	0,30	0,79	0,12	0,42	2,44	0,48	1,99	1,97	1,23	1,89
Sample	Cu	Zn	Ga	Rb	Sr	Y	Zr	Nb	Ba	La	Ce	Nd	Pb	Th	U
FP.02	1,79	2,11	1,26	2,14	2,49	1,57	2,25	1,08	3,30	1,54	1,92	0,70	1,64	0,78	0,60
FP.03	1,67	2,07	1,23	2,11	2,42	1,52	2,24	1,08	3,17	1,62	1,92	0,70	1,57	0,95	0,70
FP.04	1,90	2,16	1,28	2,18	2,42	1,57	2,32	1,15	3,23	1,40	1,93	0,70	1,59	0,95	0,60
FP.05	1,72	2,19	1,30	2,13	2,45	1,63	2,46	1,23	3,17	1,59	1,99	0,70	1,57	1,04	0,78
FP.07	1,83	2,26	1,23	2,17	2,37	1,60	2,40	1,15	3,12	1,61	1,92	0,70	1,59	1,00	0,90
FP.08	1,88	2,19	1,26	2,16	2,34	1,56	2,44	1,11	3,12	1,56	1,95	0,70	1,58	1,00	0,90
FP.09	1,68	2,20	1,23	2,10	2,27	1,61	2,33	1,08	2,96	1,76	1,90	1,08	1,59	1,08	0,70

Table 3. 17. Standardized values of the geochemical composition of the studied potsherds transformed to base 10 logarithm.

sample assemblage, as illustrated in chapter 1.5. The treatment of the geochemical data confirmed the high compositional heterogeneity (table 3.18). These situation is due to the small group of samples analysed, and to the very different pastes with high percentage of a-plastics inclusions.

A multivariate analysis (cluster analysis) was performed on the standardized values of the elements transformed to base 10 logarithm (table 3.17). Since the P_2O_5, is commonly considered a good indicator of the alteration processes that can take place during burial

Variable	A	SD	CV	MIN	IQ	MED	IIIQ	MAX	p-value
SiO2	63,03	2,41	3,83	59,22	61,15	62,72	64,80	66,43	0,92
TiO2	0,79	0,09	11,35	0,66	0,72	0,82	0,88	0,89	0,34
Al2O3	15,77	0,85	5,41	14,56	15,13	15,66	16,59	17,05	0,96
Fe2O3	5,89	0,44	7,48	5,32	5,45	5,77	6,32	6,44	0,47
MnO	0,08	0,01	10,21	0,07	0,07	0,08	0,09	0,09	0,15
MgO	1,83	0,22	11,78	1,55	1,62	1,88	2,00	2,08	0,22
CaO	5,43	2,24	41,29	2,43	3,35	5,92	8,03	8,09	0,52
Na2O	1,22	0,11	9,04	1,12	1,13	1,17	1,33	1,40	0,20
K2O	2,83	0,21	7,59	2,46	2,63	2,86	3,03	3,06	0,31
P2O5	1,96	0,61	30,95	1,00	1,73	1,78	2,68	2,75	0,30
S	431,00	308,00	71,35	88,00	274,00	392,00	434,00	1075,00	0,03
Sc	9,14	7,03	76,93	3,00	3,00	6,00	17,00	19,00	0,09
V	102,14	10,40	10,18	89,00	95,00	97,00	111,00	117,00	0,27
Cr	93,71	12,88	13,74	77,00	83,00	94,00	107,00	108,00	0,23
Co	20,29	3,82	18,82	17,00	17,00	18,00	23,00	27,00	0,12
Ni	100,70	30,20	29,97	62,00	72,00	114,00	120,00	144,00	0,35
Cu	61,57	13,33	21,65	47,00	48,00	61,00	76,00	80,00	0,51
Zn	149,29	21,63	14,49	117,00	130,00	154,00	160,00	184,00	0,77
Ga	18,00	1,16	6,42	17,00	17,00	18,00	19,00	20,00	0,16
Rb	139,00	8,94	6,43	126,00	130,00	139,00	147,00	150,00	0,80
Sr	251,00	41,70	16,59	185,00	221,00	261,00	282,00	311,00	0,93
Y	38,14	3,39	8,88	33,00	36,00	37,00	41,00	43,00	0,77
Zr	227,60	46,00	20,23	174,00	178,00	213,00	275,00	291,00	0,53
Nb	13,43	1,81	13,50	12,00	12,00	13,00	14,00	17,00	0,08
Ba	1455,00	334,00	22,97	912,00	1308,00	1465,00	1715,00	1974,00	0,70
La	39,29	9,64	24,53	25,00	35,00	39,00	42,00	57,00	0,33
Ce	86,00	5,54	6,44	80,00	83,00	84,00	89,00	97,00	0,10
Nd	6,00	2,65	44,10	5,00	5,00	5,00	5,00	12,00	0,01
Pb	39,00	2,38	6,10	37,00	37,00	39,00	39,00	44,00	0,03
Th	9,57	1,90	19,88	6,00	9,00	10,00	11,00	12,00	0,40
U	5,71	1,70	29,83	4,00	4,00	5,00	8,00	8,00	0,16

Table 3. 18. Average (A), standard deviation (SD), variance (V), coefficient of variation (CV), minimum (MIN), first quartile (IQ), median (MED), third quartile (IIIQ) and maximum (MAX) values and the p-value of the Anderson–Darling normality test for the studied potsherds

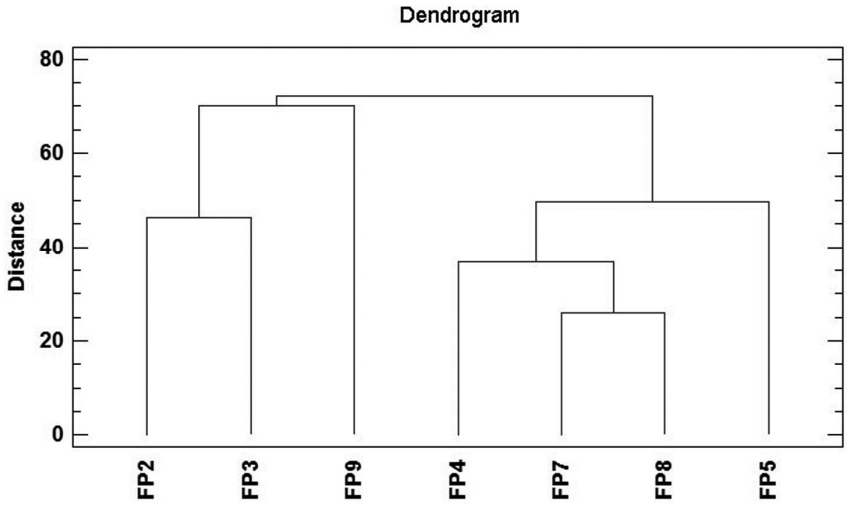

Figure 3. 53. Dendrogram obtained by cluster analysis (average algorithm) of the pottery from Fondo Paviani.

(Freestone 2001, Lemoine, Picon 1982) and here it varied over an interval: 1,00-2,75 wt% much wider than that (0.05-0.50 wt%) observed in many clayey materials from Veneto (Maritan 2002, Maritan 2004), this analysis was carried out excluding its concentration.
The cluster analysis was performed using the squared Euclidean distance and the average algorithm. The dendrogram indicates that samples tend to group into two main clusters (figure 3.53) that do not correspond perfectly to the petro-fabrics observed at the microscope. Cluster 1 is formed by the samples characterized by high quantity of carbonates (fabric 1 and sample FP2 of fabric 3). The cluster 2 is related to the fabrics 2 and sample FP4 of fabric 3, poor in carbonates, and sample FP5 (fabric 4).

3.10.6. Discussion and conclusions

The study of ten pottery from Fondo Paviani provided preliminary information about the technological skills reached by the ancient potters. The petrographic analysis of the ceramic samples revealed an extremely compositional diversity.
With the exception of fabric 2, the abundance and bimodal grain-size distribution of the inclusions suggested that most of them were artificially added. Their round shapes may suggest that potters used natural sands. The presence among the a-plastics components of rhyolite, polycrystalline quartz, chert and carbonate mudstone may relate the samples containing these inclusions to the sediments of the Adige river. Samples of fabrics 2, 4 and 5 are characterized by rounded inclusions with a well sorted unimodal grain-size distribution and a seriate grain-size distribution respectively, that seem to be naturally present in the raw clays. Only sample FP008 does not have carbonate inclusions. As none sediments were collected nearby the site, it was not possible to make any further consideration about the provenance.
Different firing temperatures were detected. All the ceramics were fired in the temperature interval of 650-850°C. Only for few specimens it could be suggest a more constrained interval (750-850°C) for the contemporary occurrence of hematite and illite.

Few samples recorded temperature less than 650°C, because of the presence of chlorite among their minerals.
Due to the small number of samples, the conclusions are not statistically representative of the real context of the site. For the same reason it was not possible to make any general correlation between the pottery productions of Fondo Paviani and Castel de Pedena. At this stage of the work any similarities between the two technological processes adopted were observed: at Fondo Paviani it seems that both raw clays with naturally present fluvial sediments were collected or sediments were added without come under a crushing process. At Castel de Pedena sediments were voluntary added by the potters at the clays, both after crushing or not. These variations may also be explained with the different geological conditions of the two regions.

Fourth chapter

THE FLARED RIM AND FLATTENED LIP POTTERY

4.1 Flared rim and flat lip pottery, historical context

During the late Final Bronze Age and Early Iron Age a distinct class of jars characterized by a flared rim and a flat lip (here called FRFL pottery) spread in the Friuli Venetia Giulia region (north-eastern Italy) in fortified settlements named "castellieri" (figure 4.1). The FRFL pottery is a well-standardized handmade production characterized by restricted orifices and coarse pastes tempered with carbonate inclusions. They are often found in highly fragmented conditions (figures 4.2-3) (Prosdocimi 2011).

Some specimens were discovered also in several Early Iron Age sites, both in settlements and in grave contexts, of the neighbouring Veneto region (figures 4. 5-7): Concordia Sagittaria, Oderzo, Montebelluna, Padova, Este and Castion di Erbè. Here the FRFL pottery slightly differs from the Friuli Venetia Giulia types: the peculiarity of the flared rim and the flat lip is less evident and generally the orifices are narrower. Moreover, in Veneto the FRFL pottery appeared later than in Friuli Venetia Giulia, in the Early Iron Age (Prosdocimi 2011)[1].

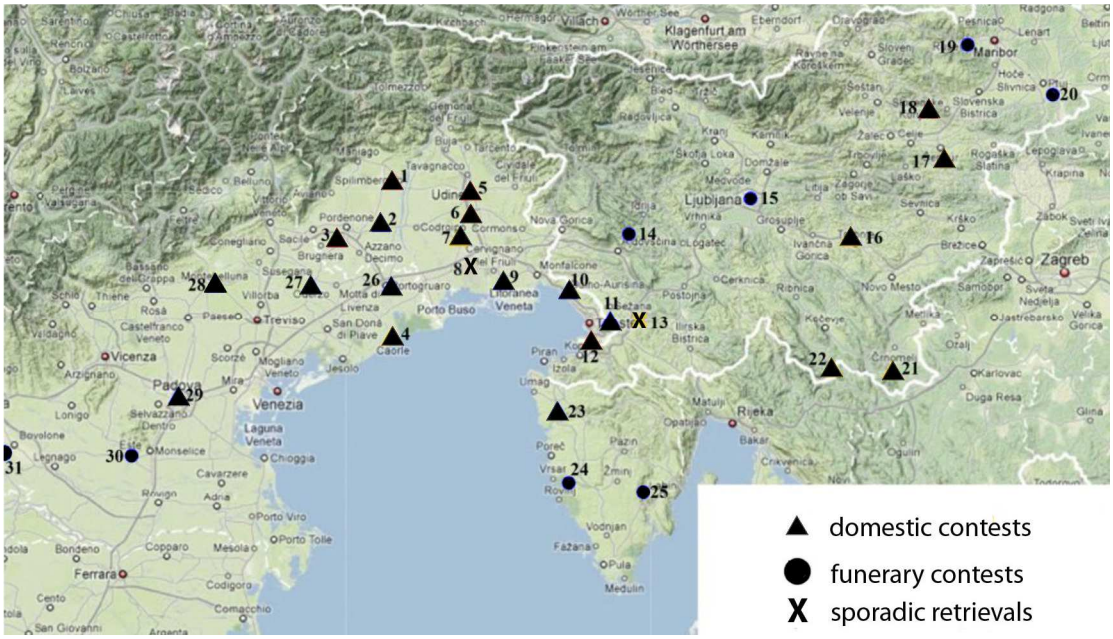

Figure 4. 1. Distribution chart of the sites where the FRFL pottery was found. After Prosdocimi 2011.

[1] Dr. Benedetta Prosdocimi recently developed a PhD study on the FRFL pottery, which analyzes its variation in time and spaces, its function, its circulation inside and outside the Friuli Venetia Giulia region and the workshops locations.

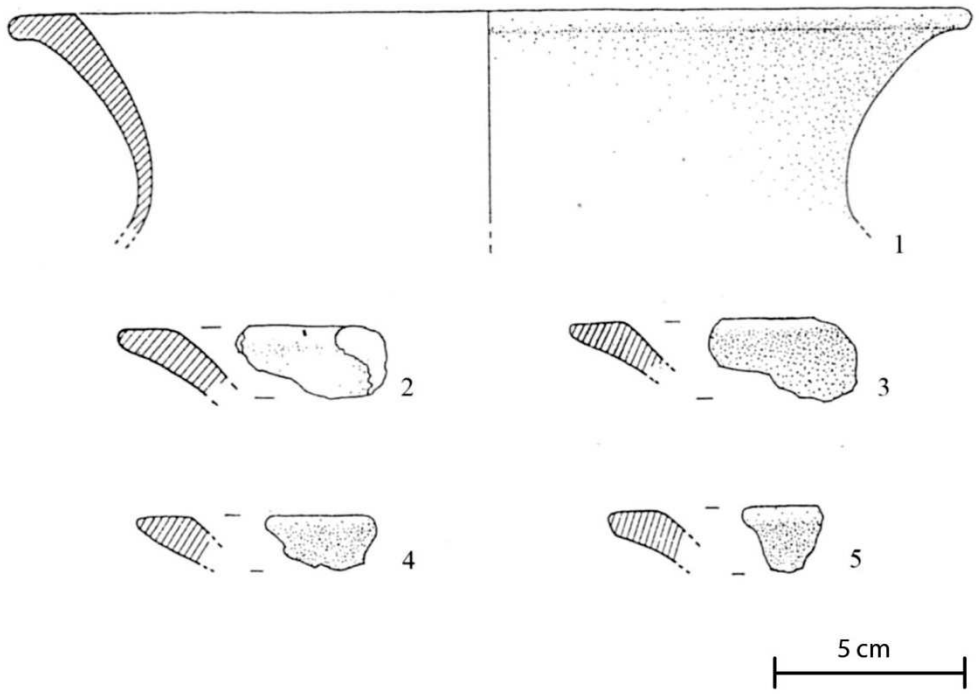

Figure 4. 2. Flared rim and flat lip fragments from Pozzuolo del Friuli. After Borgna 1994.

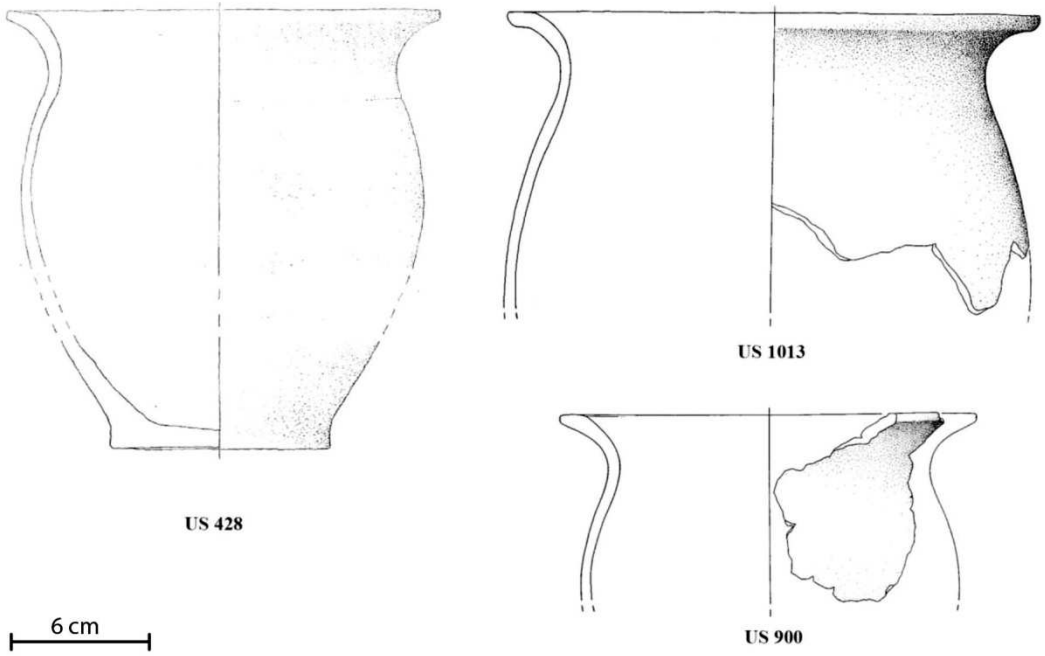

Figure 4. 3. Flared rim and flat lip ovoid jars from Variano. After Corazza 2003.

As this research focuses on FRFL pottery from few sites of the Friuli Venetia Giulia and Veneto regions, we will take in consideration the archaeological context of only the following selected settlements (figure 4.4): Terzo Ramo del Timavo, Grotta del Mitreo, Aquileia, Gradisca di Spilimbergo, Palse di Porcia (all located in the Friuli Venetia Giulia); Concordia Sagittaria, placed on the geographical and cultural boarder between these two regions and Padova and Castion d'Erbé settled in Veneto.

Terzo Ramo del Timavo

The coastal site of the Terzo Ramo del Timavo (S. Giovanni di Duino, Trieste, Italy) is located at the mouth of the third branch of the Timavo river. It is a pottery deposit of 150 m2 wide, on a highly steep floor, laying in shallow sea water, reaching nearly 7 m deep. The underwater survey and excavation took place in 1969 when an area of 80 m2 wide and 1,20 m deep was investigated. In that occasion, both protohistorical and Roman ceramics were found, among which also some FRFL pottery. These found high similarity with specimens coming from the near sites of Duino and Aquileia and were dated at the beginning of the Iron Age (Maselli Scotti 1983a, Maselli Scotti 1983b).

Grotta del Mitreo

The Grotta del Mitreo (Duino Aurisina, Trieste) is a cave site characterized by a natural clay floor and carbonate croncretions (speleothems). It is located a little way upstream of the coeval settlements of Terzo Ramo del Timavo and Duino. The archaeological survey and the dig revealed different occupational phases dated to the Neolithic, the Iron Age and the more recent in the Roman period. (Montagnari Kokelj, Crismani 1996, Progetto C.R.I.G.A. , Catasto Regionale.).

Figure 4. 4. Distribution chart of FRFL pottery with indication of the sites here studied. 1) Castion d'Erbè; 2) Padova; 3) Concordia Sagittaria; 4) Palse di Porcia; 5) Gradisca di Spilimbergo; 6) Aquileia; 7) Grotta del Mitreo; 8) Terzo Ramo del Timavo.

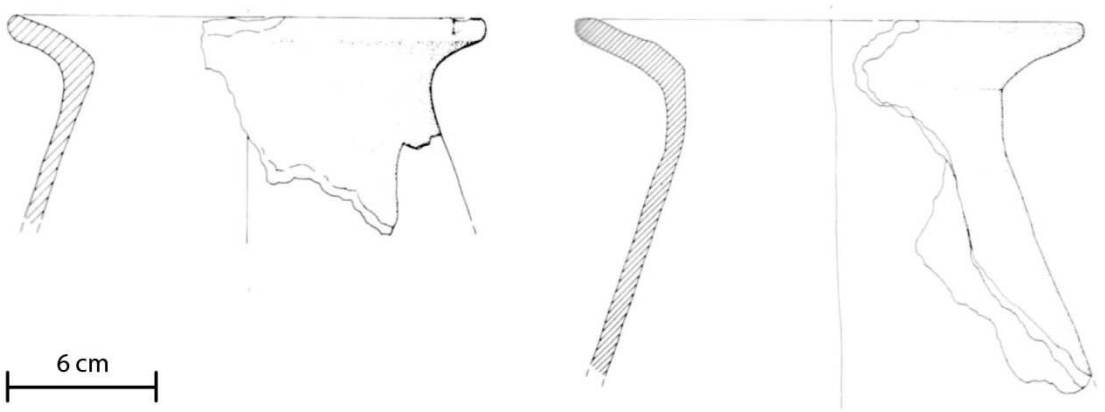

Figure 4. 5. Flared rim and flat lip double-conic vessels from Concordia Sagittaria. After AAVV. 1996.

Aquileia – Essiccatoio nord

The protohistical site of Aquileia, dated at the beginning of the Iron Age, was found in the so called "Essicatoio Nord" area of the modern city. It was located close to the sea, along the Natissa river. A floodplain alluvium 60-120 cm thick covered the Iron Age site isolating it from the more recent Roman records. The archaeological excavation interested a small area of the settlement. Remnants of domestic contexts and an updraft kiln were found. Here a fragment of carbonate mudstone classified as "calcare di Aurisina", considered by the archaeologists material used for tempering the pottery, was found. The "calcare di Aurisina" crops out near Monfalcone and Aurisna, nearly 20 km away. (Maselli Scotti, Degrassi et al. 1995, Maselli Scotti, Mandruzzato et al. 1996, Maselli Scotti, Crismani et al. 1999).

Gradisca di Spilimbergo,

The site of Gradisca di Spilimbergo is a fortified boroughs related to the Castellieri culture dated between the Final Bronze Age and the Iron Age until its abandon in the IV cent. b.C. It is located in the Pordenone plain, on the top of an alluvial terrace close to the confluence of the Cosa and the Tagliamento rivers. The first archaeological excavations brought important information on the more ancient levels of the site, and on the fortification. The first structure was built in the late Final Bronze Age-First Iron Age with the realization of a wooden palisade. Only during the beginning of the Iron Age the peculiar rampart was build. It was made of sediments composed by sands and gravels strengthen by wooden poles and an internal wall, an external ditch without water is also attested (AA. VV. 1996, Càssola Guida, Balista 2007).

Palse di Porcia,

The site of Palse di Porcia is a fortified borough settled in the alluvial plain near Pordenone. Several archaeological excavation campaigns were conducted during the years showing a varied and complex stratigraphic sequence of the site due to its long life. The more ancient levels, that preceded the fortification, were attributed to the moment of

passage between the Recent Bronze Age and the Final Bronze Age. The following phases were related to the Castellieri culture. In this phase it was built the typical earthwork made of sediments (sands and gravels) and strengthen by a wooden structure. A high vitality of the site emerges, suggested by the great size of 30 ha and by the diversity of domestic and commerical environments attested until its abandon in the IV cent. b.C. (AA. VV. 1996, Borgna, Canever et al. 1991, Càssola Guida 1980, Leonardi 1979, Vitri, Spanghero 2000).

Concordia Sagittaria

Concordia Sagittaria (Iulia Concordia) was an important Roman colony founded between 40 and 42 b.C. on the Lemene river, not far from the sea. During different archaeological excavations campaigns, under the Roman records, also remnants related to the Iron Age were found. An articulated pottery assemblage was discovered in the site of Concordia Sagittaria: a cup decorated with a goat figure, ovoid jars, double-conic vases and ollas both with or without the flat lip. The FRFL type is less standardized and might have different pastes in comparison to the specimens coming from the eastern sites. There are FRFL pottery with both coarse or fine pastes, while different shaped vases can be tempered with similar carbonatic inclusions (AA. VV. 1996, Bianchin Citton 1995, Bianchin Citton, Martinelli 2005, Croce De Villa 1991, Mizzan 1996).

P**adova**

The protohistorical site of Padova was located under the actual city centre. It was crossed by one branch of the Brenta river and settled closed to the Bacchiglione river. Different archaeological excavations were conducted over the last years thanks to the construction of new buildings in the city centre. An important number of pottery was found in the protohistorical context of Padova, among which a great number of FRFL type, here in funerary contest too (Leonardi 1976, Leonardi 1976, Rubagotti 2006).

Castion d'Erbé

The site of Castion d'Erbè (Isola della Scala, Verona, Italy), settled between the beginning of the VIII and the middle of VI cent. b.C., was located in the middle of the Venetian plain,

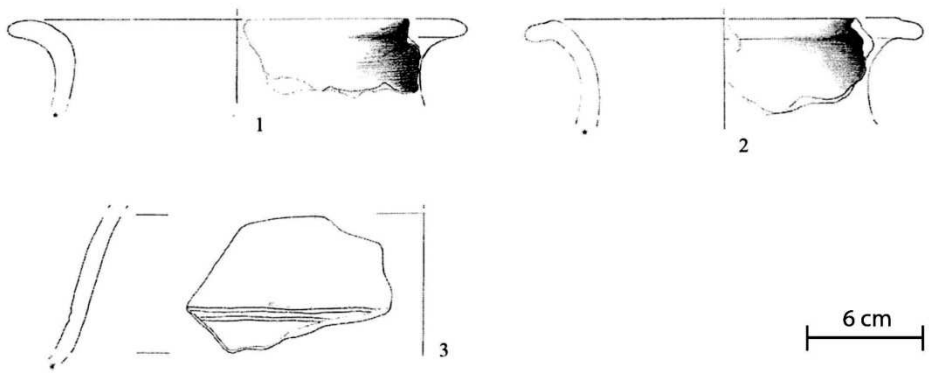

Figure 4. 6. Flared rim and flat lip double-conic vessels from Padova. After Rubagotti 2006.

on the Tartaro paleo-river valley. A series of excavations campaigns between 1971 and 1976 collected a great number of potshards related to the typical coeval Venetian types and fewer FRFL jar, comparable with those found in the neighbouring Friuli Venetia Giulia region (Prosdocimi 2011, Rossi 2008).

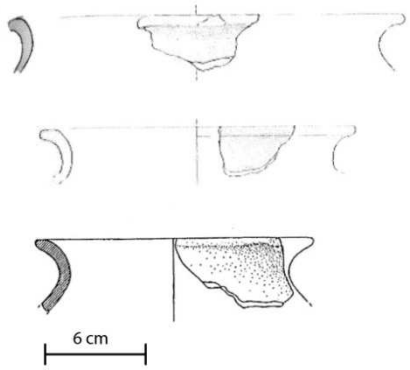

Figure 4. 7. Flared rim and flat lip jars from Castion d'Erbè. After Rossi 2008.

4.2 Macroscopic analysis

Since the object of this study was the production technology and the provenance analysis of the FRFL jars found at some sites in the Veneto region, ninety-one fragments of pottery were chosen from the ceramic assemblages of three venetian sites (Padova, Castion d'Erbè and Concordia Sagittaria), representing both this vessel type and other types of probable local origin[2]. Moreover, eleven specimens of FRFL pottery from the Friuli Venetia Giulia settlements of Gradisca di Spilimbergo, Palse di Porcia, Aquileia, Terzo Ramo del Timavo and the Grotta del Mitreo were also analyzed for comparison (table 4.1).

All the selected samples had undergone a detailed hand-examination with the unaided eye, following the methodology illustrated by P. Stienstra (1986) (see chapter 1.1). The pastes were described considering the characteristics of the non-plastic inclusions (concentration, shape and size evaluated through comparison with visual estimation charts) and the matrix. The results are reported in table 4.2.

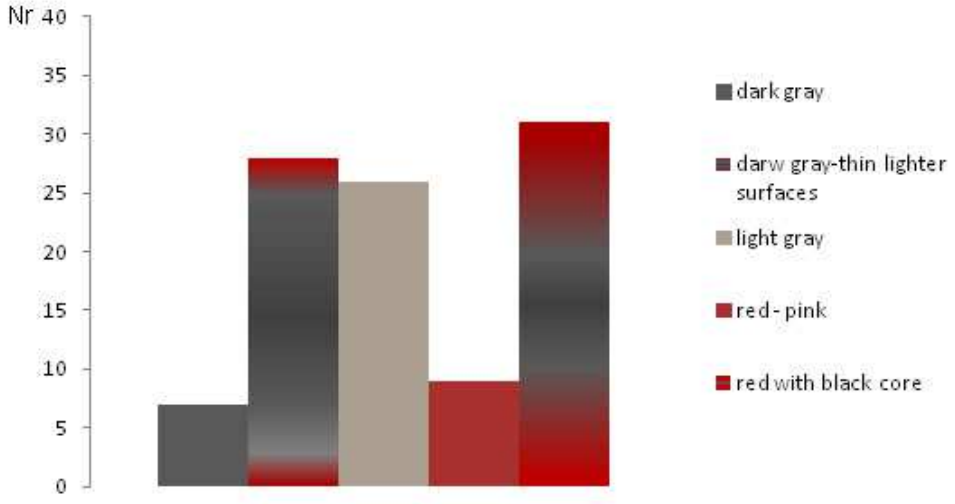

Figure 4. 8. Colour of the pastes of the studied potsherds.

[2] The pottery assemblage for the archaeometric analysis was selected by Dr. Prosdocimi. Dr. Prosdocimi recently developed a Ph.D research about FRFL pottery.

The analysis of the chromatic variations, evaluated by comparison with the Munsell's Soil Colour Charts (Munsell 2000), distinguished different situations (figure 4.8). The majority of the samples had a sandwich structure (a dark "core" with lighter reddish surfaces), or colour differentiations between the external (usually reddish), and the internal surfaces (grey-dark grey). Also homogeneous light grey bodies, or very dark grey bodies, with a lighter (pink or red) thin external layer (probably too thin to be considered as a sandwich structure) were observed. Only few had homogeneous light (reddish or pinkish) bodies or very dark grey coloured pastes.

samples	Provenance site	Form	Rim
625	TM	Jar	Flared rim, flattened lip
637	TM	Jar	Flared rim, flattened lip
6247	TM	Jar	Flared rim, flattened lip
8614	MT	Jar	Flared rim, flattened lip
14630	CS	Cup	-
14634	CS	Jar	-
14636	CS	Jar	Flared rim, flattened lip
14655	CS	Jar	-
14712	CS	Jar	Flared rim, flattened lip
14713	CS	Ovoid jar	Flared rim, slightly flattened lip
14714	CS	Glass shaped vase	Flared rim, flattened lip
14715	CS	Small jar	-
14716	CS	Double-conic jar	Flared rim, flattened lip
14717	CS	Handle	Flared rim, flattened lip
18464	MT	Jar	Flared rim, flattened lip
20783	CE	Jar	Flared rim, flattened lip
20785	CE	Jar	-
20794	CE	Jar	Flared rim, flattened lip
20796	CE	Jar	-
20799	CE	Jar	-
20959	CE	Jar	Flared rim, flattened lip
24552	CS	Small jar	Flared rim, flattened lip
24615	CS	Jar	Flared rim, flattened lip
24648	CS	Jar	Flared rim, flattened lip
24869	CS	Double-conic jar	Flared rim, flattened lip
27443	CE	Jar	-
28378	CE	Jar	-
28740	CS	Lid	-
28750	CS	Bowl	Flared rim, flattened lip
28755	CS	Ovoid jar	Flared rim, flattened lip
28770	CE	Jar	Flared rim, flattened lip
28772-28773	CS	Small ovoid jar	Flared rim, slightly flattened lip
28780	CS	Ovoid jar	Flared rim, flattened lip
28781	CS	Jar	Flared rim, flattened lip
28794-28796	CS	Situla-shaped vase	Everted rim
28798	CS	Ovoid jar	Flared rim, flattened lip
28801	CS	Ovoid jar	Flared rim, flattened lip
28806	CS	Ovoid jar	Everted rounded rim
28827	CS	Ovoid jar	Everted rim
28982	CS	Ovoid jar	Flared rim, flattened lip
29015	CS	handle	
31275	CS	Jar	Flared rim, flattened lip
31276	CS	Double-conic jar	-
31282	CS	Jar	Flared rim, flattened lip
31290	CS	Jar	Flared rim, flattened lip
31295	CS	Jar	Flared rim, flattened lip
31420	CS	Truncated conic bowl	Rounded rim
31421	CS	Jar	Flared rim, flattened lip
31479	CS	Oven	-
31490	CS	Ovoid jar	-
31492	CS	Jar	Flared rim, flattened lip

Table 4. 1. a. Details of the shards analyzed in this study.

Samples	Provenance site	Form	Rim
31493	CS	Jar*	Flared rim, flattened lip
31544	CS	Jar	Flared rim, flattened lip
31546	CS	Bowl	lip thickened to exterior
31906	CS	Jar	-
33596	CE	Jar	-
33686	CE	Jar	-
33749	CE	Jar	-
33806	CE	Jar	-
97081	CE	Jar	Flared rim, flattened lip
97151	CE	Jar	Flared rim, flattened lip
97364	CE	Jar	Flared rim, flattened lip
97442	CE	Jar	Flared rim, flattened lip
99894	CE	Jar	Flared rim, flattened lip
100568	CE	Jar	Flared rim, flattened lip
100590	CE	Jar	Flared rim, flattened lip
100691	CE	Jar	Flared rim, flattened lip
100975	CE	Jar	-
101134	CE	Jar	Flared rim, flattened lip
236738	PP	Jar	Flared rim, flattened lip
259786	GS	Jar	Flared rim, flattened lip
343769	PD	Jar	Flared rim, flattened lip
343770	PD	Jar	-
343771	PD	Jar	Flared rim, flattened lip
343772	PD	Jar	-
343773	PD	Jar	-
343774	PD	Jar	Flared rim, flattened lip
343775	PD	Jar	Flared rim, flattened lip
343776	PD	Jar	Flared rim, flattened lip
343777	PD	Jar	Flared rim, flattened lip
343778	PD	Jar	Flared rim, flattened lip
343779	PD	Jar	Flared rim, flattened lip
343780	PD	Jar	-
343781	PD	Jar	-
343782	PD	Jar	-
343783	PD	Jar	Flared rim, flattened lip
343784	PD	Jar	-
343785	PD	Jar	-
343786	PD	Jar	Flared rim, flattened lip
343787	PD	Jar	-
343788	PD	Jar	Flared rim, flattened lip
343789	PD	Jar	-
343790	PD	Jar	Flared rim, flattened lip
343791	PD	Jar	-
343792	PD	Jar	-
343793	PD	Jar	-
343794	PD	Jar	-
418269	AQ	Jar	Flared rim, flattened lip
418343	AQ	Jar	Flared rim, flattened lip
418905	AQ	Jar	Flared rim, flattened lip
424278	GS	Jar	Flared rim, flattened lip

Table 4. 1. b. Details of the shards analyzed in this study.

Samples	Pottery type	Thickness	Colour of the surfaces		Colour of the bodies		Inclusions					
			Colour	Munsell	Colour	Munsell	A (%)	sizes		shapes		
								d_{max}	$d_{average}$	A	SA	R
CASTION D'ERBÈ												
20783	FRFL	8	E: gray I: pink	E: 10YR 6/1 I: 7.5YR 7/4	E: pinkish gray I: gray	E: 7.5YR 7/2 I: GLEY1 6/N	10%	2	<1		*	
20785		8	E: light brown I: dark gray	A: 7.5YR 6/3 B: 7.5YR 4/1	light brown - very dark gray	7.5YR 6/3 – GLEY1 3/N	3%	2	<1			*
20794	FRFL	7	E: light red I: light brown	E: 2.5YR 6/6 I: 7.5YR 6/4	E: pinkish gray I: gray	E: 7.5YR 7/2 I: 7.5YR 6/1	5%	1	<<1		*	
20796		14	E: red I: light brown	E: 2.5YR 5/6 I: 7.5YR 6/3	dark gray	GLEY1 4/N	1%	3	<<1			*
20799		7	E: reddish gray I: gray	E: 5YR 5/2 I: 10YR 5/1	dark gray	GLEY1 4/N	1%	1	<<1		*	*
20959	FRFL	8	E: pink I: light brownish gray	E: 7.5YR 7/4 I: 10YR 6/2	gray	GLEY 5/N	10%	2	<1		*	
27443		7	E: gray I: gray	E: 7.5YR 6/1 I: 7.5YR 5/1	gray	GLEY 5/N	1%	1	<<1			*
28378		10	E: reddish brown I: brown	E: 5YR 5/3 I: 7.5YR 5/2	black	GLEY 2.5/N	3%	2	<<1			*
28770	FRFL	8	E: reddish yellow I: pink	E: 5YR 6/6 I: 7.5YR 7/3	gray	GLEY 5/N	20%	5	<1		*	*
33596		8	E: light brown I: gray	E: 7.5YR 6/3 I: 7.5YR 5/1	E: light brown I: gray	E: 7.5YR 6/4 I: 7.5YR 5/1	5%	1	1		*	
33686		8	E: reddish brown I: reddish brown	E: 5YR 5/3 I: 2.5YR 5/3	dark gray	GLEY 4/N	1%	1	<<1			*
33749		10	E: dark gray I: brown	E: 7.5YR 4/1 I: 7.5YR 4/2	red - dark gray	2.5YR 5/6 – 7.5YR 4/1	3%	3	<<1			*
33806			E: pinkish gray I: gray	E: 7.5YR 6/2 I: 7.5YR 5/1	E: reddish yellow I: dark gray	E: 7.5YR 6/6 I: GLEY1 4/N	3%	1	<<1			*
97081	FRFL	13	E: very pale brown I: light reddish brown	E: 10YR 7/3 I: 5YR 6/4	light gray	7.5YR 7/1	20%	3	<1		*	
97151	FRFL	7	E: pinkish gray I: reddish yellow	E: 7.5YR 6/2 I: 5YR 6/6	gray	5YR 6/1	25%	2	1		*	

Table 4. 2. Macroscopic description of the analyzed samples with indication of the pottery typology, thickness of the potsherds, colour determined using the Munsell colour charts, relative abundance of the inclusions, average size and shape.

Samples	Pottery type	Thickness	Colour of the surfaces		Colour of the bodies		Inclusions					
			Colour	Munsell	Colour	Munsell	A (%)	sizes		shapes		
								d_{max}	$d_{average}$	A	SA	R
97364	FRFL	7	E: pink I: pink	E: 5YR 7/3 I: 5YR 7/3	pinkish gray	7.5YR 6/2	10%	2	<1		*	
97442	FRFL	9	E: light gray I: pinkish gray	E: 10YR 7/2 I: 7.5YR 6/2	pinkish gray - gray	7.5YR 7/2 – GLEY1 5/N	10%	3	<1			*
99894	FRFL	6	E: light reddish brown I: pink	A: 5YR 6/4 B: 7.5YR 7/4	pink – light gray	7.5YR 7/4 – 10YR 7/2	10%	2	<1		*	*
100568	FRFL	7	E: reddish yellow I: reddish yellow	E: 5YR 7/6 I: 5YR 7/6	reddish yellow - light gray	5YR 7/6 – GLEY1 7/N	10%	2	<1		*	*
100590	FRFL	8	E: reddish yellow I: pinkish gray	E: 5YR 7/6 I: 7.5YR 6/2	gray	7.5YR 6/1	10%	3	<1		*	*
100691	FRFL	10	E: pink I: pink	E: 7.5YR 7/4 I: 7.5YR 7/4	dark gray	GLEY1 4/N	20%	2	<1		*	
100975	FRFL	8	E: light gray I: pink	E: 10YR 7/2 I: 5YR 7/4	gray	GLEY1 6/N	20%	2	<1		*	*
101134	FRFL	7	E: very pale brown I: light red	E: 10YR 8/3 I: 2.5YR 6/8	reddish yellow – dark gray	5YR 6/6 – GLEY1 4/N	10%	2	<1		*	
PADOVA												
343769	FRFL	8	E: light gray I: light gray	E: 5YR 7/1 I: 10YR 7/2	light gray	10YR 7/1	25%	2	<1		*	*
343770		8	E: dark gray I: dark gray	E: 7.5YR 4/1 I: 7.5YR 4/1	brown - very dark gray	7.5YR 5/2 – GLEY1 3/N	1%	1	<<1			*
343771	FRFL	11	E: very pale brown I: gray	E: 10YR 7/3 I: 10YR 5/1	pink	5YR 7/4	10%	1	<1		*	
343772		9	E: pink I: gray	E: 7.5YR 8/3 I: 5YR 5/1	E: pink I: dark gray	E: 7.5YR 8/3 I: GLEY1 4/N	3%	1	<1			*
343773		11	E: light brown I: pinkish gray	E: 7.5YR 6/3 I: 7.5YR 6/2	gray	GLEY1 5/N	3%	1	<<1			*
343774	FRFL	5	E: gray I: gray	E: 7.5YR 5/1 I: 5YR 5/1	gray	5YR 6/1	5%	1	<1			*
343775	FRFL	11	E: brown I: very dark gray	E: 7.5YR 5/2 I: GLEY1 3/N	dark gray	10YR 4/1	20%	4	<1		*	*

Table 4. 2. Macroscopic description of the analyzed samples.

Samples	Pottery type	Thickness	Colour of the surfaces		Colour of the bodies		Inclusions					
			Colour	Munsell	Colour	Munsell	A (%)	sizes		shapes		
								d_{max}	$d_{average}$	A	SA	R
343776	FRFL	9	E: gray I: pinkish gray	E: 7.5YR 6/1 I: 7.5YR 7/2	dark gray	GLEY1 4/N	20%	2	<1		*	*
343777	FRFL	8	E: pinkish gray I: pink	E: 7.5YR 6/2 I: 5YR 7/3	dark gray	GLEY1 4/N	20%	2	<1		*	
343778	FRFL	7	E: pinkish gray I: pinkish gray	E: 7.5YR 7/2 I: 7.5YR 7/2	pinkish gray - gray	7.5YR 7/2 – 10YR 6/1	20%	3	<1			*
343779	FRFL	8	E: light gray I: pinkish gray	E: 10YR 7/2 I: 7.5YR 7/2	pinkish gray - gray	7.5YR 6/2 - 7.5YR 5/1	10%	4	<1		*	*
343780		11	E: light gray I: gray	E: 10YR 7/2 I: 7.5YR 6/1	pinkish gray - dark gray	7.5YR 7/2 – GLEY1 4/N	5%	1	<1			*
343781		7	E: gray I: gray	E: 5YR 5/1 I: 7.5YR 5/1	dark gray	GLEY1 4/N	25%	4	<1			*
343782		8	E: pinkish gray I: pink	E: 7.5YR 7/2 I: 7.5YR 7/3	gray	GLEY1 5/N	1%	<1	<<1		*	
343783	FRFL	7	E: gray I: dark gray	E: 5YR 5/1 I: 5YR 4/1	light reddish brown	5YR 6/4	25%	3	1		*	
343784		7	E: brown I: very dark gray	E: 7.5YR 5/2 I: GLEY1 3/N	gray	7.5YR 5/1	10%	1	<<1		*	*
343785		6	E: pinkish gray I: dark gray	E: 7.5YR 6/2 I: 7.5YR 4/1	dark gray	GLEY1 4/N	1%	2	<<1		*	*
343786	FRFL	6	E: light gray I: dark reddish gray	E: 10YR 7/2 I: 2.5YR 4/1	dark gray	GLEY1 4/N	20%	2	<1		*	*
343787		5	E: gray I: gray	E: 7.5YR 5/1 I: 7.5YR 5/1	gray - gray	7.5YR 5/1 – GLEY1 5/N	3%	1	<1		*	*
343788	FRFL	7	E: gray I: pinkish gray	E: 7.5 YR 5/1 I: 7.5YR 6/2	gray	10YR 6/1	10%	2	<1		*	
343789		13	E: pink I: black	A: 5YR 7/3 B: GLEY1 2.5/N	A: pinkish gray B: dark gray	A: 5YR 6/2 B: GLEY1 4/N	5%	3	<<1			*
343790	FRFL	6	E: weak red I: pink	E: 2.5YR 5/2 I: 5YR 7/4	pinkish gray	5YR 6/2	20%	2	<1			*
343791		9	E: gray I: dark gray	E: 7.5YR 6/1 I: 5YR 4/1	E: very pale brown I: dark gray	E: 10YR 7/3 I: GLEY1 4/N	5%	3	<<1			*

Table 4. 2. Macroscopic description of the analyzed samples.

Samples	Pottery type	Thickness	Colour of the surfaces		Colour of the bodies		Inclusions					
			Colour	Munsell	Colour	Munsell	A (%)	sizes		shapes		
								d_{max}	$d_{average}$	A	SA	R
343792		9	E: pinkish gray I: gray	E: 5YR 6/2 I: 7.5YR 6/1	dark gray	GLEY1 4/N	3%	1	<<1			*
343793		7	E: pinkish gray I: gray	E: 7.5YR 6/2 I: 7.5YR 6/1	E: light reddish brown I: gray	E: 2.5YR 6/4 I: GLEY1 5/N	3%	1	<<1		*	*
343794		12	E: pinkish gray I: pink	E: 7.5YR 7/2 I: 5YR 7/4	gray	GLEY1 5/N	30%	3	<1		*	
CONCORDIA SAGITTARIA												
14630		4	E: pink I: dark gray	E: 7.5YR 7/3 I: 5YR 4/1	dark gray	GLEY1 4/N	3%	2	<1			*
14634		6	E: gray I: pinkish gray	E: 7.5YR 6/1 I: 7.5YR 7/2	very dark gray	GLEY1 3/N	1%	1	<<1			*
14636	FRFL	5	E: reddish brown I: pinkish gray	E: 2.5YR 5/3 I: 5YR 6/2	dark gray	GLEY1 4/N	10%	2	<1		*	*
14655		8	E: light red I: light reddish brown	E: 2.5YR 6/6 I: 5YR 6/4	light red	2.5YR 6/6	5%	1	<1		*	
14712	FRFL	7	E: light reddish brown I: light reddish brown	E: 2.5YR 6/4 I: 2.5YR 6/3	gray	5YR 6/1	20%	3	<1		*	
14713	FRFL	6	E: pinkish gray I: pink	E: 7.5YR 7/2 I: 7.5YR 7/3	gray	10YR 5/1	20%	2	<1		*	*
14714	FRFL	9	E: pinkish gray I: light reddish brown	E: 5YR 6/2 I: 5YR 6/3	Reddish brown	5YR 5/3	20%	2	<1			*
14715		8	E: light reddish brown I: gray	E: 5YR 6/4 I: 5YR 5/1	E: yellowish red I: dark gray	E: 5YR 5/6 I: 5YR 4/1	5%	4	<1		*	*
14716	FRFL	6	E: light reddish brown I: gray	E: 5YR 6/4 I: 7.5YR 5/1	E: light reddish brown I: gray	E: 2.5YR 6/4 I: 7.5YR 6/1	10%	2	<1		*	*
14717	FRFL	10	E: light reddish brown I: light reddish brown	A: 5YR 6/4 B: 5YR 6/4	dark gray	GLEY1 4/N	20%	4	1			*
24552	FRFL	7	E: pink I: light reddish brown	E: 7.5YR 7/4 I: 5YR 6/4	gray	GLEY1 5/1	10%	3	<1		*	*
24615	FRFL	5	E: pink I: reddish yellow	E: 7.5YR 7/4 I: 5YR 7/6	very dark gray	GLEY1 3/1	3%	1	<<1		*	*

Table 4. 2. Macroscopic description of the analyzed samples.

Samples	Pottery type	Thickness	Colour of the surfaces		Colour of the bodies		Inclusions					
			Colour	Munsell	Colour	Munsell	A (%)	sizes		shapes		
								d_{max}	$d_{average}$	A	SA	R
24648	FRFL	7	E: very pale brown I: pink	E: 10YR 8/2 I: 7.5YR 7/2	pinkish gray - gray	7.5YR 6/2 - GLEY1 5/N	5%	3	<1		*	*
24869		8	E: pink I: pinkish gray	E: 7.5YR 7/4 I: 7.5YR 6/2	dark gray	GLEY1 4/N	3%	1	0,5			*
28755	FRFL	8	E: pink I: gray	E: 7.5YR 7/4 I: 7.5YR 5/1	gray	7.5YR 5/1	10%	3	<1		*	
28772-28773	FRFL	5	E: reddish yellow I: reddish yellow	E: 5YR 7/6 I: 5YR 7/6	very dark gray	GLEY1 3/N	5%	3	<1		*	
28780	FRFL	7	E: pink I: pink	E: 5YR 7/4 I: 5YR 7/4	gray	GLEY1 5/N	10%	3	<1			*
28781	FRFL	6	E: pink I: pink	E: 7.5YR 8/3 I: 7.5YR 7/4	gray	GLEY1 5/N	20%	3	<1		*	*
28796		5	E: dark gray I: brown	E: 7.5YR 4/1 I: 7.5YR 5/2								
28798	FRFL	5	E: light red I: pink	E: 2.5YR 6/6 I: 7.5YR 8/3	gray	GLEY 5/N	5%	2	<1		*	*
28801	FRFL	5	E: pink I: pink	E: 7.5YR 7/4 I: 7.5YR 7/4	dark gray	GLEY1 4/N	5%	3	<1		*	*
28806		5	E: pink I: pink	E: 7.5YR 7/4 I: 7.5YR 7/4	gray	GLEY1 5/N	5%	3	<1			*
28827		8	E: pink I: pink	E: 7.5YR 7/3 I: 7.5YR 7/3	dark gray	GLEY1 4/1	10%	2	<1			*
28982	FRFL	7	E: light reddish brown I: light red	E: 2.5YR 6/4 I: 2.5YR 6/6	E: light red I: dark gray	E: 2.5YR 6/6 I: GLEY 5/N	3%	1	<<1	*		*
29015		5	E: pinkish gray I: gray	E: 7.5YR 6/2 I: 7.5YR 5/1	very dark gray	GLEY1 3/N	3%	1	<1		*	
31275	FRFL	12	E: pink I: reddish yellow	E: 7.5YR 7/4 I: 5YR 7/6	reddish brown - dark gray	5YR 5/4 - GLEY1 4/N	15%	4	<1		*	*
31276		12	E: reddish yellow I:	E: 5YR 6/6 I: 10YR 6/3	dark gray	GLEY1 4/N	5%	3	<1			*

Table 4. 2. Macroscopic description of the analyzed samples.

Samples	Pottery type	Thickness	Colour of the surfaces		Colour of the bodies		Inclusions					
			Colour	Munsell	Colour	Munsell	A (%)	sizes		shapes		
								d_{max}	$d_{average}$	A	SA	R
31282	FRFL	9	E: brown I: brown	E: 7.5YR 5/3 I: 10YR 5/3	dark gray	GLEY1 4/N	20%	3	<1		*	
31290	FRFL	14	E: reddish yellow I: pink	E: 5YR 6/6 I: 5YR 7/4	reddish brown - dark gray	5YR 5/4 - GLEY1 4/N	20%	2	1		*	*
31421	FRFL	9	E: yellowish red I: reddish brown	E: 5YR 5/6 I: 5YR 5/3	dark gray	GLEY1 4/N	20%	11	1	*	*	
31479		11	E: reddish yellow I: reddish yellow	A: 7.5YR 7/6 B: 5YR 6/6	reddish yellow - dark gray	7.5YR 7/6 - GLEY1 4/N	5%	3	<<1			*
31490		8	E: very dark gray I: reddish brown	E: GLEY1 3/N I: 2.5YR 5/4	very dark gray	GLEY1 3/N	10%	11	1			*
31492	FRFL	8	E: light brown I: very pale brown	E: 7.5YR 6/3 I: 10YR 7/3	gray	GLEY1 5/N	15%	2	<<1		*	*
31493	FRFL	6	E: brown I: gray	E: 7.5YR 5/2 I: 7.5YR 5/1	gray	7.5YR 5/1	15%	3	1		*	
31544	FRFL	7	E: reddish brown I: dark reddish gray	E: 2.5YR 4/3 I: 2.5YR 4/1	Dark reddish gray	2.5YR 3/1	30%	1	<1			*
31546		5	E: very dark grayish brown I: dark reddish brown	E: 10YR 3/2 I: 5YR 3/2	dark gray	GLEY1 4/N	1%	2	<<1			*
31906		8	E: pink I: pink	E: 7.5YR 7/4 I: 7.5YR 7/4	light red - dark gray	2.5YR 6/6 - GLEY1 4/N	5%	2	<<1		*	
31420		7	E: light brown I: light brown	E: 7.5YR 6/3 I: 7.5YR 6/4	light brown - gray	7.5YR 6/4 - 7.5YR 5/1	10%	4	1		*	*
31295	FRFL	6	E: pink I: pink	E: 5YR 7/4 I: 5YR 7/4	pink - dark gray	5YR 7/4 – GLEY1 4/N	10%	3	<1		*	*
28750		6	E: pink I: very pale brown	E: 7.5YR 7/4 I: 10YR 8/3	E: reddish brown I: dark gray	E: 5YR 5/4 I: 5YR 4/1	5%	2	<1			*
28740		11	E: light brown I: gray	E: 7.5YR 6/4 I: 10YR 5/1	Very dark gray	10YR 3/1	3%					

Table 4.2. Macroscopic description of the analyzed.

4.3 Petrographic fabric classification

All the samples (one-hundred and two potsherds) were analyzed under polarizing light microscope following the thin section description protocol illustrated in chapter 1.2, based on Whitbread terminology and descriptive procedure (1989, 1995).

The petrographic examination revealed a high compositional variability, mostly due to the various provenances of the potsherds, from places that are geologically different.

Thirteen petrographic groups were identified according to similarities and differences in the nature, shape and arrangement of non-plastic inclusions, voids and micromass (table 4.3). These ranged from a large dominant group to several composed of lonely samples.

- *Fabric 1: Speleothem rich potsherds (sixty samples)*

This fabric, grouping the largest number of shards, was characterized by an optically active (speckled birefringent fabric) oriented groundmass. Generally, inclusions were abundant (on average 20% of thin section area) and showed a bimodal grain-size distribution (c:f ratio from 40:60 to 95:5). The coarser fraction varied considerably in sizes (from the very fine sand to gravel sizes). It was composed of sub-angular, very peculiar carbonate fragments with concentric growing bands and saw teeth structures, showing alternation of white and dark-brown growing lamina whose microscopic features identified it as speleothems (figure 4.9.a-h). Small amounts of sub-angular and sub-rounded fragments of carbonate mudstone, sparry calcite and sandstone also occurred. The fine fraction (silt sized) was generally abundant and composed of many crystals of quartz and calcite, fragments of micritic limestone, chert, flakes of muscovite, crystals of alkali-feldspar, plagioclase and clay pellets. According to the different quantities of the main inclusions and their textural features, three subgroups were distinguished.

The *fabric 1.1* was characterized by generally abundant inclusions with the dominant presence of equant sub-angular speleothems, calcite was also common mainly with elongate angular shapes. Inclusions reached 4 mm sizes, had a bimodal grain-size distribution sometimes extremely weak, with average c:f ratio of 60:40. Voids were on average the 5-7% of the total area and consisted mainly of channels and vughs (figure 4.9.a-b). This fabric is composed of thirty-three samples: seven coming from Castion d'Erbé, sixteen from Concordia Sagittaria, seven from Padova and one from Palse di Porcia.

The *fabric 1.2* was peculiar because of the larger number of rhombohedral calcite crystals with sharp angular edges associated with the speleothems. Inclusions had a bimodal grain-size distribution moderately sorted with a c:f ratio of nearly 70:30. Voids occupied on average the 10% of the area (figure 4.9.c-d). It consists of nine samples: three coming from Castion d'Erbé, one from Concordia Sagittaria, three from Padova and two from Gradisca di Spilimbergo.

The last subgroup (*fabric 1.3*) was characterized by a fine clay, with a great number of channels voids surrounded by dark boundaries. It was characterized by less abundant

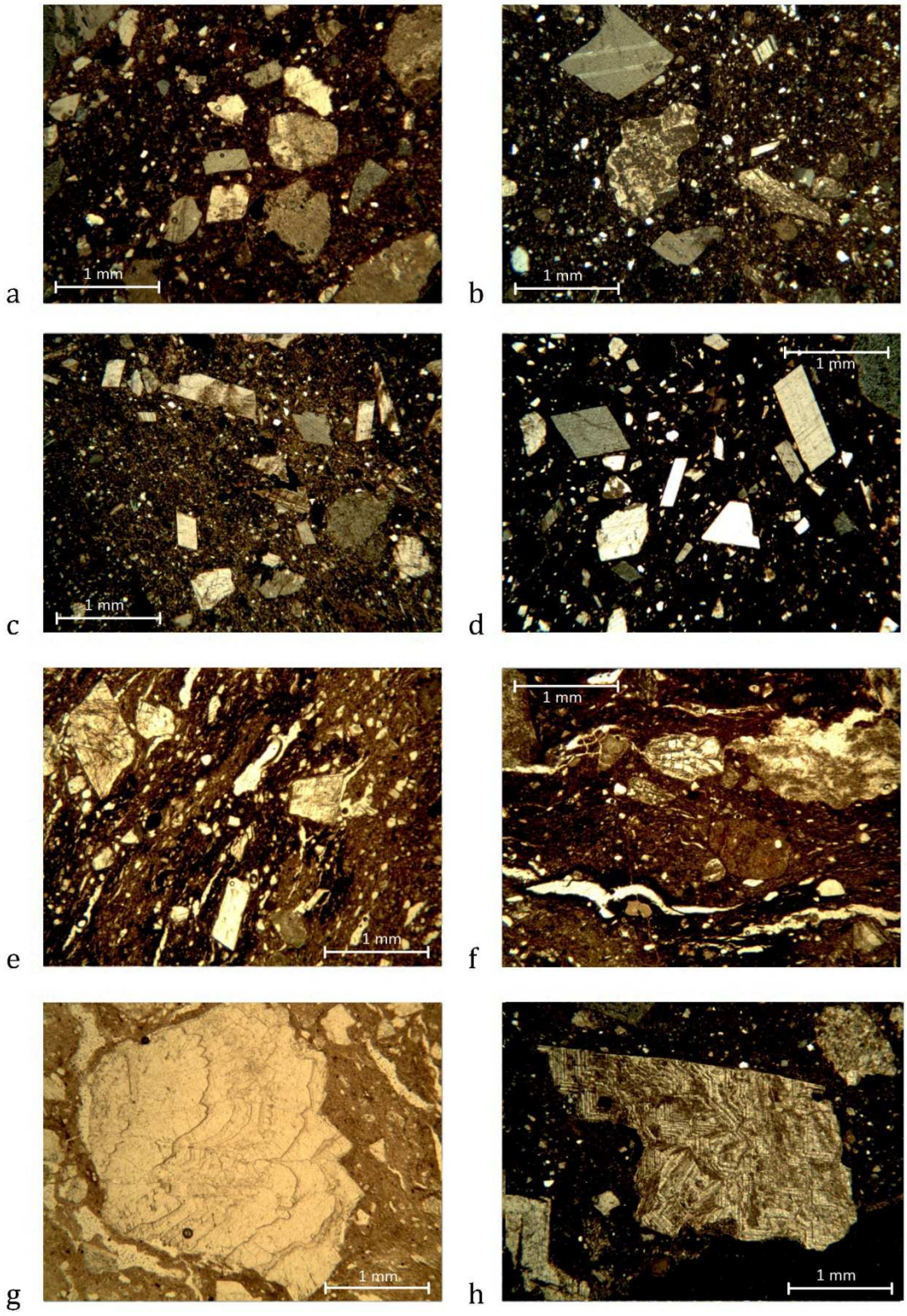

Figure 4. 9. Thin section photomicrographs of selected ceramics analysed in this study belonging to fabrics 1-2: a) Fabric 1.1 (speleothems rich potshards), sample 14636; b) fabric 1.1, sample 97442; c) fabric 1.2, sample 20783; d) fabric 1.2, sample 343776; e) fabric 1.3, sample 100590; f) fabric 1.3, sample 343783; g) detail of a speleothem, sample 14717; h) detail of a speleothem, sample 100590. Images a, b, c, d, h were taken in crossed polars, images e, f, g, were taken in plane polarized light

inclusions (15%) with a bimodal grain-size distribution (average c:f ratio 80:20). Voids were abundant (on average 15%) and consisted mainly of channels strictly aligned with the margins. The channels appear associated with burned organics inclusions because of the darkened surrounding matrix (figure 4.9.e-f). This fabric consists of twelve samples: three from Castion d'Erbé, six from Concordia Sagittaria and three from Padova.
The first fabric comprised mainly FRFL pottery and only five specimens, belonging to sub-fabrics 1.1 and 1.2, were of different type.

- *Fabric 2: Fine homogeneous sand and grog rich potsherds (nine samples)*

It was composed of a fine, sorted sand, constituted predominantly of quartz associated with crystals of plagioclase, alkali-feldspars and grogs fragments. Few small lithic fragments of chert, polycrystalline quartz, volcanic acidic rocks and mica schist were also present. Inclusions had average sizes of 1,30 mm but grog could reach 8 mm. All the samples of this fabric came from Castion d'Erbé. Two subgroups were distinguished: *fabric 2.1* (five samples) characterized by an optically active groundmass with a speckled birefringent fabric. Inclusions had a well sorted bimodal grain-size distribution (c:f ratio 50:50 on average) and were not very common (15% on average) with the dominant presence of equant, from sub-angular to rounded shaped fragments (figure 4.10. a). The *fabric 2.2* (four samples) was characterized by a optically inactive groundmass and very abundant inclusions (30-40%) with a moderately sorted bimodal size distribution (c:f ratio 50:50 on average) and sub-rounded and rounded shapes. (figure 4.10. b).

- *Fabric 3: Trachyte and grog rich potsherds (twelve samples)*

It was a homogeneous group, characterized by an optically active (speckled birefringent fabric) and iso-oriented groundmass. It had small quantities of pores (8% on average), mainly vughs and channels. Inclusions had a very weak bimodal size distribution with a c:f ratio of 10:90. All the samples contained a very fine sand of quartz and plagioclase crystals and coarse intermediate volcanic rocks, trachyte in composition, with a porphyritic structure and a fluidal microlitic groundmass. They were associated with abundant fragments of grog and, in a couple of cases, with fragments of groundmasses of acidic volcanic rocks, probably a rhyolite. All the samples of this fabric came from Padova (figure 4.10. c-d).

- *Fabric 4: Carbonate mudstone and quartz rich potsherd (one sample)*

This potsherd contained abundant inclusions (35%) with a seriate grain-size distribution (average and maximum sizes: 1,0 millimetre, 2,8 mm). It was composed by dominant sub-rounded carbonate mudstone fragments, subordinate crystals of quartz and rare clay pellets and grog. The groundmass was weakly active. Voids (15%) were mainly represented by channels and fewer vughs. This is a FRFL jar coming from Castion d'Erbé (figure 4.10. e).

- *Fabric 5: Quartz sand and trachyte and rhyolite rich potsherd (one sample)*

This potsherd presented an optically inactive groundmass with about 10% of pores, especially channels highly aligned to the margins, and abundant (25%) inclusions

showing a weakly unimodal grain-size distribution. They were mainly composed of

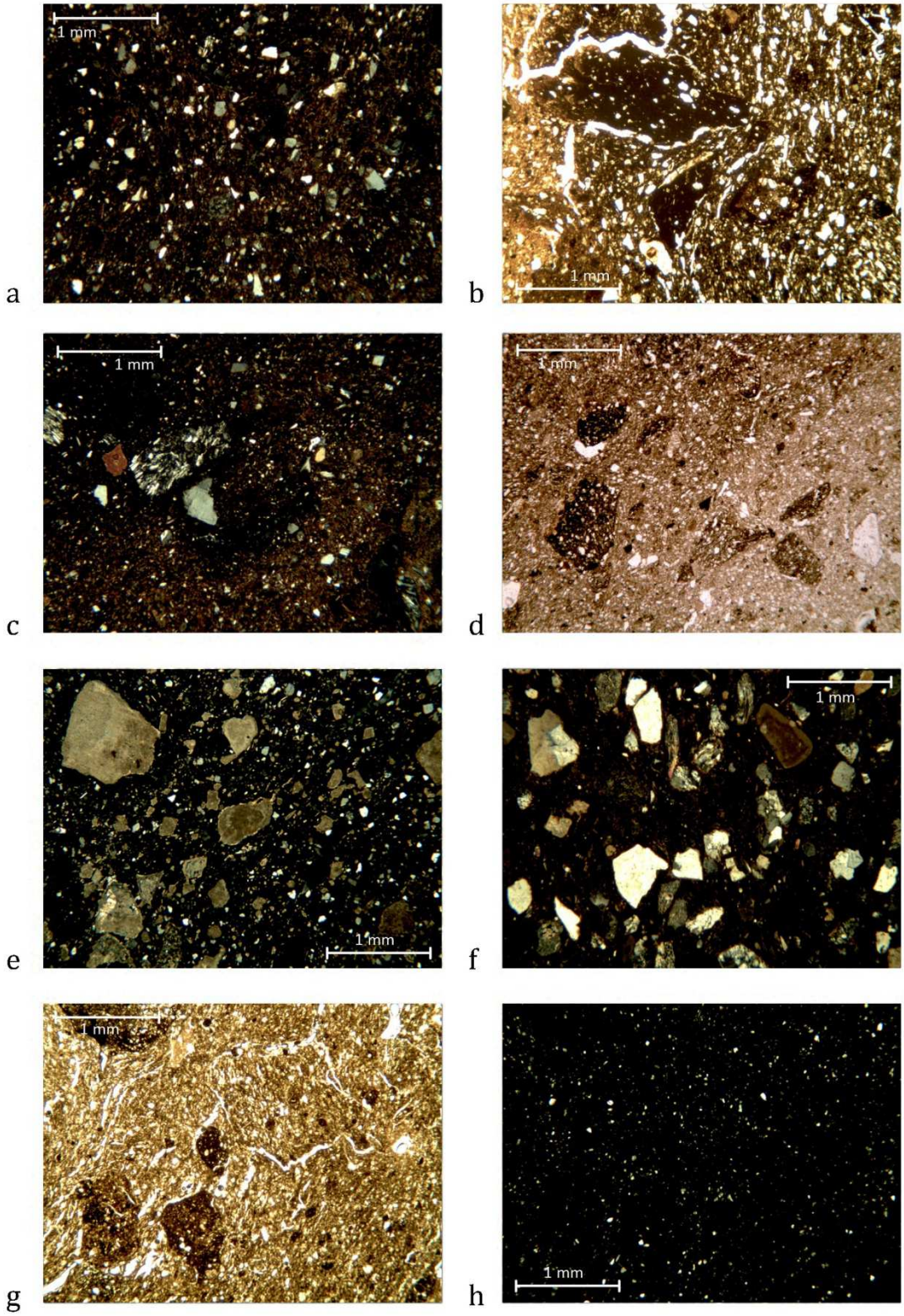

Figure 4. 10. Thin section photomicrographs of selected ceramics analysed in this study belonging to fabrics 3-8: a) fabric 2.1, sample 20796; b) fabric 2.2, sample 20785; c) fabric 3, sample 343784; d) fabric 3, sample 343791; e) fabric 4, sample 20959; f) fabric 5, sample 343781; g) fabric 6, sample 24869; h) fabric 6, sample 24869. Images a, c, e, f, h were taken in crossed polars, images b, d, g were taken in plane polarized light

quartz crystals and carbonate mudstone rocks, frequent polycrystalline quartz, rare mica schist, trachyte and rhyolite. This potsherd came from Padova (figure 4.10. f).

- *Fabric 6: Quartz sand and grog rich potsherds (seven samples)*

This group, consisting of seven samples coming from Concordia Sagittaria (two of which of FRFL type), was characterized by an often heterogeneous, only partially active, groundmass with vughs and channels well aligned to the margins. The inclusions, that occupied nearly the 15-25% of the total area, had a unimodal size distribution in the range of the coarse silt-medium sand. Sometimes a very small number of coarser inclusions were also present. They are composed of dominant crystals of quartz and fragments of grog associated with scarce crystals of feldspars, flakes of muscovite, opaque minerals, fragments of chert and polycrystalline quartz. Inclusions were mainly rounded shaped with average dimensions of 0,1 mm, but grog can reach the maximum dimension of 3,6 mm (figure 4.10. g-h).

- *Fabric 7: Coarse carbonate sand rich potsherds (two samples)*

This fabric was characterized by nearly 20% inclusions with a well bimodal grain-size distribution, where the coarser fraction represents the majority, reaching also gravel size (c:f ratio 95:5). It was mainly composed of rounded fragments of carbonate mudstone and sparry calcite, associated with fewer polycrystalline quartz, chert fragments and clay pellets. The finer fraction comprised crystals of quartz, calcite, feldspar, opaque minerals, fragments of polycrystalline quartz and chert. These two samples are FRFL jars coming from Concordia Sagittaria (figure 4.11. a).

- *Fabric 8: Trachyte rich potsherds (two samples)*

All these samples were characterized by an optically active (with a birefringent fabric of spackled type) non-calcareous groundmass and occasionally with clay pellets or stripes of different colours. Pores were rare (3%), mainly vughs and channels. There were few inclusions (10%), mostly sub-angular and sub-rounded in shape, showing a well bimodal grain-size distribution. The coarser fraction, approximately the 70%, consisted mainly of fragments of trachyte and large crystals of plagioclase. The finer sand and silt sized fraction was mainly composed of crystals of quartz, plagioclase, alkali-feldspars (sanidine) and mica flakes. Clay pellets were common. All the samples of this fabric came from Concordia Sagittaria (figure 4.11. b).

- *Fabric 9: Granite and carbonate mudstone rich potsherds (three samples)*

This was a small and heterogeneous group, composed of samples coming from Concordia Sagittaria, characterized by an optically inactive groundmass and low porosity (3-5%). Inclusions, 15-20% of the area, had an average c:f ratio of 80:20, sub-angular and sub-rounded shapes, showing a bimodal grain-size distribution where the coarser fraction reached gravel dimensions and was mainly represented by fragments of granite. Frequent sub-angular fragments of carbonate mudstone and very few crystals of feldspar, biotite and quartz were also present (figure 4.11. c).

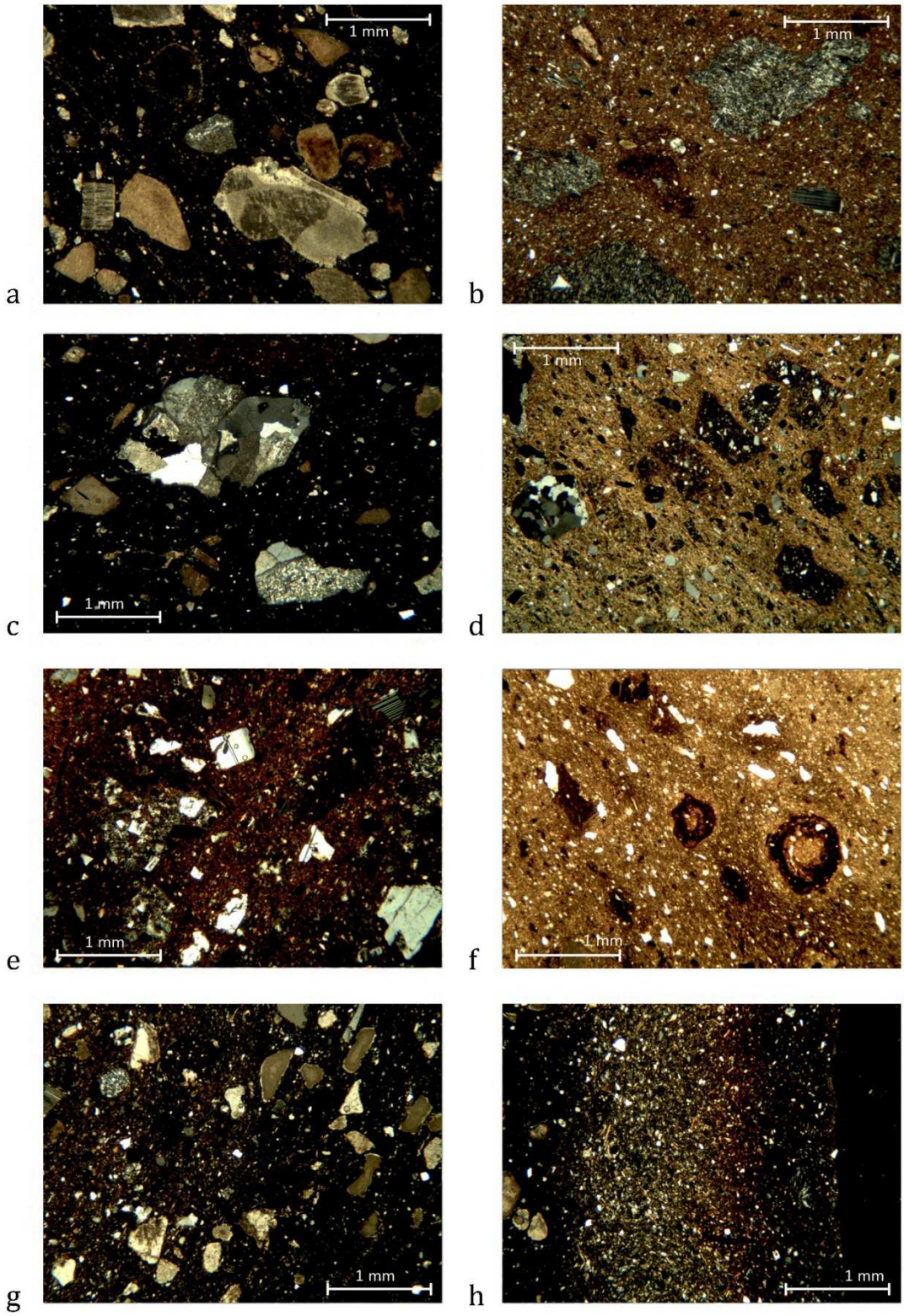

Figure 4. 11 Thin section photomicrographs of selected ceramics analysed in this study belonging to fabrics 7-13: a) fabric 7, sample 28781; b) fabric 8, sample 14715; c) Fabric 9, sample 28806; d) fabric 10, sample 28740; e) fabric 11, sample 14655; f) fabric 12, sample 31546; g) thin section photomicrographs of the inner part of the section of an oven structure (sample 31479; fabric 1.3); h) Thin section photomicrographs of the external layers of the section of an oven structure (sample 31479; fabric 1.3). Images a, b, c, d, e, g, h were taken in crossed polars, image f was taken in plane polarized light.

- *Fabric 10: Grog and clay pellets rich potsherd (one sample)*

This sample, from Concordia Sagittaria, was formed by an optically active groundmass rich in clay pellets and characterized by a low porosity (7%), mostly represented by vughs. The inclusions, nearly 15-20%, were mainly represented by large-sized fragments of grog and clay pellets, associated with few fine sand and silt-sized crystals of quartz and polycrystalline quartz fragments (figure 4.11. d).

- *Fabric 11: Coarse trachyte rich potsherd (one sample).*

This sample had an heterogeneous and weakly active groundmass. The non-plastic inclusions had a bimodal grain-size distribution with the coarser fraction, that represented the majority of all of them (c:f ratio 70:30), composed by sub-angular, coarse sand sized fragments of trachyte. This sample came from Concordia Sagittaria (figure 4.11. e).

- *Fabric 12: Clay pellets rich potsherd (one sample)*

This sample, from Concordia Sagittaria, was characterized by dominant clay pellets and iron oxides, and a very small amount (5%) of non-plastic inclusions composed of very fine sand sized opaque minerals, calcite and quartz crystals (figure 4.11. f).

- *Fabric 13: Heterogeneous groundmass potsherd (one sample)*

This sample that belonged to an oven structure found at Concordia Sagittaria was composed of two different clays: the inner part of the oven structure had nearly 20% inclusions with a bimodal grain-size distribution chiefly composed of carbonate mudstone, few fragments of grog and some clay pellets. The external margin consisted of nearly 30% inclusions, mainly composed by trachyte fragments (figure 4.11. g-h).

Table 4. 3. Minero-petrographic and micro-structural features of pottery samples analyzed under optical microscope. MATRIX: provenance and typology of the semples; area fraction occupied by the matrix (A.%); homogeneity (Hom); optical state (Opt.Ac.); birefringent fabric (b-fab); orientation (Or). VOIDS: total area fraction occupied by the voids (A.%); maximum size (max.size); shape: channel (Ch), planar voids (Pb), vugh (Vu). INCLUSIONS: total area fraction occupied by the inclusions (A.%); orientation (Or); grain-size distribution of the inclusion: unimodal (u), bimodal (bi), seriate (S), kind of sorting of the inclusions: well sorted (ws), moderately sorted (ms),poorly sorted (ps), very poorly sorted (vps); distinct description of the course and fine fractions of the inclusions (where there are present more than one mode): relative abundance of the inclusions of the fine and coarse fractions (Rel.Ab.%); maximum size of the inclusions (max.size); average size of the inclusions (av.size); shapes: equant (eq), elongate (el), angular (A), sub-angular (SA), sub-rounded (SR), rounded (R). Composition of the mineral phases and lithics: qz: quartz crystals; Fsp: feldspars in general; KF: alkali feldspar; Pl: plagioclase; Cal-Dol: calcite and dolomite crystals, Amp: amphibole; Px: pyroxene; Ms: muscovite; Bt: biotite; Srp: serpentinite; Op: opaque minerals; Glt: glauconite; Php: phosphates; Qzt: polycrystalline quartz; Mcsc: mica schist; Vlc: volcanic rock; Plt: plutonic rock; acd: acidic rock; itmd: intermediate rock; Ch: chert; Snd: sandstone; Dol: dolomite; CMt: carbonate mudstone; CSpr: sparry calcite; Sph: speleothems; CP: clay pellets; Grog: grog; ARF; CalSc: secondary calcite. Abundance of mineral phases: 8: predominant (>70%); 7: dominant (50-70%); 6: frequent (30-50%); 5: common (15-30%); 4: few (5-15%); 3: very few: (2-5%); 2: rare (0,5-2%); 1: very rare (<0,5%).

samples	prov	type	MATRIX						VOIDS						INCLUSIONS				INCLUSIONS-COARSE FRACTION								INCLUSIONS-FINE FRACTION							
			A %	Hom.	Opt. Ac.	b-fab.	Or.	d-sp.	A %	max- size	Shape				Or.	A %	Dist.	kind of sor.	Rel. Ab. %	max. size	av. size	Shape					Rel. Ab. %	max. size	av. size	Shape				
										mm	Ch	Pb	Ve	Vu						mm	mm	eq/el	A	SA	SR	R		mm	mm	eq/el	A	SA	SR	R
FABRIC 1.1																																	
6247	TM	FRFL	80	he	a	sp	i	cl-s	5	2x1,8	x			x	i	15	bi	ps	60	3,60	1,00	eq		x	x		40	0,24	0,08	eq			x	x
14636	CS	FRFL	75	ho	↓a b	sp	o	cl-d	5	2,6x0,8	x	x		x	i	20	bi	vps	70	4,80	1,40	eq-el	x		x	x	30	0,24	0,12	eq		x	x	x
14714	CS	FRFL	73	ho	i	-	↓o	cl-d	7	2,6x1,6	x	x		x	i	20	bi	vps	70	6,00	3,20	eq-el	x	x	x	x	30	0,48	0,16	eq		x	x	x
14716	CS	FRFL	75	ho	a	sp	o	cl-d	5	1,32x1	x			x	↓o	20	bi	ps	70	3,20	1,00	eq-el	x		x		30	0,40	0,16	eq		x	x	x
18464	MT	FRFL	87	ho	a	sp	↓o	cl-d	3	1,8x0,8	x			x	i	10	bi	ms	80	4,00	1,00	eq		x	x		20	0,20	0,12	eq			x	x
20794	CE	FRFL	75	he	↓a	sp		cl-s	5	1x0,6				x		20	bi	ps	60	3,60	1,20	eq			x	x	40	0,40	0,12	eq			x	
24648	CS	FRFL	80	he	a	sp	↓o	cl-d	5	5,6x2,2	x		x	x	i	15	bi	vps	60	4,00	2,00	eq-el	x	x		x	40	0,28	0,20	eq	x	x	x	x
28755	CS	FRFL	67	he	a	sp	o	cl-d	3	1,4	x		x	x	↓o	30	bi	vps	40	6,00	2,60	eq-el	x		x	x	60	0,40	0,08	eq-ql	x		x	x
28770	CE	FRFL	83	ho	a	sp	↓o	cl-o	7	2,2x0,6	x			x	i	10	bi	ms	80	6,00	1,20	eq-el	x		x	x	20	0,28	0,04	eq			x	x
28772	CS	FRFL	85	ho	i	-	o	cl-o	5	3,6x0,6	x			x		10	bi	ms	80	4,40	1,80	eq		x	x		20	0,28	0,04	eq				x
28798	CS	FRFL	83	ho	a	sp	o	cl-o	7	7x0,80	x			x	i	10	bi	ps	80	3,00	1,20	eq-el	x	x	x		20	0,20	0,08	eq			x	x
28801	CS	FRFL	78	ho	↓a b	sp	o	cl-o	7	2x0,40	x	x		x	i	15	bi	ms	80	3,00	1,60	eq		x	x		20	0,28	0,08	eq			x	x
28827	CS	-	75	ho	↓a b	sp	o	cl-s	10	4,60	x			x	↓o	15	bi	ms	80	2,60	1,20	eq		x	x	x	20	0,28	0,08	eq			x	x
31282	CS	FRFL	70	ho	a	sp	o	cl-d	10	3,2x0,6	x			x	i	20	bi	ps	80	9,20	2,00	eq	x	x		x	20	0,52	0,08	eq		x	x	
31295	CS	FRFL	68	ho	i	-	i	cl-s	7	1,4x0,4	x			x	i	25	bi	ms	50	4,40	1,60	eq		x	x		50	0,32	0,08	eq		x	x	
31420	CS	-	77	ho	↓a	sp	↓o	cl-s	3	4,2x0,8	x	x		x	i	20	bi	ms	50	3,20	2,00	eq-el	x		x		50	0,40	0,16	eq		x	x	
31421	CS	FRFL	70	he	a	sp	↓o	cl-s	10	3,20	x	x		x	i	20	bi	ps	60	4,00	2,20	eq		x	x		40	0,40	0,16	eq			x	x
31492	CS	FRFL	68	he	↓a b	sp	i	cl-s	7	2,6x1,0	x	x		x	i	25	bi	vps	50	6,00	2,00	eq		x	x	x	50	0,28	0,12	eq			x	x
31493	CS	FRFL	78	he	↓a b	-	o	cl-d	7	2,2x0,3	xx			x	i	15	bi	ps	60	3,80	0,80	eq	x	x	x		40	0,20	0,08	eq		x	x	
31544	CS	FRFL	70	ho	a	sp	o	cl-d	10	2x0,6	x	x		x	i	20	bi	vps	75	2,40	2,00	eq-el	x	x	x		25	0,20	0,04	eq-el		x	x	x
97151	CE	FRFL	73	he	↓a b	sp	o	cl-s	7	1,60	x	x		x	i	20	bi	vps	50	4,00	1,40	eq-el	x	x	x	x	50	0,40	0,12	eq			x	x
97364	CE	FRFL	77	ho	↓a	sp	↓o	cl-d	3	2,20	x			x	i	20	bi	ms	50	4,00	1,80	eq	x	x			50	0,40	0,12	eq			x	x
97442	CE	FRFL	77	ho	↓a b	sp	o	cl-s	3	0,40	x			x	↓o	20	bi	ps	60	6,00	2,20	eq-el	x		x		40	0,48	0,20	eq				x
99894	CE	FRFL	77	ho	↓a b	sp	o	cl-s	3	2,2x1,4	x			x	o	20	bi	ps	50	2,80	1,40	eq-el	x		x	x	50	0,40	0,08	eq			x	x
100691	CE	FRFL	73	ho	i	-	o	cl-d	7	1,48	x			x	↓o	20	bi	vps	60	3,80	1,60	eq-el		x	x	x	40	0,40	0,12	eq			x	x
236738	PP	FRFL	72	ho	i	-	↓o	cl-s	3	2,40	x			x	i	25	bi	ms	50	5,60	2,00	eq			x	x	50	0,40	0,16	eq		x	x	x
343769	PD	FRFL	65	ho	a	sp		cl-s	5	1,20				x	↓o	30	bi	vps	60	3,00	1,20	eq		x	x		40	0,40	0,12	eq			x	x
343771	PD	FRFL	69	he	a	sp	o	cl-s	6	1,8x0,3	xx			x	o	25	bi	ms	80	4,00	1,20	eq-el	x	x	x		20	0,40	0,08	eq			x	X
343775	PD	FRFL	78	he	a	sp	o	cl-d	7	1,8x1,2	x			xx	o	15	bi	ps	60	4,00	1,00	eq-el	x	x	x		40	0,32	0,08	eq			x	X
343777	PD	FRFL	73	he	i	-	o	cl-s	7	3,4x0,6	x	x		x	o	20	bi	ms	50	4,00	2,00	eq-el	x	x	x		50	0,40	0,12	eq			x	x
343778	PD	FRFL	78	ho	a	sp	↓o	cl-d	7	1,6x1	x			x	i	15	bi	ms	70	5,20	1,00	eq-el	x	x	x		30	0,28	0,08	eq		x	x	x
343779	PD	FRFL	67	ho	a	sp	o	cl-s	3	1,8x0,6	x			x	↓o	30	bi	vps	40	5,60	1,80	eq-el	x		x	x	60	0,40	0,12	eq			x	x
343788	PD	FRFL	70	ho	a	sp	↓o	cl-s	5	2x0,80				x	i	25	bi	ps	50	3,40	1,20	eq			x	x	50	0,40	0,08	eq			x	x
418269	AQ	FRFL	78	ho	a	sp	↓o	cl-s	7	0,68	x				↓o	15	bi	ms	70	2,80	0,80	eq		x	x		30	0,16	0,04	eq			x	x

Table 4.3. Minero-petrographic and micro-structural features of pottery samples analyzed under optical microscope.

samples	prov	type	MATRIX						VOIDS						INCLUSIONS				INCLUSIONS-COARSE FRACTION								INCLUSIONS-FINE FRACTION							
			A %	Hom.	Opt. Ac.	b-fab.	Or.	d-sp.	A. %	max- size	Shape				Or.	A %	Dist.	kind of sor.	Rel. Ab. %	max. size	av. size	Shape					Rel. Ab. %	max. size	av. size	Shape				
										mm	Ch	Pb	Ve	Vu						mm	mm	eq/el	A	SA	SR	R		mm	mm	eq/el	A	SA	SR	R
FABRIC 1.2																																	
20783	CE	FRFL	80	he	↓a b	sp	o	cl-d	5	1,6x0,8				x	↓o	15	bi	ms	60	3,00	1,40	eq-el	x		x		40	0,40	0,12	eq			x	x
24552	CS	FRFL	70	ho	↓a b	sp	o	cl-s	10	2,2x1,0	x	x		x	↓o	20	bi	ps	80	3,60	1,40	el-eq	x	x	x		20	0,40	0,08	eq		x		x
28750	CS	FRFL	83	ho	A	sp	↓o	cl-d	7	1,08	x				↓o	10	bi	ws	90	2,80	0,80	eq-el	x	x	x		10	0,28	0,06	eq		x	x	
31275	CS	FRFL	75	he	A	sp	o	cl-o	10		x			x	↓o	15	bi	ws	90	6,20	2,20	eq-el	x		x	x	10	0,32	0,08	eq-el	x		x	x
101134	CE	FRFL	70	he	↓a b	sp	o	cl-s	5	1,2x0,4		x	x	x	↓o	25	bi	vps	60	3,60	1,20	el-eq	x		x		40	0,28	0,08	eq		x		x
100975	CE	-																															
259786	GS	FRFL	-	ho	A	sp	-	cl-d	-	-	-	-	-	-	i	-	bi	ms	90	3,00	1,20	eq-el	x	x			10	0,16	0,08	eq-el		x	x	
343776	PD	FRFL	70	ho	↓a b	sp	o	cl-s	5	7x3,20		x		x	↓o	25	bi	ms	60	3,60	1,20	el	x		x		40	0,28	0,08	eq		x	x	x
343786	PD	FRFL	70	he	A	sp	o	cl-s	10	2,4x1,4	x			x	↓o	20	bi	ps	80	3,40	1,40	el-eq	x		x		20	0,20	0,08	eq		x		x
343794	PD	-	70	he	↓a b	sp	o	cl-s	5	2,4x1,4		x		x	↓o	25	bi	vps	85	5,60	2,20	eq-el	x	x	x		15	0,40	0,12	eq-el		x	x	x
418343	AQ	FRFL	65	ho	i	-	o	cl-s	15	4,8x1,0	xx			x	↓o	20	bi	vps	60	3,12	0,80	eq-el	x	x			40	0,20	0,08	eq		x	x	
424278	GS	FRFL	65	ho	a	sp	o	cl-d	15	2,8x0,8	x			x	i	20	bi	ps	85	4,40	1,60	eq-el	x	x	x		15	0,20	0,04	eq-el		x	x	
FABRIC 1.3																																	
625	TM	FRFL	70	he	a	sp	o	cl-s	20	4,8x0,3	x	x		x	↓o	10	bi	ms	70	4,80	1,00	eq-el	x	x		x	30	0,28	0,08	eq			x	x
637	TM	FRFL	75	he	↓a b	-	o	cl-s	15	4x0,28	x			x	↓o	10	bi	ps	80	4,40	1,00	eq-el		x	x		20	0,28	0,08	eq			x	x
8614	MT	FRFL	65	he	i	-	o	cl-s	15	2,6x0,7	xx			x	i	20	bi	vps	95	5,00	1,00	el-eq	x		x		5	0,20	0,08	eq		x	x	
14712	CS	FRFL	70	he	a	sp	o	cl-d	10	2,00	x			x	o	20	bi	ms	60	4,80	2,00	eq-el	x	x	x		40	0,40	0,12	eq	x	x	x	x
14713	CS	FRFL	65	he	↓a b	sp	o	cl-o	15	3,8x0,6	x				↓o	20	bi	ms	90	4,40	1,80	eq-el		x	x	x	10	0,28	0,08	eq		x	x	x
14717	CS	FRFL	65	he	a	sp	o	cl-d	15	6,4x0,3	x				i	20	bi	ps	80	5,60	2,20	eq		x	x		20	0,40	0,20	eq	x		x	x
31290	CS	FRFL	80	he	a	sp	o	cl-o	10	3,4x0,6	x			x		10	bi	ws	90	3,80	2,00	eq-el	x		x	x	10	0,28	0,08	eq				x
97081	CE	FRFL	60	he	↓a	sp	o	cl-s	20	4,4x2	x				i	20	bi	ps	60	5,20	2,00	eq		x	x	x	40	0,40	0,12	eq			x	x
100568	CE	FRFL	83	he	a	sp	o	cl-o	7	3,20	x				i	10	bi	ws	90	3,00	1,20	eq		x	x	x	10	0,52	0,08	eq		x	x	x
100590	CE	FRFL	75	he	a	sp	o	cl-o	10	1,40	x				o	15	bi	ws	70	4,80	2,00	el-eq	x		x		30	0,28	0,08	eq			x	x
343774	PD	FRFL	78	he	a	sp	o	cl-d	7	2x0,60	x			x	i	15	bi	ms	80	4,00	1,40	eq			x		20	0,40	0,16	eq			x	x
343783	PD	FRFL	83	he	a	sp	o	cl-o	7	10x1,20	x				o	10	bi	ws	90	5,00	2,20	eq			x	x	10	0,52	0,12	eq			x	x
343790	PD	FRFL	65	ho	a	sp	o	cl-d	15	2,2x0,8	x				↓o	20	bi	ps	70	6,00	1,40	eq-el		x	x	x	30	0,36	0,08	eq	x	x	x	X
418905	AQ	FRFL	75	he	a	sp	o	cl-d	10	4,4x0,3	xx				↓o	15	bi	ms	90	3,80	1,00	eq		x	x		10	0,18	0,06	eq			x	X
FABRIC 2.1																																	
20796	CE	-	65	ho	a	sp	↓o	cl-d	15	1,20	x	x		xx	i	20	bi	ws	50	4,20	1,60	eq	x	x			50	0,48	0,08	eq-el		x	xx	X
28378	CE	-	75	he	a	sp	↓o	cl-d	10	4,00	x	x		xx	i	15	bi	ps	20	2,00	1,00	eq	x	x			80	0,80	0,08	eq		x	xx	X
33686	CE	-	75	ho	a	sp	↓o	s-o	10	1,20	x	x		xx	i	15	bi	ws	50	4,60	1,20	eq	x	x		x	50	0,40	0,08	eq		x	xx	X
33749	CE	-	83	ho	a	sp	↓o	s-o	7	1,6x0,6	x			xx	i	10	bi	ws	70	5,00	2,00	eq		x	xx	x	30	0,40	0,16	eq		x	xx	X
33596	CE	-	-	ho	a	sp	-	s-o	-	-	-	-	-	-	i	10	bi	ms	80	8,00	1,40	eq	x	x		x	20	0,44	0,16	eq	-	x	xx	X

Table 4.3. Minero-petrographic and micro-structural features of pottery samples analyzed under optical microscope.

samples	prov	type	MATRIX						VOIDS						INCLUSIONS				INCLUSIONS-COARSE FRACTION								INCLUSIONS-FINE FRACTION							
			A %	Hom.	Opt. Ac.	b-fab.	Or.	d-sp.	A %	max- size	Shape				Or.	A. %	Dist.	kind of sor.	Rel. Ab. %	max. size	av. size	Shape					Rel. Ab. %	max. size	av. size	Shape				
										mm	Ch	Pb	Ve	Vu						mm	mm	eq/el	A	SA	SR	R		mm	mm	eq/el	A	SA	SR	R
FABRIC 2.2																																	
20785	CE	-	45	he	a	sp	↓o	cl-d	15	2,6x0,6	xx	x		x	i	40	bi	ms	60	5,00	1,60	eq	x	x		x	40	0,52	0,08	eq		x	xx	xx
27443	CE	-	60	he	i	-	↓o	cl-d	10	1,8x0,4	xx	x		x	i	30	bi	ms	40	1,80	1,00	eq	x	x			60	0,48	0,12	eq		x	xx	xx
33806	CE	-	63	ho	i	-	i	s-d	7	3,2x1,0	x			xx	i	30	bi	ms	60	3,40	1,20	eq	x	x			40	0,60	0,08	eq		x	xx	xx
20799	CE	-	50	he	i	-	↓o	cl-d	10	-	x			xx	i	40	bi	ps	40	2,00	0,60	eq	x	x		x	60	0,44	0,08	eq		x	xx	xx
FABRIC 3																																	
343770	PD	-	75	he	↓a	sp	↓o	s-o	10	4x0,80	xx	x		x	i	15	bi	vps	10	1,20	1,00	eq		x	x		90	0,28	0,16	eq-el		x	x	x
343772	PD	-	75	he	i	-	↓o	cl-s	5	1,80	xx	x		xx	i	20	bi	vps	5	3,60	1,20	eq-el	x	x	x		95	0,40	0,08	eq-el		x	x	x
343773	PD	-	73	he	↓a	sp	↓o	s-d	7	3,60	xx			xx	i	20	bi	vps	10	3,40	1,40	eq		x	x		90	0,24	0,12	eq			x	xx
343787	PD	-	75	ho	↓a	sp	↓o	s-d	10	1,2x0,6	x	x		xx	i	15	bi	vps	20	2,80	1,60	eq		x	x		80	0,28	0,08	eq			x	xx
343780	PD	-	80	ho	a	sp	o	s-d	5	3,00	xx	x		x	i	15	bi	vps	10	3,60	0,80	eq	x	x	x		90	0,24	0,12	eq		x	x	xx
343782	PD	-	78	ho	↓a	sp	i	cl-d	7	1,60	x	x		xx	i	15	bi	vps	20	3,40	0,80	eq		x	x	x	80	0,32	0,12	eq			x	x
343784	PD	-	75	ho	a	sp	↓o	s-d	10	2,00	x	x		xx	i	15	bi	vps	15	2,20	0,60	eq		x	x	x	85	0,16	0,08	eq			x	x
343785	PD	-	75	he	a	sp	↓o	s-d	5	3,00	xx	x		xx	i	20	bi	vps	10	2,60	0,80	eq		x	x		90	0,28	0,08	eq			x	xx
343789	PD	-	70	he	a	sp	↓o	cl-o	15	2,80	xx	x		xx	i	15	bi	ws	10	5,00	1,00	eq		x	x	x	90	0,20	0,08	eq		x	x	x
343791	PD	-	78	he	a	sp	o	cl-d	7	3,40	x			xx	i	15	bi	ws	10	4,40	0,80	eq	x	x	x	x	90	0,20	0,08	eq		x	x	x
343792	PD	-	78	he	i	-	↓o	s-d	7	2,20	xx	x		xx	i	15	bi	vps	20	2,60	1,20	eq	x	x	x		80	0,28	0,08	eq			x	x
343793	PD	-	73	he	a	sp	↓o	cl-d	7	1,8x0,5	x	x		xx	i	20	bi	vps	20	3,40	0,80	eq		x	x	x	80	0,20	0,08	eq		x	x	
FABRIC 4																																	
20959	CE	FRFL	50	ho	i	-	o	cl-s	15	1,6x0,5	xx			x	i	35	S	ms	40	2,80	1,00	eq-el	x	xx	xx	x	60	0,40	0,12	eq		x	x	x
FABRIC 5																																	
343781	PD	-	65	ho	↓a	-	o	cl-d	10	2x0,28	xx			x	↓o	25	u	ws	-	2,00	0,80	eq-el		x	x	xx	-	-	-	-	-	-	-	-
FABRIC 6																																	
14630	CS	-	78	he	↓a	sp	↓o	s-d	7	4,4x0,3	x			xx	i	15	u	ps	-	2,20	1,40	-	-	-	-	-	-	0,28	0,08	eq		x	x	xx
14634	CS	-	80	ho	a	sp	↓o	s-d	5	3,00	x			xx	i	15	u	ps	-	2,00	0,80	-	-	-	-	-	-	0,44	0,08	eq		x	xx	xx
24615	CS	FRFL	70	he	↓a b	sp	o	s-d	10	6,00	xx	x		x	↓o	20	bi	ps	10	3,60	1,00	eq		x	x	x	90	0,28	0,08	eq		x	x	xx
24869	CS	-	68	ho¯	i	-	o	s	7	3,6x1,2	xx			x	i	25	u	ws	-	2,40	1,20	-	-	-	-	-	-	0,52	0,08	eq		x	xx	x
28982	CS	FRFL	70	he	↓a	sp	o	s-d	10	2,40	xx			x	i	20	u	ps	-	2,80	1,40	-	-	-	-	-	-	0,32	0,12	eq		x	x	xx
31276	CS	-	65	ho¯	i	-	↓o	s	10	6,00	xx			x	i	25	u	ws	-	3,60	1,20	-	-	-	-	-	-	0,32	0,08	eq		x	xx	x
31906	CS	-	80	ho¯	↓a	sp	↓o	s-d	5	3,8x1,6	xx			x	i	15	u	ws	-	3,60	1,60	-	-	-	-	-	-	0,20	0,04	eq		x	x	xx
FABRIC 7																																	
28780	CS	FRFL	73	ho	a	sp	o	s	7	1,60	xx			x	i	20	u	ws	95	4,40	1,60	eq-el		x	xx	x	5	0,32	0,08	eq/el			x	X
28781	CS	FRFL	70	ho	a	sp	o	s-d	10	2,80	xx			x	i	20	u	ws	95	4,00	1,20	eq-el		x	xx	x	5	0,36	0,12	eq/el			x	X
FABRIC 8																																	
14715	CS	-	87	ho	a	sp	↓o	s-o	3	1,40	x			xx	i	10	bi	ms	70	6,60	1,80	eq		x	x	x	30	0,32	0,08	eq-el		x	x	X
28794	CS	-	-	ho	a	sp	-	s-o	-	-	-	-	-	-	i	5	u	ws	-	3,40	0,68	eq			x		-	0,40	0,08	-	-	-	-	-

Table 4.3. Minero-petrographic and micro-structural features of pottery samples analyzed under optical microscope.

samples	prov	type	MATRIX						VOIDS						INCLUSIONS				INCLUSIONS-COARSE FRACTION								INCLUSIONS-FINE FRACTION							
			Rel. Ab. %	Hom.	Opt. Ac.	b-fab.	Or.	d-sp.	Rel. Ab. %	max- size	Shape				Or.	Rel. Ab. %	Dist.	kind of sor.	Rel. Ab. %	max. size	av. size	Shape					Rel. Ab. %	max. size	av. size	Shape				
										mm	Ch	Pb	Ve	Vu						mm	mm	eq/el	A	SA	SR	R		mm	mm	eq/el	A	SA	SR	R
FABRIC 9																																	
28806	CS	-	80	he	↓a b	-	o	s-d	5	1,20	x			x	↓o	15	bi	ps	80	4,40	1,80	eq-el	x	x	x		20	0,40	0,08	eq		x	x	Xx
29015	CS	-	77	ho	i	-	↓o	cl-o	3	0,52	x			xx	↓o	20	bi	vps	25	2,40	1,00	eq		x	x		75	0,40	0,12	eq			x	Xx
31490	CS	-		ho	a	sp	↓o	cl-d		1,20	x			xx	i	15	bi	ms	80	3,60	1,20	eq		x	x	x	20	0,40	0,08	eq		x	x	Xx
FABRIC 10																																	
28740	CS	-	78	he	a	sp	↓o	s-o	7	4,4x1,6	x			xx	↓o	15	↓bi	vps	15	2,00	2,40	eq-el		x	x	x	85	0,60	0,20	eq	x	x	x	Xx
FABRIC 11																																	
14655		-	75	he	↓a b	-	↓o	s-d	5	1,00				xx	↓o	20	bi	ms	70	3,20	1,60	eq-el	x	x	xx	x	30	0,48	0,20	eq	x	x	xx	X
FABRIC 12																																	
31546	CS	-	92	he	a	sp		d-o	0	0,80	x	x		x	i	5	bi	ws	20%	1,00	-	eq	x	x	x	x	80	0,32	0,08	eq	x	x	x	X
FABRIC 13																																	
31479	CS	-	70	he	a	sp	o		10	1,2x0,5	xx			x		20	bi	ms															
31479	INT.							cl-d								20	bi	ms	70	2,40	1,00	eq			xx	x	30	0,28	0,12	eq		x	x	X
	EXT							cl-s								30	u	ws	100	1,00	0,12	eq-el		x	x									

Table 4.3. Minero-petrographic and micro-structural features of pottery samples analyzed under optical microscope.

COARSE FRACTION																														
samples	CRYSTALS												MET.R.		IGNEOUS R.			SEDIMENTARY ROCKS						OTHER FEATURES						
	Qz	Fsp	KF	Pl	Cal-Dol	Amp	Px	Bt	Srp	Op	Glt	Php	Qzt	Mcsc	vlc		plt	Ch	sdn	Dol	CMt	CSpr		Sph	CP	Grog	ARF	AtR	CalSc	
															acd	itmd	acida													
FABRIC 1.1																														
6247										4											3			8						
14636	1				7				1												5			6	1					
14714					6																4			7	4					
14716	1				5						2										5			7	3					
18464					3					1											1	2		7						
20794	1				1																3			8	5					
24648					5															4	5			5						
28755	1				5															3	5			6	3	1				
28770					2					1											1			8	2	3				
28772																					6			6	5					
28798					5													2		1	4			7	4					
28801	1				4								1								1			7	3	1				
28827																					4			7	3					
31282					1					2											4			7						
31295																					3			8		3				
31420					4					1											3			8	3	1				
31421																					5			5	5	1				
31492																					3			7	5	5				
31493	1				5					3														7						
31544					6				2											3				5	5					
97151	1				4																4			7	3	5				
97364																					4			8		5				
97442	1				5																	4		8	2	1				
99894	1				4																	1		8	3					
100691					2																5			6	3					
236738					3					2											4			8	4	2				
343769					2				1												5			8						
343771					6																2			7						
343775	1				5				2	1	4										5			6	2	3				
343777					5						1										5			7						
343778					6																	5		6		5				
343779	1				5															2	3			8	2					
343788					3																3			8	3	5				
418269					3																			8	3	2				
FABRIC 1.2																														
20783					5																5	2		7	3					
24552					5								1					1			2			7	6					

Table 4.3. Minero-petrographic and micro-structural features of pottery samples analyzed under optical microscope.

COARSE FRACTION																													
samples	CRYSTALS												MET.R.		IGNEOUS R.			SEDIMENTARY ROCKS						OTHER FEATURES						
	Qz	Fsp	KF	Pl	Cal-Dol	Amp	Px	Bt	Srp	Op	Glt	Php	Qzt	Mcsc	vlc	itmd	plt	Ch	sdn	Dol	CMt	CSpr		Sph	CP	Grog	ARF	AtR	CalSc	
															acd		acida													
28750					6					3								3				5		6	3		2			
31275					6																2			6		5				
100975	1				6				1				2											7	3					
101134					7								2								2			7	4					
259786					7					2														5						
343776					7																5			6	3					
343786					5																2			7	5					
343794					6								1					1						7	3	1				
418343					7					3					3			4	4			2		6						
424278					7														2		1			4		4				
FABRIC 1.3																														
625					4					3											3	2		7	3					
637					4																	3		7		2				
8614					3																			8						
14712					2																4			8	2	4				
14713					5																3			7	4	2				
14717					5																2			8	1					
31290					6							3									2			6	3	4				
97081	1				2																5			8	3	1	2			
100568	1				1								2								4			8	2		1			
100590					3																5			7	3	1				
343774					2						4										4			8	4	3	4			
343783					4																4			8	3	3				
343790	1				5								1							1	3			7	4	3				
418905					4						3								2			5		7						
FABRIC 2.1																														
20796																										8				
28378																										8				
33686																									5	7				
33749													5								5					7			2	
33596																									3	8				
FABRIC 2.2																														
20785																									4	8				
27443													2													8				
33806																					3				2	8				
20799															3		2	3			6					6				
FABRIC 3																														
343770	7	6	2	6		1	4			2					4	2									2	4				

Table 4.3. Minero-petrographic and micro-structural features of pottery samples analyzed under optical microscope.

COARSE FRACTION																													
samples	CRYSTALS												MET.R.		IGNEOUS R.			SEDIMENTARY ROCKS						OTHER FEATURES					
	Qz	Fsp	KF	Pl	Cal-Dol	Amp	Px	Bt	Srp	Op	Glt	Php	Qzt	Mcsc	vlc		plt	Ch	sdn	Dol	CMt	CSpr		Sph	CP	Grog	ARF	AtR	CalSc	
															acd	itmd	acida													
343772	4	4		4	4		3			3			1		2	5									3	7		3		
343773	7	6	2	5			3		1	2			1												2	7				
343780	3	5	5	4	4		2			3			1		3	1									2	7		6 vlc.itmd.		
343782	7	6	2	5		1	2		2	2					2	7		1							2	6				
343784	5	6	2	5		1	4		2	1			2		2	7		2							2	4				
343785	5	7	5	7			1		2	4			1		2	5		1							1	4				
343787	4	5	4	4	4		2			4			4		3	2									2	6		5 vlc.itmd		
343789	5	4		3		1			3	4	2		1	1	3	4		2							2	7		4		
343791	5	5		5		1	4			2					1										2	7			4	
343792	4	2		2						2	4		6		6		3	1			6				2	4		2		
343793	6	6		6					1	3			3		1	3		1							2	7				
FABRIC 4																														
20959	3																				8				2	2				
FABRIC 5																														
343781	5	3	2	3				1					6	2	3	2	2	2			6									
FABRIC 6																														
14630	-	-	-	-	-	-	-	-	-	-	-	-	-	-	-	-	-	-		-	-	-		-	-	7	-	-	-	
14634	-	-	-	-	-	-	-	-	-	-	-	-	-	-	-	-	-	-		-	-	-		-	-	8	-	-	-	
24615					4					1											6			3		6				
24869	-	-	-	-	-	-	-	-	-	-	-	-	-	-	-	-	-	-		-	-	-		-	-	-	-	-	-	
28982	-	-	-	-	-	-	-	-	-	-	-	-	-	-	-	-	-	-		-	-	-		-	-	6	-	-	-	
31276	-	-	-	-	-	-	-	-	-	-	-	-	-	-	-	-	-	-		-	-	-		-	-	-	-	-	-	
31906	-	-	-	-	-	-	-	-	-	-	-	-	-	-	-	-	-	-		-	-	-		-	-	-	-	-	-	
FABRIC 7																														
28780					1								4		1		1	4			6	6			2					
28781					1								4	1		1		4			6	7			2					
FABRIC 8																														
14715				2												8									4					
28794																8									4					
FABRIC 9																														
28806			2					1					3		1		6				7			4	2					
29015	2			3													6				6				5					
31490	2			1		1		1					3		1		8								2					
FABRIC 10																														
28740	3	3											4								4				6	6				
FABRIC 11																														
14655		6	2	2				4	2	3						7									2	1				
FABRIC 12																														
31546	2				5					6			1												7	2				
FABRIC 13																														
31479	3	1							3	4	3		3					3			7	2			5	5				

Table 4.3. Minero-petrographic and micro-structural features of pottery samples analyzed under optical microscope.

INE FRACTION																											
Samples	CRYSTALS													MTM.R.	IGNEOUS R.			SEDIMENTARY R:					OTHER FEASTURES				
	Qz	Fsp	KF	Pl	Cal-Dol	Amp	Px	Ms	Bt	Srp	Op	Glt	Php	Qzt	vlc		plt	Ch	Dol	CMt	CSpr		Sph	CP	Grog	ARF	CalSc
															ac.	int.	ac.										
FABRIC 1.1																											
6247	7	2	2		1			2			3			2				2					4				
14636	6				6			1			2			1				2									1
14714	7	1			4			1			2			1				2					2				
14716	6				5			1			2	2	1	2				2		2			3				1
18464	2				4			1			3												7				
20794	6	1			4			1						3				2		3			5				1
24648	7				5			2			2			1				1		4			3				
28755	6				7			1		1	2							1					4	1			3
28770	8				4			1			3																2
28772	8				3			2										1									2
28798	6				6			2		1	1							1									
28801	7				6			2						3				3									
28827	6				6			1																			1
31282	6				6			2			3									3			4				
31295	6							1			4												6				
31420	7				5			1			2	1		1				3					2				
31421	6	1	1					1		2		1		3				1		6				3			5
31492	6				5			1						2				1		5			5				5
31493	7				5			1						1				1					3				
31544	5				7			2		5	2	5		1				1									
97151	7				5			1		2	1			2				1		1			2				
97364	7				5			1			3												5				
97442	7	1	1		4			1	1			1		1				2		3			3	2			2
99894	7				6			2			2			1				2		1			2				
100691	6	1	1		5			1					2	1				1					2	1			1
236738	8				2			1			3							2						2			2
343769	6				5			3				1		3				3		4			6				
343771	7	2			4			2			2	2		4				3					4				
343775	7	1		1				1			3	3		1				2					3	2			1
343777	7		1		2			2				1		1				2		5			2				5
343778	6	1	1		6			2		2	1	1		3				2		1			3				
343779	7				4			1			2			1				5		4			3				4
343788	8				3			2		1	1	1		2				2		3			4				
418269	7	2	2		4			1			1	1		1				2		1			6				
FABRIC 1.2																											
20783					5															5	2		7	3			
24552					5									1				1		2			7	6			
28750	7				4			3			4	2						2									
31275	3	1			8			1					1							1			5				
100975	1				6					1				2									7	3			
101134					7									2						2			7	4			

Table 4.3. Minero-petrographic and micro-structural features of pottery samples analyzed under optical microscope.

INE FRACTION																											
Samples	CRYSTALS													MTM.R.	IGNEOUS R.			SEDIMENTARY R:					OTHER FEASTURES				
	Qz	Fsp	KF	Pl	Cal-Dol	Amp	Px	Ms	Bt	Srp	Op	Glt	Php	Qzt	vlc		plt	Ch	Dol	CMt	CSpr		Sph	CP	Grog	ARF	CalSc
															ac.	int.	ac.										
259786	6				6			5			2																
343776					7															5			6	3			
343786					5															2			7	5			
343794					6									1				1					7	3	1		
418343	7				2			2												5			5				
424278	6				6			1			2																
FABRIC 1.3																											
625	7	2	2					1			4			1				2					5				
637	7				3			1			2			2									5				
8614	2																						8				
14712	5	2	2		6			1			2	1		2				3		3			3				3
14713	5	1	1		6			1			2			1				1		5			2				3
14717	3				8			1			2	1											2				2
31290	5				8			1			3		1					1		2			2				4
97081	6	1	1		5			1			2	1		3				2		4			5				2
100568	5				6			1		1				2				1					4				1
100590	6				5			1		1	2			2				1		4			4				1
343774	5				4			1		1	2	1		1				2		2			7				
343783	4				4	1		1										1		2			7				1
343790	5				6			1		1		1		1				1		1			6				
418905	7	2			2			1			1	1											6				
FABRIC 2.1																											
20796	7	2	1	2		1		1		1		1	5		5	2	1	2		1							
28378	8	2	2	1		1		1		1			3		3			2									1
33686	7	2	2	1		1		1		1			2											2			1
33749	7							3										4		4							
33596	7	2	3	1		1		1		1			2		4												
FABRIC 2.2																											
20785	7	2	2	2		3		1	1	1	1		3	3	2			2									2
27443	8	2	2	2		3	1	1	1					3	2			3									1
33806	7	6		2				1	1				1	2	2			3									
20799	7	2	3	2				2	1					3				3									2
FABRIC 3																											
343770	8	6	4	4				2			4			1				1									4
343772	7	6	2	6		4		3		1	4			2													
343773	8	6		4				2			4																
343787	8	6		4		1		2			2	2															
343780	7	6	4	4	1	1		3	1		2	1															1
343782	8	6		5				2	1		4					4		1									
343784	8	6	4	4		2		3		4	3							1									
343785	8	6	3	4				3			3							1									
343789	8	5		3				3	1	2	2																
343791	8	5		3				3	1		2																
343792	8	5		3		2	1	2	1		1																

Table 4.3. Minero-petrographic and micro-structural features of pottery samples analyzed under optical microscope.

INE FRACTION																												
Samples	CRYSTALS													MTM.R.	IGNEOUS R.			SEDIMENTARY R:					OTHER FEASTURES					
	Qz	Fsp	KF	Pl	Cal-Dol	Amp	Px	Ms	Bt	Srp	Op	Glt	Php	Qzt	vlc		plt	Ch	Dol	CMt	CSpr		Sph	CP	Grog	ARF	CalSc	
															ac.	int.	ac.											
343793	8	6		6				2	1		2																	
FABRIC 4																												
20959	6	2	2					1	1		3			3	2			2		6							4	
GRUPO 5																												
343781	7	4	2	2				1	1		1							1		6								
FABRIC 6																												
14630	7	4			3			1			1							3		3			2					
14634	7	4						2		1	1																4	
24615	8	5						1			1	1	1					1		1							1	
24869	7	2						1	1		2			3				2		1				2	5		4	
28982	8	5						1			1							1		1							2	
31276	7	2	2					2	1		1		1	2	1			1						2	6		4	
31906	6	2						3	1		1			1				1						4	5		2	
FABRIC 7																												
28780	6	4			6			1	1		2							3									3	
28781	6	4			6			1	1		2			2				3									2	
FABRIC 8																												
14715	6	6	4	5		2	1	4	3	1	2			1	1	2				2							2	
28794	7	4	4	4				4	1	1	2	1				1												
FABRIC 9																												
28806	8	3				1		4			2						1	2		4							2	
29015	8	4						4	1								2	1									5	
31490	8	2				1		4	1		2							1										
FABRIC 10																												
28740	7	6	2	2				1		1	1			5				1		2				2			4	
FABRIC 11																												
14655	3	6	2	2				2	2	4	3					4												
FABRIC 12																												
31546	6				5			5			6							1		1								
FABRIC 13																												
31479_INT.	6	3	2	2				3		3	4							2		4								
31479_EXT.	6	5	2	2		2		5	4		5					4		1		1								

Table 4.3. Minero-petrographic and micro-structural features of pottery samples analyzed under optical microscope.

4.4 Digital Image Analysis (DIA)

The Digital Image Analysis (DIA) was performed to gain precise information about quantity, grain-size distribution and shapes of inclusions, as well as on the ratio between matrix, inclusions and pores. It was performed on a selection of five samples (20794, 28772, 31290, 343771, 343777) characteristic of the first fabric group identified by the optical microscopy, of interest because of the presence of speleothems.

SEM-BSE images were acquired for this purpose (figures 4.12-16). For each sample nearly ten SEM-BSE images were taken at nearly 30x magnification, in order to obtain a well representation of each thin section. Before undertaking the DIA it was necessary to process all the images with graphical software as described in chapter 1.6. The files so elaborated had undergone the segmentation process: the extraction of the pottery features (voids, matrix, type of inclusions).

Since it was not possible to separate all the different kind of rocks and crystals, for maintained high accuracy, only the distinction between matrix, voids and inclusions (in general) was considered. Particle analysis was then performed. For each image the *area fraction,* the maximum *Feret's diameter (Feret)* and the *aspect ratio (AR)* were statistically treated in order to analyze the grain-size distribution of the inclusions present in the thin sections. For each sample the *Feret* results of the inclusions data-set were illustrated through histograms overlaid by the probability distribution functions that best matches with them (figures 4.12-16). As the finer inclusions are extremely greater in terms of number of particles than the coarser ones, they appear predominant also when are insignificant considering the total area occupied. For that reason it is difficult to see any real presence of one or more modes in the grain-size distribution. Therefore the inclusions were divided on the basis of the different grain-size distribution referred to the Wentworth grain-size chart and the total area fractions occupied by each class were calculated. Where more than one sample for fabric was available, their average data were

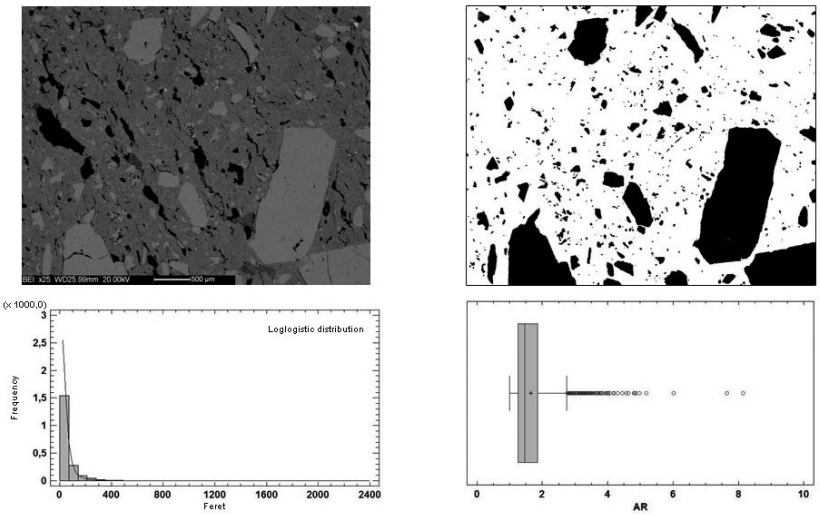

Figure 4. 12. a) SEM- BSE image of the sample 20794; b) segmented image of all the inclusions present. C) Frequency distribution diagram of the whole inclusions; d) AR values of the inclusions.

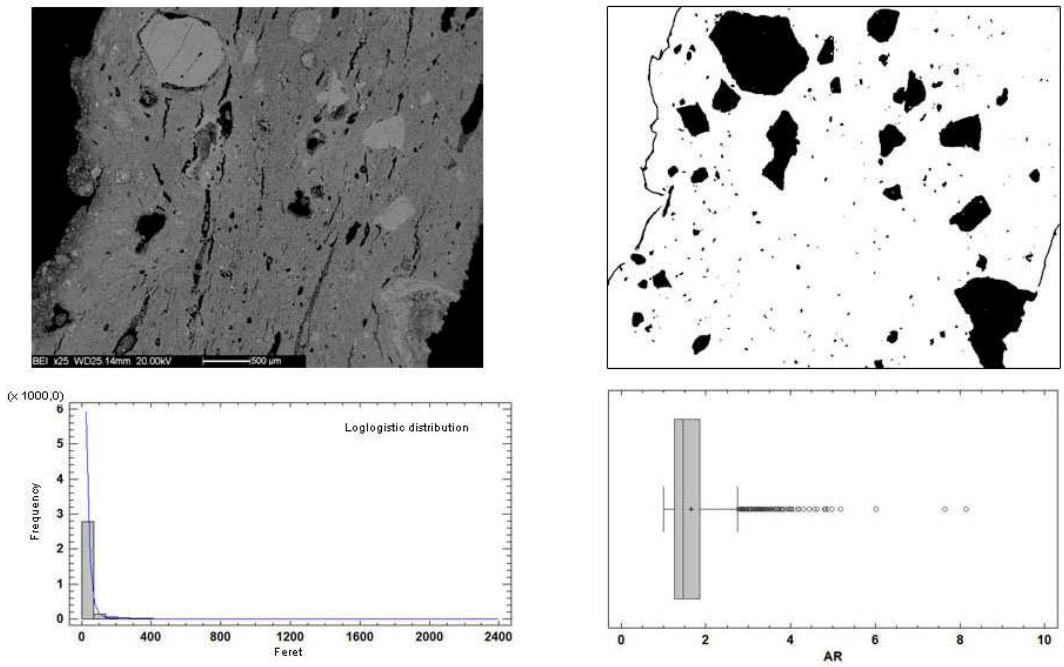

Figure 4. 13. a) SEM- BSE image of the sample 28772; b) segmented image of all the inclusions present. C) Frequency distribution diagram of the whole inclusions; d) AR values of the inclusions.

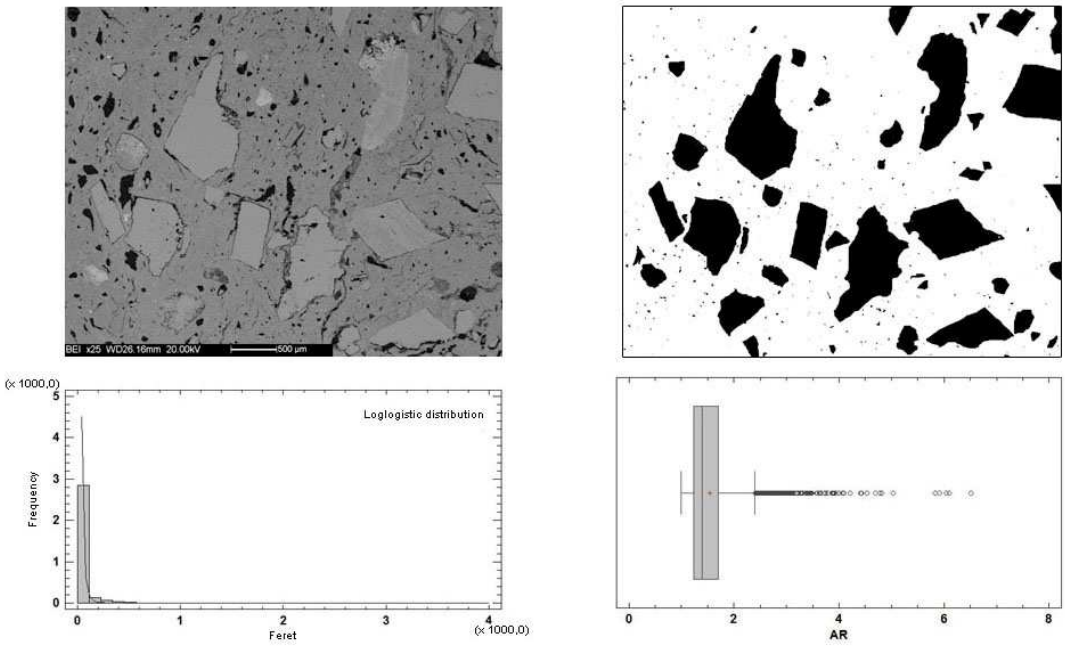

Figure 4. 14. a) SEM- BSE image of the sample 31290; b) segmented image of all the inclusions present. C) Frequency distribution diagram of the whole inclusions; d) AR values of the inclusions.

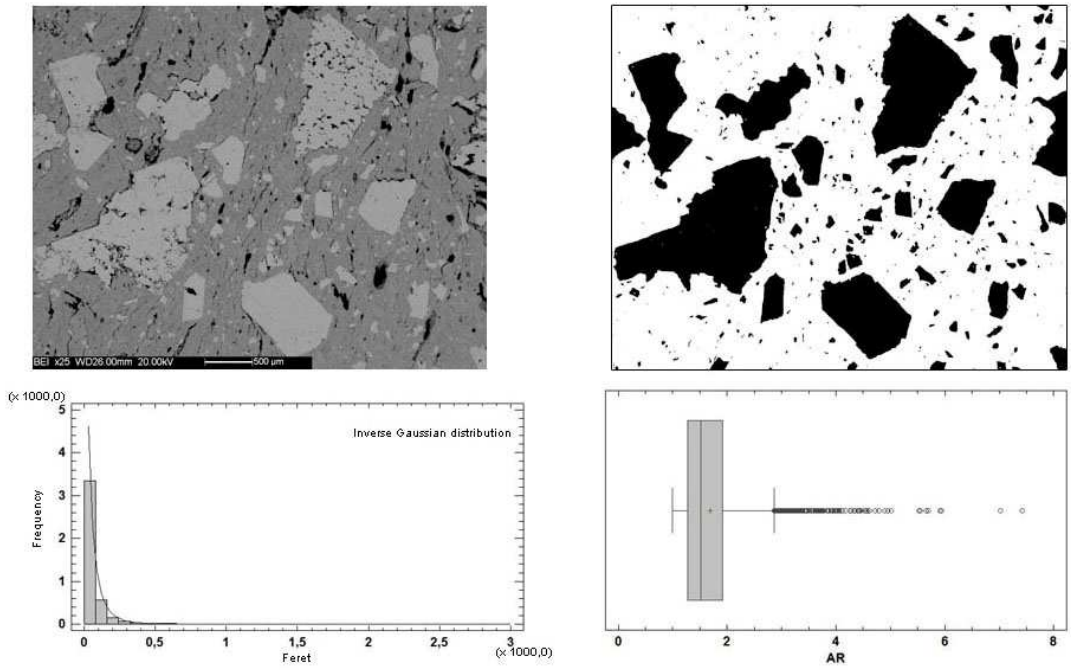

Figure 4. 15. a) SEM- BSE image of the sample 343771; b) segmented image of all the inclusions present. C) Frequency distribution diagram of the whole inclusions; d) AR values of the inclusions.

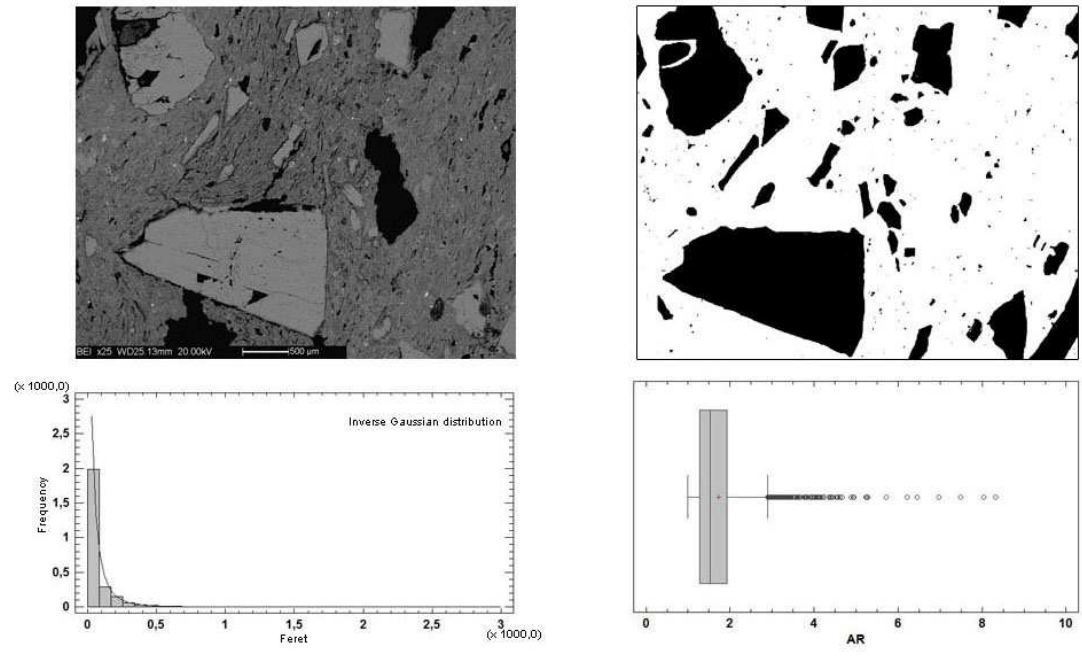

Figure 4. 16. a) SEM- BSE image of the sample 343777; b) segmented image of all the inclusions present. C) Frequency distribution diagram of the whole inclusions; d) AR values of the inclusions.

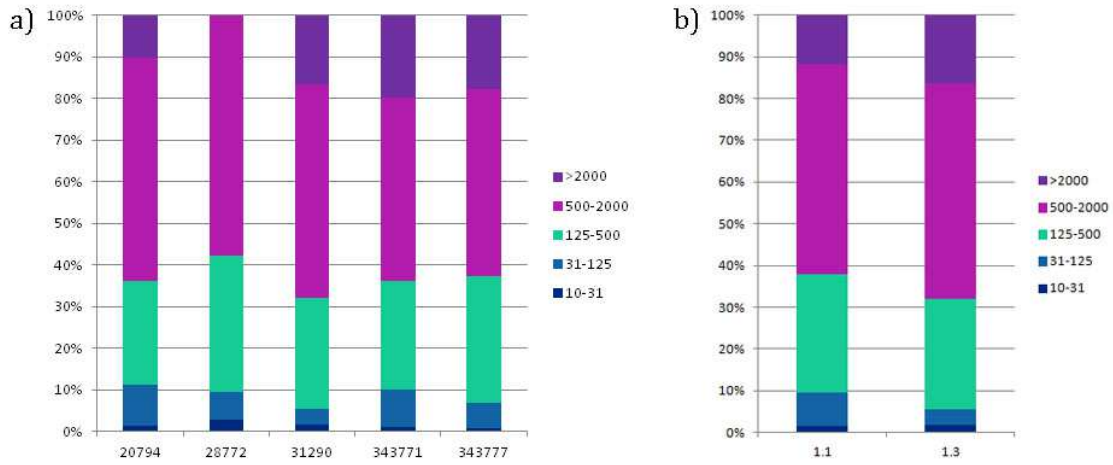

Figure 4. 17. a) area fraction occupied by each grain-size class of the inclusions for each sample; b) average area fraction occupied by each grain-size class of the inclusions for the fabrics 1.1 and 1.2.

considered. It was observed that clustering together two by two the Wentworth grain-size classes is clearer and still well comparable with the fabric description (figure 4.17).

According with Whitbread (1995) only the fragments greater than 10 μm were considered.

Box-plots displaying the Aspect Ratio (AR) values were obtained in order to give indication of the average shapes of the inclusions for each sample (figure 4.12-16). Since the inclusions were analyzed without discriminating the different rock types, this result must be considered with great caution. The AR was referred simultaneously to different rock fragments and minerals that usually have different aspects (angularity, elongation, size). Moreover, the finer fraction of the grains -much numerous than the coarser fragments- is mostly represented by small sub-angular equant quartz crystals (table 4.3). This aspect deeply affects the results displayed in the box-plots where the median and the range between the first and third quartiles have low values of AR, indicating a high sphericity, but there is always a great number of outliers.

Then, the m:v:i (matrix:voids:inclusions) ratio was estimated through the area fraction occupied by the matrix, voids and all the inclusions and displayed in a 100% stacked bar

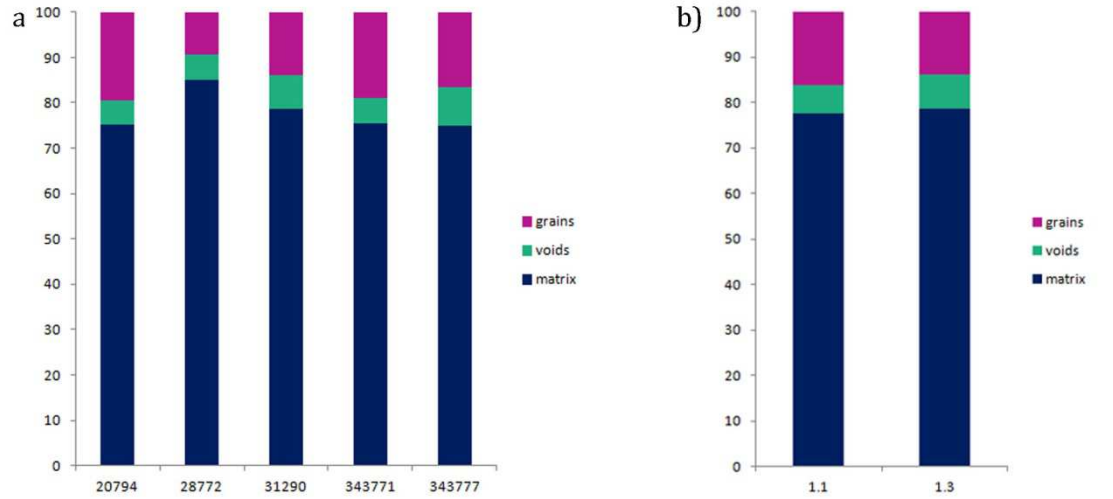

Figure 4. 18. a) Area fraction of each sample occupied by the matrix, voids and inclusions; b) average area fraction of each fabric (fabrics 1.1, 1.3) occupied by the matrix, voids and inclusions.

chart (figure 4.18). Comparing the results obtained from DIA with those gained by microscopy observation (figure 4.18; table 4.3), it appeared a good correspondence. For petrographic group 1.1 the average area of the different components of pottery (matrix:voids:inclusions) is 78:6:16. The grain-size distributions have average c:f ratio of 65:35 with maximum size of the fine fraction of 0,5 cm. For fabric 1.3, the area fraction of the different components (matrix:voids:inclusions) is 79:8:14, similarly to fabric 1.1. The grain-size distributions had average c:f ratio of 65:35 with maximum size of the fine fraction of 0,5 cm. None sample of fabric 1.2 were analyzed by digital image analysis.

4.5 Mineralogical composition

The mineralogical association of the samples was identified by X-ray powder diffraction (XRPD) analysis. The high compositional variability noticed during the optical microscopy observation was also confirmed by the XRPD data: considering the presence or absence and the relative abundance of some specific mineral phases, it was possible to distinguish several groups (tables 4.4-5).

The *first group* (A_{xrd}) is characterized by abundant quartz and calcite associated with scarce illite. Plagioclase and alkali-feldspars (like microcline) are occasionally present in small amounts. In few samples ($A2_{xrd}$, $A3_{xrd}$) there are also trace of high temperature minerals like gehlenite and hematite while clay minerals like chlorite and smectites are totally absent. In four specimens also occur traces of pyrite, in two of which it is associated with gypsum. The majority of the samples of this cluster are of the FRFL type.

The *second* group (B_{xrd}) is composed by only two samples characterized by predominant quartz, and subordinate plagioclase and alkali-feldspar (like microcline). Clay minerals (illite, smectites and chlorite) are totally absent and were replaced by the high temperature phases spinel and pyroxene. These are secondary phases that crystallize at temperature higher than 950° (Maggetti 1982, Veniale 1990).

GROUPS	Qz	Pl	Kfs		Cal	Ilt	Sme	Chl	Spl	Zeo	Px	**Gh**	Hem	Amp	Gp	pyr	Ant
		Ab	Mc	Ano/Snd										Tr			
$A1_{xrd}$	***/****	-/*	-/**		***/****	*/**										-/*	-/*
$A2_{xrd}$	****	-/*			***	*/**						*			-/*	-/*	
$A3_{xrd}$	****	-/*	-/*		***/****	*/**						- /*	*				
B_{xrd}	****	**/***	**/***						*								
$C1_{xrd}$	***/****	**/***		**/***	-/*	*/**					-/*			-/*			-/*
$C2_{xrd}$	***/****	**/***		**	-/**	**	-/*	-/*			-/*			-/*			
$D1_{xrd}$	****	**	*/**		-/**	*/**				-/*	-/*			-/*			
$D2_{xrd}$	****	**	***									*					
$D3_{xrd}$	****	**	**		-/*	*/**	-/*	-/**			-/*			-/*			
E_{xrd}	***	**		****		**							*				

Table 4. 4. Mineralogical associations. Qz: quartz; Pl: plagioclase; KF: alkali feldspar; Cal: calcite; Ilt: illite; Sme: smectites; Chl: chlorite; Spl: spinel; Zeo: zeolite; Px: pyroxene; Gh: ghelenite; Hem: hematite; Amp: amphibole; Gp: gypsum; Pyr: pyrite; Ant: Ti oxide atanasio.

SAMPLES	GROUPS	POTTERY TYPE	Qz	Pl	Kfs		Cal	Ilt	Sme	Chl	Spl	Zeo	Px	**Gh**	Hem	Amp	Gp	Pyr	Ant
				Ab	Mc	Ano/Snd										Tr			
625	A1	FRFL	****		*		***	*										*	
14636	A1	FRFL	****		**		****	**											*
14712	A1	FRFL	***		*		****	*											
14713	A1	FRFL	***		*		****	*											*
14714	A1	FRFL	****		*		***	**											
14716	A1	FRFL	****				****	*											*
14717	A1	FRFL	***				****	**											*
18464	A1	FRFL	***				****	**											
20783	A1	FRFL	****		*		***	*											
24552	A1	FRFL	****	*	*		****	*											
24648	A1	FRFL	****				***	**											
28755	A1	FRFL	****				****	*											
28770	A1	FRFL	***				****	*											
28772	A1	FRFL	****	*	**		***	*											
28780	A1	FRFL	****	*	*		***	*											
28781	A1	FRFL	***	*	*		****	*											
28798	A1	FRFL	****	*	*		***	*											
28801	A1	FRFL	****	*	*		***	*											
28827	A1	-	****	**	*		***	*											
31282	A1	FRFL	****		*		***	*											
31295	A1	FRFL	****	*			***	**											
31420	A1	-	****		*		***	*											
31492	A1	FRFL	****	*	*		***	*											
31493	A1	FRFL	****	*			***	**											
97081	A1	FRFL	****				***	*											
97151	A1	FRFL	****		*		***	*											
97364	A1	FRFL	****		*		***	*											
97442	A1	FRFL	****		*		***	*											
99894	A1	FRFL	****		*		***	*											
100691	A1	FRFL	****				****	*											
100975	A1	FRFL	****		*		****	*											
101134	A1	FRFL	****	*			***	*											
236738	A1	FRFL	****		*		***	*											
343769	A1	FRFL	****		*		***	*											
343774	A1	FRFL	****		*		****	**											
343776	A1	FRFL	****		*		***	*											
343777	A1	FRFL	****				***	*											*
343778	A1	FRFL	***		*		****	**											
343781	A1	-	****		*		***	**											
343786	A1	FRFL	****	*	*		***	**											
343787	A1	-	****		*		***	*											
343788	A1	FRFL	****				***	*											
418269	A1	FRFL	****	**			***	*											
418905	A1	FRFL	****		*		***	*										*	
20794	A1	FRFL	****				***	**											
637	A2	FRFL	****				***	*						*			*	*	
6247	A2	FRFL	****		*		***	*						*			*	*	
8614	A2	FRFL	***	*			****	*						*					
20959	A2	FRFL	****	**			***	*						*					
31275	A3	FRFL	****		*		***	**							*				
31290	A3	FRFL	****				***	**							*				
31421	A3	FRFL	****	*			***	*							*				
31544	A3	FRFL	****	*			****	**							*				
100568	A3	FRFL	****				****	*							*				
343775	A3	FRFL	****				***	*							*				
343783	A3	FRFL	***		*		****	**							*				
343790	A3	FRFL	***				****	**							*				
343794	A3	-	****				****	*						*	*				
418343	A3	FRFL	****				****	*							*				

Table 4. 5. a. XRPD results. Qz: quartz; Pl: plagioclase; KF: alkali feldspar; Cal: calcite; Ilt: illite; Sme: smectites; Chl: chlorite; Spl: spinel; Zeo: zeolite; Px: pyroxene; Gh: ghelenite; Hem: hematite; Amp: amphibole; Gp: gypsum; Pyr: pyrite; Ant: Ti oxide atanasio.

SAMPLES	GROUPS	POTTERY TYPE	Qz	Pl	Kfs		Cal	Ilt	Sme	Chl	Spl	Zeo	Px	**Gh**	Hem	Amp	Gp	Pyr	Ant
				Ab	Mc	Ano/Snd										Tr			
24869	B	-	****	**	***						*								
33806	B	-	****	***	**						*								
14715	C1	-	***	**		***		**					*						
343770	C1	-	****	**		**		**					*						
343771	C1	FRFL	****	**		**		**											*
343772	C1	-	****	**		**	*	**											
343773	C1	-	****	**		**		**											
343782	C1	-	****	***		*		*					*						
343785	C1	-	****	**		**		**					*						
343793	C1	-	****	**		**		*					*			*			
28794	C2	-	***	**		***		**		*			*			*			
343780	C2	-	****	***		**	**	**	*							*			
343784	C2	-	****	**		**		**	*				*						
343789	C2	-	***	**		**		**	*				*						
343791	C2	-	****	**		*		**	*				*			*			
343792	C2	-	****	**		**		**		*			*						
14630	D1	-	****	**	**		*	**											
14634	D1	-	****	**	**		*	**											
20785	D1	-	****	**	**		*	**					*						
24615	D1	FRFL	****	**	*		**	**											
27443	D1	-	****	**	**			*					*			*			
28740	D1	-	****	**	*		*	**											
28750	D1	-	****	**	**		**	**											
28806	D1	-	****	**	**		*	**											
28982	D1	FRFL	****	**	*		*	**											
29015	D1	-	****	**	**		*	*											
31276	D1	-	****	**	**			*											
31479	D1	-	****	**	**		**	*				*							
31906	D1	-	****	**	**			**											
33686	D1	-	****	**	**		*	*											
20799	D2	-	****	**	***									*					
20796	D3	-	****	**	**			*		*			*			*			
28378	D3	-	****	**	**			**	*				*						
31490	D3	-	****	**	**			**	*										
31546	D3	-	****	**	**		*	**		**									
33596	D3	-	****	**	**			*	*							*			
33749	D3	-	****	**	**		*	**	*							*			
100590	D3	FRFL	****	**	**			**	*				*						
343779	D3	FRFL	****	**	**		*	**		*									
14655	E	-	***	**		****		**							*				

Table 4. 6. b. XRPD results. Qz: quartz; Pl: plagioclase; KF: alkali feldspar; Cal: calcite; Ilt: illite; Sme: smectites; Chl: chlorite; Spl: spinel; Zeo: zeolite; Px: pyroxene; Gh: ghelenite; Hem: hematite; Amp: amphibole; Gp: gypsum; Pyr: pyrite; Ant: Ti oxide atanasio.

The *third assemblage* (C_{xrd}) is characterized by predominant quartz, and subordinate feldspar (both plagioclase and alkali feldspar like sanidine) and illite. Calcite, pyroxene amphibole -like tremolite- can be present in few amount. Few samples ($C2_{xrd}$) bear also clay minerals like smectites and chlorite. The *fourth cluster* (D_{xrd}) is similar to group C_{xrd}. It differs in the type of alkali-feldspar present: like sanidine or anorthoclase the first and like microcline that one. Few samples ($D2_{xrd}$) present also clay minerals like smectites and chlorite. Only in the sample 20799 there are the high temperature secondary phase ghelenite and the absence of calcite and mica. The last group (E_{xrd}) is composed only by sample 14655. It has predominant alkali-feldspar like anorthoclase/sanidine associated with less amount of quartz, plagioclase, illite and traces of hematite.

4.6 Chemical composition and statistical treatment of data

The chemical composition of eighty-five samples was determined by XRF. Of these, fifty were of FRFL type and the other thirty-five were of supposed local vessels, here considered for comparison. Thirty chemical elements were calculated: the major elements (SiO_2, TiO_2, Al_2O_3, Fe_2O_3, MnO, MgO, CaO, Na_2O, K_2O, P_2O_5) whose concentrations are expressed in wt% of their oxides, and trace elements (Sc, V, Cr, Co, Ni, Cu, Zn, Ga, Rb, Sr, Y, Zr, Nb, Ba, La, Ce, Nd, Pb, Th, and U), expressed in ppm (table 4.8).

In a first approach descriptive statistic analyses were performed on the variable concentrations calculated for the whole sample assemblage, as illustrated in chapter 1.5. The treatment of the geochemical data showed compositional heterogeneity, expressed by the high variance and the wide distribution intervals. Furthermore, generally variables had high coefficient of variations and the Anderson Darling normality test indicated that only seven chemical elements (Al_2O_3, Fe_2O_3, K_2O, V, Ga, Rb, Y) follow a normal distribution (table 4.7).. These situation is due to the different provenance of the samples, with reference to those of local origin, characterized by very different pastes with high percentage of a-plastics inclusions of several different rock types.

Variable	S	SD	V	CV	MIN	IQ	MED	IIIQ	MAX	p-value
SiO2	55,944	6,984	48,772	12,48	39,47	50,78	56,24	62,42	68,48	0,019
TiO2	0,9034	0,2492	0,0621	27,59	0,65	0,78	0,83	0,89	2	< 0,005
Al2O3	15,921	1,895	3,589	11,9	11,64	14,445	15,97	17,39	20,11	**0,248**
Fe2O3	5,81	1,231	1,516	21,19	2,74	4,91	5,94	6,68	8,64	**0,381**
MnO	0,10329	0,05862	0,00344	56,75	0,02	0,06	0,1	0,12	0,42	< 0,005
MgO	1,6325	0,6455	0,4166	39,54	0,56	1,125	1,47	2,095	3,49	< 0,005
CaO	14,89	10,1	102,05	67,87	1,58	3,21	17,51	22,2	38,48	< 0,005
Na2O	0,7027	0,669	0,4475	95,2	0,01	0,19	0,58	1,095	3,87	< 0,005
K2O	2,4876	0,6777	0,4593	27,24	1	1,995	2,42	2,885	4,07	**0,639**
P2O5	0,8329	0,7094	0,5033	85,17	0,14	0,385	0,62	1,065	5,6	< 0,005
V	143,32	30,32	919,53	21,16	59	119,5	141	162,5	210	**0,097**
Cr	168,6	61,36	3765,43	36,4	32	114,5	182	217	290	< 0,005
Co	19,953	5,548	30,783	27,81	5	17	19	22	39	< 0,005
Ni	103,24	43,83	1921,49	42,46	31	66,5	94	138	289	< 0,005
Cu	88,72	39,78	1582,3	44,84	30	65	80	98,5	290	< 0,005
Zn	134,65	37,6	1413,47	27,92	66	108	128	150,5	279	0,026
Ga	19,812	5,317	28,274	26,84	2	17	20	24	32	**0,208**
Rb	127,08	26,71	713,6	21,02	71	107	127	142	210	**0,502**
Sr	144,94	55,42	3071,41	38,24	71	108	133	161,5	408	< 0,005
Y	35,024	5,728	32,809	16,35	22	31	34	39	51	**0,474**
Zr	228,14	91	8280,74	39,89	127	177,5	200	232,5	639	< 0,005
Nb	18,95	12,89	166,07	67,99	10	12,5	14	16	67	< 0,005
Ba	552,7	233,5	54532,8	42,25	259	381,5	472	676	1207	< 0,005
La	39,82	11,32	128,17	28,43	16	32,5	38	45	72	< 0,005
Ce	72,45	23,23	539,61	32,06	38	56,5	68	85	138	< 0,005
Nd	21,76	10,26	105,3	47,15	5	12,5	23	29,5	42	0,006
Pb	28,106	7,955	63,286	28,3	13	23	26	32	52	< 0,005
Th	7,247	2,841	8,069	39,2	1	6	7	9	15	< 0,005
U	3,188	1,835	3,369	57,57	1	1	4	5	7	< 0,005

Table 4. 7. Average (A), standard deviation (SD), variance (V), coefficient of variation (CV), minimum (MIN), first quartile (IQ), median (MED), third quartile (IIIQ) and maximum (MAX) values and the p-value of the Anderson–Darling normality test for the studied potsherds.

samples	SiO_2	TiO_2	Al_2O_3	Fe_2O_3	MnO	MgO	CaO	Na_2O	K_2O	P_2O_5	V	Cr	Co	Ni	Cu	Zn	Ga	Rb	Sr	Y	Zr	Nb	Ba	La	Ce	Nd	Pb	Th	U		L.O.I.	FeO
6247	58,17	0,92	12,91	4,38	0,05	1,13	18,99	0,61	1,75	0,27	153	290	26	211	68	243	14	89	76	39	259	14	259	25	69	40	23	15	5		16,56	-
8614	41,04	0,76	15,89	5,41	0,21	1,41	32,23	0,14	2,3	0,25	199	182	21	148	59	163	19	151	116	40	133	12	286	33	61	41	23	13	1		19,39	-
14630	64,76	0,83	16,05	4,85	0,06	2,02	4,41	0,85	3,5	0,8	112	129	13	91	290	150	26	142	142	34	221	16	497	39	66	11	31	7	3		8,9	-
14636	50,07	0,8	13,27	4,51	0,12	1,06	26,86	0,25	1,75	0,65	148	211	19	143	193	91	10	85	144	33	208	13	354	36	71	22	24	7	4		21,69	1,28
14655	62,13	0,96	18,72	5,95	0,06	1,31	1,91	3,87	4,07	0,26	59	32	12	31	164	106	25	115	282	33	639	67	659	72	134	40	32	6	5		2,41	1,14
14712	42,91	0,84	15,44	5	0,12	1,81	30,24	0,09	1,97	0,69	182	212	18	140	80	118	20	114	144	33	213	16	331	32	75	31	19	9	1		21,56	1,94
14713	47,79	0,82	16,18	6,68	0,13	1,45	24,01	0,21	2,32	0,35	161	198	20	138	87	109	17	127	102	29	157	12	337	31	51	31	27	9	1		16,85	3,53
14714	53,68	0,77	11,86	4,09	0,06	1,15	25,57	0,16	2	0,8	124	224	18	111	205	83	8	96	121	29	188	13	325	32	49	29	18	10	1		21,54	0,99
14715	64,39	0,91	17,36	5,34	0,08	1,41	2,6	2,61	3,91	0,57	69	67	15	44	106	104	28	130	201	38	518	51	631	60	126	34	19	12	3		5,17	0,75
14716	51,46	0,69	14,25	4,31	0,05	0,91	23,73	0,12	2,07	0,89	141	199	17	104	145	107	21	103	133	34	149	12	395	33	47	12	20	9	3		19,14	1,35
14717	43,21	0,74	15,16	4,91	0,1	1,47	30,36	0,09	2,5	0,58	166	166	19	155	163	109	16	142	97	32	127	12	298	38	42	33	15	9	4		23,92	1,12
18464	39,47	0,79	13,41	4,46	0,17	0,74	38,48	0,06	1,69	0,37	123	189	20	167	87	150	14	104	85	34	162	13	312	19	50	34	21	13	1		27,75	-
20783	56,71	0,82	13,56	3,63	0,03	0,8	19,55	0,2	1,91	0,62	103	224	14	63	50	89	11	101	104	24	202	12	363	26	43	12	17	6	4		15,63	1,36
20785	63,85	0,86	17,43	6,68	0,14	2,34	2,6	1,17	3,55	0,56	147	127	25	85	72	138	22	175	134	36	196	15	532	30	84	24	36	7	1		2,64	4,62
20794	51,25	0,71	13,13	4,23	0,13	1,15	26,61	0,18	1,87	0,46	132	188	18	114	30	85	10	113	136	28	156	13	374	34	59	5	13	9	1		18,42	1,47
20796	65,53	0,85	17,16	6,77	0,1	1,65	2,3	1,16	2,97	1,13	116	103	14	67	105	149	20	148	148	42	221	15	842	53	82	16	40	6	1		9,31	2
20799	64,55	0,84	17,86	6,78	0,09	2,12	2,32	1,1	3,32	0,38	136	109	19	75	89	147	25	157	117	42	219	14	510	45	88	22	37	5	4		1,83	4,76
20959	54,86	0,93	15,88	6,57	0,1	1,08	17,05	0,14	1,29	1,73	208	284	28	154	86	141	20	86	108	45	267	17	348	35	86	29	27	7	4		11,96	2,44
24552	51,36	0,69	14,56	5,4	0,07	2,15	22,27	0,75	2,61	0,19	108	88	11	46	65	87	22	130	99	32	191	12	374	20	55	23	24	8	4		16,48	3,54
24615	57,74	0,83	17,05	6,57	0,06	2,94	10,46	0,86	2,96	0,42	174	212	24	127	174	123	17	141	161	32	177	12	470	37	68	10	25	8	3		8,62	3,92
24869	64,42	0,87	18,32	5,72	0,1	2,6	1,7	0,82	3,88	0,96	131	114	14	39	65	149	21	162	108	38	230	15	387	40	90	32	24	9	5		2,25	3,51
27443	64,23	0,87	18	7,06	0,12	2,41	1,98	1,08	3,57	0,31	152	122	22	85	69	138	18	179	122	36	194	15	516	39	72	27	31	7	5		1,53	6,11
28378	63,69	0,81	17,93	7,15	0,09	2,09	3,25	0,97	2,89	0,86	127	104	20	75	76	129	17	165	167	44	200	14	1207	54	93	5	37	5	1		13,24	2,41
28740	67,28	0,8	15,97	6,3	0,08	1,74	2,75	1,13	1,84	0,53	117	144	19	83	130	80	19	106	163	31	288	17	567	38	73	20	33	6	1		8,63	1,62
28750	57,23	0,75	14,73	6,53	0,29	2,92	12,62	0,73	2,79	0,6	120	124	35	75	107	113	14	128	129	30	187	13	521	16	65	14	31	4	1		14,25	0,82
28755	43,03	0,89	13,93	4,88	0,15	0,98	33,67	0,22	1,21	0,43	167	217	18	156	88	101	16	78	169	38	223	16	393	32	75	23	23	6	1		23,43	2,1
28772	57,71	0,77	15,34	5,95	0,13	2,42	14,55	0,74	2,51	0,24	122	134	19	83	64	96	20	131	118	34	188	12	444	39	71	32	29	8	1		12,12	3,43
28780	50,31	0,67	14,33	5,34	0,08	3,19	22,12	0,8	2,6	0,33	109	102	15	66	54	84	21	115	142	29	151	12	422	29	61	26	28	4	1		18,44	1,55
28781	49,48	0,65	13,99	4,91	0,06	2,76	23,33	0,58	2,4	0,31	109	99	12	52	38	86	17	119	146	31	150	11	387	36	48	27	15	10	1		19,06	2,2
28796	62,22	1,04	18,29	8,21	0,42	1,82	1,91	2,32	2,84	0,37	109	67	32	69	97	125	27	126	199	34	494	48	716	61	111	26	25	10	1		9,32	0,82
28798	52,62	0,76	14,65	5,94	0,17	1,65	20,57	0,58	2,26	0,44	117	110	25	59	69	91	17	127	143	31	178	13	524	41	65	19	29	5	4		17,41	1,88
28806	63,27	0,86	15,82	5,87	0,11	2,17	6,64	1,16	3,02	0,39	107	119	15	65	76	126	25	142	121	34	207	14	424	42	76	24	40	4	3		8,28	1,6
28827	54,64	0,82	15,13	5,88	0,1	2,07	16,69	0,66	2,39	0,33	117	118	16	66	56	101	18	131	123	31	188	13	437	42	68	21	29	6	6		14,03	3,17
28982	59,21	0,84	18,47	6,94	0,06	3,32	6,24	0,87	2,68	0,38	140	113	18	64	87	106	25	137	148	38	221	14	512	42	87	15	32	7	5		8,82	3,21
31275	54,69	0,88	17,42	6,79	0,03	1,6	13,4	0,45	3,1	0,62	160	197	17	110	140	125	27	148	147	22	145	11	435	36	56	21	33	1	1		12,68	1,8
31276	61,15	0,79	18,53	6,51	0,1	3,49	3,31	0,76	3,96	0,52	137	118	16	61	92	144	27	163	107	39	204	14	429	50	95	32	38	6	4		-88,22	4,83
31282	48,62	0,78	13,85	5,56	0,16	1,08	27,3	0,29	1,85	0,49	153	192	17	119	77	95	23	106	139	37	194	13	471	42	61	20	40	1	1		20,57	2,66
31290	54,93	0,87	17,23	6,75	0,03	1,57	12,64	0,45	3,07	0,61	162	198	16	110	104	120	23	146	149	24	151	16	443	36	48	10	24	8	3		12,12	1,77

Table 4. 8. Geochemical composition of samples obtained by XRF. The FeO values ware obtained by titration.

samples	SiO_2	TiO_2	Al_2O_3	Fe_2O_3	MnO	MgO	CaO	Na_2O	K_2O	P_2O_5	V	Cr	Co	Ni	Cu	Zn	Ga	Rb	Sr	Y	Zr	Nb	Ba	La	Ce	Nd	Pb	Th	U		L.O.I.	FeO
31295	51,7	0,85	15,33	4,59	0,14	1,64	21,23	0,41	2,21	0,35	192	243	27	153	80	121	21	139	119	46	194	13	316	38	77	30	45	1	6		15,87	2,24
31420	57,29	0,8	13,53	5,07	0,05	1,23	18,39	0,12	2,31	0,35	141	241	15	115	82	106	16	99	91	30	227	15	359	36	55	15	29	7	5		15,87	1,19
31421	50,29	0,84	17,46	7,45	0,13	1,72	19,09	0,22	1,52	0,38	171	226	23	129	89	116	17	96	111	45	231	15	387	54	72	42	43	7	4		15,66	2,97
31490	68,48	0,68	17,33	5,6	0,02	1,04	1,58	1,16	2,51	0,14	110	124	5	41	93	66	25	129	71	30	183	13	319	28	58	20	43	6	7		12,38	0,94
31492	55,83	0,84	15,17	6,52	0,19	1,18	17,38	0,21	1,86	0,48	166	227	23	136	72	118	24	119	124	41	215	15	402	39	72	30	52	1	1		12,49	3,91
31544	46,31	0,81	19,09	7,64	0,09	1	21,4	0,2	1,65	1,27	193	217	26	159	123	151	17	117	166	51	221	15	709	60	98	32	39	5	5		23,71	0,92
31546	59,47	0,76	19,89	6,64	0,12	2,1	4,08	1,03	4,01	0,84	136	106	20	59	135	141	32	210	133	39	185	14	737	51	86	16	52	1	1		9,24	2,11
33596	63,41	0,85	16,92	6,75	0,11	2,4	3,17	1,1	3,4	0,94	132	114	20	93	92	143	23	191	157	32	174	14	1049	33	55	5	36	7	4		8,55	1,23
33686	64,01	0,89	17,52	6,26	0,08	2,11	2,64	0,87	2,79	0,84	142	123	19	80	76	146	24	188	144	36	183	14	941	37	58	5	35	5	1		10,61	1,98
33749	63,09	0,78	16,81	6,91	0,11	1,82	4,84	0,91	2,65	1,24	120	97	17	89	103	145	25	156	174	39	185	14	1185	43	70	5	38	4	4		10,14	-
33806	63,7	0,86	16,87	6,53	0,12	2,3	2,82	1,09	3,26	0,29	140	115	19	74	65	122	22	169	130	36	203	15	524	43	62	28	26	8	4		1,41	4,5
97081	51,47	0,8	15,26	4,98	0,1	1,01	23,4	0,14	1,98	0,47	163	275	17	124	51	117	17	120	97	33	254	14	658	33	62	12	23	6	6		16,74	3
97151	51,62	0,91	16,4	4,93	0,11	1,12	19,91	0,19	1,51	0,59	189	241	24	143	65	127	21	104	103	39	229	16	442	46	73	28	29	8	5		15,04	3,12
97442	55,87	0,84	14,37	4,63	0,08	0,91	20,03	0,17	1,38	0,72	155	244	22	126	57	118	18	94	105	38	241	14	770	34	57	5	23	7	6		15,92	2,13
100568	48,66	0,88	18,05	6,01	0,13	1,44	20,77	0,16	2,37	0,63	193	213	23	155	70	127	18	147	118	31	163	13	379	40	51	29	22	8	1		14,89	2,59
100590	54,28	0,87	15,77	5,59	0,11	1,18	19,56	0,15	2,16	0,37	159	230	21	150	64	112	13	125	408	31	197	13	620	28	64	13	23	5	1		14,96	2,27
100691	43,37	0,88	16,23	5,37	0,17	0,74	28,9	0,08	1	2,24	195	220	22	150	49	118	20	71	183	40	219	15	872	43	74	5	30	5	4		24,27	1,99
100975	49,93	0,78	14,77	4,73	0,09	1,14	24,95	0,14	2,04	0,34	152	199	21	129	45	103	16	123	105	31	173	12	311	25	40	26	24	5	5		16,86	2,87
101134	54,02	0,78	14,57	5,54	0,08	1,25	20,6	0,34	1,52	1,03	127	158	14	90	89	161	19	103	134	32	223	13	818	41	74	5	20	8	6		17,17	1,63
236738	47,66	0,9	14,47	7,72	0,1	0,56	19,94	0,01	1,34	5,6	145	263	21	160	139	201	12	71	162	40	225	13	767	32	47	5	39	5	6		22,5	0,91
343769	56,48	0,76	11,64	3,12	0,03	0,82	24,48	0,17	1,99	0,42	105	207	14	77	41	80	17	102	76	26	210	13	279	21	56	17	23	8	4		17,48	2,21
343770	60,32	1,68	18,13	8,64	0,09	2,13	2,96	1,58	2,84	0,92	141	111	19	59	77	178	25	105	234	36	353	45	605	50	120	24	26	9	5		8,1	3,46
343771	53,76	0,73	14,43	4,34	0,04	0,95	21,66	0,11	2,35	0,97	164	208	18	125	73	123	24	121	77	30	144	12	320	42	55	36	24	7	1		18,85	0,95
343772	63,36	1,16	16,63	5,85	0,11	1,46	5,28	1,34	2,62	2,11	113	116	17	59	104	180	21	129	234	38	325	43	1199	45	81	5	24	11	5		8,94	3,3
343773	64,73	1,47	17,71	6,01	0,13	1,43	2,65	1,66	2,67	1,86	115	89	16	50	83	206	29	138	277	44	414	44	948	65	114	26	31	9	4		8,11	2,68
343775	51,68	0,83	14,75	6,67	0,11	1,14	18,7	0,2	2,42	1,35	210	249	26	146	106	163	18	130	119	45	197	14	367	34	68	31	37	6	1		16,71	2,7
343776	56,24	0,83	12,36	3,55	0,05	0,92	21,92	0,19	2,22	0,93	115	192	17	92	82	142	2	107	98	26	191	12	453	23	57	20	21	7	4		17,1	1,64
343777	60,17	0,79	12,98	3,79	0,08	1,04	16,75	0,19	2,33	1,3	119	192	22	99	73	155	14	110	114	27	200	11	434	36	52	17	22	6	3		14,24	1,54
343778	49,38	0,81	15,23	3,76	0,11	0,96	25,84	0,19	2,31	0,85	174	215	18	127	75	142	18	131	112	40	184	14	453	44	57	22	23	8	1		20,3	1,12
343779	58,54	0,78	13,18	3,79	0,05	0,94	19,47	0,28	2	0,66	157	251	17	98	58	113	14	114	104	33	234	13	299	38	62	21	29	6	4		15,48	2,04
343780	58,34	1,48	17,09	6,59	0,09	1,83	6,52	1,39	2,54	1,39	152	127	35	75	74	172	29	135	253	40	330	40	774	61	113	29	29	5	4		10,32	2,27
343781	66,2	0,77	16,88	5,94	0,04	2,13	3,48	1	2,88	0,97	135	120	17	71	81	168	24	156	119	31	164	16	452	31	73	26	28	9	1		9,58	2,41
343783	47,24	0,92	17,26	6,63	0,2	2,02	20,52	0,19	2,72	1,12	186	196	27	147	82	183	18	157	134	41	181	15	540	49	58	21	28	7	4		16,42	2,34
343784	61,38	1,45	17,88	6,84	0,08	1,98	2,44	1,86	2,97	1,12	147	107	25	61	71	147	28	134	242	42	383	49	595	71	138	41	22	11	5		8,13	2,18
343785	60,21	2	18,61	7,79	0,07	1,88	2,66	1,42	2,75	1,59	149	124	22	77	80	207	22	119	226	31	387	44	656	47	113	31	32	4	6		8,93	2,79
343786	51,73	0,76	13,58	5,97	0,11	2,17	20,71	0,69	2,38	1,68	132	198	21	124	115	166	20	114	138	34	152	12	708	32	60	5	21	8	1		18,45	2,04
343787	63,62	1,18	16,5	6,35	0,06	1,97	4,33	1,25	2,97	1,36	117	116	16	69	91	170	25	129	202	37	309	39	982	37	102	10	20	11	5		8,7	2,33
343788	59,69	0,95	15,34	2,74	0,04	0,85	16,8	0,26	2,05	0,88	151	254	22	94	62	142	13	91	108	35	235	16	384	51	65	24	23	7	1		15,45	1,75

Table 4. 8. Geochemical composition of samples obtained by XRF. The FeO values ware obtained by titration.

samples	SiO_2	TiO_2	Al_2O_3	Fe_2O_3	MnO	MgO	CaO	Na_2O	K_2O	P_2O_5	V	Cr	Co	Ni	Cu	Zn	Ga	Rb	Sr	Y	Zr	Nb	Ba	La	Ce	Nd	Pb	Th	U		L.O.I.	FeO
343789	61,03	1,35	20,11	6,42	0,19	1,37	2,6	1,89	3,23	1,91	104	59	17	56	97	193	27	115	275	45	433	57	1145	65	135	11	24	9	5		9,41	2,17
343790	43,07	0,71	16,5	7,3	0,06	1,14	27,88	0,2	2,57	0,61	193	182	22	139	88	170	17	147	122	23	160	10	501	38	57	12	24	7	1		20,75	2,28
343791	63,82	1,34	16,87	7,2	0,1	1,75	2,31	1,55	2,81	1,48	120	103	17	56	67	146	18	129	192	34	358	46	641	39	91	24	25	10	1		7,7	2,3
343792	60,95	1,46	17,15	8,2	0,19	2,49	2,83	1,15	3,38	1,37	138	154	39	113	100	279	27	146	159	37	274	34	700	46	92	32	32	6	3		9,96	-
343793	62,62	1,73	18,38	7,29	0,07	1,86	2,4	1,66	2,75	1,1	134	110	20	51	83	170	25	120	229	36	390	47	693	53	118	28	25	8	4		4,52	4,53
343794	50,21	0,69	14,34	5,29	0,05	1,18	23,86	0,18	2,18	0,41	187	241	20	127	60	128	16	137	111	34	156	10	472	34	38	29	17	7	4		16,44	3,62
418269	56,08	0,83	14,4	5,49	0,12	1,94	17,51	0,8	1,99	0,48	147	223	18	150	51	128	18	113	95	35	160	11	574	31	53	23	24	13	4		14,27	-
418343	48,81	0,78	14,46	5,45	0,1	1,34	25,91	0,19	2,34	0,52	149	200	24	138	46	134	15	137	108	28	149	11	516	32	46	31	29	13	5		17,94	-
418905	51,42	0,87	16,05	4,55	0,07	1,2	20,87	0,21	2,55	1,64	190	285	34	289	75	200	20	107	137	39	198	11	991	41	58	5	23	13	4		18,43	-

Table 4. 8. Geochemical composition of samples obtained by XRF. The FeO values ware obtained by titration.

samples	SiO2	TiO2	Al2O3	Fe2O3	MnO	MgO	CaO	Na2O	K2O	V	Cr	Co	Ni	Cu	Zn	Ga	Rb	Sr	Y	Zr	Nb	Ba	La	Ce	Nd	Pb	Th	U
6247	1,76	-0,04	1,11	0,64	-1,3	0,05	1,28	-0,21	0,24	2,18	2,46	1,41	2,32	1,83	2,39	1,15	1,95	1,88	1,59	2,41	1,15	2,41	1,4	1,84	1,6	1,36	1,18	0,7
8614	1,61	-0,12	1,2	0,73	-0,68	0,15	1,51	-0,85	0,36	2,3	2,26	1,32	2,17	1,77	2,21	1,28	2,18	2,06	1,6	2,12	1,08	2,46	1,52	1,79	1,61	1,36	1,11	0
14630	1,81	-0,08	1,21	0,69	-1,22	0,31	0,64	-0,07	0,54	2,05	2,11	1,1	1,96	2,46	2,18	1,42	2,15	2,15	1,53	2,34	1,2	2,7	1,59	1,82	1,04	1,49	0,83	0,49
14636	1,7	-0,1	1,12	0,65	-0,92	0,03	1,43	-0,6	0,24	2,17	2,32	1,28	2,16	2,28	1,96	0,98	1,93	2,16	1,52	2,32	1,13	2,55	1,56	1,85	1,34	1,39	0,82	0,62
14655	1,79	-0,02	1,27	0,77	-1,22	0,12	0,28	0,59	0,61	1,77	1,5	1,06	1,49	2,21	2,02	1,4	2,06	2,45	1,51	2,81	1,83	2,82	1,86	2,13	1,6	1,51	0,8	0,7
14712	1,63	-0,08	1,19	0,7	-0,92	0,26	1,48	-1,05	0,29	2,26	2,33	1,26	2,15	1,9	2,07	1,3	2,06	2,16	1,52	2,33	1,21	2,52	1,5	1,88	1,49	1,28	0,94	0
14713	1,68	-0,09	1,21	0,82	-0,89	0,16	1,38	-0,68	0,37	2,21	2,3	1,3	2,14	1,94	2,04	1,24	2,1	2,01	1,46	2,19	1,07	2,53	1,49	1,71	1,49	1,44	0,96	0
14714	1,73	-0,11	1,07	0,61	-1,22	0,06	1,41	-0,8	0,3	2,09	2,35	1,26	2,04	2,31	1,92	0,89	1,98	2,08	1,47	2,27	1,12	2,51	1,5	1,69	1,46	1,26	1,02	0
14715	1,81	-0,04	1,24	0,73	-1,1	0,15	0,41	0,42	0,59	1,84	1,82	1,17	1,64	2,03	2,02	1,45	2,11	2,3	1,58	2,71	1,71	2,8	1,78	2,1	1,53	1,27	1,1	0,5
14716	1,71	-0,16	1,15	0,63	-1,3	-0,04	1,38	-0,92	0,32	2,15	2,3	1,24	2,02	2,16	2,03	1,32	2,01	2,12	1,53	2,17	1,08	2,6	1,52	1,67	1,09	1,3	0,93	0,53
14717	1,64	-0,13	1,18	0,69	-1	0,17	1,48	-1,05	0,4	2,22	2,22	1,27	2,19	2,21	2,04	1,21	2,15	1,99	1,5	2,1	1,09	2,47	1,58	1,63	1,52	1,16	0,94	0,61
18464	1,6	-0,1	1,13	0,65	-0,77	-0,13	1,59	-1,22	0,23	2,09	2,28	1,3	2,22	1,94	2,18	1,15	2,02	1,93	1,53	2,21	1,11	2,49	1,28	1,7	1,53	1,32	1,11	0
20783	1,75	-0,09	1,13	0,56	-1,52	-0,1	1,29	-0,7	0,28	2,01	2,35	1,14	1,8	1,7	1,95	1,04	2	2,02	1,38	2,3	1,09	2,56	1,41	1,63	1,09	1,24	0,8	0,61
20785	1,81	-0,07	1,24	0,82	-0,85	0,37	0,41	0,07	0,55	2,17	2,1	1,39	1,93	1,86	2,14	1,35	2,24	2,13	1,55	2,29	1,18	2,73	1,48	1,92	1,38	1,55	0,86	0
20794	1,71	-0,15	1,12	0,63	-0,89	0,06	1,43	-0,74	0,27	2,12	2,27	1,25	2,06	1,48	1,93	1,01	2,05	2,13	1,45	2,19	1,12	2,57	1,53	1,77	0,7	1,13	0,97	0
20796	1,82	-0,07	1,23	0,83	-1	0,22	0,36	0,06	0,47	2,06	2,01	1,15	1,83	2,02	2,17	1,31	2,17	2,17	1,62	2,34	1,17	2,93	1,72	1,91	1,21	1,6	0,8	0
20799	1,81	-0,08	1,25	0,83	-1,05	0,33	0,37	0,04	0,52	2,13	2,04	1,27	1,88	1,95	2,17	1,39	2,2	2,07	1,62	2,34	1,16	2,71	1,65	1,94	1,34	1,57	0,7	0,61
20959	1,74	-0,03	1,2	0,82	-1	0,03	1,23	-0,85	0,11	2,32	2,45	1,45	2,19	1,94	2,15	1,31	1,93	2,03	1,65	2,43	1,23	2,54	1,54	1,93	1,46	1,44	0,86	0,57
24552	1,71	-0,16	1,16	0,73	-1,15	0,33	1,35	-0,12	0,42	2,03	1,94	1,02	1,67	1,81	1,94	1,35	2,11	1,99	1,5	2,28	1,07	2,57	1,31	1,74	1,36	1,37	0,91	0,65
24615	1,76	-0,08	1,23	0,82	-1,22	0,47	1,02	-0,07	0,47	2,24	2,33	1,38	2,1	2,24	2,09	1,24	2,15	2,21	1,51	2,25	1,09	2,67	1,57	1,83	1,01	1,39	0,89	0,54
24869	1,81	-0,06	1,26	0,76	-1	0,41	0,23	-0,09	0,59	2,12	2,06	1,16	1,59	1,82	2,17	1,32	2,21	2,03	1,58	2,36	1,16	2,59	1,6	1,96	1,51	1,38	0,96	0,71
27443	1,81	-0,06	1,26	0,85	-0,92	0,38	0,3	0,03	0,55	2,18	2,09	1,33	1,93	1,84	2,14	1,26	2,25	2,09	1,56	2,29	1,17	2,71	1,59	1,86	1,43	1,49	0,86	0,68
28378	1,8	-0,09	1,25	0,85	-1,05	0,32	0,51	-0,01	0,46	2,1	2,02	1,29	1,88	1,88	2,11	1,23	2,22	2,22	1,64	2,3	1,16	3,08	1,73	1,97	0,7	1,57	0,69	0
28740	1,83	-0,1	1,2	0,8	-1,1	0,24	0,44	0,05	0,26	2,07	2,16	1,29	1,92	2,11	1,9	1,29	2,03	2,21	1,5	2,46	1,22	2,75	1,58	1,86	1,29	1,52	0,8	0
28750	1,76	-0,12	1,17	0,81	-0,54	0,47	1,1	-0,14	0,45	2,08	2,09	1,54	1,88	2,03	2,05	1,15	2,11	2,11	1,48	2,27	1,13	2,72	1,21	1,81	1,15	1,49	0,59	0
28755	1,63	-0,05	1,14	0,69	-0,82	-0,01	1,53	-0,66	0,08	2,22	2,34	1,26	2,19	1,95	2	1,21	1,89	2,23	1,58	2,35	1,19	2,59	1,5	1,88	1,37	1,36	0,78	0
28772	1,76	-0,11	1,19	0,77	-0,89	0,38	1,16	-0,13	0,4	2,09	2,13	1,29	1,92	1,8	1,98	1,29	2,12	2,07	1,53	2,27	1,08	2,65	1,59	1,85	1,51	1,47	0,92	0
28780	1,7	-0,17	1,16	0,73	-1,1	0,5	1,34	-0,1	0,41	2,04	2,01	1,17	1,82	1,73	1,92	1,33	2,06	2,15	1,47	2,18	1,07	2,63	1,46	1,79	1,42	1,44	0,63	0
28781	1,69	-0,19	1,15	0,69	-1,22	0,44	1,37	-0,24	0,38	2,04	2	1,08	1,71	1,58	1,93	1,23	2,08	2,16	1,49	2,18	1,04	2,59	1,56	1,68	1,43	1,17	0,98	0
28796	1,79	0,02	1,26	0,91	-0,38	0,26	0,28	0,37	0,45	2,04	1,82	1,5	1,84	1,99	2,1	1,43	2,1	2,3	1,53	2,69	1,68	2,85	1,79	2,04	1,42	1,4	1	0
28798	1,72	-0,12	1,17	0,77	-0,77	0,22	1,31	-0,24	0,35	2,07	2,04	1,39	1,77	1,84	1,96	1,24	2,1	2,16	1,49	2,25	1,11	2,72	1,62	1,81	1,27	1,46	0,67	0,56
28806	1,8	-0,07	1,2	0,77	-0,96	0,34	0,82	0,06	0,48	2,03	2,07	1,17	1,81	1,88	2,1	1,4	2,15	2,08	1,54	2,32	1,14	2,63	1,63	1,88	1,37	1,6	0,64	0,51
28827	1,74	-0,09	1,18	0,77	-1	0,32	1,22	-0,18	0,38	2,07	2,07	1,2	1,82	1,74	2	1,25	2,12	2,09	1,49	2,27	1,11	2,64	1,62	1,83	1,33	1,46	0,74	0,75
28982	1,77	-0,08	1,27	0,84	-1,22	0,52	0,8	-0,06	0,43	2,14	2,05	1,26	1,81	1,94	2,03	1,39	2,14	2,17	1,58	2,34	1,14	2,71	1,63	1,94	1,19	1,51	0,86	0,74
31275	1,74	-0,06	1,24	0,83	-1,52	0,2	1,13	-0,35	0,49	2,2	2,29	1,23	2,04	2,15	2,1	1,43	2,17	2,17	1,35	2,16	1,06	2,64	1,55	1,75	1,33	1,52	0	0
31276	1,79	-0,1	1,27	0,81	-1	0,54	0,52	-0,12	0,6	2,14	2,07	1,21	1,78	1,97	2,16	1,43	2,21	2,03	1,59	2,31	1,13	2,63	1,7	1,98	1,5	1,58	0,74	0,61
31282	1,69	-0,11	1,14	0,75	-0,8	0,03	1,44	-0,54	0,27	2,18	2,28	1,23	2,08	1,88	1,98	1,36	2,03	2,14	1,57	2,29	1,11	2,67	1,62	1,79	1,31	1,6	0	0
31290	1,74	-0,06	1,24	0,83	-1,52	0,2	1,1	-0,35	0,49	2,21	2,3	1,21	2,04	2,02	2,08	1,36	2,17	2,17	1,39	2,18	1,19	2,65	1,56	1,69	1,01	1,38	0,9	0,48

Table 4.9. Matrix used for multivariate statistical analysis: Log10 of the geochemical composition of samples obtained by XRF.

samples	SiO2	TiO2	Al2O3	Fe2O3	MnO	MgO	CaO	Na2O	K2O	V	Cr	Co	Ni	Cu	Zn	Ga	Rb	Sr	Y	Zr	Nb	Ba	La	Ce	Nd	Pb	Th	U
31295	1,71	-0,07	1,19	0,66	-0,85	0,21	1,33	-0,39	0,34	2,28	2,39	1,43	2,18	1,9	2,08	1,32	2,14	2,08	1,66	2,29	1,12	2,5	1,59	1,89	1,47	1,66	0	0,79
31420	1,76	-0,1	1,13	0,71	-1,3	0,09	1,26	-0,92	0,36	2,15	2,38	1,18	2,06	1,91	2,03	1,2	2	1,96	1,48	2,36	1,19	2,56	1,56	1,74	1,18	1,47	0,83	0,66
31421	1,7	-0,08	1,24	0,87	-0,89	0,24	1,28	-0,66	0,18	2,23	2,35	1,35	2,11	1,95	2,07	1,23	1,98	2,05	1,66	2,36	1,18	2,59	1,73	1,86	1,62	1,63	0,83	0,64
31490	1,84	-0,17	1,24	0,75	-1,7	0,02	0,2	0,06	0,4	2,04	2,09	0,74	1,62	1,97	1,82	1,39	2,11	1,85	1,48	2,26	1,1	2,5	1,44	1,77	1,3	1,64	0,77	0,82
31492	1,75	-0,08	1,18	0,81	-0,72	0,07	1,24	-0,68	0,27	2,22	2,36	1,37	2,13	1,85	2,07	1,39	2,08	2,09	1,61	2,33	1,16	2,6	1,59	1,86	1,48	1,71	0	0
31544	1,67	-0,09	1,28	0,88	-1,05	0	1,33	-0,7	0,22	2,29	2,34	1,41	2,2	2,09	2,18	1,22	2,07	2,22	1,71	2,34	1,18	2,85	1,78	1,99	1,51	1,59	0,73	0,69
31546	1,77	-0,12	1,3	0,82	-0,92	0,32	0,61	0,01	0,6	2,13	2,03	1,29	1,77	2,13	2,15	1,51	2,32	2,12	1,59	2,27	1,15	2,87	1,71	1,94	1,21	1,71	0	0
33596	1,8	-0,07	1,23	0,83	-0,96	0,38	0,5	0,04	0,53	2,12	2,06	1,3	1,97	1,96	2,16	1,37	2,28	2,19	1,5	2,24	1,15	3,02	1,52	1,74	0,7	1,56	0,84	0,63
33686	1,81	-0,05	1,24	0,8	-1,1	0,32	0,42	-0,06	0,45	2,15	2,09	1,29	1,9	1,88	2,16	1,38	2,27	2,16	1,55	2,26	1,13	2,97	1,57	1,77	0,7	1,54	0,65	0
33749	1,8	-0,11	1,23	0,84	-0,96	0,26	0,68	-0,04	0,42	2,08	1,99	1,22	1,95	2,01	2,16	1,4	2,19	2,24	1,59	2,27	1,16	3,07	1,63	1,84	0,7	1,57	0,59	0,63
33806	1,8	-0,07	1,23	0,81	-0,92	0,36	0,45	0,04	0,51	2,14	2,06	1,29	1,87	1,81	2,09	1,35	2,23	2,11	1,55	2,31	1,17	2,72	1,63	1,79	1,45	1,42	0,88	0,59
97081	1,71	-0,1	1,18	0,7	-1	0	1,37	-0,85	0,3	2,21	2,44	1,24	2,09	1,71	2,07	1,23	2,08	1,99	1,52	2,4	1,13	2,82	1,52	1,79	1,09	1,36	0,79	0,77
97151	1,71	-0,04	1,21	0,69	-0,96	0,05	1,3	-0,72	0,18	2,28	2,38	1,37	2,15	1,81	2,1	1,33	2,02	2,01	1,59	2,36	1,19	2,65	1,66	1,86	1,45	1,46	0,89	0,71
97442	1,75	-0,08	1,16	0,67	-1,1	-0,04	1,3	-0,77	0,14	2,19	2,39	1,35	2,1	1,76	2,07	1,25	1,97	2,02	1,58	2,38	1,13	2,89	1,53	1,75	0,7	1,36	0,85	0,76
100568	1,69	-0,06	1,26	0,78	-0,89	0,16	1,32	-0,8	0,37	2,28	2,33	1,36	2,19	1,85	2,1	1,24	2,17	2,07	1,5	2,21	1,11	2,58	1,6	1,71	1,46	1,34	0,88	0
100590	1,73	-0,06	1,2	0,75	-0,96	0,07	1,29	-0,82	0,33	2,2	2,36	1,31	2,18	1,81	2,05	1,12	2,1	2,61	1,5	2,29	1,12	2,79	1,45	1,81	1,12	1,36	0,66	0
100691	1,64	-0,06	1,21	0,73	-0,77	-0,13	1,46	-1,1	0	2,29	2,34	1,34	2,18	1,69	2,07	1,29	1,85	2,26	1,6	2,34	1,19	2,94	1,63	1,87	0,7	1,48	0,72	0,59
100975	1,7	-0,11	1,17	0,67	-1,05	0,06	1,4	-0,85	0,31	2,18	2,3	1,33	2,11	1,65	2,01	1,2	2,09	2,02	1,49	2,24	1,08	2,49	1,4	1,6	1,41	1,39	0,71	0,66
101134	1,73	-0,11	1,16	0,74	-1,1	0,1	1,31	-0,47	0,18	2,1	2,2	1,14	1,96	1,95	2,21	1,29	2,01	2,13	1,5	2,35	1,12	2,91	1,62	1,87	0,7	1,3	0,88	0,76
236738	1,68	-0,05	1,16	0,89	-1	-0,25	1,3	-2	0,13	2,16	2,42	1,32	2,2	2,14	2,3	1,08	1,85	2,21	1,6	2,35	1,12	2,88	1,5	1,67	0,7	1,6	0,66	0,8
343769	1,75	-0,12	1,07	0,49	-1,52	-0,09	1,39	-0,77	0,3	2,02	2,32	1,14	1,89	1,61	1,91	1,23	2,01	1,88	1,41	2,32	1,11	2,44	1,31	1,75	1,23	1,36	0,89	0,65
343770	1,78	0,23	1,26	0,94	-1,05	0,33	0,47	0,2	0,45	2,15	2,05	1,29	1,77	1,89	2,25	1,4	2,02	2,37	1,56	2,55	1,65	2,78	1,7	2,08	1,38	1,41	0,95	0,74
343771	1,73	-0,14	1,16	0,64	-1,4	-0,02	1,34	-0,96	0,37	2,21	2,32	1,24	2,1	1,87	2,09	1,39	2,08	1,89	1,48	2,16	1,07	2,51	1,63	1,74	1,56	1,38	0,83	0
343772	1,8	0,06	1,22	0,77	-0,96	0,16	0,72	0,13	0,42	2,05	2,06	1,24	1,77	2,02	2,25	1,32	2,11	2,37	1,58	2,51	1,63	3,08	1,66	1,91	0,7	1,38	1,05	0,74
343773	1,81	0,17	1,25	0,78	-0,89	0,16	0,42	0,22	0,43	2,06	1,95	1,21	1,7	1,92	2,31	1,46	2,14	2,44	1,64	2,62	1,65	2,98	1,81	2,06	1,41	1,49	0,95	0,57
343775	1,71	-0,08	1,17	0,82	-0,96	0,06	1,27	-0,7	0,38	2,32	2,4	1,41	2,17	2,03	2,21	1,25	2,11	2,07	1,65	2,3	1,15	2,56	1,53	1,83	1,49	1,57	0,75	0
343776	1,75	-0,08	1,09	0,55	-1,3	-0,04	1,34	-0,72	0,35	2,06	2,28	1,24	1,97	1,91	2,15	0,3	2,03	1,99	1,41	2,28	1,08	2,66	1,37	1,76	1,3	1,31	0,86	0,61
343777	1,78	-0,1	1,11	0,58	-1,1	0,02	1,22	-0,72	0,37	2,08	2,28	1,34	2	1,86	2,19	1,13	2,04	2,06	1,44	2,3	1,04	2,64	1,56	1,71	1,22	1,34	0,8	0,51
343778	1,69	-0,09	1,18	0,58	-0,96	-0,02	1,41	-0,72	0,36	2,24	2,33	1,26	2,1	1,87	2,15	1,26	2,12	2,05	1,6	2,27	1,14	2,66	1,64	1,75	1,35	1,36	0,9	0
343779	1,77	-0,11	1,12	0,58	-1,3	-0,03	1,29	-0,55	0,3	2,19	2,4	1,24	1,99	1,76	2,05	1,14	2,06	2,02	1,52	2,37	1,12	2,47	1,58	1,79	1,32	1,46	0,8	0,65
343780	1,77	0,17	1,23	0,82	-1,05	0,26	0,81	0,14	0,4	2,18	2,1	1,55	1,88	1,87	2,24	1,46	2,13	2,4	1,6	2,52	1,61	2,89	1,78	2,05	1,46	1,46	0,71	0,64
343781	1,82	-0,11	1,23	0,77	-1,4	0,33	0,54	0	0,46	2,13	2,08	1,22	1,85	1,91	2,23	1,39	2,19	2,07	1,49	2,22	1,2	2,66	1,48	1,86	1,42	1,45	0,94	0
343783	1,67	-0,04	1,24	0,82	-0,7	0,31	1,31	-0,72	0,43	2,27	2,29	1,43	2,17	1,91	2,26	1,25	2,2	2,13	1,61	2,26	1,17	2,73	1,69	1,76	1,33	1,45	0,82	0,64
343784	1,79	0,16	1,25	0,84	-1,1	0,3	0,39	0,27	0,47	2,17	2,03	1,39	1,79	1,85	2,17	1,44	2,13	2,38	1,63	2,58	1,69	2,77	1,85	2,14	1,62	1,35	1,03	0,74
343785	1,78	0,3	1,27	0,89	-1,15	0,27	0,42	0,15	0,44	2,17	2,09	1,35	1,89	1,9	2,32	1,35	2,08	2,35	1,49	2,59	1,65	2,82	1,67	2,05	1,5	1,51	0,64	0,75
343786	1,71	-0,12	1,13	0,78	-0,96	0,34	1,32	-0,16	0,38	2,12	2,3	1,32	2,09	2,06	2,22	1,29	2,06	2,14	1,53	2,18	1,07	2,85	1,5	1,78	0,7	1,32	0,88	0
343787	1,8	0,07	1,22	0,8	-1,22	0,29	0,64	0,1	0,47	2,07	2,06	1,2	1,84	1,96	2,23	1,4	2,11	2,31	1,57	2,49	1,59	2,99	1,57	2,01	1,01	1,29	1,02	0,74
343788	1,78	-0,02	1,19	0,44	-1,4	-0,07	1,23	-0,59	0,31	2,18	2,4	1,35	1,97	1,79	2,15	1,1	1,96	2,04	1,54	2,37	1,19	2,58	1,71	1,82	1,38	1,37	0,85	0

Table 4.9. Matrix used for multivariate statistical analysis: Log10 of the geochemical composition of samples obtained by XRF.

samples	SiO2	TiO2	Al2O3	Fe2O3	MnO	MgO	CaO	Na2O	K2O	V	Cr	Co	Ni	Cu	Zn	Ga	Rb	Sr	Y	Zr	Nb	Ba	La	Ce	Nd	Pb	Th	U
343789	1,79	0,13	1,3	0,81	-0,72	0,14	0,41	0,28	0,51	2,02	1,77	1,23	1,75	1,99	2,29	1,43	2,06	2,44	1,65	2,64	1,76	3,06	1,81	2,13	1,05	1,38	0,94	0,69
343790	1,63	-0,15	1,22	0,86	-1,22	0,06	1,45	-0,7	0,41	2,29	2,26	1,34	2,14	1,94	2,23	1,23	2,17	2,08	1,36	2,2	0,99	2,7	1,58	1,76	1,08	1,39	0,85	0
343791	1,8	0,13	1,23	0,86	-1	0,24	0,36	0,19	0,45	2,08	2,01	1,24	1,75	1,82	2,16	1,25	2,11	2,28	1,53	2,55	1,66	2,81	1,59	1,96	1,39	1,4	0,98	0
343792	1,78	0,16	1,23	0,91	-0,72	0,4	0,45	0,06	0,53	2,14	2,19	1,6	2,05	2	2,45	1,44	2,16	2,2	1,57	2,44	1,53	2,85	1,66	1,96	1,5	1,51	0,81	0,51
343793	1,8	0,24	1,26	0,86	-1,15	0,27	0,38	0,22	0,44	2,13	2,04	1,29	1,71	1,92	2,23	1,4	2,08	2,36	1,56	2,59	1,67	2,84	1,73	2,07	1,45	1,4	0,89	0,56
343794	1,7	-0,16	1,16	0,72	-1,3	0,07	1,38	-0,74	0,34	2,27	2,38	1,31	2,1	1,78	2,11	1,21	2,14	2,05	1,53	2,19	1	2,67	1,53	1,58	1,46	1,22	0,87	0,62
418269	1,75	-0,08	1,16	0,74	-0,92	0,29	1,24	-0,1	0,3	2,17	2,35	1,26	2,18	1,71	2,11	1,26	2,05	1,98	1,54	2,2	1,04	2,76	1,49	1,72	1,36	1,38	1,11	0,6
418343	1,69	-0,11	1,16	0,74	-1	0,13	1,41	-0,72	0,37	2,17	2,3	1,38	2,14	1,66	2,13	1,18	2,14	2,03	1,45	2,17	1,04	2,71	1,51	1,66	1,49	1,46	1,11	0,7
418905	1,71	-0,06	1,21	0,66	-1,15	0,08	1,32	-0,68	0,41	2,28	2,45	1,53	2,46	1,88	2,3	1,3	2,03	2,14	1,59	2,3	1,04	3	1,61	1,76	0,7	1,36	1,11	0,6

Table 4.9. Matrix used for multivariate statistical analysis: Log10 of the geochemical composition of samples obtained by XRF.

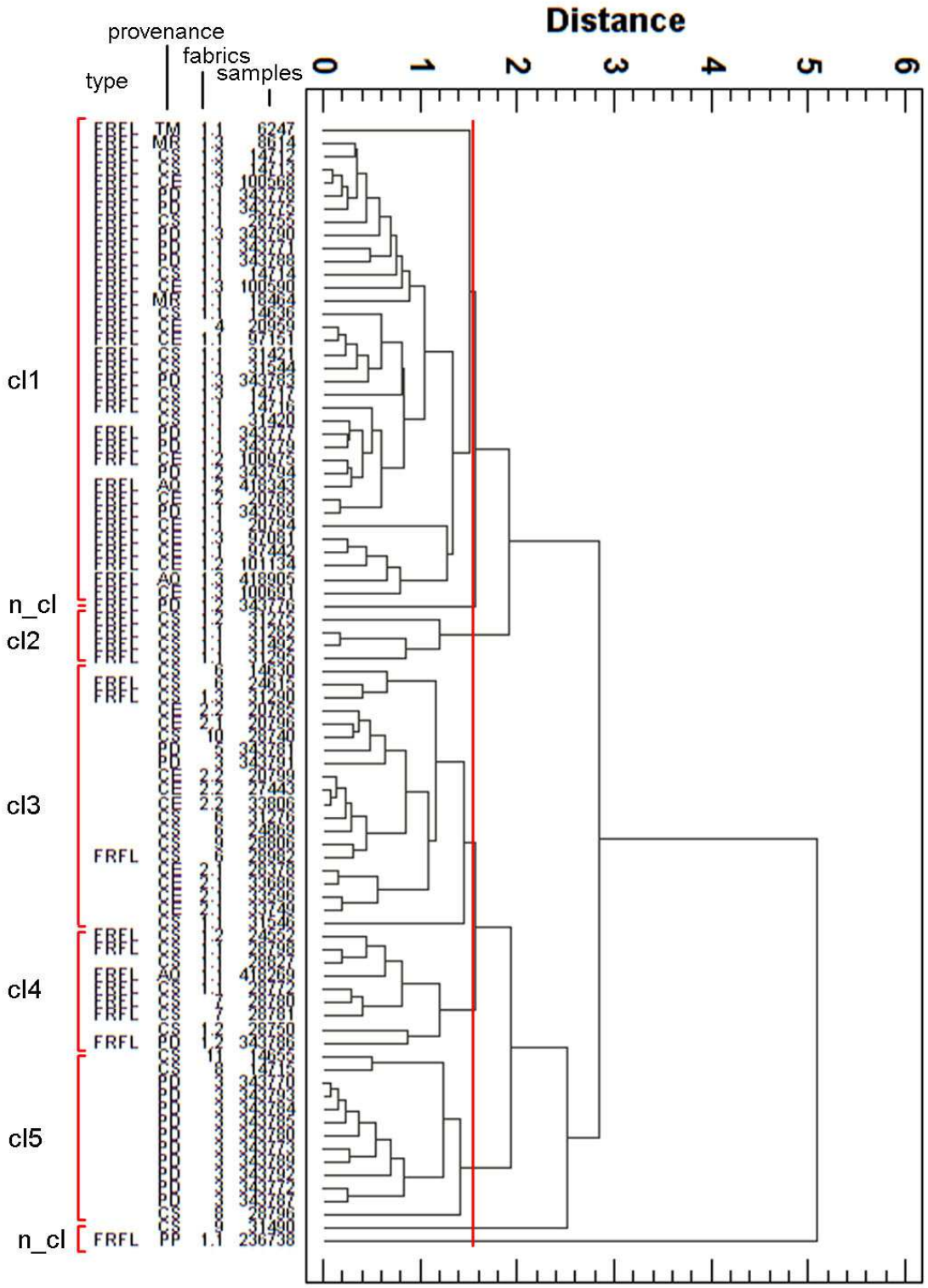

Figure 4. 19. Dendrogram obtained by cluster analysis (average linkage) of the studied pottery. Petrographic fabrics, provenance and the pottery type are also indicated.

Multivariate analyses (cluster and principal component analyses) were performed on the standardized values of the elements transformed to base 10 logarithm (table 4.9). These analyses were carried out excluding the concentration of P_2O_5, since here it varied over a wide interval: 0,14-5,60 wt%, much greater than that (0.05-0.50 wt%) observed in many clayey materials from Veneto (Maritan 2002, Maritan 2004). As explained in chapters 1.5 and 3.6, this oxide is commonly considered a good indicator of the alteration processes that can take place during burial (Freestone 2001, Lemoine, Picon 1982).

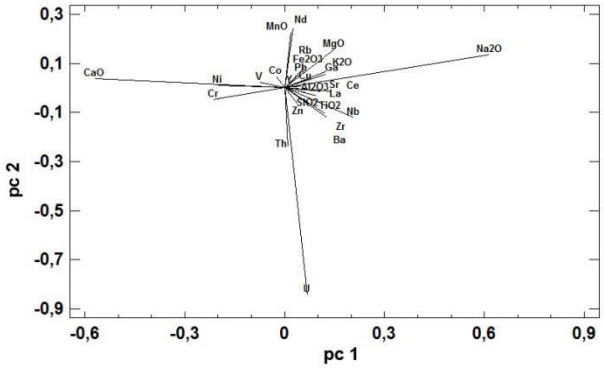

Figure 4. 20. Loading plot of the variables considered for the pca, respect pc1-pc2.

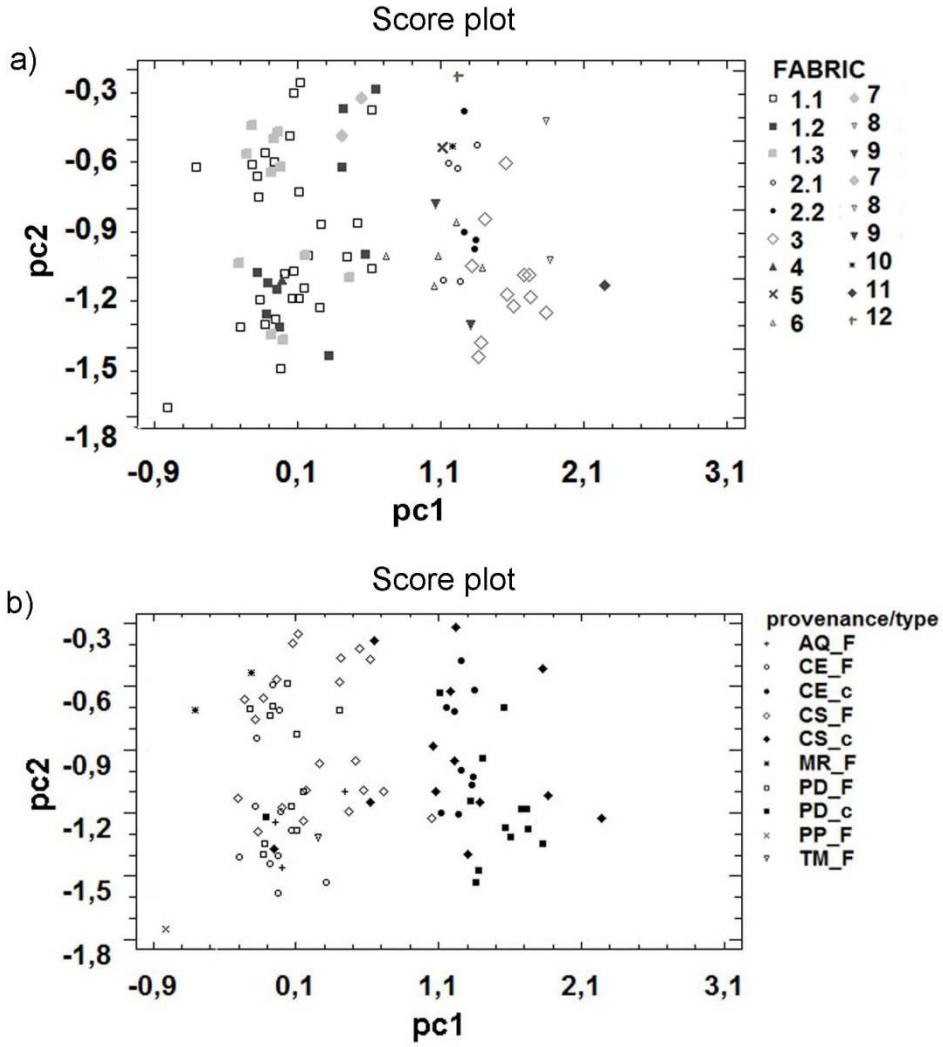

Figure 4. 21. a-b. Principal component analysis of the chemical data with indication of the fabric (a) and of the provenance site and pottery type (F: FRFL pottery, c: other tyoes for comparison) (b). Plot of PC1 versus PC2, explaining 47% and 11,% of the total variance, respectively.

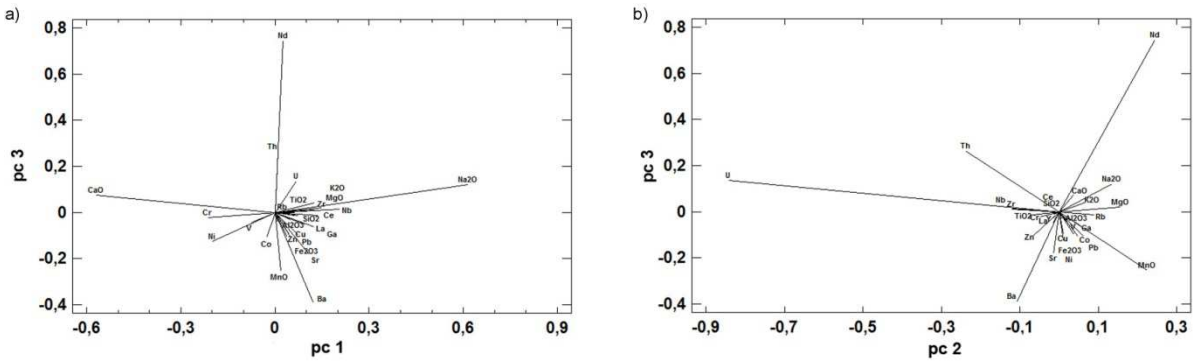

Figure 4. 22. Loading plot of the variables considered for the pca, respect pc1-pc3 (a); pc2-pc3 (b).

The cluster analysis was performed using the squared Euclidean distance and the average algorithm. The dendrogram indicates that samples tend to group into five main clusters (figure 4.19) based on the petro-fabrics observed at microscope together with their provenance sites**.** The Cluster 1 (cl1) is formed by the samples of fabric 1, characterized by abundant speleothems. They are all FRFL ceramic except for two potsherds of different

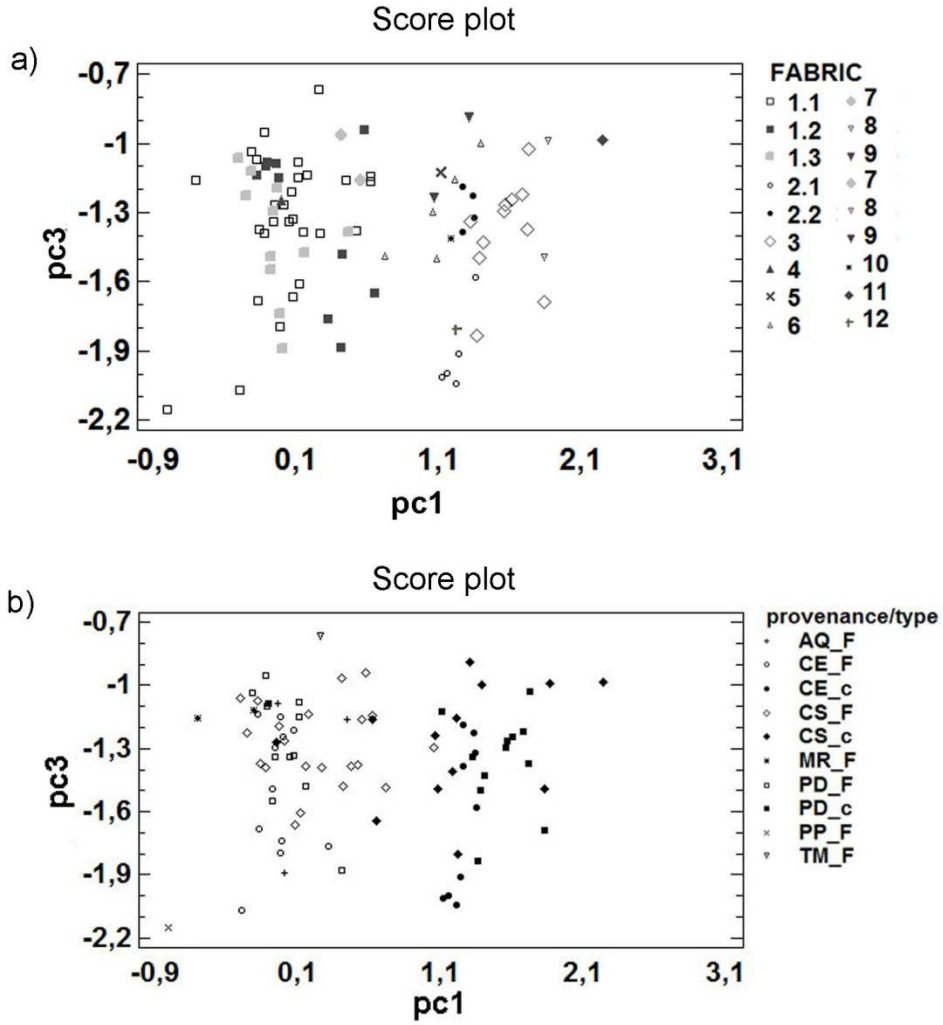

Figure 4. 23. Principal component analysis of the chemical data with indication of the fabric group (a) and of the provenance site and pottery type (b). Plot of pc1 versus pc3, explaining 47% and 8% of the total variance, respectively.

type coming from Padova and Concordia Sagittaria. They came from several sites (Padova, Concordia Sagittaria, Castion d'Erbè, Aquileia, Grotta del Mitreo and Terzo Ramo del Timavo) and mostly belong to the mineralogical assemblage A_{xrd}. The clusters 2 (cl2) is a small group formed by four samplesof FRFL pottery, that belong to the fabrics 1.1 and 1.2.. They all come from Concordia Sagittaria. The cluster 3 (cl 3) is related to the fabrics 2 and 6, rich in crystals of quartz and grog, with the exception of few samples characterized by the presence of trachyte and rhyolite (fabrics 3 and 5), grog and clay pellets (fabrics 10 and 12) and one sample belonging to fabric 1.3. They come from Castion d'Erbè (fabric 2), Concordia Sagittaria (fabrics 1.3, 6, 10, 12), and from Padova (fabrics 3, 5). The clusters 4 (cl4) is a small heterogeneous small group formed by samples that belong to the fabrics 1.1, 1.2 and 7. They are all potsherds coming from Concordia Sagittaria plus two fragments from Aquileia and Padova. The pottery types are of both FRFL ceramic and local typology. They are related to the mineralogical assemblage A_{xrd} (rich in calcite), the presence of one sample of group D_{xrd} is probably due to particular abundant calcite among its phases. The cluster 5 (cl5) is a homogeneous group

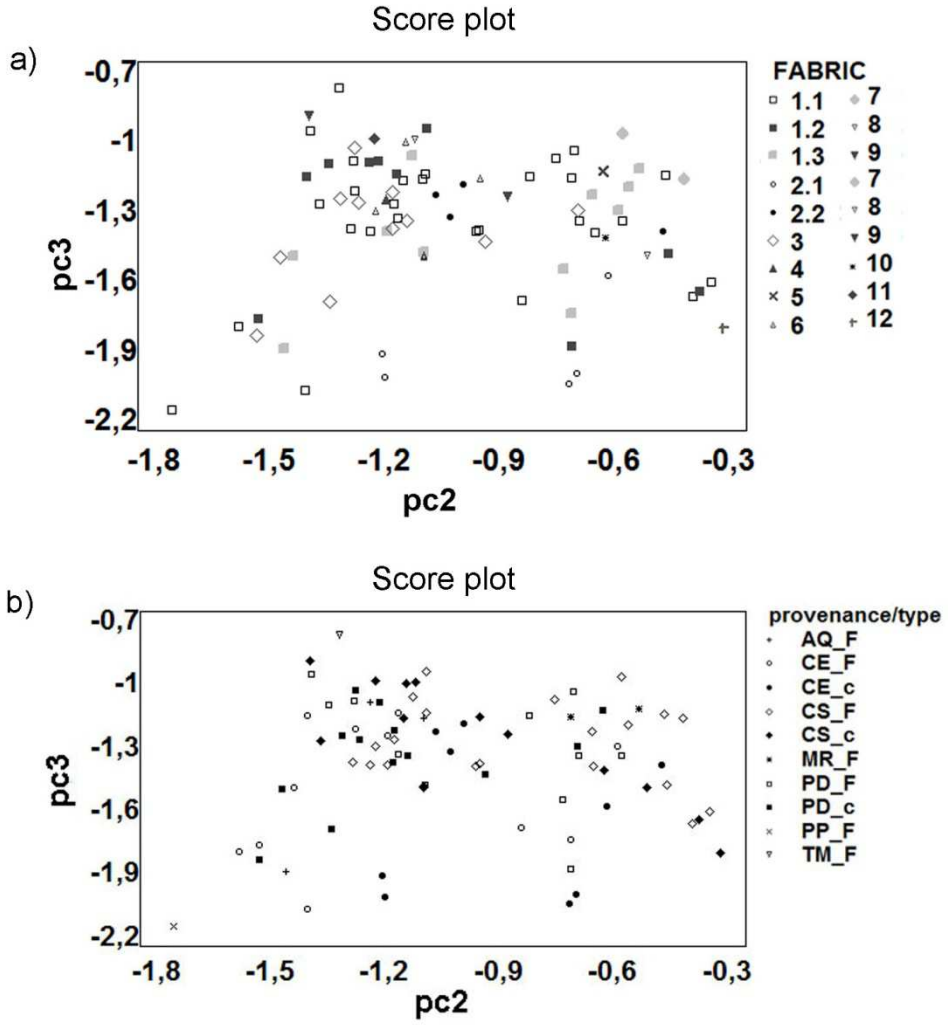

Figure 4. 24. Principal component analysis of the chemical data with indication of the provenance site and pottery type. Plot of PC2 versus PC3, explaining 11% and 8% of the total variance, respectively.

formed by specimens of fabrics 3, 8 and 11, rich in trachyte rock fragments. They come respectively from Padova and Concordia Sagittaria and are ceramic types supposed to be of local origins. They are associated to the XRD group C_{xrd}.and E_{xrd}. Only two FRFL pottery from Padova (sample 343776, fabric 1.2) and Palse di Porcia (sample 236738, fabric 1.1) and one small olla from Concordia Sagittaria (sample 31490, fabric 9) appeared to be outliers.

The score plots of principal component analysis (PCA) shows a well defined situation (figures 4.20-25). Considering the plot of the first and second factors, the samples are shared in two main groups: those samples classified as FRFL vases (fabric 1) are concentrate on the direction of high content of CaO (lower values of pc1). Of these, the samples of petrofabric 1.3 (associated to burned organic inclusions) are concentrate mostly toward positive values of pc2, along the direction of higher content in MnO and Nd, while samples of group 1.2 (rich in calcite crystals) toward higher content of U and Th (lower value of pc2 and greater of pc3). Pottery supposed to be of local origin are concentrate toward positive values of pc1 (at higher content in SiO_2 and Na_2O): samples from Padova (fabric 3, rich in trachyte fragments) are well concentrate towards higher contents of U, Th, Ba, Zr associated with fabrics 2.2, 6, 8, 9 and 11 (respectively rich in quartz sand, grog, trachyte rocks, granite associated with carbonate mudstone fragments). Samples from Castion d'Erbé belonging to the fabric 2.1 (fine sand and grog rich potsherds) are partly concentrated toward the direction of higher content of MgO,

Variable	A	SD	V	CV	MIN	IQ	MED	IIIQ	MAX	p_value
SiO2	51,51	5,12	26,20	9,94	39,47	48,65	51,55	55,84	60,17	**0,23**
TiO2	0,81	0,07	0,00	8,63	0,65	0,77	0,82	0,87	0,95	**0,80**
Al2O3	15,02	1,66	2,76	11,06	11,64	13,91	14,76	16,08	19,09	**0,67**
Fe2O3	5,32	1,22	1,48	22,89	2,74	4,44	5,36	6,53	7,72	**0,46**
MnO	0,10	0,05	0,00	47,14	0,03	0,06	0,10	0,13	0,21	**0,21**
MgO	1,40	0,64	0,41	45,46	0,56	0,98	1,15	1,64	3,32	< 0,005
CaO	21,93	5,83	33,96	26,57	6,24	19,07	21,05	25,64	38,48	**0,17**
Na2O	0,30	0,24	0,06	77,74	0,01	0,16	0,20	0,42	0,87	< 0,005
K2O	2,11	0,47	0,23	22,52	1,00	1,83	2,12	2,41	3,10	**0,74**
P2O5	0,80	0,82	0,67	102,58	0,19	0,38	0,60	0,90	5,60	< 0,005
V	155,06	29,41	865,00	18,97	103,00	130,75	156,00	176,00	210,00	**0,30**
Cr	204,74	46,63	2174,56	22,78	88,00	191,25	209,50	227,75	290,00	< 0,005
Co	20,28	4,45	19,80	21,94	11,00	17,00	20,00	23,00	34,00	**0,31**
Ni	125,78	41,57	1727,69	33,05	46,00	98,75	128,00	150,00	289,00	0,01
Cu	84,66	39,09	1527,70	46,17	30,00	58,75	75,00	89,00	205,00	< 0,005
Zn	126,66	34,47	1187,90	27,21	80,00	102,50	119,00	144,00	243,00	0,01
Ga	17,38	4,57	20,89	26,30	2,00	14,75	17,50	20,00	27,00	**0,11**
Rb	115,98	21,24	451,16	18,31	71,00	102,75	114,50	131,00	157,00	**0,92**
Sr	128,08	47,46	2252,77	37,06	76,00	104,00	119,00	143,25	408,00	< 0,005
Y	34,16	6,45	41,65	18,89	22,00	29,75	33,00	39,00	51,00	**0,37**
Zr	191,40	35,00	1225,06	18,29	127,00	159,25	192,50	221,00	267,00	**0,25**
Nb	13,14	1,64	2,69	12,49	10,00	12,00	13,00	14,00	17,00	< 0,005
Ba	462,50	167,50	28059,00	36,21	259,00	345,30	412,00	518,00	991,00	< 0,005
La	35,78	8,23	67,73	23,00	19,00	32,00	36,00	41,00	60,00	**0,22**
Ce	61,26	12,24	149,87	19,98	40,00	51,75	59,50	71,00	98,00	**0,29**
Nd	21,84	10,45	109,28	47,86	5,00	12,00	22,50	30,25	42,00	**0,08**
Pb	26,24	7,87	61,98	30,00	13,00	22,00	24,00	29,00	52,00	< 0,005
Th	7,38	3,09	9,55	41,87	1,00	6,00	7,00	9,00	15,00	< 0,005
U	2,98	1,85	3,41	61,95	1,00	1,00	3,50	4,00	6,00	< 0,005

Table 4. 10. Average (A), standard deviation (SD), variance (V), coefficient of variation (CV), minimum (MIN), first quartile (IQ), median (MED), third quartile (IIIQ) and maximum (MAX) values and the p-value of the Anderson–Darling normality test for the studied potsherds of FRFL type.

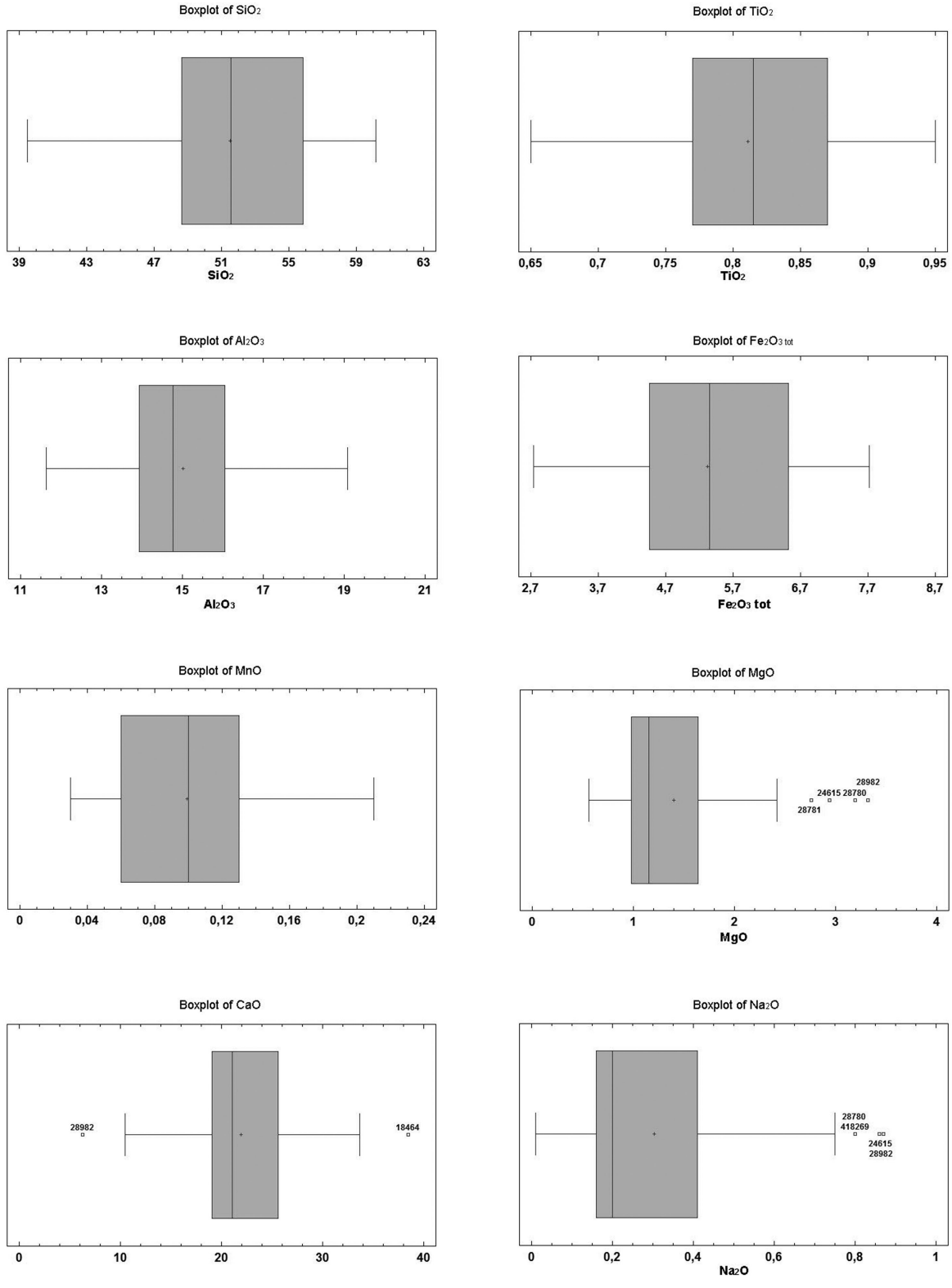

Figure 4. 25. a. Box-plot representing the chemical data with indication of the outliers.

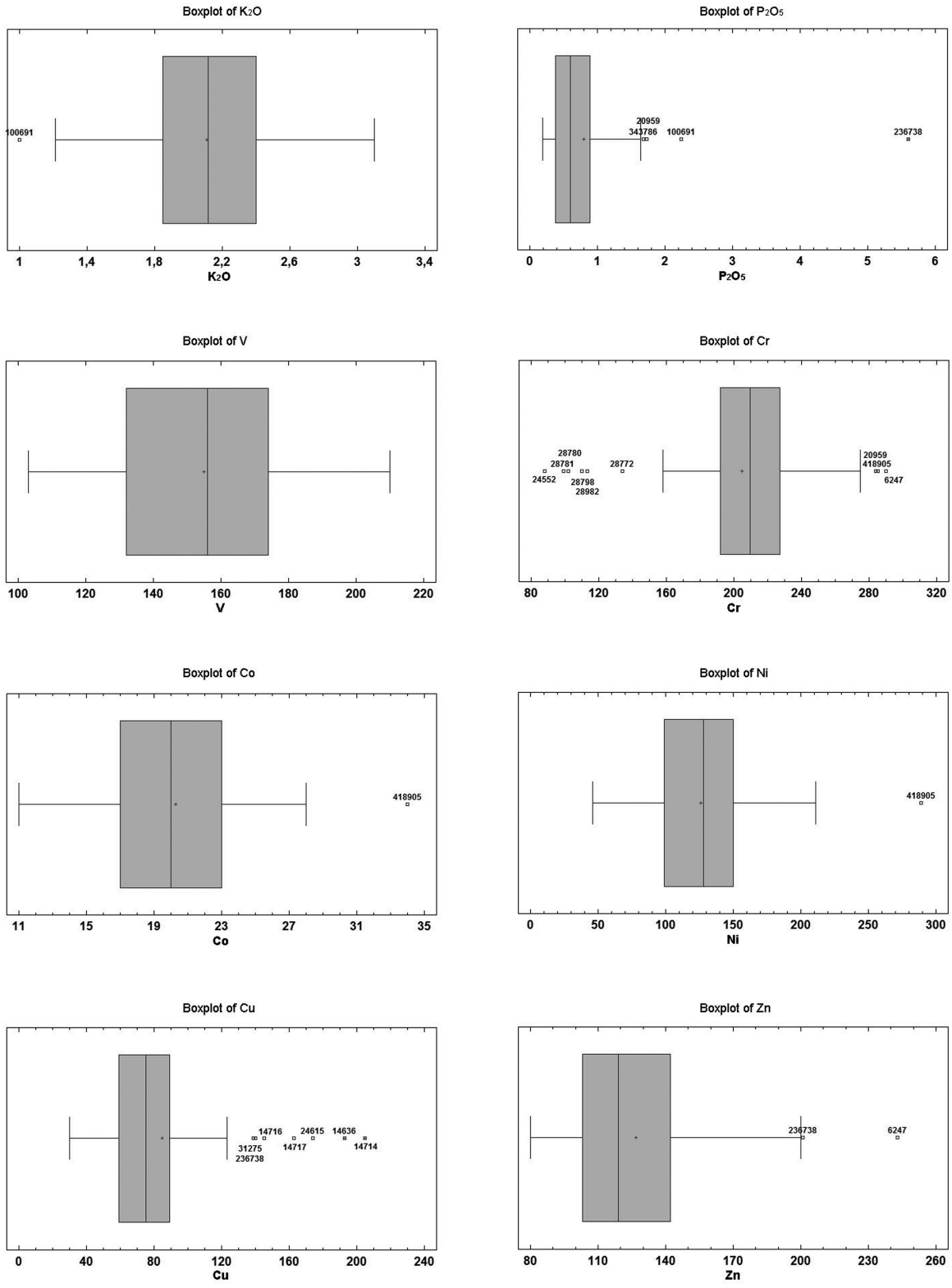

Figure 4. 25. b. Box-plot representing the chemical data with indication of the outliers.

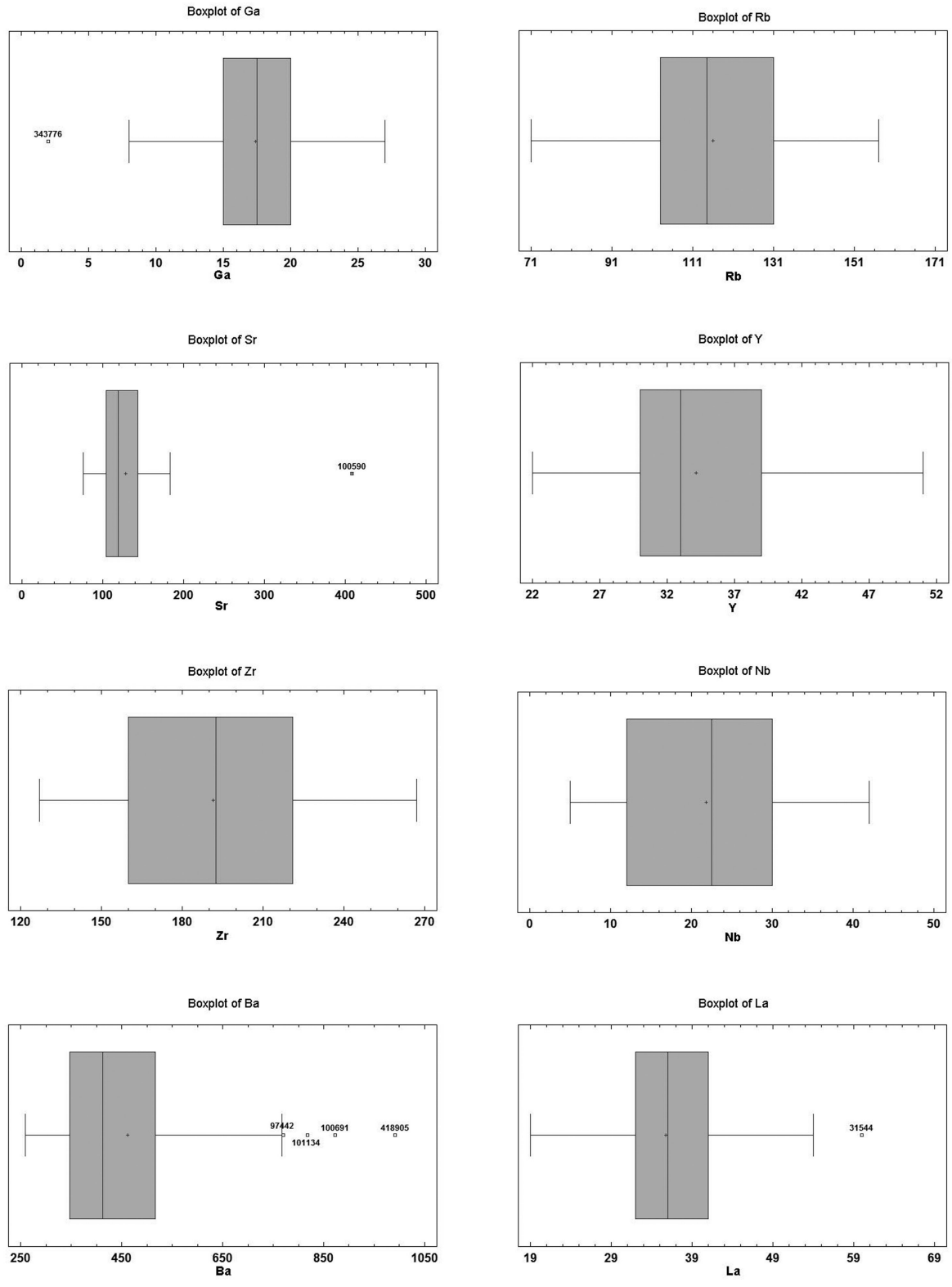

Figure 4. 25. c. Box-plot representing the chemical data with indication of the outliers.

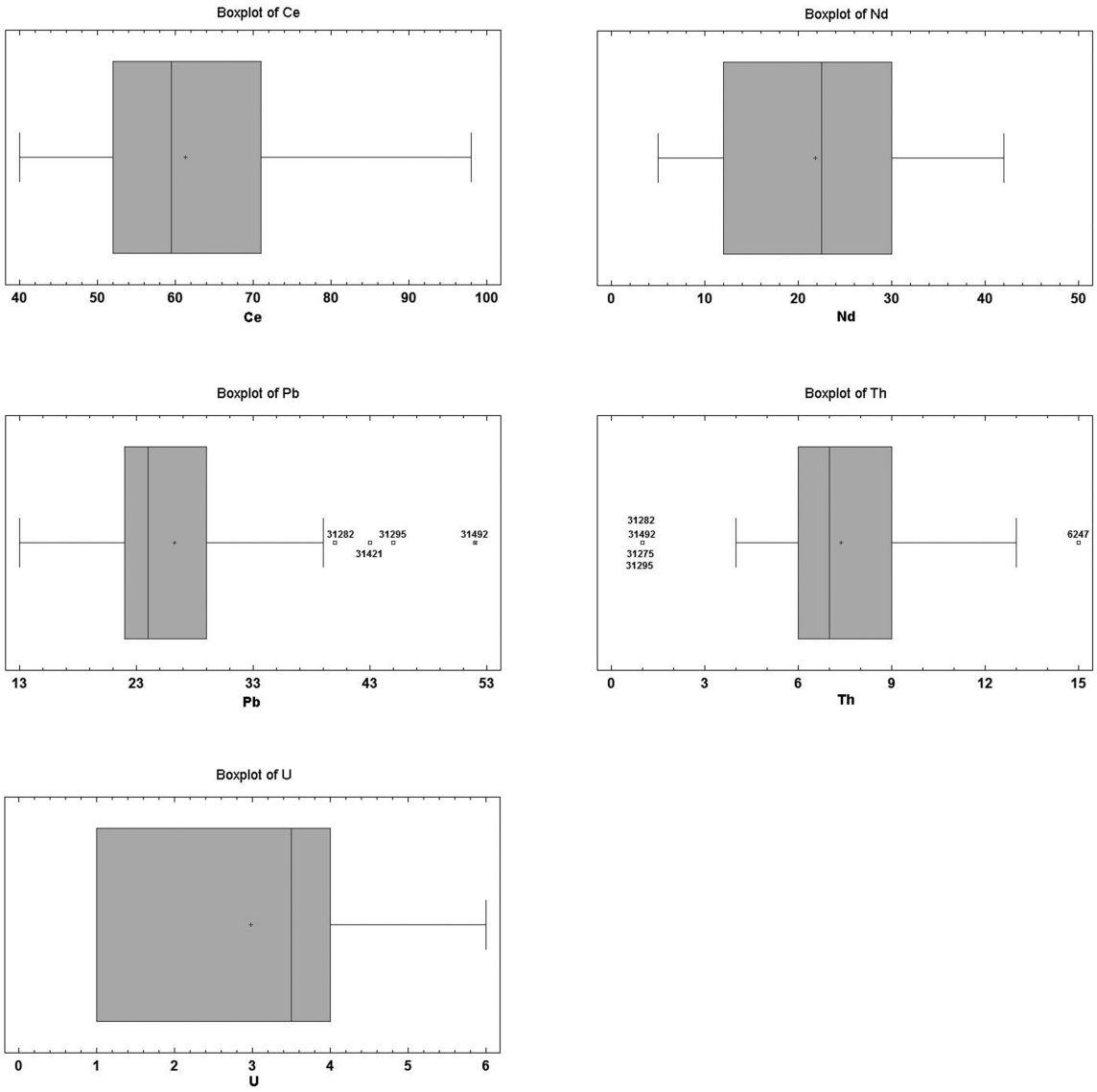

Figure 4. 25. d. Box-plot representing the chemical data with indication of the outliers.

Fe_2O_3, K_2O associated with fabrics 5, 10, 12 and one sample of fabrics 2.2. This grouping respects well the petrographic fabric classification observed through microscopy analysis and described in chapter 4.3.

Statistical analyses were repeated selectively on the samples of FRFL type. Descriptive statistics results show a more homogeneous situation with less wide distribution intervals and lower or in few cases (Fe_2O_3, P_2O_5, Cu, Y, Nd, Pb, Th, U) similar coefficient of varaiations. The Anderson Darling normality test indicates that the 55% of the variables follow a normal distribution (table 4.10). The box-plots display the presence of less outliers, the most of which due to the samples belonging to different fabric from the first petrographic group (samples 20959, 24615, 28780, 28781, 28982), the only pottery of FRFL type not characterized by speleothems among their inclusions (figures 4.25).

Multivariate analyses (cluster and principal component analyses) were performed on the standardized values of the elements transformed to base 10 logarithm. These analyses were carried out excluding the concentration of P_2O_5 because its high value (0,19-5,60

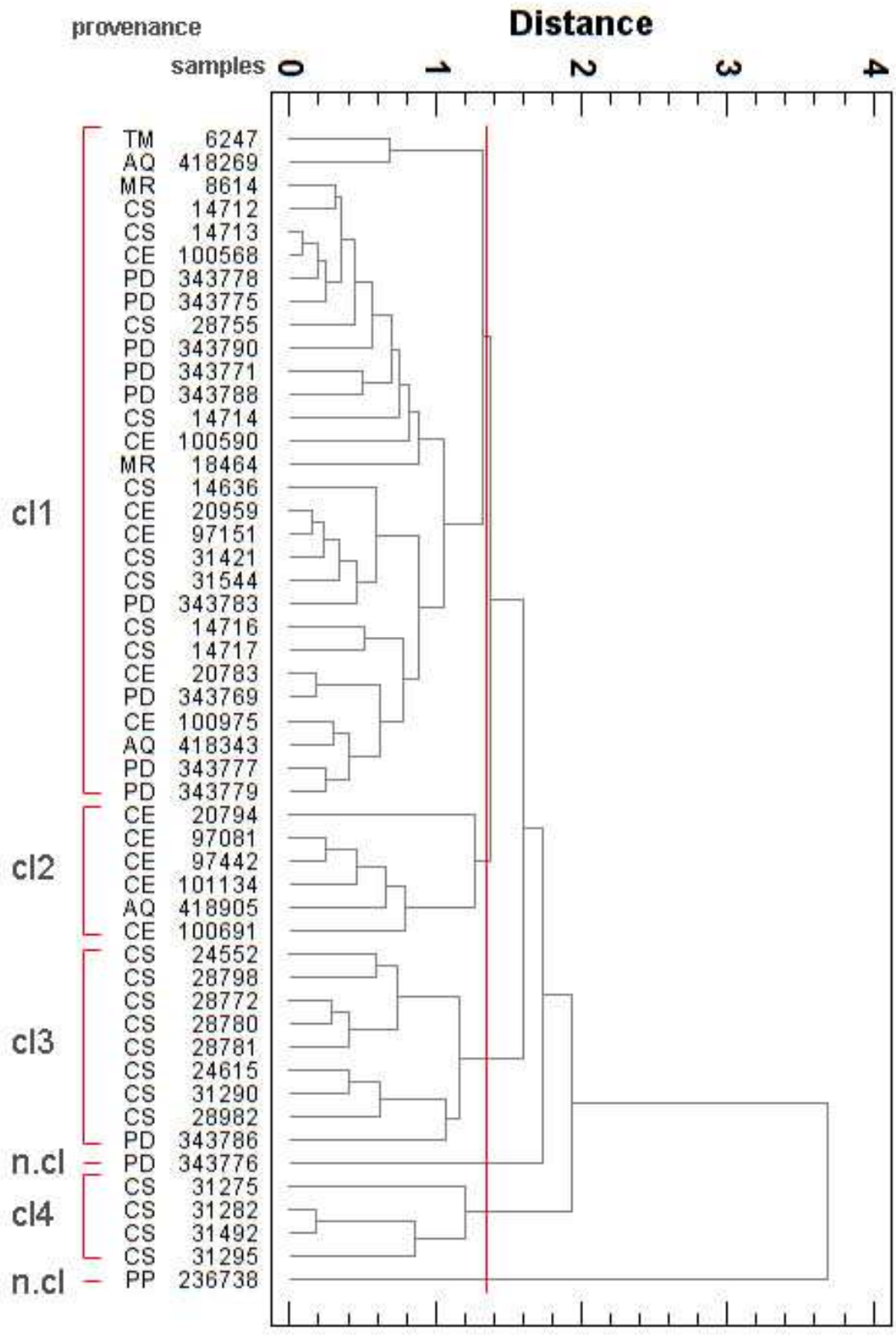

Figure 4. 26 Dendrogram obtained by cluster analysis (Further Neighbor) of pottery from Castel de Pedena. Petrographic groups are also shown.

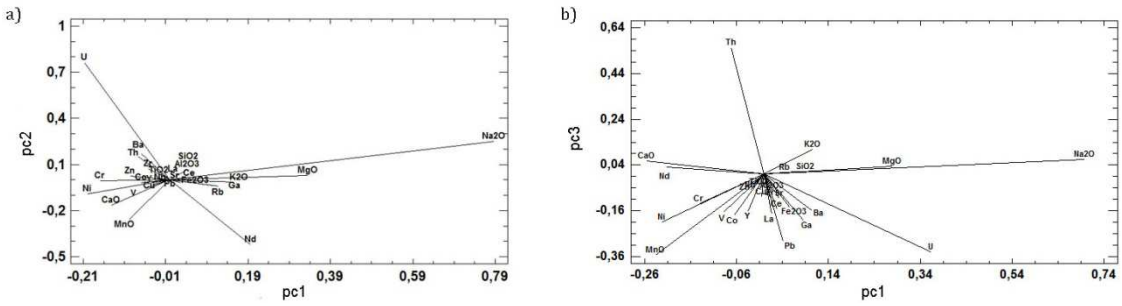

Figure 4. 27. Loading plot of the variables considered for the pca performed on the FRFL pottery data, respect pc1-pc2 (a) and pc1-pc3 (b).

wt%) is here considered a consequence of alteration processes that took place during burial (Lemoine and Picon, 1982; Freestone, 2001). The cluster analysis was performed using the squared Euclidean distance and the average algorithm. The dendrogram indicates that samples tend to group into four main clusters apparently not related to the provenance sites neither to the fabric subgroups except for the cluster 3 that groups the

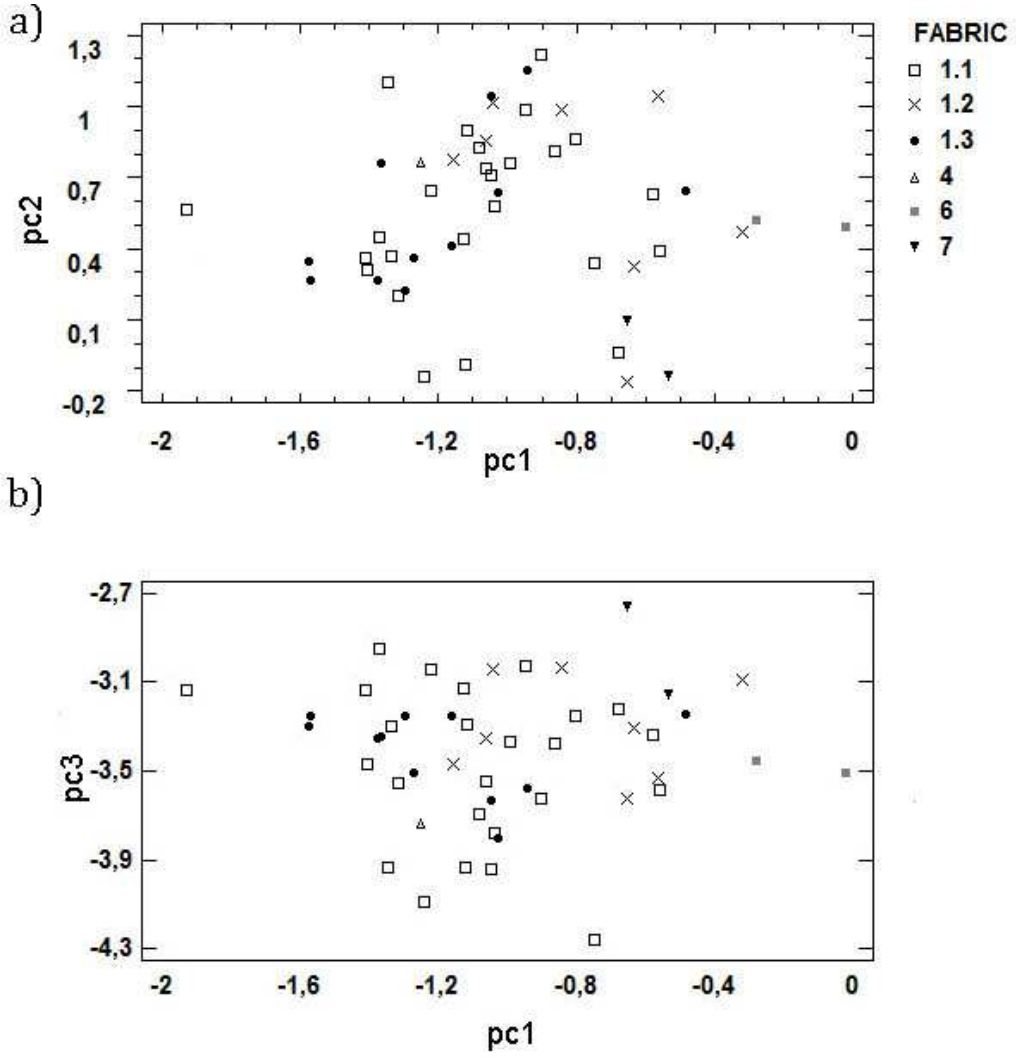

Figure 4. 28. Principal component analysis of the chemical data performed on the FRFL pottery, with indication of the fabrics. Plot of pc1 versus pc2, explaining 20% and 19% of the total variance, respectively (a); plot of pc1 versus pc3, explaining 20% and 14% of the total variance, respectively.

samples belonging to the fabrics 6 and 7 (rich in a quartz sand and grog and a coarse 14 carbonate sand respectively) together with samples of fabrics 1.1, 1.2 and 1.3. Only two samples (343776, 236738), coming from Padova and Palse di Porcia, are classified as outlier (figure 4.26). The dendrogram performed without these outliers do not show any difference.

Although, the score plot resulting from the pca do not seems to be strictly related to the provenance sites neither to the fabric groups and subgroups, as for the cluster analysis, it can help to better understand the clusters previously illustrated. In general all the samples are concentrated toward the direction of high content in CaO. More in details samples of cluster one (cl1) are concentrated toward high values of pc3, average values of pc1 and they are all spread for pc2, that means that they are characterized by the higher contents of CaO. Samples of cluster two (cl2) are concentrated toward average values of pc1 and pc3, and high values of pc2 that corresponds to higher content in Na_2O, U, Th but also of SiO_2 and MgO. The Cluster three (cl3) is concentrated towards higher values of pc1, medium/high values of pc2 (a part of three samples characterized by high content in MnO and CaO) and of pc3 due to the high content in Na_2O, MgO, K_2O and SiO_2. The cluster four is well grouped toward low value of pc2 and pc3, along the direction of MnO, Pb and Fe_2O_3. Sample 236738 appears to be an outlier also from pca and it isolated in respect of low values of pc1, toward the direction where U, CaO and Mn are more consistent. The principal component analysis repeated without consider sample 236738 gave some further clarification. Considering the score plot resulted from pc2 and pc3 axes, samples belonging to the cl1 is shared in two subgroups: one, together with cl3, toward the direction characterized by higher content in NaO and K_2O (low values of pc2 and high of pc3) and the other, together with cl2, toward higher content in U (higher values of pc2 and lower of pc3). The cl4 is concentrated for low values of pc2 and pc3 (toward the direction where MnO and Pb are more important). Respect pc1, the cl1 and cl2 have low average values (towards higher contents of SiO_2), cl3 is concentrated for higher values (corresponding to more abundance of Na_2O, MgO and K_2O) while cl4 is shared in the two different directions.

4.7 Geological setting

The flared rim and flattened lip (FRFL pottery) was widely present in the Friuli Venetia Giulia region, in settlements related to the Castellieri *phacies*, and it can be considered peculiar of this culture. As very similar ceramics were found in few Venetian sites during the Iron Age, one of the main goal of this project was to answer whether the vessels found in Veneto were manufactured locally or imported and if there was any evidence of trade. Since the involved regions are a wide area and the sites with presence of FRFL pottery, especially in the Friuli Venetia Giulia region, are numerous, the samples selection was carried out considering the main aims of this project: FRFL potsherds were chosen, mostly in the Venetian sites, and some different vessels type of probable local production were sampled for comparison.

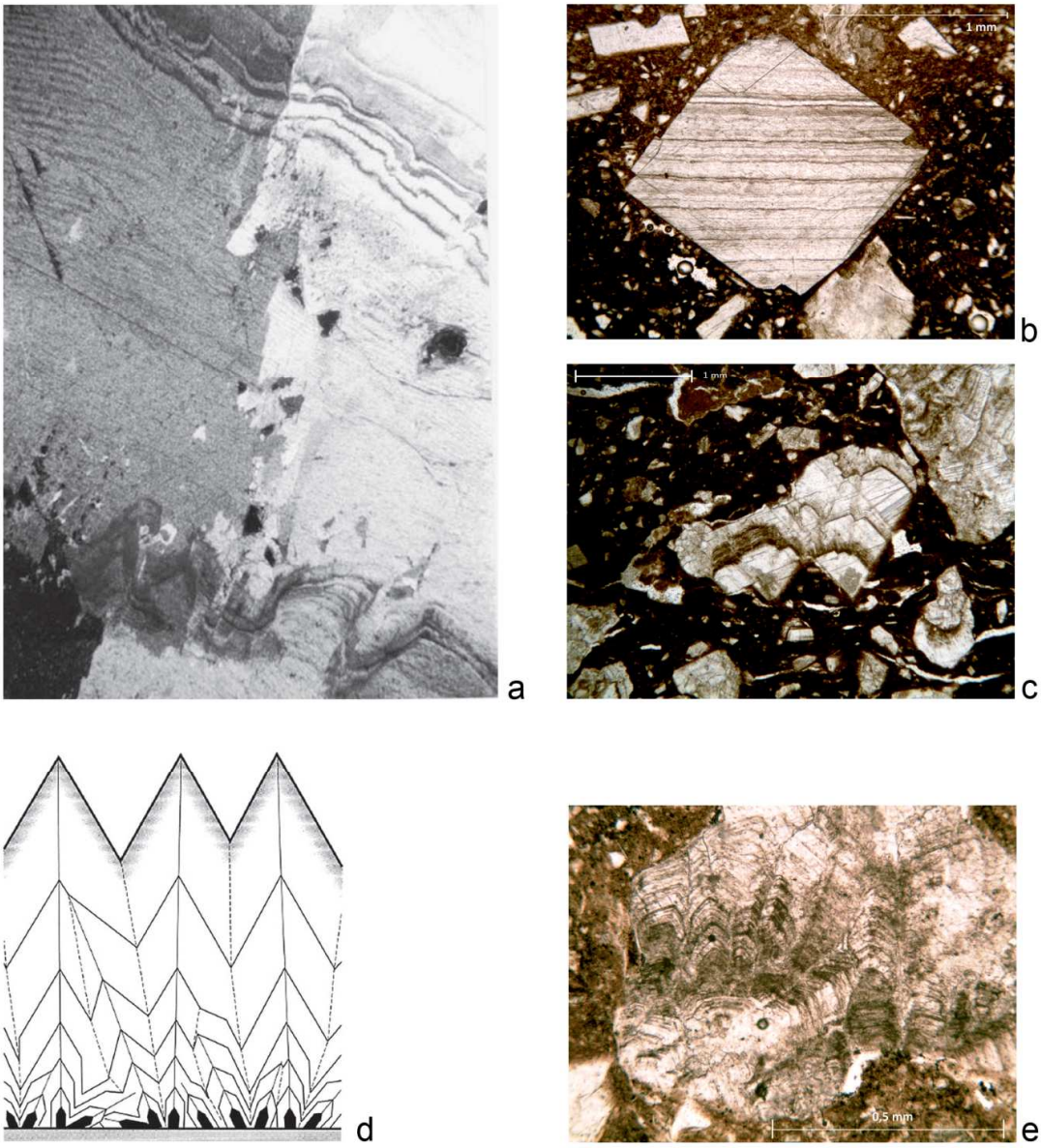

Figure 4. 29. Thin section photomicrographs of speleothems. a) Photomicrograph of the microcrystalline fabric in a stalagmite from the Grotta di Ernesto (Trentino, Italy) showing the annual growth lamina and irregular domains with the same optical orientation. Base of the photograph = 5.0 mm (From Frisia 2005). b) Photomicrograph of sample 343776, detail of a carbonate inclusion (speleothem). Image width = 2,45 mm. c) Photomicrograph of sample 14717, detail of a carbonate inclusion (speleothem). Image width = 3,85 mm. d) Geometric selection on a flat growth surface. (From Kantor 2003). e) Photomicrograph of sample 343778, detail of a carbonate inclusion (speleothem). Image width = 0,97 mm. Images b, c and e were taken in plane polarized light.

The minero-petrographic composition of the potsherds of the first fabric is characterized by the presence of peculiar carbonate inclusions that indicates the use of a similar temper, consisting in fragments of speleothems (figures 4.9 4.29). Speleothems are secondary mineral deposits, composed of calcium carbonate (calcite or aragonite) formed in karst caves (Moore, 1952), that occur mainly as stalactites and stalagmites. The minerals forming these deposits are therefore homogeneous solids with a definite chemical composition and a 3-D ordered atomic arrangement (Self and Hill, 2003). Five

different speleothem fabrics have been identified in Alpine caves on the basis of morphological and microstructural characteristics, and related to growth mechanisms and growth environment: columnar and fibrous, microcrystalline, dendritic, and calcareous tufa fabrics (Frisia et al., 2000). Due to the small size of the inclusions that occur in the studied potsherds, they cannot be related to one or other structure however, the thin section observations show great similarity between them (figure 4.29).

This interpretation acquires great importance if we consider the geological setting of the interested areas. The regions involved are highly geologically diversified. In the Veneto region karst environments are nearly absent, except of very few karstic caves (e.g. in the Berici Hills). Whereas they are widely diffuse in the Friuli Venetia Giulia, a limestone hill region typically karstic, with common dolines and heavy clay-rich soils where more than seven thousands caves have been discovered (figure 4.30) (Catasto 2008).

Moreover, none of the Venetian sites where FRFL pottery was found are really closed to any karstic region. The sites here studied (Castion d'Erbé, Padova and Concordia Sagittaria) are all settled in the Venetian-Friulan plain, a wide alluvial basin originated by the infilling of the subsiding foreland basin started in the Pleistocene–(Doglioni1993) and are all linked to specific hydrographic basins. Padova is settled in the middle of the eastern Po plain, not far from the Adriatic sea and few kilometers north of the Euganean Hills. It insists on the Brenta and the Bacchiglione alluvial deposits, containing the former subordinate alpine sediments. Castion d'Erbé is settled in the Valli Grandi Veronesi, in the central-west of the Po plain, on the Adige and Tartaro system, within the Tartaro palaeo-river valley. Concordia Sagittaria is located on the borderline between the Friuli Venetia Giulia and the Veneto regions, not far from the sea. It is related to the Tagliamento-Lemene-Livenza fluvial system. The Adige, Brenta, Bacchiglione, Livenza and Tagliamento fluvial systems during the past were fed by the Alpine glaciers. Clasts of rock types

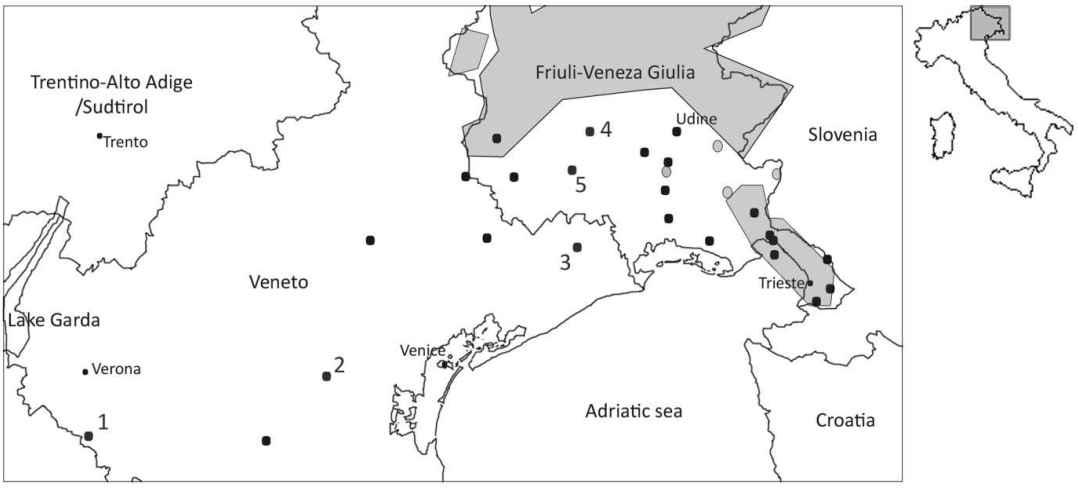

Figure 4. 30. Distribution of the sites where FRFL pottery was found in the Veneto region and in Friuli Venetia Giulia with indication of the settlements where the studied pots come from: 1) Castion d'Erbè, 2) Padova, 3) Concordia Sagittaria, 4) Gradisca di Spilimbergo, 5) Palse di Porcia. Indication of the caves distribution in Friuli Venetia Giulia region (grey pattern).

common in the Alpine hydrographic basins can be easily found in the sandy fraction of these rivers sediments while none speleothem is present (Jobstraibitzer and Mallesani, 1973).

In addition the suspected imported pots (FRFL types) and the Venetian local products appear compositionally distinct. Except three samples found at Concordia Sagittaria and Padova, none of these latter present speleothems among their inclusions. Instead inclusions are generally compatible with the alluvial deposits of the fluvial systems correlated to the provenance sites, with some exceptions which are probably related to the reuse of imported lithic materials as temper. This is the case of few samples from Concordia Sagittaria that contain among their inclusions also fragments of trachyte. This rock crops out in the Euganean Hills, in the middle of the Padan plain, far from the site, and it is not geologically locally available. The use of this type of rock is well established for the production of lithic objects (such as stone mortars) since the prehistoric periods in other areas also far from the Euganean District (Cattani, Lazzarini et al. 1997)

On the contrary, the comparison between the FRFL pots from Vento with eleven shards of the same pottery type coming from several Friuli Venetia Giulia sites (Gradisca di Spilimbergo, Palse di Porcia, Grotta del Mitreo, Terzo Ramo del Timavo) revealed great similarity. Both these assemblages present speleothems among their inclusions, this is greatly significant giving evidence of a common place of origin.

Previously, Boschian and Floreano (2007, 2009) archaeometrically studied coeval ceramics found in the Friuli Venetia Giulia settlements of Gradisca di Spilimbergo, Variano di Basiliano, and Pozzuolo del Friuli, focusing on the petrographic analysis on one hundred-one shards and on sediments sampled in thirteen sites of the Friuli plain. The average mineral composition of the sands transported by the main rivers was determined and compared with that of the ceramic pastes, in order to define the possible source of temper. On the basis of microscopic analyses, Boschian and Floreano (2007) grouped the pottery pastes into 12 distinct fabrics. All the FRFL pots were grouped in the same fabric (namely number 2) discriminated from all the other contemporaneous type of pottery by the presence of dominant unsorted euhedral calcite (sparite) with the size range from fine sand to very fine gravel. Fewer subhedral or anhedral sparite with “dusty concentric growing bands” were also identified. This fabric, as described by the authors, seems to correspond with the petrographic group 1.2 illustrated in this work (chapter 4.3).

Taking into consideration all these facts, the source area of the raw materials used for the production of these potsherds is likely to be located in the Friuli Venetia Giulia region, probably in the territory near Trieste, where most of the karsic caves are located.

4.8 Production technology

The object of this study was a peculiar ceramics with the flared rim and flattened lip (FRFL pottery) widely present in the Friuli Venetia Giulia region, but found also in the Veneto region. This archaeometrical study was conducted with the aim of defining the production technology (clay selection and processing choices, pottery forming methods,

firing conditions...), of characterizing in detail their compositional variability (if presents), and of distinguishing between local and imported artefacts. That was carried out through the combined petrographic and chemical analyses of the ceramic samples.

According to the petro-fabric classification, it resulted that pottery of FRFL type coming from both the Venetian sites (Concordia Sagittaria, Padova, Castion d'Erbè) and the Friuli Venetia Giulia region (Aquileia, Palse di Porcia, Gradisca di Spilimbergo, Terzo Ramo del Timavo, Grotta del Mitreo) are very similar in terms of recipes. Moreover, the compositional variability of the locally produced pottery from the same Venetian sites for most of the studied potsherds, indicates that FRFL ceramics were imported from the Friuli Venetia Giulia region, and that it may be considered a reference group and be described like that.

In details, it arose that the pots of FRFL type were prepared following similar recipes with little differences in terms of temper and clay ratio and type of temper (fabrics 1.1, 1.2, 1.3), except of few samples found at Concordia Sagittaria (14630, 28982, 31276: fabric 6; 28780, 28781: fabric 7) and at Castion d'Erbé (20959: fabric 4).

According to Prosdocimi (2011), the FRFL pottery was made using the coiling technique. The presence of clay pellets and oxides into the groundmass of most samples indicates that the clay was not seasoned, or at least not for a long period.

The petrographic microscopy observation suggests that most of the non-plastic elements were artificially added. Inclusions have angular to sub-rounded outlines (speleothems), and range between 10 vol% and 30 vol% with a hiatal grain-size distribution. In the majority of the samples (fabric 1.1) the coarser temper is represented selectively by speleothems, with few carbonate mudstone. Only in some situations speleothems are associated to comparable amount of rombohedral calcite crystals with splintery, angular outlines (fabric 1.2; 18% of the studied FRFL pottery) while twelve samples (fabric 1.3; 22% of samples) present evidences of burned organics inclusions (like straw), as indicated by the abundant channels voids surrounded by a darkened matrix. Grog is seldom present, always in very few amount. Generally there are fewer inclusions with a well sorted bimodal grain-size distribution (c:f ratio 80:20). These data were demonstrated also by the digital image analysis.

It can therefore be concluded that potters added speleothems and sometimes calcite crystals. Controlled crushing can be surely detected for calcite, and supposed for the most of the speleothems (Maggetti 1982). Also organics elements were quite surely voluntary added to some of the studied samples.

These little diversities among the FRFL pottery are not related to different provenances and all the three sub-groups contain samples coming from both the Venetian and the Friuli Venetia Giulia sites.

Only few pots of FRFL type were prepared following different recipes. Samples 14634, 28982, 31276 (fabric 6), all coming from Concordia Sagittaria, presented a fine quartz sand and abundant grog. Grains have round shapes, a well sorted unimodal distribution, with similar dimensions (average diameter 0.8–1.6 mm). It can be concluded that potters

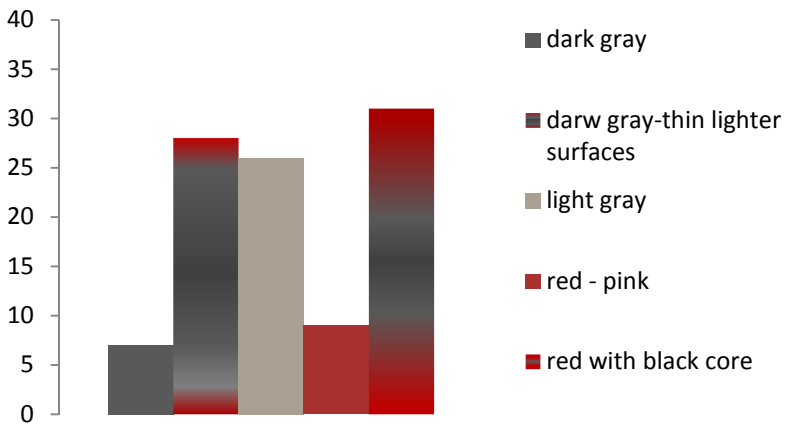

Figure 4. 31. Paste color differentiations of FRFL pottery bodies.

used a clay with the natural presence of the quartz sand and the addition of abundant grog. These samples are associated to other potsherds still coming from Concodia Sagittaria.

Two other samples from Concordia Sagittaria (28780, 28781; fabric 7) presented a well sorted hiatal structure of the inclusions mostly given by rounded fragments of carbonate mudstone and sparry calcite. It seems likely that here potters added a natural sand to the raw clay.

A lonely sample (fabric 4), coming from Castion d'Erbé, has abundant inclusions mainly represented by a fine quartz sand associated to coarser sub-rounded carbonate mudstone presents with a seriate grain-size distribution. It is difficult to say if the carbonate mudstone was already present in the original clay or if it was voluntary added by potters using a natural sand. None other potsherd among the studied samples from this site is referred to this one.

It is singular that the most of the dissimilarities occur among samples from Concordia Sagittaria, a Venetian site located on the cultural boarder between the Veneto and the Friuli Venetia Giulia regions, where differences among pastes and inclusions types of FRFL pottery were yet macroscopically observed (Prosdocimi 2011). It seems likely that the FRFL was there locally copied, using new production recipes with respect to those traditionally used for other types of pottery.

Firing conditions (redox atmosphere and maximum fire temperatures) were also deduced. Initially, chromatic variations of pottery were evaluated (chapter 3.2) and different situations were described (figure 4.31). The majority of the samples have homogeneous grey or very dark grey body, sometimes with a lighter (pink or red) extremely thin external layer, usually indicative of cooling in reducing atmosphere, independently of the organic matter content, or with a fast exposure to oxidising atmosphere. Some samples present a sandwich structure (a dark "core" with lighter reddish surfaces) or colour differentiations along the external, usually reddish, and the internal, grey-dark grey, surfaces. This is generally related to a reducing atmosphere during firing and oxidising cooling, or oxidising firing and cooling atmospheres in presence of organic matters. Only few of potsherds have homogeneous brown or reddish bodies, probably due to firing in oxidising atmosphere. The redox conditions of firing were deduced also from the Reduction Index (see chapter 3.8). Conventionally RI values higher than 0,20 are related to a reducing firing atmosphere. The RI calculated for the

analyzed samples highly varies and ranges between 0,13 and 0,82. According to the macroscopic colour evaluation, only one sample has value related to a oxidising firing atmosphere while all the other range from slightly reducing to reducing atmospheres (figure 4.32).

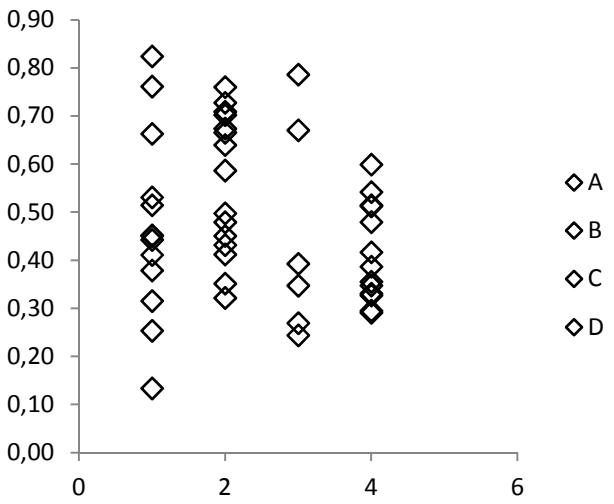

Figure 4. 32. RI indicated for the different color type pottery. A: dark grey or dark grey with thin lighter surfaces; B) light grey; C) red-pinkish; D: red body with dark core (sandwich structure).

The firing temperatures were deduced from the stability range of selected critical minerals phases, defined by X-ray powder diffraction. Based on the results of XRPD analysis, the samples were clustered in groups and sub-groups related to specific temperature intervals (chapter 4.5). The most of the FRFL pottery belong to the group A_{XRD}, characterized by a illitic clay rich in carbonates. The presence of calcite and illite and the absence of chlorite or smectites minerals indicate firing temperature between 650-850°C ($A1_{XRD}$). The nucleation of hematite in presence of carbonates (calcite and dolomite) indicate a temperature interval of 750-850°C (group $A3_{xrd}$). The presence of gehlenite is indicative of temperature higher than 900°C. The occurrence just of trace of gehlenite together with abundant calcite means that this temperature was just reached but not exceeded or, at least, higher temperatures were held for a very short time. Only two samples of fabric 1 (1.1 and 1.3) belong to group $D3_{xrd}$, probably for particular low amount of calcite among their components respect of the other samples. The presence of chlorite and smectites, lowers the temperature at less than 650°C.

Some additional information was given by the SEM investigation of speleothem present as inclusions in the studied pottery that reveals small rounded pores along their growing laminas. Since a similar behaviour was already observed in fragments of mollusc shell inclusions and was related to the transformation and/or decomposition of calcite related

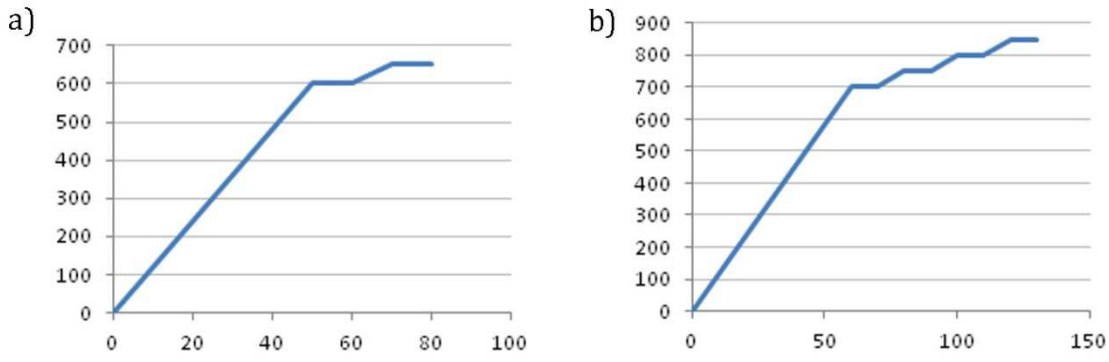

Figure 4. 33 Fire rating adopted for the first (a) and second (b) experimental firings.

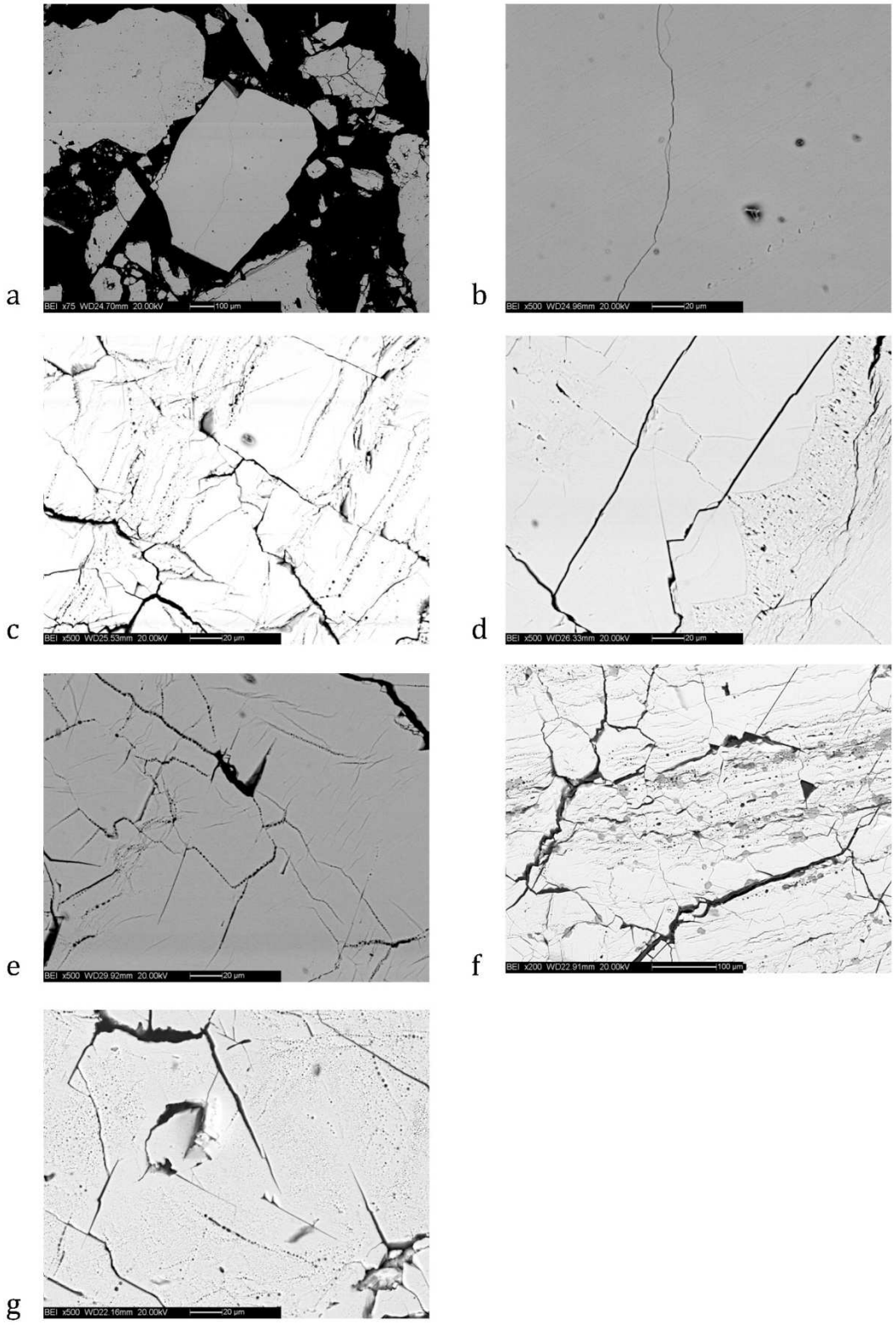

Figure 4. 34. SEM- BSE images of speleothems undergone to firing experiments. a) Speleothem SP.1, not fired; b) detail of figure (a); c-d) speleothem SP.1 fired at 600°C; e) detail of speleothem SP.1 fired at 650°C; f) Sample SP.2, fired at 700°C; g) sample SP.1, fired at 750°C.

to temperature (Maritan et al. 2007), firing experiments were carried out on speleothems with the aim to observe whether this porosity had the same origin. As a matter of fact, speleothems are secondary mineral deposits, composed of calcium carbonate (calcite or aragonite) characterized by a multilayer microstructure, often showing "concentric growing bands". Similarly the shells of bivalves are characterized by a multilayer microstructure, often showing several crossed-lamellae internal layers related to different stages of growth.

Two speleothems (SP.1, SP.2) coming from karst caves of the Friuli Venetia Giulia were crushed at grain-sizes compatible with those observed for the studied pottery (0,001-4,50 mm). The samples were fired in the temperatures interval from 600°C to 850°C, in successive temperature steps of 50° C, at a heating rate of 5°C min^{-1}, residence time at each step of 10 min and fast cooling (figures 4.33. a-b). Firing experiments were seated in order to reproduce open firings, characterised by a low oxygen fugacity and fast heating rates (Rye, 1981). A reducing atmosphere was forced by firing the speleothem fragments with charcoal pieces. Kiln firing conditions were reproduced with an MT furnace at DMP, equipped with a digital microprocessor (Digitronik DCP200, Yamateke-Honeywell) for firing curve control. All of the fired samples, in addition of the unfired one, were then analysed by scanning electron microscopy (SEM) in order to identify possible structure changes and microstructure development with increasing firing temperature.

Similarly to what observed in the shell fragments (Maritan and Mazzoli 2007), the microstructural analysis revealed that during firing speleothems maintain their structure up to 600°C (figures 4.34.a-b). At 600°C, regardless of the dimension of the fragments, the internal structure of the growth layers tended to fade, showing more clearly the limit between two adjacent growing bands, and small rounded pores along their borders appear (figures 4.34.c-d). The number and size of the pores progressively increase with the firing temperature. Between 650°C and 700°C, pores are mostly slightly bigger and are located along the contact between adjacent growth layers (inter-layer pores) (figures 4.34.e-f). At temperature higher then 750°C, pores become much larger and occur within each of the growth layers (intra-layer pores), especially in proximity to the external surface and in thinner fragments (figure 4.34.g). At temperature of 800°C, and more explicitly at 850°C, the inter-layer pores are so thick to become real fractures and the intra-layer pores increase. In that way the growing laminas of speleothems become more evident than in the original natural situation (figures 4.35. a-f) and numerous intra-layer porous structures develop. The shape, dimension and location of the pores within the microstructure were found to be directly related to the firing temperature and to the fragments sizes. Smaller fragments undergone more easily to decomposition while on the bigger ones it occurs previously on the edges and further in the inner portions. In some cases it was possible to make direct correlation between the speleothems experimentally fired and those present in the potter. Particularly those potsherds whose speleothems were investigated by SEM in detail, were used for making comparisons. Sample 343779, for which a firing temperature lower than 650°C was estimated, presents few inter-layer

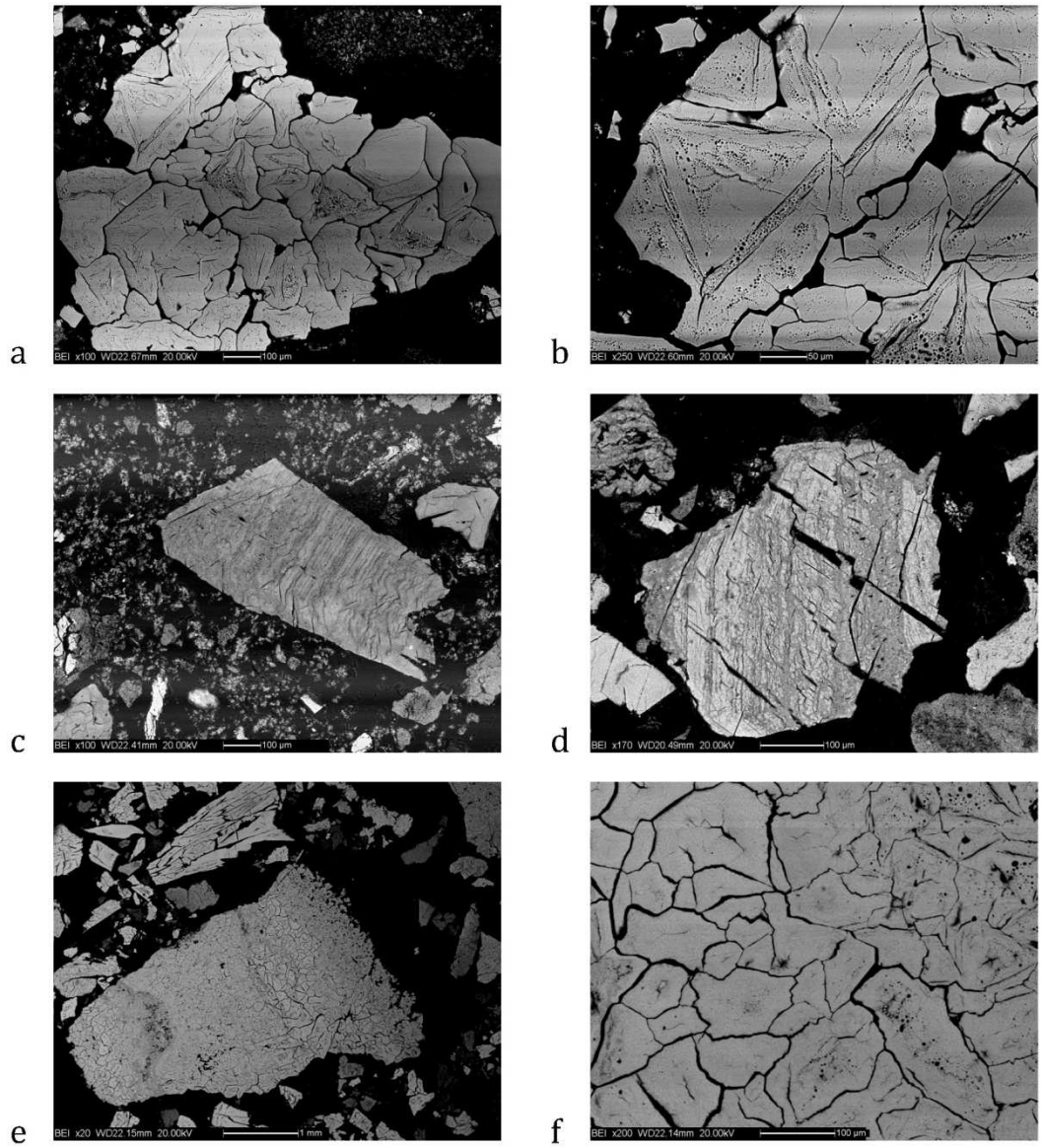

Figure 4. 35. SEM-BSE images of speleothems that undergone to firing experiments. a) Speleothem SP.1 fired at 800°C; b) detail of figure (a); c) speleothem SP.1 fired at 800°C; d) speleothem SP.1 fired at 850°C; e) sample SP.2 fired at 850°C; f) detail of figure (e).

pores in one fragment but also rare intra-layer pores occur in a small fragment (figures 4.36.a-b). Samples 20794, 343771 and 343777, whose estimated firing temperatures range between 650°C and 850°C, present more similarities with speleothems fragments fired at low temperatures, between 650-750°C (figures 4.36.c-e). Sample 31290, probably fired between 750-850°C, present inclusions with both inter-layer and intra-layer pores of bigger dimensions than the previous samples, that seem to confirm a higher temperature interval (figures 4.36.f-g).

At a higher scale these consideration were address at the thin sections. We tried to compare the general display of the fragments in term of evidences of the growing layers of the speleothems fragments analyzed by SEM and those observed in the potsherds by optical microscope. In that cases, although it was not possible to reach the same precision

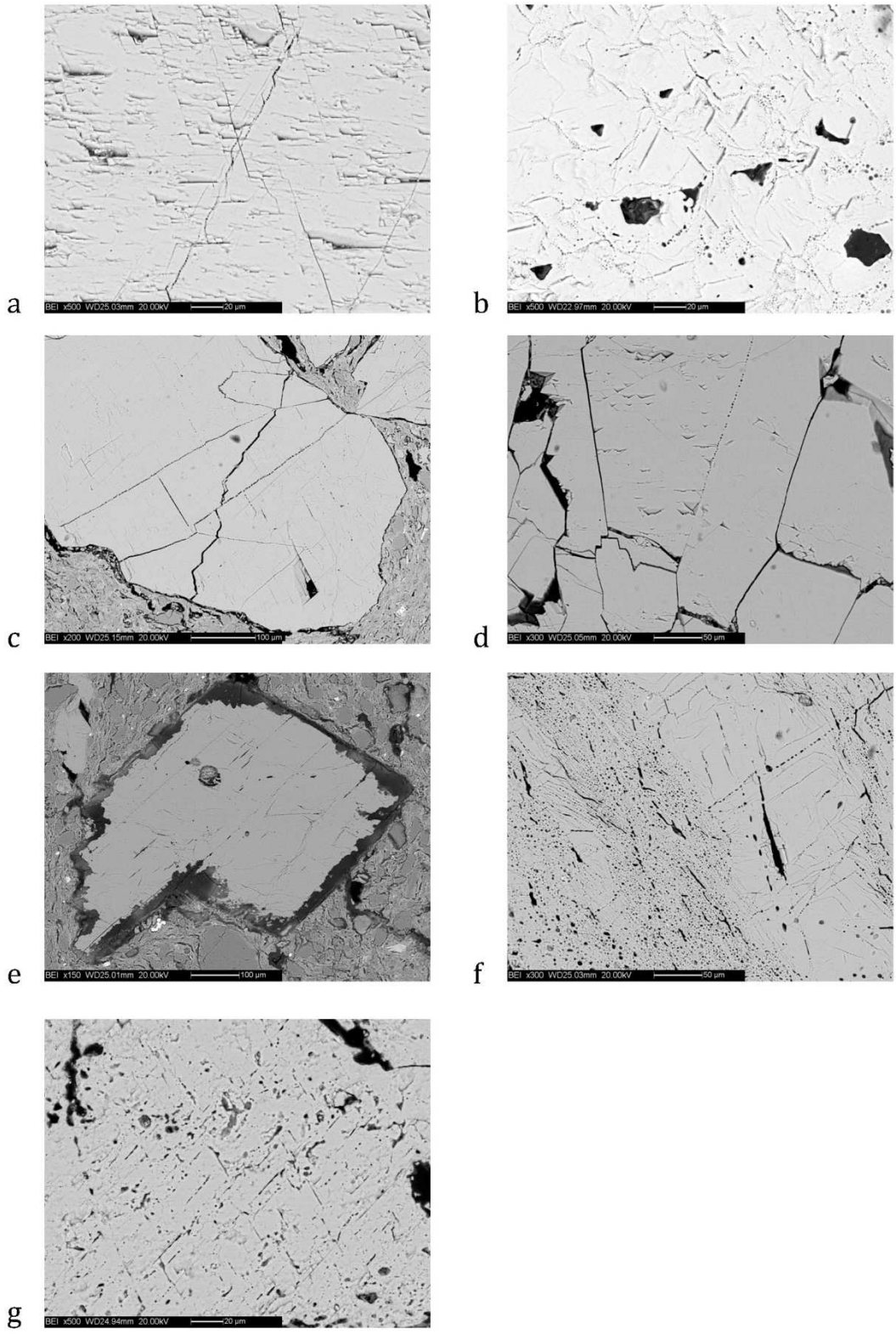

Figure 4. 36 SEM-BSE images of speleothems present in the studied samples. a) sample 343779; b) speleothem SP.1 fired at 650°C; c) sample 20794; d) sample 343771; e) sample 343777; f-g) sample 31290.

acquired at SEM, we observed different situations, and the firing temperatures estimated on the basis of the X-ray diffraction were constrained to a closer temperature interval on the basis of the microstructures observed within the speleothems (figures 4.9.g-h).

4.9 Discussion and conclusions

The study of flared rim and flattened lip ceramics (FRFL pottery) provided interesting results and information about the networks and contacts in the proto-historical north-eastern Italy. Starting point of this work was the PhD research carried out by B. Prosdocimi (2011) about this pottery type and its circulation, with particular regard at the Friuli Venetia Giulia region, under an archaeological point of view. The preliminary information was:

1) the typical FRFL ceramic was widely present, during the late Final Bronze Age and the Iron Age, in the Friuli Venetia Giulia region, in sites related at the Castellieri culture.

2) there was evidence of FRFL pottery also in few sites of the neighboring region of Veneto, where it appeared in a further moment during the Iron Age.

3) the FRFL were not luxury products and rather seemed to have storage functions.

This archaeometrical study was conducted on FRFL pottery found in Venetian sites with the aim of understand whether it was local or imported, of recognizing trades and contacts and defining its production technology. The combined petrographic and chemical analyses of the ceramic samples revealed that the FRFL pots found in Veneto, except six samples from Concrodia Sagittaria and Castion d'Erbé, have high similarity due to the use of temper with very peculiar inclusions: concretions of speleothems. Moreover, the analysis of vases coming from the same Venetian sites but supposed of local origin (because of the different lip and rim forms) reveals a high compositional variability in respect of the FRFL pots. None of these Venetian vases presented speleothems among their inclusions.

The high peculiarity of inclusions and the similarity among the pastes (corresponding to fabric 1) of FRFL pottery found in Veneto suggests that they can be considered real "paste compositional reference units" (PCRUs), archaeologically meaningful. Moreover, this assumption is also enhanced by the high differences with all the Venetian local assemblages analyzed and compared.

Flared rim and flattened lip pots were prepared following similar recipes with slight differences (fabrics 1.1, 1.2, 1.3), except of the few samples from Concordia Sagittaria and Castion d'Erbé that present completely diverse pastes. More in details, this pottery type was hand-made by coiling technique. The frequent presence of clay-pellets suggests that potters were not used to season the raw clay, or at least not for a long period. Most of the non-plastic elements were added: indeed, they range between 10 vol% and 30 vol% with a hiatal structure. In the majority of the samples (fabric 1.1) the coarser temper is represented selectively by speleothems. Only in some situations speleothems are associated to comparable amount of rombohedral calcite crystals with splintery, angular outlines (fabric 1.2) or with burned organics inclusions (like straw), as suggested by

channels voids surrounded by a darkened matrix (fabric 1.3). Ceramic were fired within a wide temperature interval (low of 650-900°C), under reducing atmosphere, likely using rudimental kiln firing techniques. Other pastes and recipes (fabrics 4, 6, 7) must be considered as outliers since only few samples or lonely one belong to them. Therefore, it is not possible to make any consideration about them.

Since the presence of a temper of so unusual composition (speleothems), the high similarity within most of the FRFL pots and the differences within the local potsherds analyzed for comparison allow to consider the FRFL type a production-related group, it is likely that the raw material used came from the same sources. In addition, the comparison with some FRFL pots coming from sites settled in the Friuli Venetia Giulia showed high similarity due to the tempering of these pottery with speleothems. The Friuli Venetia Giulia region is a karsic region with presence of more of seven-thousand caves, natural source of speleothems. Despite the small number of samples here analyzed and coming from the interested area, it seems rational that ceramic import took place from the Friuli Venetia Giulia to Veneto. The low quality of these pots (coarse hand-made ceramic) and their shapes (ovoid jars or double-conic jars among which the Venetian ones have usually narrower orifices) induce to think that their presence in Veneto was the result of exchanges or trades, of the movement of pottery as a container for some other commodity.

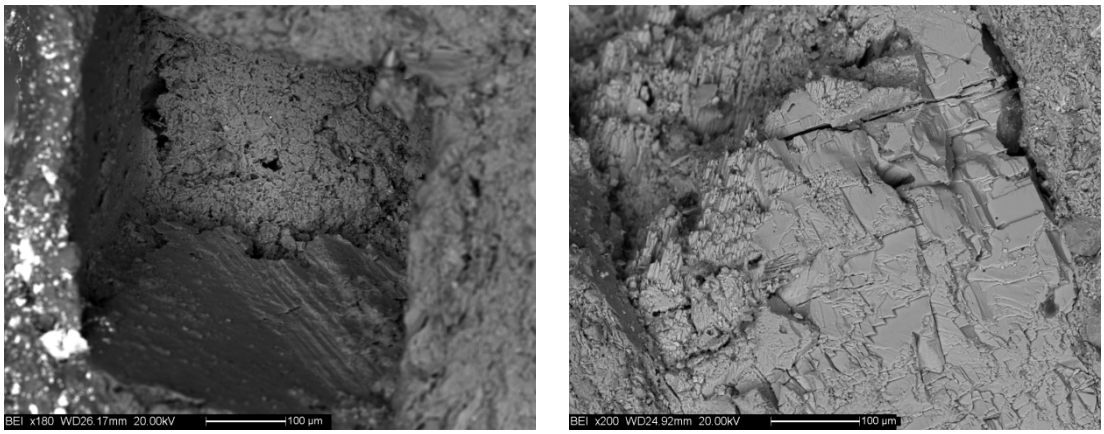

Figure 4. 37 Traces of carbonate fragments undergone to dissolution due to acidic attack.

This interpretation is also supported by the observation that numerous pots have wether/demaged internal surfaces where carbonatic inclusions had undergone dissolution (figure 4.37). This may be due to the original products contained, probably consisting in some acidic substance/material characterized by a PH lower than 7,6 (Berna, Matthews et al. 2003). However, this project must be considered a preliminary work. In order to gain more precise data, a large-scale research should be planned with the aim to widely study the pottery assemblages from settlements of Friuli Venetia Giulia, with particular regard to the Venetia Giulia, of both FRFL types and other forms for comparison. In that way it could be possible to observe whether this temper type was really generally used for the FRFL pottery or whether there were differences in the paste types and in the production recipes adopted, to discriminate between likely production

groups, to observed whether speleothems were used selectively for FRFL pottery or also for other vases.

Since at this stage of the work it is not clear if, in the supposed provenance regions, speleothems were generally used for pottery manufacturing or if they were adopted selectively for FRFL pots, it is difficult to make further considerations about the motivation of this temper selection: if it was the result of purely cultural factors or if it was due to its specific technological characteristics. Indeed, it is known that limestone-tempered pottery, shell tempered pottery (whose behavior is similar to that of speleothems; chapter 4.8) and organic-tempered pottery have superior performance characteristics like impact resistance, resistance to mechanical stress, thermal shock resistance, ease of manufacture, and heating effectiveness (Bronitsky and Hamer 1986, Feathers 1989, Feathers 2003, Feathers 2006, Feathers et al. 2003, Hoard et al. 1995, Skibo et al. 1999, Tite et al. 2001).

Chapter five

5. POST DEPOSITIONAL ALTERATION OCCURRED IN SOME OF THE STUDIED POTSHERDS

Buried pottery may undergo post-depositional alterations. Temperature cycles, freezing, load pressure, groundwater composition, acidity, saturation and redox conditions are the main environmental parameters controlling burial alteration processes. Of these, groundwater is the main weathering agent determining chemical and mineralogical transformations of pottery by dissolution, alteration and/or precipitation of secondary mineral phases on the surface or, through open pores, inside the potsherds (Freestone 2001, Maritan, Mazzoli 2004, Schwedt, Mommsen et al. 2006). Variations in the pristine chemical composition of the pottery represent good evidence of chemical-physical alterations of archaeological finds during burial. This suggests caution when interpreting archaeometrical data since post depositional alterations of chemical and mineralogical composition may cause changes in the chemical and physical properties of pottery and give false interpretation about provenance and production technologies (Freestone 2001, Secco, Maritan et al. 2011).

Post-depositional secondary phases (phosphates and sulphates) were observed also in few samples of potsherds with flared rim and flattened lip. They were analyzed here using a multidisciplinary approach.

5.1 Secondary phosphates in ceramic fragments from Concordia Sagittaria

A good indicator of the alteration processes that can take place during burial is commonly considered the high concentrations of phosphorous oxides (P_2O_5) (Freestone 2001, Lemoine, Meille et al. 1981, Lemoine, Picon 1982). Two phosphate aggregates were detected by optical microscope in sample 31290, from Concordia Sagittaria, indicating a secondary deposition through infilling of the voids, mainly represented by channels and vughs. Source of phosphorous may be bone fragments, seldom used for tempering the pots, or they may be due to the human wastes (Maritan, Angelini et al. 2009).

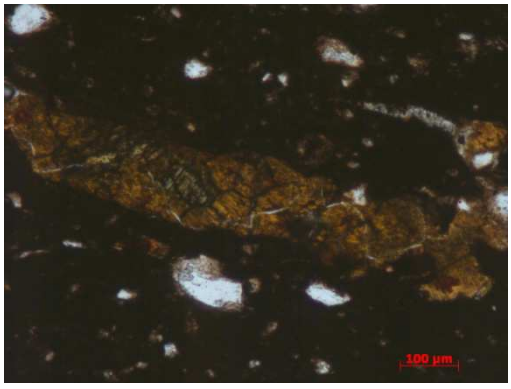

Figure 5. 1. Thin section photomicrographs of phosphate aggregate (P.1). The image was taken in crossed polars.

At Concordia Sagittaria a protohistorical occupation is testified, followed by the foundation of the Roman colony, Iulia

Samples	Provenance	Type	Fabric	SiO_2	TiO_2	Al_2O_3	Fe_2O_3	MnO	MgO	CaO	Na_2O	K_2O	P_2O_5
31490	CS_cemetery area	-	9	68,48	0,68	17,33	5,60	0,02	1,04	1,58	1,16	2,51	0,14
31295	CS_cemetery area	FRFL	1.1	51,70	0,85	15,33	4,59	0,14	1,64	21,23	0,41	2,21	0,35
31420	CS_cemetery area	-	1.1	57,29	0,80	13,53	5,07	0,05	1,23	18,39	0,12	2,31	0,35
31421	CS_cemetery area	FRFL	1.1	50,29	0,84	17,46	7,45	0,13	1,72	19,09	0,22	1,52	0,38
31492	CS_cemetery area	FRFL	1.1	55,83	0,84	15,17	6,52	0,19	1,18	17,38	0,21	1,86	0,48
31282	CS_cemetery area	FRFL	1.1	48,62	0,78	13,85	5,56	0,16	1,08	27,30	0,29	1,85	0,49
31276	CS_cemetery area	-	6	61,15	0,79	18,53	6,51	0,10	3,49	3,31	0,76	3,96	0,52
31290	CS_cemetery area	FRFL	1.3	54,93	0,87	17,23	6,75	0,03	1,57	12,64	0,45	3,07	0,61
31275	CS_cemetery area	FRFL	1.2	54,69	0,88	17,42	6,79	0,03	1,60	13,40	0,45	3,10	0,62
31546	CS_cemetery area	-	12	59,47	0,76	19,89	6,64	0,12	2,10	4,08	1,03	4,01	0,84
31544	CS_cemetery area	FRFL	1.1	46,31	0,81	19,09	7,64	0,09	1,00	21,40	0,20	1,65	1,27

Table 5. 1. Geochemical composition of the major elements whose concentration is expressed as wt% of their oxides.

Concordia. The sample bearing phosphate aggregates was found in domestic settings of the protohistorical record, neighbour the modern cemetery (AA. VV. 1996, Bianchin Citton 1995, Bianchin Citton, Martinelli 2005, Croce De Villa 1991, Mizzan 1996).

In general potsherds from Concordia Sagittaria, and in particular from the area closed to the modern cemetery, had often medium/high content of P_2O_5 that range between 0,14-1,27 wt% (table 5.1). This high concentration can be interpreted as a contamination effect (Freestone 2001, Freestone, Middleton et al. 1994, Lemoine, Picon 1982, Maritan, Mazzoli 2004, Picon 1985).

The two aggregates were identified by optical microscopy in sample 31290. From the digital image analysis performed by SEM and the microscopic analysis, this sample has low porosity (8 vol%) and few inclusions (14 vol%). Pores are generally constituted by

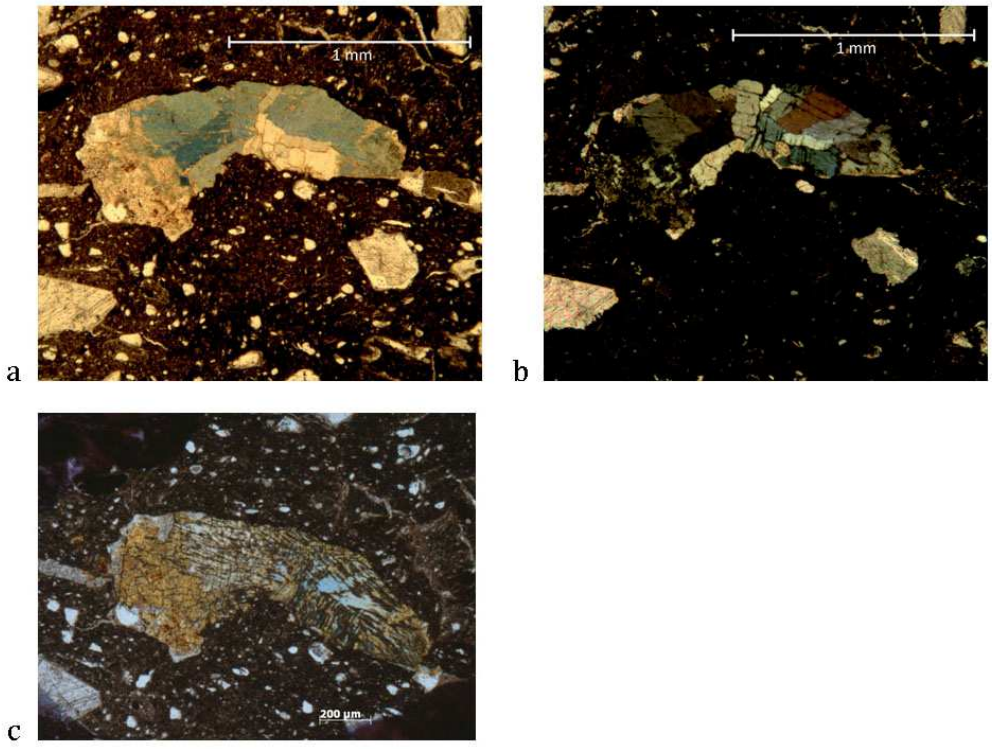

Figure 5. 2. Thin section photomicrographs of phosphate aggregate (P.2). The images were taken in plain polars (a) and in crossed polars (b-c), respectively.

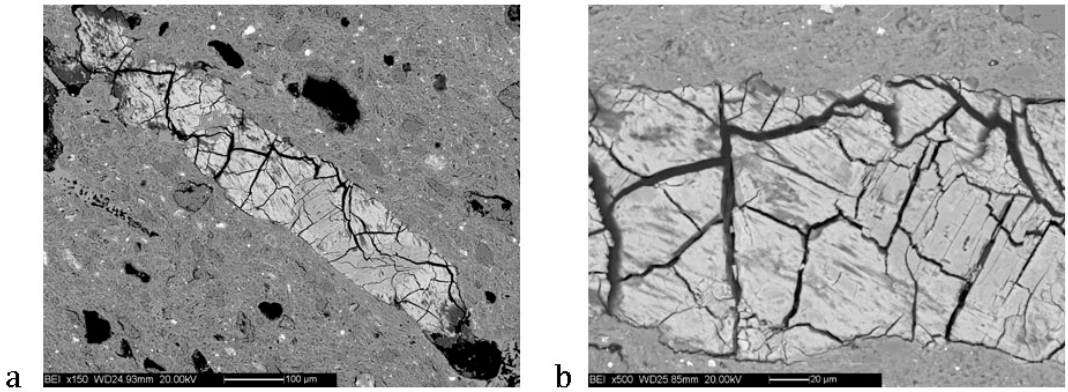

Figure 5. 3. a) SEM-BSE image of the phosphate aggregate P.1; b) Detail of P.1.

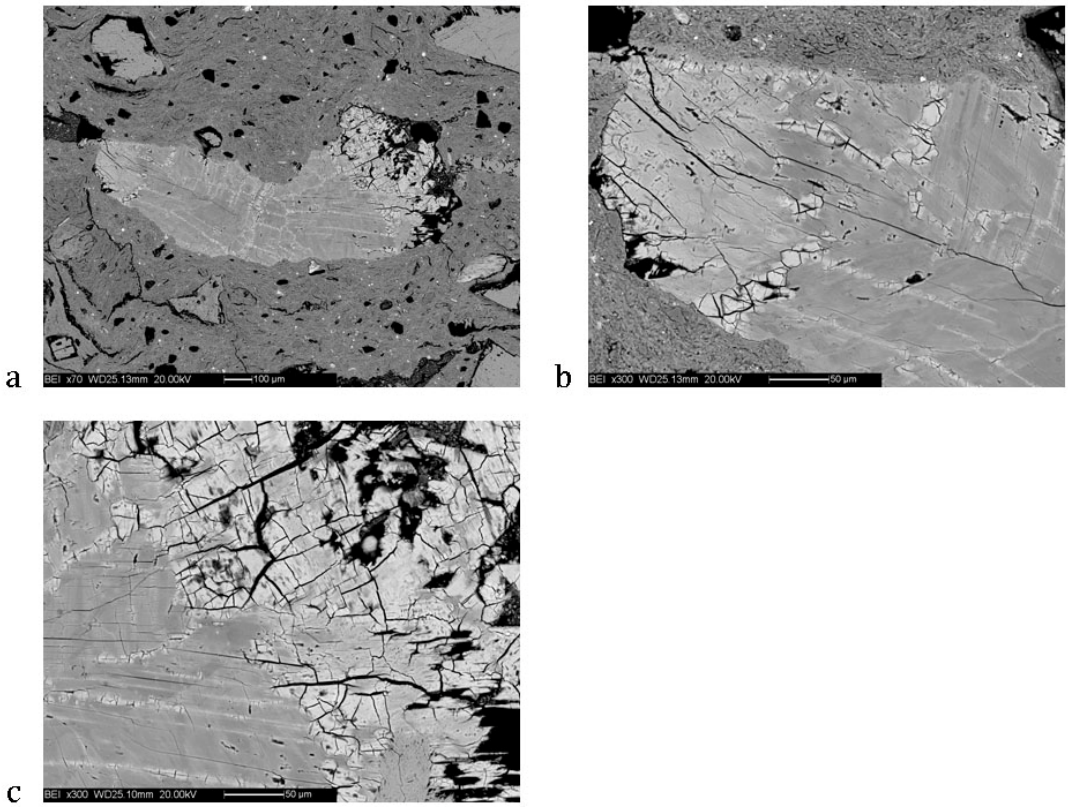

Figure 5. 4. a) SEM-BSE image of phosphate aggregate P.2. b-c) Details of P.2.

vughs and elongated channels strictly aligned with the margins that can reach the dimension of 3,40 x 0,60 mm. The channels appear associated with burnt organics inclusions because of the darkened surrounding matrix. Inclusions have a bimodal grain-size distribution. The coarser fraction varied considerably in sizes (from the very fine sand to gravel sizes). It is composed of sub-angular speleothems fragments. Small amounts of sub-angular and sub-rounded fragments of carbonate mudstone and grog also occurred. The fine fraction (silt sized) is mainly composed of crystals of quartz and calcite, fragments of carbonate mudstone, chert, flakes of muscovite and secondary calcite.

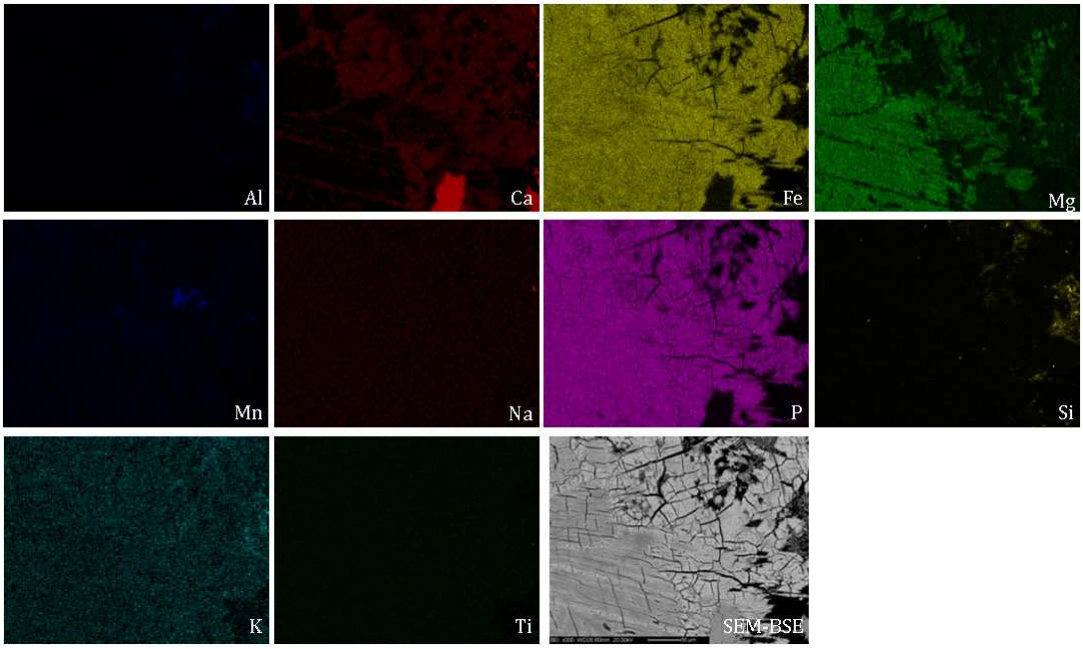

Figure 5. 5. Elemental chemical map of a detailed of P.2.

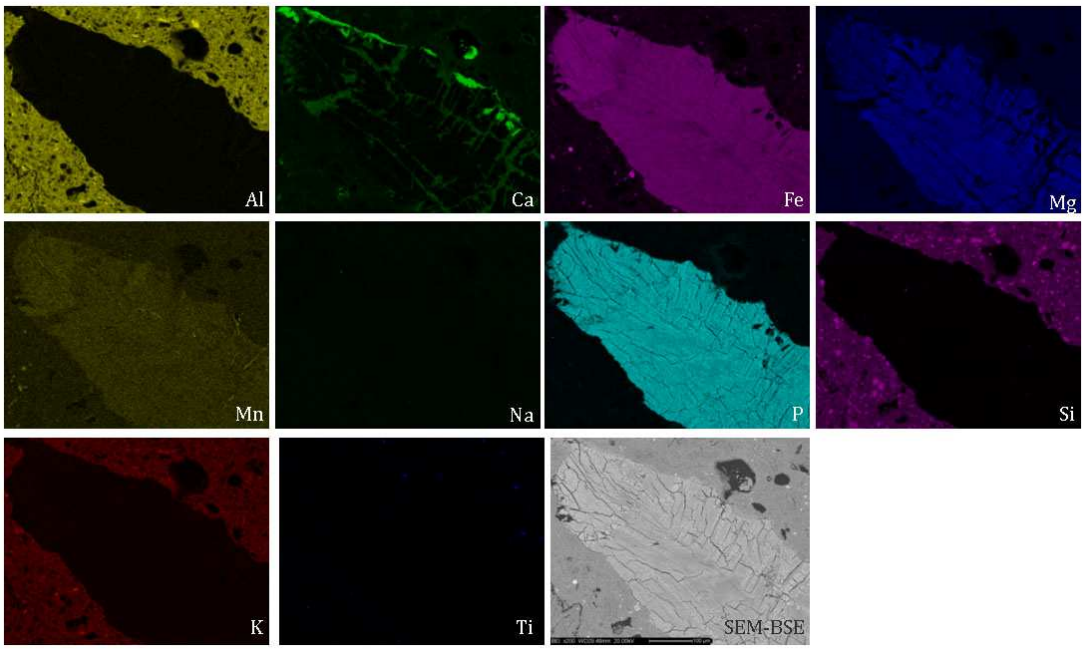

Figure 5. 6 Elemental chemical map of a detailed of P.2.

By optical microscopy the phosphate aggregates properties identify two different mineral species: P.1, phosphate crystallized filling a vugh, characterized by good cleavage and low interference colours on the tone of yellow (figure 5.1). P.2, fan-shaped aggregates of a phosphate where prismatic crystals display perfect cleavage, pleochroism from deep cobalt blue/light blue to pale yellow/colourless, from medium to low interference colours (on the hues of blue, brown, grey) (figure 5. 2). A similar structure was observed also by Dr. Maritan, Angelini et al. (2009) in some phosphate aggregates detected in ceramics from the archaeological site of Frattesina there identified as vivianite.

Since it was not possible to precisely recognize them by the merely optical observation and their concentration was too low to be detected by XRPD, also SEM analysis was performed on the phosphate aggregates in order to investigate their microstructure (figures 5. 3-5.4). Chemical maps of phosphate P.2 were acquired in order to identify the chemical composition and possible changes in the elemental concentration of this aggregate (figures 5.5-5.6). It derived that P.2 was mainly composed of P, Fe and Mg and traces of Mn, Ca was detected mostly along cleavage plains.

Quantitative analyses of major and minor elements (Na, Mg, Al, Si, P, K, Ca, Mn, Fe) were carried out by microprobe in order to define precisely the composition of the two different phosphates. On the two aggregates thirteen and sixteen points analysis, respectively, were acquired (figure 5.7).

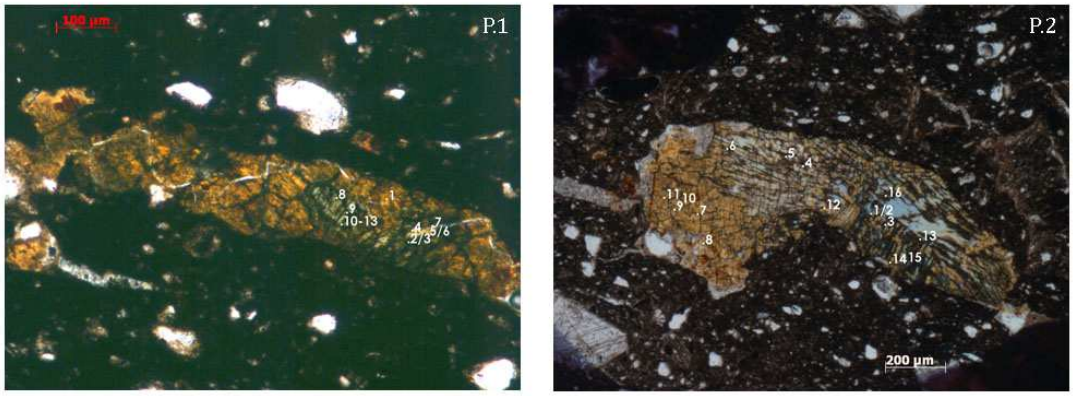

Figure 5. 7. Thin section photomicrographs of the phosphate aggregates (P.1, P.2) with indication of the EMPA points analysis.

The results indicated that the two mineral phases are different (table 5.2). The first one (P.1) is chemically uniform: it is a Fe, Mg phosphate with 34,01-37,11% P_2O_5, 32,92-38,70% Fe_2O_{3tot} and 8,74-11,71% MgO. Only one point analysis (point 1) revealed a different composition with a lower phosphorous content: P_2O_5 (30,54 %), FeO (32,97 %), MgO (1,05%), CaO (15,90 %). Its composition is compatible with a Mg-bearing mitridatite ($Ca_2Fe_3(PO_4)_3O_2 \bullet 3H_2O$) (Maritan, Angelini et al. 2009). The second phosphate (P.2) is a solid solution with a varying composition. It is a Fe, Mg phosphates with 29,74-36,91% P_2O_5, 25,60-35,08% Fe_2O_{3tot}, 9,21-14,01% MgO and 0,31-2,27% CaO, on one extremity the composition changes: the percentage quantities of CaO, SiO_2 and Al_2O_3 increase and P_2O_5, FeO and MgO lowers. Mg, Fe^{2+}, Mn, Ca are all interchangeable elements in the chemical formula of these minerals.

For the second aggregate, although there are various phosphates with similar composition possibly compatible with those detected, since the high compositional variability it was not possible to identify anyone that perfectly matched with it. However, considering that Mg, Fe, Mn and Ca interchanges may have occurred, possible phases are those listed in table 5.3.

To further integrate the mineralogy of the phosphate aggregates, profile high-resolution micro X-ray diffraction was performed on the two aggregates. Since the sample was mounted on a thin-section, it had a glass carrier that contributes to the background

intensity. Unlikely although the carrier thickness was reduced as much as possible so as to reduce at most its noise, it was still too high and the peaks peculiar of the mineral phases were mostly hidden by the high background (figure 5.8). Therefore, none of the phosphates previously identified as suitable constituent of the aggregates perfectly corresponded.

phosphate P.1																	
		1	2	3	4	5	6	7	8	9	10	11	12	13			
Ox%(O)		0,00	0,00	0,00	0,00	0,00	0,00	0,00	0,00	0,00	0,00	0,00	0,00	0,00			
Ox%(Na)		0,06	0,23	0,16	0,07	0,05	0,07	0,00	0,22	0,16	0,16	0,06	0,19	0,28			
Ox%(Mg)		1,06	8,74	8,88	10,82	10,78	11,14	11,61	9,70	9,28	10,61	9,18	8,92	10,00			
Ox%(Al)		0,93	0,22	0,18	0,04	0,03	0,02	0,02	0,06	0,04	0,06	0,06	0,10	0,00			
Ox%(Si)		1,35	0,43	0,52	0,21	0,15	0,13	0,17	0,19	0,18	0,17	0,25	0,22	0,16			
Ox%(P)		30,53	36,01	37,05	35,08	34,56	34,01	37,11	35,52	35,30	34,95	36,07	35,27	35,40			
Ox%(K)		0,11	0,14	0,15	0,04	0,00	0,00	0,02	0,12	0,05	0,06	0,18	0,25	0,08			
Ox%(Ca)		15,90	2,02	2,14	1,76	0,61	0,50	0,60	1,13	0,73	0,45	1,27	1,03	0,54			
Ox%(Mn)		0,00	0,74	0,73	0,74	0,71	0,71	0,72	0,81	0,66	0,63	0,69	0,83	0,79			
Ox%(Fe)		32,97	36,81	38,37	33,23	32,92	33,07	37,07	36,00	34,63	35,22	37,03	38,70	35,90			
W%(O)		33,27	35,99	37,15	34,88	34,10	33,93	37,09	35,40	34,51	34,94	35,82	35,78	35,21			
W%(Na)		0,05	0,17	0,12	0,05	0,04	0,05	0,00	0,17	0,12	0,12	0,04	0,14	0,21			
W%(Mg)		0,64	5,27	5,36	6,52	6,50	6,72	7,00	5,85	5,60	6,40	5,53	5,38	6,03			
W%(Al)		0,49	0,12	0,10	0,02	0,02	0,01	0,01	0,03	0,02	0,03	0,03	0,05	0,00			
W%(Si)		0,63	0,20	0,25	0,10	0,07	0,06	0,08	0,09	0,08	0,08	0,12	0,10	0,08			
W%(P)		13,32	15,72	16,17	15,31	15,08	14,84	16,19	15,50	15,41	15,25	15,74	15,39	15,45			
W%(K)		0,09	0,11	0,12	0,04	0,00	0,00	0,02	0,10	0,04	0,05	0,15	0,21	0,07			
W%(Ca)		11,36	1,44	1,53	1,26	0,43	0,36	0,43	0,81	0,52	0,32	0,90	0,73	0,39			
W%(Mn)		0,00	0,57	0,57	0,57	0,55	0,55	0,55	0,63	0,51	0,49	0,53	0,64	0,61			
W%(Fe)		23,06	25,75	26,84	23,24	23,03	23,13	25,93	25,18	24,22	24,63	25,90	27,07	25,11			
phosphate P.2																	
		1	2	3	4	5	6	7	8	9	10	11	12	13	14	15	16
Ox%(O)		0,00	0,00	0,00	0,00	0,00	0,00	0,00	0,00	0,00	0,00	0,00	0,00	0,00	0,00	0,00	0,00
Ox%(Na)		0,00	0,00	0,07	0,05	0,00	0,03	0,26	0,02	0,17	0,09	0,15	0,08	0,09	0,00	0,00	0,05
Ox%(Mg)		12,20	14,01	13,26	11,10	11,48	11,17	9,21	0,90	0,96	1,01	1,05	13,62	10,14	12,06	12,03	4,72
Ox%(Al)		0,00	0,07	0,05	0,08	0,08	0,03	0,05	2,95	1,71	6,91	1,92	0,00	0,03	0,01	0,03	0,06
Ox%(Si)		0,18	0,11	0,15	0,15	0,09	0,15	0,20	3,18	1,83	9,47	1,39	0,31	0,26	0,23	0,68	0,43
Ox%(P)		32,63	36,91	33,42	29,75	32,86	32,95	34,92	26,09	28,88	13,73	29,68	34,23	33,80	34,65	35,71	32,35
Ox%(K)		0,03	0,00	0,03	0,00	0,00	0,03	0,17	0,08	0,17	0,11	0,12	0,00	0,02	0,06	0,02	0,03
Ox%(Ca)		0,32	0,35	0,42	0,33	0,38	0,34	2,27	13,41	14,40	9,98	15,49	0,52	0,55	0,31	0,44	11,47
Ox%(Mn)		0,41	0,37	0,56	0,49	0,49	0,47	0,77	2,42	0,86	12,09	0,04	0,58	0,47	0,53	0,57	0,26
Ox%(Fe)		27,39	31,47	27,07	25,60	29,26	30,44	34,52	31,49	33,59	19,29	33,54	25,98	32,76	30,22	35,08	30,60
W%(O)		31,75	36,09	32,61	29,20	32,17	32,46	34,76	32,00	32,90	27,84	33,35	32,97	33,36	33,74	36,09	32,91
W%(Na)		0,00	0,00	0,05	0,03	0,00	0,02	0,19	0,01	0,12	0,07	0,11	0,06	0,06	0,00	0,00	0,04
W%(Mg)		7,36	8,45	8,00	6,69	6,92	6,74	5,56	0,54	0,58	0,61	0,63	8,21	6,11	7,27	7,26	2,85
W%(Al)		0,00	0,03	0,02	0,04	0,04	0,02	0,02	1,56	0,90	3,66	1,01	0,00	0,01	0,00	0,02	0,03
W%(Si)		0,09	0,05	0,07	0,07	0,04	0,07	0,09	1,49	0,85	4,42	0,65	0,14	0,12	0,11	0,32	0,20
W%(P)		14,24	16,11	14,59	12,98	14,34	14,38	15,24	11,39	12,61	5,99	12,95	14,94	14,75	15,12	15,59	14,12
W%(K)		0,02	0,00	0,03	0,00	0,00	0,03	0,14	0,07	0,14	0,09	0,10	0,00	0,02	0,05	0,02	0,03
W%(Ca)		0,23	0,25	0,30	0,24	0,27	0,24	1,62	9,59	10,30	7,13	11,07	0,37	0,39	0,22	0,32	8,20
W%(Mn)		0,32	0,28	0,43	0,38	0,38	0,37	0,59	1,87	0,66	9,36	0,03	0,45	0,37	0,41	0,45	0,20
W%(Fe)		19,16	22,01	18,93	17,90	20,47	21,29	24,14	22,02	23,49	13,49	23,46	18,17	22,92	21,14	24,54	21,40

Table 5. 2. Microprobe analysis results for phosphates P.1 and P.2 (Ox%; wt%).

Jahnsite-(CaMgMg)	$CaMg(Mg_2)Fe_2^{3+}(PO_4)_4(OH)_2•8H_2O$
Rittmannite	$(Mn^{2+},Ca)Mn^{2+}Fe^{2+}Al2(OH)2(PO4)4•8(H2O)$
Whiteite –(CaFeMg)	$Ca(Fe^{2+},Mn^{2+})Mg_2Al_2(PO_4)_4(OH)_2•8(H_2O)$
Kaluginite	$(Mn^{2+},Ca)MgFe^{3+}(PO_4)_2(OH)•4(H_2O)$
Segelerite	$CaMgFe^{3+}(PO_4)_2(OH)•4(H_2O)$
Satterlyite	$(Fe_{2+},Mg)_2(PO_4)(OH)$
Ushkovite	$MgFe^{3+}{}_2(PO_4)_2(OH)_2•8(H_2O)$
Baricite	$(Mg,Fe^{2+})_3(PO_4)_2•8(H_2O)$
Richellite	$Ca3Fe^{3+}{}_{10}(PO_4)_8(OH)_{12}•n(H2O)$
Zodacite	$Ca_4Mn^{2+}Fe^{3+}{}_4(PO_4)_6(OH)_4•12(H_2O)$

Table 5. 3. List of the phosphates that may correspond in composition to P.2.

Finally, in order to gain additional information, on P.1. we also performed analysis of Electron Backscatter Diffraction (EBSD) patterns through SEM. This is a powerful tool for crystalline microstructural characterization. It detects crystallographic orientation, grain-boundary character, and phase-distribution information from single and poly-phase crystalline materials. During EBSD analysis any pattern was visible.

The appearance of these phosphate aggregates and the high amount of P_2O_5 in some samples can be related to the presence of the modern cemetery of the city. Here the source of phosphorous seems likely to be related to the dissolution of bone fragments. In soils the precipitation and re-crystallization of phosphates is related to the presence of groundwater and of bacteria activity that control the environmental condition (pH and Eh) (Maritan, Angelini et al. 2009, Maritan, Mazzoli 2004).

The multidisciplinary analyses led to the following considerations: through the combined XRF and microscopy analyses it was observed that high quantity of phosphorous in the bulk chemical data did not correspond necessarily to the presence of phosphate aggregates in the ceramic paste visible at the optical microscopy. The sample with presence of phosphates crystals observed at the optical microscope did not have the higher quantity of P_2O_5, this is in agreement with that observed also by Maritan and

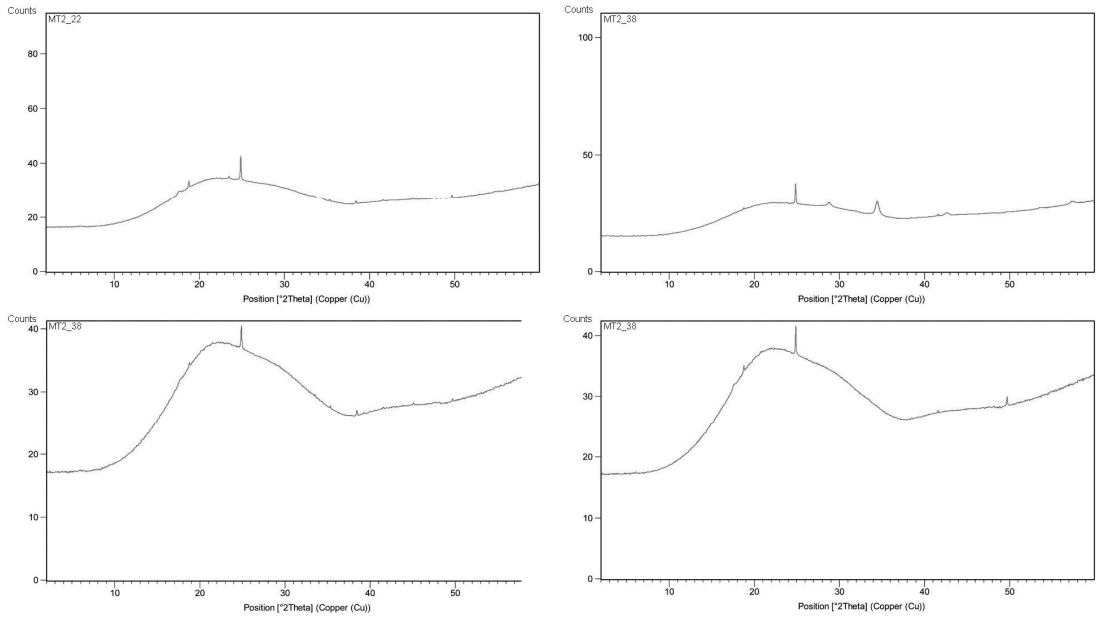

Figure 5. 8. Pattern gained by high-resolution micro-X-Ray diffraction analysis performed on phosphates P.1, here corresponding to sample MT2, and P.2, here corresponding to sample MT1.

Mazzoli (2004). This situation may be explained considering that phosphates can precipitate in the pottery through aqueous solution with a subsequent re-crystallized, or they can even be adsorbed at the surface of primary mineral phases, leading in that way at a variation in the bulk composition (Freestone 2001, Freestone, Meeks et al. 1985, Maritan, Mazzoli 2004, Walter, Besnus 1989).

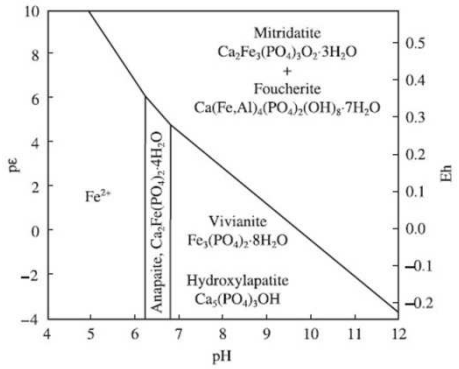

Figure 5. 9. Stability relations for Ca- and Fe-phosphates for dissolved phosphate. After Nriagu and Dell (1974).

The phosphate aggregate P.1 was recognized as a Mg-bearing mitridatite, a phase that forms in relatively alkaline and oxidising environment (Maritan, Angelini et al. 2009, Maritan, Mazzoli 2004). These conditions are also compatible with the presence of secondary calcite that forms for pH higher than 8 (figure 5.9). Secondary calcite can occur in potsherds as a re-crystallized phase, which forms after firing for carbonation of CaO or $Ca(OH)_2$ formed during firing for decomposition of calcite, or can be the result of re-crystallization of soil components (Buxeda i Garrigós, Cau 1995). Generally it requires alkaline conditions of the solution at normal concentrations of calcium and hydrogen carbonate, and precipitates according to the following reaction:

$$Ca^{2+}_{(aq)} + HCO^{-}_{3} \rightarrow CaCO_{3(s)} + H^{+}$$

It was not possible to identify precisely the phosphate aggregate P.2, although we found numerous phases that could be compatible.

5.2 Secondary sulphates formed in potsherds coming from lagoon-like environments

Post-depositional sulphates were observed in few potsherds from Aquileia and Terzo Ramo del Timavo, two coastal sites located in the Friuli Venetia Giulia region. Both these settlements may be considered transitional environment characterized by burial conditions between land and marine-base, with the typical lagoon-like environmental chemical-physical conditions.

The site of the Terzo Ramo del Timavo (S. Giovanni di Duino, Trieste, Italy) was located at the mouth of the third branch of the Timavo river. It was a 150 m^2 wide pottery deposit, on a highly steep floor lying in shallow sea water reaching nearly 7 m deep that can be considered as a lagoon-like place.

The protohistical site of Aquileia, dated at the beginning of the Iron Age, was located close to the sea, along the Natissa river. The archaeological excavation interested a small area of the settlement, particularly it found part of domestic places (through which a “fired clay floor”, suitable for humid environments) settled on wooden drainage structures. Moreover, a 60-120 cm thick floodplain alluvium covered the Iron Age site isolating it

from the more recent Roman records. Besides, presences of important waterways in the Aquileia deltaic plain in antiquity and rivers flooding have been recently attested indicating a swamp environment (Arnaud-Fassetta, Carré et al. 2003). In addition, periodic sea-level rise and subsidence affected its chemical-physical conditions and produced changes in salinity (Arnaud-Fassetta, Carré et al. 2003, Secco, Maritan et al. 2011).

Post-depositional modifications that occurred in potsherds, mostly in land and marine environments, are commonly observed and described in archaeometric researches by several authors (Buxeda 1999, Buxeda i Garrigós, Cau Ontiveros et al. 2005, Heimann, Maggetti 1981, Maggetti, Westley et al. 1984, Maritan, Mazzoli 2004, Pradell, Vendrell-Saz et al. 1996, Schleicher, Miller et al. 2008, Schwedt, Mommsen et al. 2006, Secco, Maritan et al. 2011). A study about alteration processes of pottery in lagoon-like environments was recently carried out by Secco, Maritan et al. (2011). Lagoon-like environments are generally characterized by high salinity, alkaline and reducing water conditions, and high anaerobicity, due to the intense activity of micro-organisms, the abundance of organic matter, and low water exchanges. Salinity is generally between the level in freshwater and in the open sea, and may vary significantly over time, depending on different freshwater versus seawater contributions, the evolution of local geomorphological features, and hydrology (Secco, Maritan et al. 2011). All these features contribute to the formation of reductive basic environmental conditions, with Eh between -0.3 and -0.6 V and pH often exceeding 8 (Garrels 1960, Secco, Maritan et al. 2011), suitable for sulphate-reducing bacterial colonies to flourish (Dellwig, Böttcher et al. 2002, Fors, Nilsson et al. 2008, Howarth, Giblin 1983, Howarth, Teal 1979, Preda, Cox 2004). The micro-organisms are able to reduce sulphate ions in salt water to sulphur or hydrogen sulphide, by a variety of metabolic processes. Sulphate ions act as final electron acceptors in concomitant oxidation of simple organic compounds such as acetic and fatty acids, which donate electrons by reactions such as (Secco, Maritan et al. 2011, Sørensen, Christensen et al. 1981):

$$CH_3COO^- + SO_4^{2-} \rightarrow HS^- + 2HCO_3^-$$

All the sulphate-bearing potsherds belong to the fabrics 1.1 (sample 6247) and 1.3 (samples 625, 637, 418905). Sample 6247 (fabric 1.1) has an optically active (speckled birefringent fabric) heterogeneous groundmass. There are few voids (5% of the total area) consisted mainly of channels and vughs of medium sizes (d_{max} 2mm). Inclusions are the 15% of the total area that can reach 3, 60 mm sizes, they have a poorly sorted bimodal grain-size distribution. They are mainly composed of speleothems and few small quartz crystals.

Samples 625, 637 and 418905 (fabric 1.3) have an optically active (speckled birefringent fabric) heterogeneous groundmass. Voids are abundant (10-20% of the total area) consisted mainly of long channels surrounded by dark boundaries and fewer vughs (d_{max} 4,8 x 0,3 mm). Inclusions are the 10-15% of the total area, that can reach sizes of 4,80

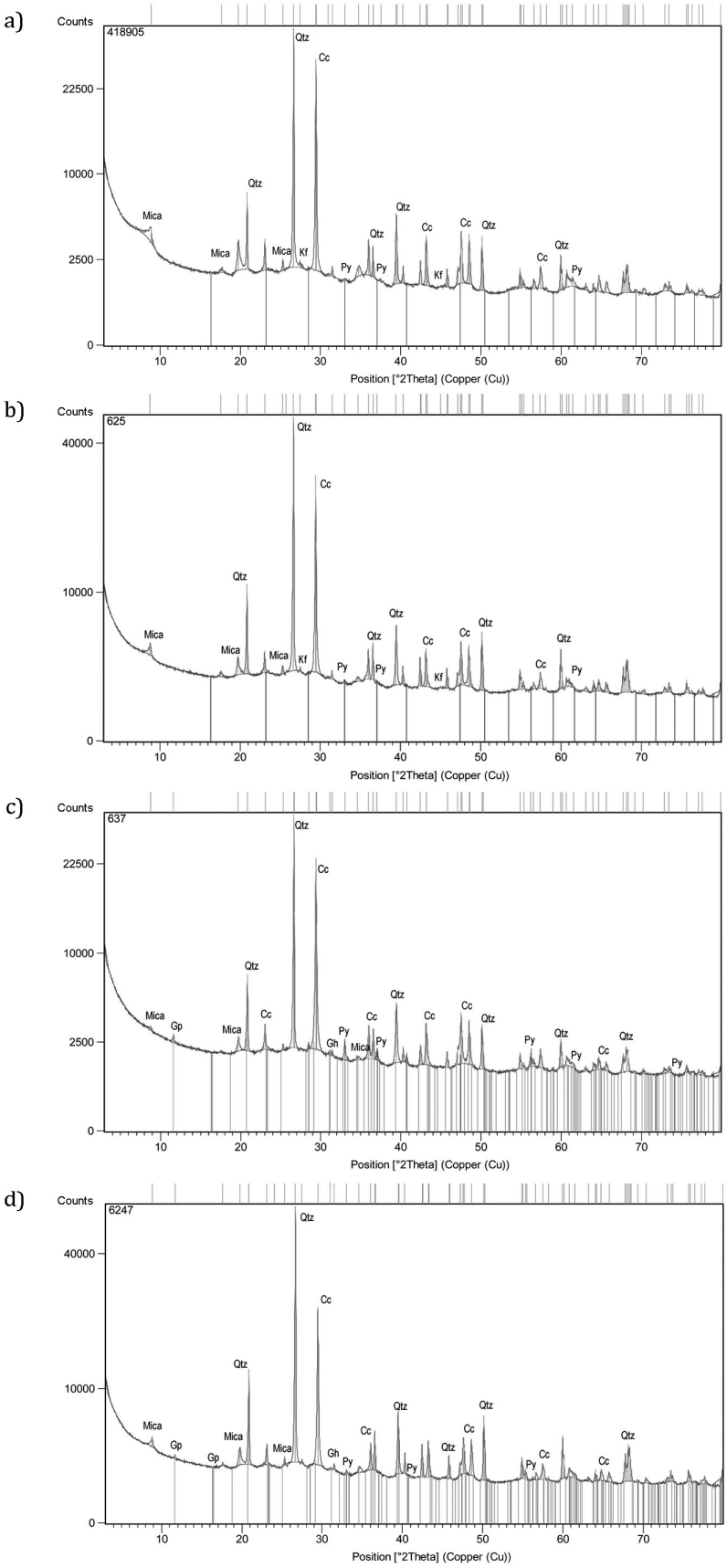

Figure 5. 10. X-ray diffraction patterns of sample 418905 from Aquileia and samples 625, 637 and 6247 from Terzo Ramo del Timavo site. Abbreviations for mineral names: Qtz, quartz; Kf, K-feldspar; Mica, mica; Cc, calcite; Py, pyrite; Gp, gypsum; Gh, gehlenite. Pyrite and gypsum are underlined by the coloured lines.

mm, they have a moderately sorted bimodal grain-size distribution and are mainly composed of speleothems and fewer calcite, sparry calcite and small quartz crystals. The channel voids are associated to burnt organics inclusions because of the darkened surrounding matrix. None secondary calcite was observed in any pores.

XRPD analysis indicates that the sample coming from Aquileia belongs to groups $A1_{xrd}$ and those coming from Terzo Ramo del Timavo to the groups $A1_{xrd}$ and $A2_{xrd}$ (see chapter 4.5). They are characterized by abundant quartz and calcite associated with scarce illite, plagioclase and alkali-feldspars (like microcline) are occasionally present in small amounts. In few samples ($A2_{xrd}$) there are also traces of high temperature minerals like gehlenite while hematite is absent. All samples contain also pyrite, while only in two of them (637 and 6247 from Terzo Ramo del Timavo) it is associated to gypsum (figure 5.10). Sulphates are always present in few quantities. XRPD analysis was carried out on the bulk composition of samples and core and margins were not differentiated.

A model to describe post-depositional alteration effects and processes that pottery may undergone during burial in lagoon-like environments was recently developed by Secco, Maritan et al. (2011) and it was here followed applied to the interested potsherds.

The presence of pyrite and the absence of hematite may suggest the decomposition of hematite through reduction from Fe^{3+} to Fe^{2+} and solubilisation. Two main mechanisms have been proposed in the literature. The first considers hematite hydroxylation to goethite, according to the following reaction (Bedarida, Flamini et al. 1973, Secco, Maritan et al. 2011):

$$Fe_2O_3 + H_2O \rightarrow 2FeOOH$$

and goethite dissolution by either bacterial reduction or reaction with hydrogen sulphide in water solution according to the following reactions, respectively (Pyzik, Sommer 1981):

$$2FeOOH + R\text{-}CH_2OH + 2H^+ \rightarrow 2Fe_2{}^+{}_{(aq)} + R\text{-}COOH + 3H_2O$$

$$2FeOOH + H_2S \rightarrow 2Fe_2{}^+{}_{(aq)} + S + 4OH^-$$

As the concentration of hydrogen sulphide produced by the trophic processes of sulphate reducing bacteria is generally high in lagoon environments, goethite most probably dissolved according to the last reaction (Secco, Maritan et al. 2011).

An alternative mechanism consists of direct reductive dissolution of hematite by hydrogen

sulphide, according to the reaction (Neal, Techkarnjanaruk et al. 2001, Secco, Maritan et al. 2011):

$$Fe_2O_3 + H_2S + 4H+ \rightarrow 2Fe_2{}^+{}_{(aq)} + S + 3H_2O$$

Ferrous iron then reacts with additional hydrogen sulphide and forms pyrite, following various reactions, strongly depending on local environmental conditions (Secco, Maritan et al. 2011). Pyrite can crystallize through the reaction between ferrous iron (Fe^{2+}) and HS^- with the formation of unstable iron monosulphide, disordered mackinawite ('FeS') (Secco, Maritan et al. 2011, Wilkin, Barnes 1997):

$$Fe_2^{+}{}_{(aq)} + HS^{-} \rightarrow \text{'FeS'} + H^{+}$$

('FeS') is then transformed to pyrite (Secco, Maritan et al. 2011, Wilkin, Barnes 1997):

$$\text{'FeS'} + H_2S_{(aq)} \rightarrow FeS_2 + H_{2(g)}$$

$$\text{'FeS'} + S \rightarrow FeS_2$$

$$2\text{'FeS'} + 2H+ \rightarrow FeS_2 + Fe_2^{+} + H_{2(g)}$$

The occurrence of gypsum in some samples from Terzo Ramo del Timavo is due to the intense acidification caused by pyrite oxidation, to the reaction of released sulphate anions with Ca^{2+}, either present in pore-water (first formula) or derived by dissolution of secondary calcite previously precipitated within pores (second formula):

$$Ca^{2+}{}_{(aq)} + SO_4^{2-}{}_{(aq)} + 2H_2O \rightarrow CaSO_4 \bullet 2H_2O_{(s)}$$

$$CaCO_{3(s)} + SO_4^{2-}{}_{(aq)}2H_2O \rightarrow CaSO_4 \bullet 2H_2O_{(s)} + CO_3^{2-}{}_{(g)}$$

According with Secco (2011), the presence in two samples from Terzo Ramo del Timavo, of gypsum -crystallized during pyrite oxidation in seawater- generally indicates considerable changes in the chemical-physical conditions of burial, from pH > 8 and Eh between -0.3 and -0.6 V to lower pH and more positive Eh values.

Differences in the habit of pyrite crystals are related to diverse environmental burial conditions. Since this specific study must be considered at a preliminary level, none sulphide aggregate is visible at the optical microscopy and no SEM microstructural analyses have already carried out, it is not possible to make any consideration about the different pyrite crystals habits and possible relations with the burial environments.

All these secondary processes were thermodynamically described by Secco, Maritan et al. (2011) using the PHREEQC package (for major details about this modelisation see (Secco, Maritan et al. 2011).

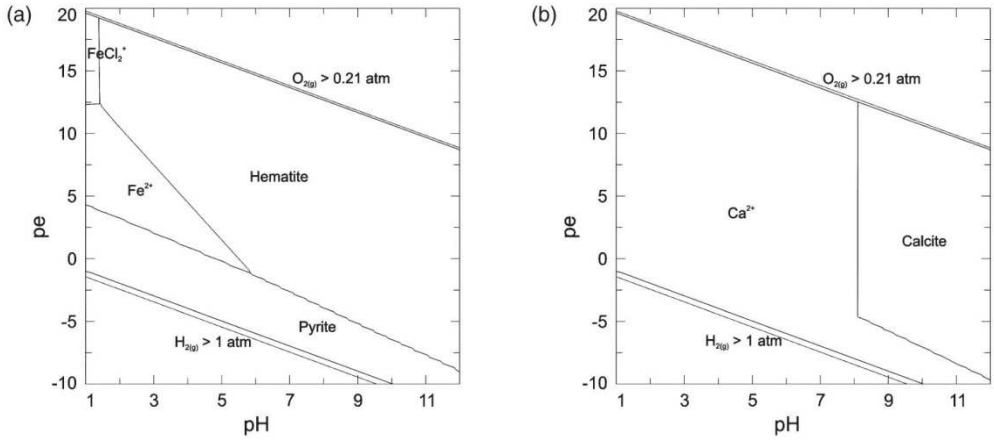

Figure 5. 11. a) A pe–pH diagram of iron calculated by PhreePlot (Kinniburgh and Cooper 2009), and referring to a solution of seawater composition. Common iron oxides and sulphides (hematite, goethite, magnetite, jarosite, mackinawite, pyrrhotite and pyrite) were examined. b) A pe–pH diagram of calcium calculated by PhreePlot, referring to a solution of seawater composition. Common calcium carbonates and sulphates (calcite, aragonite, gypsum and anhydrite) were examined

The Eh–pH diagram (figure 5.11.a) shows that pyrite is stable for negative values of the redox potential while calcite, which may be also present in secondary assemblages, can precipitate from seawater at pH>8 (figure 5.11.b), providing further constraints on the model. These results were consistent with an environment dominated by the action of sulphate-reducing bacteria and with the observation that pyrite is the only low-Eh iron phase present in the studied samples (Raiswell, Canfield 1998).

Post-depositional secondary phases of sulphates were detected by XRPD in four potsherds coming from Aquileia and Terzo Ramo del Timavo, two coastal sites located in the Friuli Venetia Giulia region. Both these settlements may be considered lagoon-like environments characterized by high salinity, basic and reducing water conditions and highly anaerobic, subjected by an intense activity of sulphate-reducing bacterial colonies.

The salinity in the burial environment at Aquileia was probably lower than at the Terzo Ramo del Timavo due to the greater distance from the open sea.

The presence of pyrite in these samples is probable due by the replacement of hematite originally contained in the pottery. Generally this occurs at negative values of the redox potential and basic conditions of burial.

The crystallization of gypsum after pyrite in two samples from the Terzo Ramo del Timavo suggests drainage and oxidation of the sediments. Gypsum formed at very low pH values and high concentrations of dissolved salt.

CONCLUSIONS

This project concerned the study of pottery coming from protohistorical sites of the north-east of Italy dated between the Early Bronze Age and the first Iron Age. Through the archaeometric results on ceramic technology and provenance, it contributed to wider themes about these protohistoric communities: particularly, provenance data were useful to examine trades, exchanges and migrations while the interpretations of technology to examine the craft tradition, its evolution and the relationships to large scale processes that took place in the societies over time.

In order to gain these aims, three 'case studies' involving all the north-east of Italy and the whole interested period were developed and undergone to an integrated analytical approach: 1) Castel de Pedena and the Luco/Laugen-Meluno/Melaun ceramics, 2) the flared rim and flattened lip pottery (here called FRFL) widely present in the Friuli Venetia Giulia region but found also in the neighbouring Veneto, 3) pottery from the terramara site of Fondo Paviani. These locations were selected depending on the presence, among the archaeological fictile finds, of shards peculiar of other places and cultures. Firstly the study aimed to identify possible importation cases (due to the products circulation), to define if they were produced in different places by the same potters (due to the people circulation), or rather if they were local objects produced by locals thanks to the circulation of different ceramic models.

In that way a better comprehension of the relationships between populations settled in the Veneto region with the neighbouring cultures were achieve:

- between mountain and plain sites during the Recent Bronze Age through the study of pottery from Castel de Pedena and Fondo Paviani,
- with the near Luco/Laugen-Meluno/Melaun culture present in the Italian South Tyrol and Trentino, the Austrian East Tyrol, in Liechtenstein and in the Swiss Grisons during the Final Bronze Age through the study of Castel de Pedena pottery assemblage,
- with the Friuli Venetia Giulia region during the Final Bronze Age and the first Iron Age, through the study of FRFL pottery coming mostly from Venetian sites.

From the study of the pottery assemblage from Castel de Pedena, and in particular of the Luco/Laugen-Meluno/Melaun ceramic, a pottery type peculiar of north-western regions, important information arose. Although it appears that this pottery was produced locally and no ceramic trade could be identified for these vases, a so high similarity in the shapes of vessels proves the existence of intensive contacts with the northern regions. This type of ceramic may have been manufactured by local people who adopted a new style or by potters who had migrated but who may have continued to use their traditional methods. Further important information gained by the study of the ceramics from Castel de Pedena

was the possibility to delineate the evolution of the production technology from the Recent Bronze Age to the first Iron Age. Paste compositional reference units (PCRUs), archaeologically meaningful, were identified, indicating significant changes over time in the potters technological habits.

Through the combined petrographic and chemical analyses of flared rim and flattened lip ceramics, the FRFL pots found in Veneto and Friuli Venetia Giulia regions appeared to have high similarity. This was due to the preparation following similar recipes and the selection of very peculiar inclusions (concretions of speleothems) as temper. The presence of speleothems links this pottery to the Friuli Venetia Giulia, a karsic region with presence of more of seven-thousand caves natural source of speleothems. The presence of this ceramic type in the Veneto region can be related to the trade of some specific products probably contained into these vases, starting from the Friuli Venetia Giulia towards the Veneto.

The third 'case study' concerns a small sample of potsherds coming from the site of Fondo Paviani (Verona, Italy) and it must be consider a preliminary study. It was observed that during the Recent Bronze Age the common use of produce coarse pottery with macroscopically similar pastes spread in all the 'Palafitticolo Terramaricola' culture sites. Moreover in the coeval level of the site of Castel de Pedena specimens typical of the 'Palafitticolo Terramaricola' culture were found. This induced to analyze also this small assemblage from Fondo Paviani with the intention to compare it with similar shards from Castel de Pedena. The number of samples analyzed was very small and not statistically representative of the real context of the site. For the same reason it was not possible to make any general correlation between the pottery productions of Fondo Paviani and Castel de Pedena.

This project must be considered a preliminary step toward a better comprehension of trades and exchanges between prehistoric populations of the north-eastern Italy and toward a better knowledge of the technical choices and habits of the ancient potters. In order to gain this, large-scale projects and collaborations between researchers with scientific and archaeological expertises should be planned.

REFERENCES

AA VV., 1984. *Preistoria del Caput Adriae, Atti del Convegno Internazionale (Trieste, 19-20 novembre 1983).* Trieste.

AA VV., 1996. *La protostoria tra Sile e Tagliamento. Antiche genti tra Veneto e Friuli, Catalogo della mostra (Concordia Sagittaria, 14 settembre-10 novembre 1996; Pordenone, 23 novembre 1996-8 gennaio 1997).* Padova.

AA VV., 2010. *Il villaggio di Frattesina e le sue necropoli (XII-X secolo a.C.).* Museo Archeologico Nazionale di Fratta Polesine.

ARNAUD-FASSETTA, G., CARRÉ, M., MAROCCO, R., MASELLI SCOTTI, F., PUGLIESE, N., ZACCARIA, C., BANDELLI, A., BRESSON, V., MANZONI, G., MONTENEGRO, M.E., MORHANGE, C., PIPAN, M., PRIZZON, A. and SICHÉ, I., 2003. The site of Aquileia (northeastern Italy): example of fluvial geoarchaeology in a Mediterranean deltaic plain / Le site d'Aquilée (Italie nord-orientale): exemple de géoarchéologie fluviale dans une plaine deltaïque méditerranéenne. *Géomorphologie: relief, processus, environnement,* **9**(4), pp. 227-245.

ARPAV, 2005. *Carta dei Suoli del Veneto in scala 1:250.000.* ARPAV.

BAGOLAN, M. and LEONARDI, G., 2000. Il Bronzo finale nel Veneto. In: M. HARARI and M. PEARCE, eds. In: *Il Protovillanoviano al di qua e al di là dell'Appennino, Atti della giornata di studio (Pavia, Collegio Ghislieri, 17 giugno 1995)*, 17 giugno 1995, 2000, New Press, pp. 15-46.

BALISTA, C. and DE GUIO, A., 1997. Ambiente ed insediamenti dell'età del bronzo nelle Valli Grandi Veronesi. In: M. BERNABÒ BREA, A. CARDARELLI and M. CREMASCHI, eds, *Le Terramare. La Più Antica Civiltà Padana.* Modena, pp. 137-165.

BALISTA, C. and LEONARDI, G., 2003. Le strategie di insediamento tra II e inizio I millennio a.C. in Italia settentrionale centro-orientale, *Atti della XXXV Riunione Scientifica dell'Istituto Italiano di Preistoria e Protostoria, Firenze* 2003, pp. 159-171.

BALISTA, C. and LEONARDI, G., 1998. Gli abitati di ambiente umido in Italia settentrionale. In: D. COCCHI GENICK, ed, *L'antica età del bronzo in Italia.* Firenze, pp. 199-228.

BAXTER, M.J., 2006. A review of supervised and unsupervised pattern recognition in archaeometry. *Archaeometry,* 48 (4), pp. 671-694.

BAXTER, M.J., 2001. Multivariate analysis in archaeology. In: D.R. BROTHWELL and A.M. POLLARD, eds, *Handbook of archaeological sciences.* Chichester: Wiley, pp. 687-694.

BAXTER, M.J., 1999. Detecting multivariate outliers in artefact compositional data. *Archaeometry,* 41.

BAXTER, M.J. and FREESTON, I.C., 2006. Log-ratio compositional data analysis in archaeometry. *Archaeometry,* 48 (3), pp. 511-531.

BEDARIDA, F., FLAMINI, F., GRUBESSI, O. and PEDEMONTE, G.M., 1973. Hematite to goethite surface weathering: scanning electron microscopy. *American Mineralogist,* **58**, pp. 794-795.

BELLINTANI, P., 1998. Cànar di San Pietro Polesine. Breve sintesi sugli studi archeologici. In: C. BALISTA and P. BELLINTANI, eds, *Cànar di San Pietro Polesine. Ricerche paleoambientali sul sito palafitticolo, Quaderni di Padusa, 2.* pp. 15-21.

BELLINTANI, P., 1987. I materiali dell'età del bronzo di Cànar (Castelnovo Bariano - Rovigo): le raccolte di superficie. *Padusa,* XXIII, pp. 147-188.

BERNABÒ BREA, M. and CARDARELLI, A., 1997. Le terramare nel tempo. In: M. BERNABÒ BREA, A. CARDARELLI and M. CREMASCHI, eds, *Le Terramare. La più antica civiltà padana, Catalogo della Mostra, Milano.* Milano, pp. 295-301.

BERNABÒ BREA, M., CARDARELLI, A. and CREMASCHI, M., 1997. Il crollo del sistema terramaricolo. In: M. BERNABÒ BREA, A. CARDARELLI and M. CREMASCHI, eds, *Le Terramare. La più antica civiltà padana, Catalogo della Mostra, Milano.* Milano, pp. 745-753.

BERNABÒ BREA, M. and CREMASCHI, M., 1997. Le terramare: "palafitte a secco" o "villaggi arginati"?. In: M. BERNABÒ BREA, A. CARDARELLI and M. CREMASCHI, eds, *Le Terramare. La più antica civiltà padana, Catalogo della Mostra, Milano.* Milano: pp. 187-195.

BETTELLI, M. and VAGNETTI, L., 1997. Aspetti delle relazioni fra l'area egeo-micenea e l'Italia settentrionale. In: M. BERNABÒ BREA, A. CARDARELLI and M. CREMASCHI, eds, *Le Terramare. La più antica civiltà padana, Catalogo della Mostra, Milano.* Milano, pp. 614-620.

BIANCHIN CITTON, E., 1995. Concordia Sagittaria in età preromana: lo stato della ricerca. *Concordia e la X regio,* pp. 229-254.

BIANCHIN CITTON, E., 1989. Considerazioni metodologiche relative alla presenza di ceramica di stile appenninico nei complessi veneti: funzione e cronologia, *Atti della XXVI Riunione Scientifica dell'Istituto Italiano di Preistoria e Protostoria, Ferrara*, 1987. 1989, pp. 171-179.

BIANCHIN CITTON, E. and MARTINELLI, N., 2005. Cronologia relativa e assoluta in alcuni contesti veneti dell'età del Bronzo recente, finale e degli inizi dell'età del Ferro. Nota preliminare. *Oriente e Occidente,* pp. 239-253.

BIETTI SESTIERI, A.M., 1996. *Protostoria. Teoria e pratica.* Roma: La Nuova Italia Scientifica.

BISHOP, R.L. and NEFF, H., 1989. Compositional data analysis in archaeology. In: R.O. ALLEN, ed, *Archaeological Chemistry IV.* Washington: pp. 57-86.

BORGNA, E., CANEVER, L., SPANGHERO, T. and VITRI, S., 1991. S. Ruffina di Palse di Porcìa. Scavi 1991. *Aquileia Nostra,* LXII, pp. 276-280.

BRADLEY, W.F., 1945. Molecular ssociations between montmorillonite and some polyfunctional organic liquid. *Journal of American Chemical Society,* 67 (6), pp. 975-981.

BUXEDA, J., 1999. Alteration and Contamination of Archaeological Ceramics: The Perturbation Problem. *Journal of Archaeological Science,* 26, pp. 295-313.

BUXEDA, J., KILIKOGLOU, V. and DAY, P., 2001. Chemical and mineralogical alteration of ceramics from a Late Bronze Age kiln at Kommos, Crete: the effect on the formation of a reference group. *Archaeometry,* 43 (3), pp. 349-371.

BUXEDA, J., MOMMSEN, H. and TSOLAKIDOU, A., 2002. Alterations of Na, K and Rb concentrations in Mycenaean pottery and a proposed explanation using X-ray diffraction. *Archaeometry,* 44 (2), pp. 187-198.

BUXEDA I GARRIGÓS, J., CAU ONTIVEROS, M.A., MADRID I FERNÁNDEZ, M. and TONIOLO, A., 2005. Roman amphorae from the *Iulia Felix* ship wreck: alteration and provenance. In: H. HARS and E. BURKE, eds, *Proceedings of the 33rd International Symposium on Archaeometry, Geoarchaeological and Bioarchaeological Studies, Vol. 3, Institute for Geo- and Bio-archaeology, Vrije Universiteit.* Amsterdam: pp. 149-151.

BUXEDA I GARRIGÓS, J. and CAU, M., 1995. Identificación y significado de la calcita secondaria en cerámicas arqueológicas. *Complutum,* **6**, pp. 293-309.

BUXEDA, J., 1999. Alteration and Contamination of Archaeological Ceramics: The Perturbation Problem. *Journal of Archaeological Science,* **26**, pp. 295-313.

BUXEDA, J., CAU, M.À, GURT, J. and TUSET, F., 1996. Análisis tradicional y análisis arqueométrico en el estudio de las cerámicas comunes de la época romana. *Ceràmica comuna romana d'època alto-imperial a la península ibèrica. Estat de la qüestió.* Empúries, pp. 39-60.

CAPUIS, L., 1999. I Veneti. In: G. CIURLETTI and F. MARZATICO, eds, *I Reti/Die Räter. Atti del simposio 23-25 settembre 1993, Castello di Stenico.* Trento: pp. 650-670.

CAPUIS, L., 1993. *I Veneti. Società e cultura di un popolo dell'Italia preromana.* Milano: Longanesi & C.

CARANCINI, G. and PERONI, R., 1997. La koiné metallurgica. In: M. BERNABÒ BREA, A. CARDARELLI and M. CREMASCHI, eds, *Le Terramare. La più antica civiltà padana, Catalogo della Mostra, Milano.* Milano, pp. 595-601.

CARDARELLI, A., 2009. The collapse of the Terramare Culture and growth of new economic and social system during the Late Bronze Age in Italy, A. CARDARELLI, A. CAZZELLA, M. FRANGIPANE and R. PERONI, eds. In: *Le ragioni del cambiamento "Nascita", "declino" e "crollo" delle società tra fine del IV e inizio del I millennio a.C., in Scienze dell'Antichità, vol. 15*, 15-18 giugno 2006, 2009, pp. 449-520.

CARDARELLI, A., 1997. Terramare: l'organizzazione sociale e politica delle comunità. In: M. BERNABÒ BREA, A. CARDARELLI and M. CREMASCHI, eds, *Le Terramare. La più antica civiltà padana, Catalogo della Mostra, Milano.* Milano, pp. 653-660.

CÀSSOLA GUIDA, P., 1980. L'area orientale della civiltà paleoveneta. In: AA. VV., ed, *Este e la civiltà paleoveneta a cento anni dalle prime scoperte, Atti dell' XI Convegno di Studi etruschi e italici (Este-Padova, 1976).* Firenze, pp. 107-122.

CÀSSOLA GUIDA, P. and BALISTA, C., 2007. *Gradisca di Spilimbergo (Pordenone). Indagini di scavo in un castelliere protostorico (1987-1992)*. *Studi e ricerche di protostoria mediterranea,* 7.

CATASTO REGIONALE., Catasto regionale delle grotte del Friuli Venezia Giulia. Available: http://www.catastogrotte.fvg.it/.

CATTANI, M., LAZZARINI, L. and FALCONE, R., 1997. Macine protostoriche dall'Emilia e dal Veneto: note archeologiche, caratterizzazione chimico-petrografica e determinazione della provenienza. *Padusa,* XXXI, pp. 105-137.

CHUNG, F.H., 1974. Quantitative interpretation of X-ray diffraction patterns, I. Matrix-flushing method of quantitative multicomponent analysis. *Journal of Applied Crystallography,* 7, pp. 513-519.

COSTANTINI, E.A.C., 1992. I suoli e i paesaggi del comprensorio tabacchicolo veronese. In: E.A.C. COSTANTINI, F. CASTELLI, D. CASTALDINI, G. RODOLFI, R. NAPOLI, T. PANINI, G. BRAGATO, S. PELLEGRINI, P.G. ARCARA, P. CHERUBINI, P. SPALLACCI, D. BIDINI and S. SIMONCINI, eds, *Valutazione del territorio per la produzione di tabacco di tipo Virginia Bright: uno studio interdisciplinare nel comprensorio veronese (Italia settentrionale),* pp. 45-66.

CROCE DE VILLA, P., 1991. Concordia Sagittaria. Scavo nell'abitato protostorico. *Quaderni di Archeologia del Veneto,* VII, pp. 79-92.

CUPITÒ, M. and LEONARDI, G., c.s. L'insediamento arginato di Fondo Paviani nel quadro delle relazioni tra mondo egeo-miceneo e Pianura Padana. *Ambra per Agamennone. Indigeni e Micenei tra Egeo, Ionio e Adriatico nel II millennio a.C., Catalogo della Mostra, Bari, maggio 2010.* Bari: Adda.

CUPITÒ, M. and LEONARDI, G., 2005. Proposta di lettura sociale delle necropoli di Olmo di Nogara. In: L. SALZANI, ed, *La necropoli dell'età del bronzo all'Olmo di Nogara, Memorie del Museo Civico di Storia Naturale di Verona, 2. serie, Sezione Scienze dell'Uomo, 8,* pp. 488-494.

DALLA LONGA, E., 2012. I materiali dal Bronzo antico al Bronzo recente. In: A. ANGELINI and G. LEONARDI, eds, *Il castelliere di Castel de Pedena. Un sito di frontiera del II e I millennio a.C.* Silea, pp. 77-94.

DAMIANI, I., 1997. La ceramica appenninica e subappenninica come modelli ed elementi di scambio. In: M. BERNABÒ BREA, A. CARDARELLI and M. CREMASCHI, eds, *Le Terramare. La più antica civiltà padana, Catalogo della Mostra, Milano.* Milano, pp. 621-628.

DAY, P.M. and KIRIATZI, E., 1999. Group therapy in Crete: a comparison between analyses by NAA and thin section petrography of Early Minoan pottery. *Journal of Archaeological Science,* 26, pp. 1025-1036.

DE MARINIS, R.C., ed, 2000. *Il Museo Civico Archeologico Giovanni Rambotti, una introduzione alla preistoria del lago di Garda.* , Castiglione delle Stiviere (MN).

DE MARINIS, R.C., 1999. Towards a Relative and Absolute Chronology of the Bronze Age in Northern Italy. *Notizie Archeologiche Bergomensi,* 7, pp. 23-100.

DE MARINIS, R.C., 1997. L'età del bronzo nella regione benacense e nella pianura padana a nord del Po. In: M. BERNABÒ BREA, A. CARDARELLI and M. CREMASCHI, eds, *Le Terramare. La più antica civiltà padana, Catalogo della Mostra, Milano.* Milano, pp. 405-419.

DELLWIG, O., BÖTTCHER, M.E., LIPINSKI, M. and BRUMSACK, H.J., 2002. Trace metals in Holocene coastal peats and their relation to pyrite formation (NW Germany). *Chemical Geology,* **182**, pp. 423-442.

DONADEL, V., 2012. I materiali dal Bronzo recente avanzato alla prima età del Ferro. In: A. ANGELINI and G. LEONARDI, eds, *Il castelliere di Castel de Pedena. Un sito di frontiera del II e I millennio a.C.* Silea, pp. 95-108.

ERKO, A., SCHÄFERS, F., FIRSOV, A., PEATMAN, W.B., EBERHARDT, W. and SIGNORATO, R., 2004. The BESSY X-ray microfocus beamline project. *Spectrochimica Acta Part B: Atomic Spectroscopy,* 59(10-11), pp. 1543-1548.

FASANI, L. and SALZANI, L., 1975. Nuovo insediamento dell'età del Bronzo in località «Fondo Paviani» presso Legnago (VR). *Bollettino del Museo Civico di Storia Naturale di Verona,* II, pp. 259-281.

FREESTON, I.C. and MIDDLETON, A.P., 1987. Mineralogical applications of the analitycal SEM in archaeology. *Mineralogical Magazine,* 51, pp. 21-31.

FREESTONE, I.C., 2001. Post-depositional changes in archaeological ceramics and glasses. In: D.R. BROTHWELL and A.M. POLLARD, eds, *Handbook of archaeological sciences.* Chichester: John Wiley, pp. 615-625.

FREESTONE, I.C., 1995. Ceramic Petrography. *American Journal of Archaeology,* 99 (1), pp. 111-115.

FREESTONE, I.C., MEEKS, N.D. and MIDDLETON, A.P., 1985. Retention of phosphate in buried ceramics: an electron microbeam approach. *Archaeometry,* **27**, pp. 161-177.

FREESTONE, I.C., MIDDLETON, A.P. and MEEKS, N.D., 1994. Significance of phosphate in ceramic bodies: discussion of paper by Bollong et al. *Journal of Archaeological Science,* 21 (425), pp. 426.

FORS, Y., NILSSON, T., RISBERG, E.D., SANDSTRÖM, M. and TORSSANDER, P., 2008. Sulfur accumulation in pinewood (Pinus sylvestris) induced by bacteria in a simulated seabed environment: implications for marine archaeological wood and fossil fuels. *International Biodeterioration and Biodegradation,* (63), pp. 1-12.

GORNER, W., HENTSCHEL, M.P., MULLER, B.R., RIESEMEIER, H., KRUMREY, M., ULM, G., DIETE, W., KLEIN, U. and FRAHM, R., 2001. BAMline: the first hard X-ray beamline at BESSY II. *Nuclear Instruments and Methods in Physics Research Section A: Accelerators, Spectrometers, Detectors and Associated Equipment,* 467–468 (1), pp. 703-706.

GARRELS, R.M., 1960. *Mineral equilibria at low temperature and pressure.* New York: Harper and Row.

GOVINDARAJU, K., 1994. 1994 Compilation of working values and sample description for 383 geostandards. *Geostandards Newsletter,* 18, pp. 1-158.

HARARI, M. and PEARCE, M., eds, 2000. *Il Protovillanoviano al di qua e al di là dell'Appennino. Atti della giornata di Studio (Pavia 17 Giugno 1995).* Como.

HEIMANN, R.B. and MAGGETTI, M., 1981. Experiments on simulated burial of calcareous terra sigillata (mineralogical change). Preliminary results. *British Museum occasional paper,* **19**.

HOWARTH, R.W. and GIBLIN, A.E., 1983. Sulfate reduction in the salt marshes at Sapelo. *Limnology and Oceanography,* **28**, pp. 70-82.

HOWARTH, R.W. and TEAL, J.M., 1979. Sulfate reduction in a New England salt marsh. *Limnology and Oceanography,* **24**, pp. 999-1013.

JONES, R., VAGNETTI, L., LEVI, S., WILLIAMS., J., JENKINS, D. and DE GUIO, A., 2002. Mycenean and Aegean pottery from Northern Italy. Archaeological and archaeometrical studies. *Studi Micenei ed Egeo-Anatolici,* (XLIV/2), pp. 221-261.

JOSEPHS, R., 2005. Short contribution: Applying micromorphological terminology to ceramic petrography. *Geoarchaeology,* 20, pp. 861-865.

KILIKOGLOU, V., MANIATIS, Y. and GRIMANIS, P., 1988. The effect of purification and firing of clays on trace element provenance studies. *Archaeometry,* 30 (1), pp. 37-46.

LANDGREBE, D., 1997, Multispectral data analysis: a signal theory perspective. Available: https://engineering.purdue.edu/~biehl/MultiSpec/.

LANZINGER, M., MARZATICO, F. and PEDROTTI, A., eds, 2000. *Storia del Trentino vol 1. La preistoria e la protostoria.* Bologna: Il mulino.

LEMOINE, C., MEILLE, E., POUPET, P., BARRANDON, J.N. and BORDEIRE, B., 1981. Etude de quelques altérations de composition chimique de céramique en milieu marin et terrestre. *Revue d'Archéometrie,* Supplément 5, pp. 349-353.

LEMOINE, C. and PICON, M., 1982. La fixation du phosphore par les céramiques lors de leur enfouissement et ses incidences analytiques. *Revue d'Archéometrie,* 6, pp. 101-112.

LEONARDI, G., 2012. Castel de Pedena nel propio contesto storico e territoriale. In: A. ANGELINI and G. LEONARDI, eds, *Il castelliere di Castel de Pedena. Un sito di frontiera del II e I millennio a.C.* Silea, pp. 153-166.

LEONARDI, G., 1976. Ex Storione (Canton del Gallo). In: AA. VV., ed, *Catalogo della mostra (Padova, 27 giugno-15 novembre 1976).* Padova, pp. 102-132.

LEONARDI, G., 1976. S. Sofia, angolo nord via Cesare Battisti. In: AA. VV., ed, *Padova Preromana, Catalogo della mostra (Padova, 27 giugno-15 novembre 1976).* Padova, pp. 140-146.

LEONARDI, G., 2010. Le problematiche connesse ai siti d'altura nel Veneto tra antica età del Bronzo e romanizzazione. In: L. DAL RI, P. GAMPER and H. STEINER, eds, *Höhensiedlungen der Bronze- und Eisenzeit. Kontrolle der Verbindungswege über die Alpen. Abitati dell'età del Bronzo e del Ferro. Controllo delle vie di comunicazione attraverso le Alpi. Atti del convegno (Schluderns 2001).* Trento, pp. 251-274.

LEONARDI, G., 1979. Il Bronzo finale nell'Italia nord-orientale, proposta per una suddivisione in fasi, *Atti XXI Riunione Scientifica dell'Istituto Italiano di Preistoria e Protostoria, Firenze 21-23 ottobre 1977*, 21-23 ottobre 1977 1979, pp. 155-188.

LEONARDI, G. and CUPITÒ, M., 2008. Il sito arginato dell'età del Bronzo di Fondo Paviani-Legnago. Notizia preliminare sulla campagna di indagine 2007. *Quaderni di Archeologia del Veneto,* pp. 90-93.

MAGGETTI, M., 1991. Mineralogical and petrographical methods for the study of ancient pottery, F. BURRAGATO, O. GRUBESSI and L. LAZZARINI, eds. In: *1st European Workshop on archaeological ceramics,10-12. 10. 1991, Roma* 1991, pp. 23-35.

MAGGETTI, M., 1982. Phase analysis and its significance for technology and origin. *Archaeological ceramics, Smithsonian Institute, Washington,* pp. 121-133.

MAGGETTI, M., MARRO, C. and PERINI, R., 1979. Risultati delle analisi mineralogiche-petrografiche della ceramica "Luco": l'importazione di ceramiche dal Trentino-Alto Adige alla bassa Engadina. *Studi trentini di scienze storiche,* 4, pp. 3-19.

MAGGETTI, M., WESTLEY, H. and OLIN, J.S., 1984. Provenance and technical studies of Mexican majolica using elemental and phase analysis. In: J.B. LAMBERT, ed, *Archaeological chemistry III, Advances in Chemistry Series 205.* Washington DC: American Chemical Society, pp. 151-191.

MALIK, J., BELONGIE, S., LEUNG, T. and SHI, J., 2001. Contour and Texture Analysis for Image Segmentation. *International Journal of Computer Vision,* 43 (1), pp. 7-27.

MARITAN, L., 2004. Archaeometric study of Etruscan-Padan type pottery from the Veneto region: petrographic, mineralogical and geochemical-physical characterisation. *European Journal of Mineralogy,* 16.

MARITAN, L., 2002. *Studio archeometrico di ceramiche di tipo etrusco padano nell'area veneta: indagini petrografiche, chimiche e fisiche e confronto con i risultati ottenuti da prove sperimentali di cottura di materiali argillosi.* PhD edn. Padova: Geological Department, University of Padova.

MARITAN, L., ANGELINI, I., ARTIOLI, G., MAZZOLI, C. and SARACINO, M., 2009. Secondary phosphates in the ceramic materials from Frattesina (Rovigo, North-Eastern Italy). *Journal of Cultural Heritage,* **10**, pp. 144-151.

MARITAN, L. and MAZZOLI, C., 2004. Phosphates in archaeological finds: implications for environmental conditions of burial. *Archaeometry,* 46.

MARZATICO, F., 2000. L'età del Bronzo Recente e Finale. In: M. LANZINGER, F. MARZATICO and A. PEDROTTI, eds, *Storia del Trentino, vol.1, La preistoria e la protostoria.* Il mulino, pp. 367-416.

MASELLI SCOTTI, F., DEGRASSI, V., MEZZI, M.R. and MANDRUZZATO, L., 1995. Aquileia. Essiccatoio Nord, scavi 1995. *Aquileia Nostra,* LXVI, pp. 192-199.

MASELLI SCOTTI, F., MANDRUZZATO, L. and TIUSSI, C., 1996. Aquileia. Essiccatoio Nord, scavi 1996. *Aquileia Nostra,* LXVII, pp. 267-272.

MASELLI SCOTTI, F., 1983. Insediamento di Duino. *Caput Adriae,* pp. 211-214.

MASELLI SCOTTI, F., 1983. Stazione del Terzo Ramo del Timavo. *Caput Adriae,* pp. 209-210.

MASELLI SCOTTI, F., CRISMANI, A., SENARDI, F. and VENTURA, P., 1999. Aquileia. Essiccatoio Nord. *Aquileia Nostra,* LXX, pp. 329-340.

MATTHEW, A.J., WOODS, A.J. and OLIVER, C., 1991. Spots before the eyes: new comparison charts for visual percentage estimation in archaeological material. In: A.P. MIDDLETON and I.C. FREESTONE, eds, *Recent developments in ceramic petrology, No. 81.* London: British Museum Occasional Paper, pp. 211-263.

METZER, I. and GLEIRSCHER, P., eds, 1992. *I Reti/Die Räter.* Bolzano.

MIDDLETON, A.P., FREESTON, I.C. and LEESE, M.N., 1985. Textural analysis of ceramic thin sections: evaluation of grain sampling procedures. *Archaeometry,* 27 (1), pp. 64-74.

MIZZAN, S., 1996. La ceramica. In: P. CÀSSOLA GUIDA and S. MIZZAN, eds, *Pozzuolo del Friuli II,1. La prima età del ferro nel settore meridionale del castelliere. Lo scavo e la ceramica (Studi e ricerche di protostoria mediterranea 4).* Roma, pp. 43-203.

MONTAGNARI KOKELJ, E. and CRISMANI, A., 1996. La grotta del Mitreo nel Carso triestino. *Atti Società della Priestoria e Protostoria del Friuli Venezia Giulia,* X, pp. 7-98.

MOORE, D.M. and REYNOLDS JR., R.C., 1997. *X-ray diffraction and the identification and analysis of clay minerals.* Oxford-New York. Oxford University Press.

MOZZI, P., 2005. Alluvial plain formation during the late Quaternary between the southern Alpine margin and the Lagoon of Venice (northern Italy). *Geografia Fisica e Dinamica Quaternaria,* Suppl. 7, pp. 219-230.

MUNSELL, A.H., 2000. *Soil color chart.*

NEAL, A.L., TECHKARNJANARUK, S., DOHNALKOVA, A., MCCREADY, D., PEYTON, B.M. and GEESEY, G.G., 2001. Iron sulfides and sulfur species produced at hematite surfaces in the presence of sulfate-reducing bacteria. *Geochimica et Cosmochimica Acta,* **65**, pp. 223-235.

NEUGERBAUER, J.W., 1994. *Bronzezeit in Ostösterreich.* St. Pölten-Wien.

NICOSIA, C., BALISTA, C., CUPITÒ, M., ERTANI, A., LEONARDI, G., NARDI, S. and VIDALE, M., 2010. Anthropogenic deposits from the Bronze Age site of Fondo Paviani (Verona, Italy): Pedochemical and micropedological characteristics. *Quaternary International,* 243, pp. 280-292.

PACCIARELLI, M., 1997. Il Bronzo Medio-Recente della Romagna. In: M. BERNABÒ BREA, A. CARDARELLI and M. CREMASCHI, eds, *Le Terramare. La più antica civiltà padana, Catalogo della Mostra, Milano.* Milano, pp. 423-430.

PAPAGEORGIOU, I. and BAXTER, M.J., 2001. Model-based cluster analysis of artefact compositional data. *Archaeometry,* 43.

PARIS, O., LI, C., SIEGEL, S., WESELOH, G., EMMERLING, F., RIESEMEIER, H., ERKOD, A. and FRATZLA, P., 2007. A new experimental station for simultaneous X-ray microbeam scanning for small- and wide-angle scattering and fluorescence at BESSY II. *Journal of Applied Crystallography,* 40, pp. 466-470.

PELLEGRINI, E., 1989. Aspetti regionali e relazioni interregionali nella produzione metallurgica del Bronzo Finale nell'Italia continentale: i ripostigli con pani a piccone. In: E. ANTONACCI SANPAOLO, ed, *Archeometallurgia. Ricerche e prospettive. Atti del Colloquio Internazionale di Archeometallurgia, Bologna (Bologna – Dozza Imolese 1988).* Bologna, pp. 589-603.

PERINI, R., 1976. Appunti per una definizione delle fasi della cultura Luco sulla base delle recenti ricerche nel territorio. *Studi trentini di scienze storiche,* 2, pp. 151.

PERONI, R., 2004. *L'Italia alle soglie della storia.* Roma-Bari, Laterza.

PERONI, R., 1971. *L'età del Bronzo nella penisola italiana, I, L'Antica età del Bronzo.* Firenze.

PICON, M., 1985. Un exemple de pollution aux dimensions kilométriques: la fixation du baryum par les céramiques. *Revue d'Archéometrie,* 9, pp. 27-29.

PRATT, J.H., 1894. On the determination of ferrous iron in silicates. *American Journal of Science,* 48 (284), pp. 149-151.

PREDA, M. and COX, M.E., 2004. Temporal variations of mineral character of acid-producing pyritic coastal sediments, southeast Queensland, Australia. *Science of the Total Environment,* **326**, pp. 257-269.

PROGETTO C.R.I.G.A., , Progetto C.R.I.G.A. - Catasto Ragionato Informatico delle Grotte Archeologiche. Available: http://progetti.divulgando.eu/criga/.

PROSDOCIMI, B., 2011. *Una produzione di ceramica della prima età del ferro tra Veneto e Friuli: le olle ad orlo appiattito.* PhD edn. Udine: University of Udine.

PYZIK, A.J. and SOMMER, S.E., 1981. Sedimentary iron monosulfides-kinetics and mechanism of formation. *Geochimica et Cosmochimica Acta,* **45**, pp. 687-698.

RAPI, M., 2002. Lavagnone di Desenzano del Garda (BS), settore B: la ceramica del Bronzo Antico I. *Notizie Archeologiche Bergomensi,* 10, pp. 132-145.

RAISWELL, R. and CANFIELD, D.E., 1998. Sources of iron for pyrite formation in marine sediments. *American Journal of Science,* **298**, pp. 219-245.

REEDY, C., 1994. Thin-section petrography in studies of cultural materials. *Journal of the American Institute for Conservation,* 33, pp. 115-129.

REEDY, C.L., 2008. *Thin-section petrography of stone and ceramic cultural materials.* London: Archetype Publications Ltd.

REEDY, C.L., 2006. Review of digital image analysis of petrographic thin sections in conservation research. *Journal of the American Institute for Conservation,* 45(2), pp. 127-146.

RICE, M.P., 1987. *Pottery analysis.* 2005 edn. USA: The University of Chicago Press.

RIEDERER, J., 2004. Thin section microscopy applied to the study of archaeological ceramics. *Hyperfine Interactions,* 154, pp. 143-158.

ROSSI, S., 2008. *L'abitato arginato di Castion di Erbè (VR) alla luce dei risultati dello studio cronotipologico della ceramica vascolare e considerazioni sulla prima età del ferro nel territorio veronese.* PhD edn. Padova: University of Padova.

RUBAGOTTI, A., 2006. *Padova, un rinvenimento fortuito: materiali veneti da via S. Sofia angolo via C. Battisti.* Padova: University of Padova.

SCHLEGEL, M.C., MUELLER, U., PANNE, U. and EMMERLING, F., 2011. Deciphering the sulfate attack of cementitious materials by high-resolution micro-X-ray diffraction. *Analytical Chemistry,* 83, pp. 3744-3749.

SCHLEICHER, L., MILLER, W., WATKINS-KENNEY, S., CARNES-MCNAUGHTON, L. and WILDE-RAMSING, M., 2008. Non-destructive chemical characterization of ceramic sherds from Shipwreck 31CR314 and Brunswick Town, North Carolina. *Journal of Archaeological Science,* **35**, pp. 2824-2838.

SCHWEDT, A., MOMMSEN, H., ZACHARIAS, N. and BUXEDA, J., 2006. Analcime crystallization and compositional profiles — Comparing approaches to detect post-depositional alterations in archaeological pottery. *Archaeometry,* 48 (2), pp. 237-251.

SECCO, M., MARITAN, L., MAZZOLI, C., LAMPRONTI, G., ZORZI, F., NODARI, L., RUSSO, U. and MATTIOLI, S., 2011. Alteration processes of pottery in lagoon-like environments. *Archaeometry,* 53 (4), pp. 809-829.

SHELDON, M.R., 2003. *Probabilità e statistica per l'ingegneria e le scienze.* Apogeo.

SILLAR, B. and TITE, M.S., 2000. The challenge of 'technological choices' for materials science approaches in archaeology. *Archaeometry,* 42, pp. 2-20.

SORBINI, L., ACCORSI, C.A., BANDINI MAZZANTI, M., FORLANI, L., GANDINI, F., MENEGHEL, M., RIGONI, A. and SOMMARUGA, M., 1984. Geologia e Geomorfologia di una porzione della pianura a sud-est di Verona. *Memorie del Museo Civico di Storia Naturale di Verona. Sez. Sc. Della Terra,* 2, pp. 1-91.

SØRENSEN, J., CHRISTENSEN, D. and JØRGENSEN, B.B., 1981. Volatile fatty acids and hydrogen as substrates for sulfate reducing bacteria in anaerobic marine sediment. *Applied and Environmental Microbiology,* **42**, pp. 5-11.

STIENSTRA, P., 1986. *Systematic macroscopic description of the texture and composition of ancient pottery – some basic methods*. *Newsletter Department of Pottery Technology, University of Leiden,* IV.

STOLTMAN, J.B., 1989. A quantitative approach to the petrographic analysis of ceramic thin sections. *American Antiquity,* 54 (1), pp. 147-160.

TITE, M.S., FREESTON, I.C. and MEEKS, M., 1982. The use of scanning electron microscopy in the technological examination of ancient ceramics. In: J.S. OLIN and A.D. FRANKLIN, eds, *Archaeological ceramics.* Washington: Smithsonian Institution Press, pp. 109-120.

TITE, M.S. and MANIATIS, Y., 1975. Examination of ancient pottery using the scanning electron microscope. *Nature,* pp. 122-123.

VENIALE, F., 1990. Modern techniques of analysis applied to ancient ceramics, *Advanced Workshop, «Analytical Methodologies for the Investigation of Damaged Stones», Pavia (Italy)*, 14-12 September 1990, 1990.

VITRI, S. and SPANGHERO, T., 2000. Porcìa, loc. S. Ruffina di Palse. Scavi 1999-2000. *Aquileia Nostra,* LXXI, pp. 671-677.

WALTER, V. and BESNUS, Y., 1989. Un exemple de pollution en phosphore et en manganèse de céramiques anciennes. *Revue d'Archéometrie,* **13**, pp. 55-64.

WEIGAND, P.C., HARBOTTLE, G. and SAYRE, V., 1977. Turquoise sources and source analysis: Mesoamerica and the Southwestern U.S.A. In: T.K. EARLE and J.E. ERICSON, eds, *Exchange system in prehistory.* New York: Academic Press, pp. 15-34.

WILKIN, R.T. and BARNES, H.L., 1997. Formation processes of framboidal pyrite. *Geochimica et Cosmochimica Acta,* **61**, pp. 323-339

WHITBREAD, I.K., 1996. Detection and interpretation of preferred orientation in ceramic thin section, *Proceeding of the 2nd Symposium of the Hellenic Archaeometrical Society (26-28 March 1993)*, 26-28 March 1993. 1996, pp. 413-425.

WHITBREAD, I.K., 1995. Greek transport of amphorae – A petrological and archaeological study. *British School at Athens, Fitch laboratory occasional paper,* 4.

WOODS, A.J., 1982. An introductory note on the use of tangential thin sections for distinguishing between wheel-thrown and coil/ring-built vessels. *Bulletin on the Experimental Firing Group,* 3, pp. 100-114.